MEDICAL PHYSICS
International

- *EDITORIALS*
- *NEW IOMP EDUCATIONAL AND PROFESSIONAL ACTIVITIES*
- *CURRENT STATUS OF MEDICAL PHYSICS RECOGNITION IN SEAFOMP COUNTRIES*
- *THE ASEAN COLLEGE OF MEDICAL PHYSICS (ACOMP) – THE FIRST TWO YEARS*
- *MEDICAL PHYSICS EDUCATION AND TRAINING IN BRAZIL*
- *EDUCATION AND CLINICAL TRAINING OF MEDICAL PHYSICS IN THAILAND*
- *OPTIMIZING CLINICAL IMAGE QUALITY: AN EXPANDING ROLE FOR MEDICAL PHYSICISTS*
- *AN e-LEARNING PACKAGE FOR PERSONAL DOSIMETRY TRAINING PURPOSES*
- *THE SOCIAL WEB: THE FUTURE IS NOW*
- *THE APPEARANCE AND ORIGIN OF COMMON MRI ARTIFACTS*
- *COMPUTED TOMOGRAPHY DOSIMETRY: FROM BASIC TO STATE-OF-THE-ART TECHNIQUES*
- *HISTORY OF MEDICAL PHYSICS – A BRIEF PROJECT DESCRIPTION*
- *INTERVIEW WITH PROFESSOR JOHN MALLARD*
- *MEDICAL PHYSICS PROFESSIONAL BODIES IN THE UNITED KINGDOM: A BRIEF HISTORY*
- *COLLABORATING TOPICS AND BOOK REVIEWS*
- *REPORT OF AN UPDATE TO THE PERSIAN TRANSLATION OF MEDICAL PHYSICS TERMS*
- *RAD-AID, AN ORGANIZATION BRINGING RADIOLOGY TO RESOURCELIMITED REGIONS OF THE WORLD*
- *INTERNATIONAL DAY OF MEDICAL PHYSICS*
- *WELCOME TO PINK CITY JAIPUR*
- *IMPLEMENTING STEREOTACTIC RAPIDARC TREATMENTS INTO CLINICAL ROUTINE*

IOMP

MPI

World Congress on Medical Physics & Biomedical Engineering

June 3–8, 2018
Prague, Czech Republic
www.iupesm2018.org

IUPESM
PRAGUE 2018

TOPICS

1 Diagnostic Imaging
2 Image Processing
3 Information Technology in Healthcare
4 Modelling and Simulation
5 BME and MP Education, Training and Professional Development
6 Patient Safety
7 Accreditation and Certification
8 Health Technology Assessment
9 Biosignals Processing
10 Biomechanics, Rehabilitation and Prosthetics
11 Minimum Invasive Surgery, Robotics, Image Guided Therapies, Endoscopy
12 Diagnostic and Therapeutic Instrumentation
13 Micro- and Nanosystems, Active Implants, Biosensors
14 Neuroengineering, Neural Systems
15 Biomaterials, Cellular and Tissue Engineering, Artificial Organs
16 Assistive Technologies
17 Biological Effects of Electromagnetic Fields
18 Clinical Engineering
19 Radiation Oncology Physics and Systems
20 Dosimetry and Radiation Protection
21 Advanced Technologies in Cancer Research and Treatment
22 Biological Effects of Ionizing Radiation

ORGANISERS

Czech Society for Biomedical Engineering and Medical Informatics
Member of Czech Medical Association JEP
Prague, Czech Republic

Czech Association of Medical Physicists
Prague, Czech Republic

CONTACTS

Congress Organising Committee
E-mail: coc@iupesm2018.org

Supporting Agency
GUARANT International spol. s r.o., Na Pankráci 17, 140 21 Prague, Czech Republic
Tel: +420 284 001 444, fax: +420 284 001 448, e-mail: agency@iupesm2018.org

MEDICAL PHYSICS INTERNATIONAL

THE JOURNAL OF

THE INTERNATIONAL ORGANIZATION FOR MEDICAL PHYSICS

Volume 5, Number 1, April 2017

MEDICAL PHYSICS INTERNATIONAL

The Journal of the International Organization for Medical Physics

MPI web address: www.mpijournal.org

CONTENTS

EDITORIALS

Medical Physics Education – Challenges and Opportunities

Perry Sprawls, Co-Editor

The future holds many opportunities for medical physicists to make greater contributions to improved care for patients, especially in the field of medical imaging. We continue to experience around the world many innovations in both medical imaging technology for diagnosis and therapeutic methods especially for the treatment of cancer. These provide greatly increased capabilities for both diagnosis and treatment, they are also much more complex. This is both a challenge and opportunity for medical physicists in all countries. As the new methods and technology becomes available there is a critical need for physics education to support effective and safe clinical procedures. In the area of medical imaging much of our physics education and activities has focused on the equipment, how it produces images and evaluating performance in the context of quality control procedures. While this is important, it does not address the most significant factors determining image quality for clinical procedures. That is the imaging procedure itself that

is controlled by the complex combination of protocol factors. The goal is to optimize every clinical procedure so that the individual image quality characteristics are balanced to provide the necessary clinical visibility without unnecessary radiation exposure or acquisition times. The focus must be on the image and the procedures and not just the equipment. Medical physicists are becoming major contributors to this both as clinical consultants and educators for the other imaging professionals, especially radiologists and technologists.

One of the special purposes of this journal is to publish articles to serve as resources for this type of education. There are two in this edition.

I will continue to support medical physics educators in this effort with resources through the opportunities of Collaborative Teaching on the web at:
www.sprawls.org/resources

The accents of this MPI Issue

Slavik Tabakov, Co-Editor

This issue of the Medical Physics International (MPI) Journal (2017, No.1) includes a number of useful educational and professional papers from the International Conference on Medical Physics in Bangkok (ICMP2016). These strengthen the impact of the first IOMP School and the IOMP/IUPAP Workshop at ICMP2016, and provide good materials, which can be used in many medical physics lectures and courses.

The current MPI issue includes also detailed educational papers, some very extensive, as the one on MRI Imaging Artifacts and the one on Implementation of RapidArc Treatment. Our statistics shows that such papers have many downloads. We shall continue to invite and publish various papers explaining clinical applications and hands-on practical solutions. In future these will also be used in the IOMP collection of educational materials (Digital Library) – a shared resource to support our teaching and learning.

A specific emphasis of the current MPI issue is the inclusion of several papers with historical emphasis. These include the first public announcement of the large

project History of Medical Physics, which was discussed and supported in IOMP about one year ago. The project will take many years to complete, and will surely attract hundreds of contributors – specialists in various fields. It will be published on parts in MPI, and will be left open for future updates, thus forming a constantly growing record of the achievements of the profession and its benefit for healthcare.

This MPI issue (and the next one, already in development) will also try to include as much as possible papers on professional development in all continents. This is vital for the harmonious global development of medical physics. This will also strengthen the links between the IOMP Federations and will provide additional background for cooperation.

Finally we want to remind our readers that we do not publish research papers – these have to be addressed to the other research-orientated professional journals. At the same time we want to encourage colleagues to send educational, professional, historical and other types of materials (large papers will be in Annex). We want to specially thank all colleagues who contribute to the MPI Journal.

PROFESSIONAL ISSUES

NEW IOMP EDUCATIONAL AND PROFESSIONAL ACTIVITIES: IOMP SCHOOL AND IOMP/IUPAP WORKSHOP "BUILDING PROFESSIONAL CAPACITY IN DEVELOPING COUNTRIES"

S. Tabakov[1,2]

[1] Dept. Medical Engineering and Physics, King's College London, King's College Hospital, London SE5 9RS, UK
[2] President IOMP (International Organization for Medical Physics), IPEM, York YO24 1ES, UK

I. INTRODUCTION

The International Organization for Medical Physics (IOMP) launched a new regular activity during the 22nd International Conference on Medical Physics (ICMP2016), which took place in Bangkok (9-12 December 2016). This activity – IOMP School was a sequence of 41 educational mini-Symposia, covering various topics of importance for the profession (please see the Book with Abstracts at MPI Journal vol.4 No.2, p.532-574).

Also at the ICMP2016 IOMP organized, with support from the IUPAP, a specific Workshop "Building Professional Capacity in Developing Countries". Materials from both activities are now included in the current MPI issue.

II. IOMP SCHOOL

The new IOMP activity IOMP School was approved by the IOMP ExCom at the end of 2015. During ICMP2016 it was made in the form sequence of Mini-symposia. Topics of the Mini Symposia and the main presenters were as follows:

-Physics, dosimetry and radiation protection; Speakers: KH Ng, K Matsubara, J Damilakis (IOMP)

-New horizon of medical physics and synergetic effect with medical engineering and information science; Speaker: K Inamura

-Current trends of medical physics in radiotherapy and imaging; Speaker: GA Zakaria (U. of Cologne)

-The evolving posture of MP as a profession: medical physics 3.0; Speaker: E Samei (Duke U.)

-The new era of medical physics in Asia; Speaker: K Doi (JSRT)

-Novel retrieval technologies for similar images and personal identification in computer-aided diagnosis and radiation therapy; Speakers: H Arimura, C Muramatsu, H Fujita, YW Chen, K Wakasugi, A Katsumata, T Aoki (JSRT)

-Comprehensive audits in radiotherapy, diagnostic and interventional radiology, nuclear medicine; Speakers: A Meghzifene (IAEA), A Krisanachinda

-Radiation protection in dental radiography; Speakers: J Vassileva, R Pauwels, V Tsapaki (IAEA/IOMP)

-Eye lens dosimetry and study on radiation cataract with interventional cardiologists; Speakers: K Matsubara, S Srimahashota, A Krisanachinda

-Dosimetry of small static photon fields: challenges and solutions; Speakers: MS Huq & S Suriyapee

-Recent developments in dosimetry, treatment planning and quality assurance for intensity modulated proton therapy; Speaker: N Sahoo (MD Anderson)

-Robust optimization and robustness quantification in intensity modulated proton therapy; Speaker: W Liu (Mayo Clinic)

-Stereotactic body radiation therapy: technical challenges and clinical aspects; Speakers: MS Huq, D Kannarunimit, S Oonsiri

-Digital radiography detectors: overview and acceptance testing/quality control update.

Implementation of the IEC 62494-1 exposure index standard; Speaker: JA Seibert (UC Davis)

-Precision medicine through dose optimization and monitoring of medical imaging; Speaker: E Samei (Duke Univ.)

-Radiation dose metrics and dose monitoring for medical imaging procedures; Speaker: JA Seibert (UC Davis)

-Dosimetry in radiopharmaceutical therapy treatment planning; Speaker: G Sgouros (Johns Hopkins U.)

-Medical physics training and education collaboration among both regional organizations; Speakers: H Round, I Duhaini, LA Balooshi

-Dose Tracking and Quality Assurance; Speakers: M Rehani, N Fitousi, V Tsapaki (IOMP)

-ASEAN College of Medical Physics: Workshop on Digital Radiography; Speakers: KH Ng, N Jamal, CH Yeong

-Women in MP conference/meeting; Speakers: HA Azhari, M Stoeva, S Kodlulovich Renha (IOMP women group)

-Pilot survey in participation on women in MP conferences; Speakers: G Martin, S Kodlulovich Renha, P Platoni, A Peralta (IOMP women group)

- European initiatives on medical radiation protection; Speakers: J Damilakis, V Tsapaki, E Lief (EFOMP)

- IAEA/RCA project, RAS6077, "Strengthening the effectiveness and extent of MP education and training; Speaker: A Meghzifene

-Proton therapy (Physics); Speaker: T Bortfeld (MGH)

- Proton therapy (Clinical); Speaker: S MacDonald (MGH)

-New approaches to quality management in radiation therapy; Speakers: MS Huq, P Tangboonduangjit, T Sanghangthum

-Latest MDCT technologies in Japan; Speakers: K Tsujioka & K Ichikawa (JSRT)

- Dosimetry in terms of absorbed dose to water in photon brachytherapy; Speaker: GA Zakaria (U. of Cologne)

-Experience-based lecture on ROC observer studies in diagnostic medical physics; Speakers: J Shiraishi & R Tanaka (JSRT)

-Safety in MRI; Speaker: S Keevil (IOMP)

-The role of medical physicist in clinical trials; Speaker: T Kron

-Radiobiophotonics in cancer therapy; Speaker: R Papineni (KUMC)

-Normal tissue protection in disease and disaster; Speaker: R Papineni (KUMC)

- Current status of mammography in Asia; Speakers: T Endo, H Nishide, P Hansakul, A Krisanachinda

-Radio-adaptive response — more than tumor resistant; Speaker: D Nantajit

-Tumor microenvironment: challenges and perspectives; Speaker: T Tippayamontri

-Practical application of Moodle for e-learning courses in MP; Speaker: V Tabakova (King's College London)

-Fetal dose in radiotherapy – managing the physics aspects; Speaker: JCL Lee

-Three-dimensional (3D) dosimetry; Speaker: GS Ibbott (MD Anderson)

The mini-symposia attracted many colleagues and students and some of the topics were later invited for presentation as educational topics at the MPI Journal. The

paper here about CT Dosimetry (by Dr Matsubara) is one of these excellent presentations.

To accommodate this large number of mini-Symposia, ICMP2016 included a novel organisation of the Programme: having all mornings associated with the mini-Symposia and all afternoons for scientific presentations and poster sessions. This re-organisation of the programme was accepted very well by all participants. It was discussed some of the mini-Symposia to be presented again at the next IOMP-Schools, associated with the AOCMP-AMPICON 2017 in Jaipur, India and with the World Congress in Prague WC2018.

IOMP wants to thank all colleagues who contributed to the IOMP School Mini-symposia

III. WORKSHOP

Another educational and professional activity during the ICMP2016 was 3rd jointly sponsored IOMP-IUPAP Workshop "Building Professional Capacity in Developing Countries". The Workshop was Co-organised by S Tabakov, A Krisanachinda, Y Pipman, V Tsapaki, SD Charma, and KY Cheung.

The Workshop discussed the global growth of medical physics in the past 20 years. It highlighted the need of more medical physicists specifically in the regions of South-East Asia, Africa and Latin America. It was decided to concentrate on positive examples for building professional capacities. The reports stressed the need of inter-professional collaboration and support for building medical physics educational courses. The new IOMP activities related to International Accreditation of MSc courses and International Certification of medical physicists were also underlined. Examples were given from Thailand, Indonesia, Nepal, Nigeria, Brazil, Cuba, Bulgaria, Philippines, India and South Africa.

The Workshop Programme included:

- Growth of medical physics profession from 1965 to our days; S Tabakov

-The Role of Professional Organizations; KY Cheung

-Current Status of Medical Physics Recognition in SEAFOMP Countries; S Pawiro

-Research innovation stimulates professional growth; Kwan Ng

-IOMP Professional Relations Committee activities; Y Pipman

-Medical Physics in Nepal; M Adhikari

-Examples from developments in Latin America; S Kudlulovich Renha

-Medical physics developments in Thailand; A Krisanachinda:

-IAEA Projects; A Meghzifene

-Discussion and Way Forward

The need of including research elements, together with practical training, was discussed as specific need for building professional capacities in developing countries. Special thanks were expressed to the ICTP College on Medical Physics and related MSc programme for their support for the development of medical physics in these countries. The IOMP Library programme and the AAPM Virtual library initiative were also praised. The IAEA report showed some of the latest international projects in this field. The role of professional organisations, such as IOMP and IUPAP, was underlined and gratitude was expressed to the Organisations for the financial support of the Workshop.

Some of the presentations from the Workshop are included in the current MPI issue (related to SEAFOMP, ACOMP and Thailand)

Some of the participants at the IOMP-IUPAP Workshop

Current Status of Medical Physics Recognition in SEAFOMP Countries

S.A. Pawiro[1], J.C.L. Lee[2], F. Haryanto[3], K.H. Ng[4], A. Krisanachinda[5], D.S. Soejoko[1,] A. Peralta[6],
N.T. Chau[7], D. Manlapaz[8], S.S. Lin[9], C.H. Yeong[4], S. Chhom[10], E.O. Voon[11]

[1] Department of Physics, FMIPA, Universitas Indonesia, Depok, Indonesia
[2] Department of Radiotherapy, National Cancer Center of Singapore
[3] Department of Physics, FMIPA, Institut Teknologi Bandung, Indonesia
[4] Department of Biomedical Imaging, University of Malaya Medical Center, Kuala Lumpur, Malaysia
[5] Department of Radiology, Faculty of Medicine, King Chulalongkorn University, Bangkok, Thailand
[6] Ministry of Health, The Republic of Philippines
[7] Unit of PET-CT & Cyclotron, Cho Ray Hospital, Ho Chi Minh City, Vietnam
[8] Lung Center Center, Quezon Avenue , Manila, Philippines
[9] Pinlon Cancer Center, North Dagon Township, YangonMyanmar
[10] National Cancer Centre, Calmette Hospital, Phnom Penh, Cambodia

[11] Radiation safety & Quality Unit, Energy and Industry Department, Brunei Darussalam

Abstract— **South East Asian Federation of Organizations for Medical Physics (SEAFOMP) was established in 1997. Many efforts and activities have been conducted by the founding fathers and mothers of SEAFOMP to develop medical physics at both national and regional level. The recognition of medical physicists by the governments of the member countries is one of the goals of their efforts. The federation has conducted a survey on the current status of medical physics recognition in SEAFOMP countries, focusing on the profile of society members, medical physics education and clinical training program, as well as recognition of medical physics profession in the region. There is still a gap among medical physicists in SEAFOMP member countries. Five countries have established the role of professional society, education and training for the enhancement of medical physicists, however the recognition of medical physicists as a profession is only achieved by less than 60% of SEAFOMP member countries.**

Keywords — **medical physics, recognition, education, SEAFOMP, ASEAN.**

I. Introduction

The Association of Southeast Asian Nations, commonly referred to as ASEAN, is an organization comprising of 10 countries located in Southeast Asia. The organization was formed on 8 August 1967 in Bangkok, Thailand by its five original member countries, i.e. Indonesia, Malaysia, Philippines, Singapore and Thailand. Over the years, the organization grew when Brunei Darussalam joined in as the sixth member on 8 January 1984, Vietnam on 28 July 1995, Laos and Myanmar on 23 July 1997 and Cambodia on 30 April 1999. Its objectives include accelerating economic growth, social progress and cultural development among its members, as well as to promote regional peace [1].

The spirit of ASEAN is resounded in SEAFOMP. The idea of setting up an organization for South-east Asian medical physics societies was first mooted in 1996. During the International Organization of Medical Physics (IOMP) World Congress at Nice in 1997, the formation of SEAFOMP was endorsed by member countries. The South East Asian Federation of Organizations for Medical Physics (SEAFOMP) was officially accepted as a regional chapter of the IOMP at the Chicago World Congress in 2000 with five member countries, viz. Indonesia, Malaysia, Philippines, Singapore and Thailand. At that time, the founding members of SEAFOMP were Anchali Krisanachinda and Ratana Pirabul from Thailand, Kwan-Hoong Ng from Malaysia, Agnette Peralta from the Philippines, Djarwani S Soejoko from Indonesia and Toh-Jui Wong from Singapore. Prof. Kwan-Hoong Ng served as the founding president until 2006. Three other countries joined SEAFOMP subsequently: Brunei (2002), Vietnam (2005), Cambodia (2016), and Myanmar (2016).

The objectives of SEAFOMP are to promote (i) co-operation and communication between medical physics organizations in the region; (ii) medical physics and related activities in the region; (iii) the advancement in status and standard of practice of the medical physics profession; (iv) to organize and/or sponsor international and regional conferences, meetings or courses; (v) to collaborate or affiliate with other scientific organizations. SEAFOMP has a complementary and synergistic relationship with AFOMP in moving medical physics forward in the region [2].

II. Medical Physics Recognition

2.1. Profile of Clinical Medical Physicists in SEAFOMP Countries

A survey of medical physicist professional status; education and training as well as the recognition of medical physics profession, has been performed. The survey was conducted through the executive committee of SEAFOMP between October 2016 and March 2017. The result of this survey was presented at the track 'Capacity building in medical physics' at the International Conference on Medical Physics on 11th December 2016 in Bangkok, Thailand. This survey has updated the data which was published in previous works [3,4].

The survey data was presented in Table 1 to Table 4. Table 1 describes the profile of medical physicists in the SEAFOMP countries which consist of the members of societies include the academics, beaurocrats, product specialists and clinical medical physicists. We also refer the certified medical physicists as part of clinical medical physicists.

Table 1 shows that there are currently 1027 medical physicists serving in various aspects of medical physics in this region. Among all, 745 are clinical medical physicists who are working in clinical setting. The clinical medical physcists who are working at clinical institutions and comply with international qualification standard (eg. minimum academic qualification of master's degree) may be qualified to receive certification from international or national body. Until recently, the number of certified medical physicists (i.e. clinically qualified medical physcists, CQMP) in SEAFOMP countries is about 88 (8.5%) out of 1027 medical physicists. The table also points out the number of clinical medical physicists in the region who hold international certification (< 1%), while the remaining certified medical physicists are recognized by the respective national bodies or institutions.

Table 1. The profile of society members including clinical medical physicists and certified medical physicists

Country	Society Members	No. Clinical MedPhys	Certified-MP
Brunei Darussalam	8	8	None
Cambodia	4	4	None
Indonesia	290	161	13 (national certification)
Malaysia	266	200	1 (ABMP)
Myanmar	34	26	3 (overseas training)
Philippines	110	85	35 (national certification)
Singapore	35	31	1 (ABR), 20 (institution)
Thailand	150	150	30 (national certification)
Vietnam	130	80	5 (Overseas training)

2.2. Profile of Medical Physics Education and Training in SEAFOMP Countries

Table 2 shows that only four countries in this region offer medical physics post-graduate education by coursework (master degree), while the others offer medical physics as an elective subject or in final year's syllabus in bachelor's degree. Most of these countries do not have doctoral program in medical physics. On the other hand, some universities are beginning to consider to start medical physics postgraduate (Master's degree) coursework program as per international recommendation.

International Atomic Energy Agency (IAEA) through the Regional Technical Cooperation project in Asia Pacific (RAS6038), conducted the pilot project to initiate the clinical residency program in SEAFOMP countries, as presented in Table 3. In this project, Thailand, Philippines, Malaysia and Singapore participated with 30, 12, 14 and 3 residents, respectively. The residency clinical training program was coordinated by external coordinator who was appointed by the IAEA. These clinical residency program followed the IAEA Training Course Series (TCS) publication 37, 47, and 50. In the end of the project, 51 residents have successfully graduated from the program. Subsequently, the pilot project was continued through the new project RAS6077. This new program also followed the IAEA TCS, however it was translated to e-learning system called the Advanced Medical Physics Learning Environment (AMPLE). This e-learning system provides the possibility for residents to submit their work and the supervisor to grade their work. Table 3 also presents the data on countries that had taken part in the pilot project.

Table 2. Profile of Medical Physics Post-graduate Education (master degree and doctoral) in SEAFOMP countries

Country	No. Univerities	Estimated students /year	Qualification
Brunei	None	-	-
Cambodia	None	-	-
Indonesia	4	40	MSc, PhD
Malaysia	2	30	MSc, PhD
Myanmar	None	-	-
Philihines	1	12-15	MSc
Singapore	None	5	PhD
Thailand	3	30	MSc, PhD
Vietnam	None	-	-

Table 3. Pilot projects in medical physics clinical residency program through RAS6038 and RAS6077

Country	Start year	No. Enrolled RAS 6038 +(RAS6077)	No. Graduated
Brunei	None	None	None
Cambodia	None	None	None
Indonesia	2016	0+ (7)	None
Malaysia	2010	14+(0)	6
Myanmar	2016	0+(2*)	None
Philippines	2009	12 + (51)	12
Singapore	2015	3 +(0)	3
Thailand	2007	30 +(29)	30

| Vietnam | 2016 | 0 +(1*) | None |

*Residents of Mnyamar and Vietnam are registered in AMPLE under remote supervision by medical physicists from Thailand through RAS6077 IAEA project

2.3 Profile of Medical Physics Recognition in SEAFOMP countries

Formal recognition of medical physicists has been a major task of the SEAFOMP leadership. Numerous efforts and activities have been implemented to raise the profile of medical physics in the region. The result of the survey on formal recognition is presented in Table 4. It describes that only 5 out of 9 countries have included medical physics profession in the scope of their national regulation. It means that the recognition of medical physics profession in SEAFOMP is less than 60% of all members. This is proven to be a major challenge, underlining the need of medical physics societies at SEAFOMP countries to enhance their efforts in communicating with their governments/regulators.

Table 4 also indicates that the certification status of clinical medical physicist in the region reflects the state of recognition. On the other hand, the registration of medical physics profession has just been established in Indonesia; and Malaysia has recently begun to register the medical physicists working in clinical setting. The registration of medical physics profession in Indonesia and Malaysia are similar; both are performed under a council of allied health profession under the Ministry of Health. The clinical medical physicists who have registered as the allied health profession are required to collect a designated credit points from activities related to continuing medical education (CME). By regulation, the re-registration of clinical medical physicist in Indonesia has also been implemented in 2017. The formal requirements for re-registration of clinical medical physicists was stated by the professional society (Indonesian Association of Physicists in Medicine).

Table 4. Medical Physics recognition in SEAFOMP countries

Country	Recognition	Certification	Registration
Brunei D	Yes, Gov	None	none
Cambodia	None	None	none
Indonesia	Yes, Gov. Law 36/2014	Gov & Society	Council of Allied Health Prof. (MOH)
Malaysia	Yes, Ministry of Health (MOH)	Allied Health Professions, MOH	Allied Health Professions, (MOH)
Myanmar	None	None	none
Philippines	Yes, MOH	Society	none
Singapore	Yes, MOH	None	none
Thailand	Yes	Society	none
Vietnam	None	None	none

Table 1 to Table 4 express the gap in the medical physics infrastructure among nine SEAFOMP countries.

Five have not started the medical physics education at postgraduate level as per international recomendation. Therefore it is a challenge for SEAFOMP to support and encourage the countries like Cambodia, Myanmar, Vietnam and Brunei to start the formal medical physics education program. On the other hand, Singapore offers their program as elective course in bachelor's and doctoral degree in physics because the demand of medical physcists in the country is relatively low. Most positions of medical physicists in Singapore are filled by medical physcists who are graduated from overseas.

2.4 Capacity Building of Medical Physics Activities in the Region

In order to promote scientific exchange and mutual support in the region, SEAFOMP has organized a series of congresses since her formation. SEAFOMP congresses have been held annually since its inception and these congresses have stimulated much growth and progress in medical physics in the region. The history of SEAFOMP and her role in ASEAN has been well documented [5,6].

The South East Asian Congress of Medical Physics (SEACOMP) series were held respectively in Kuala Lumpur (2001), Bangkok (2003), Kuala Lumpur (2004), Jakarta (2006), Manila (2007), Ho Chi Minh City (2008), Chiang Mai (2009), Bandung (2010), Manila (2011), Chiang Mai (2012), Singapore (2013), Ho Chi Minh City (2014), Yogyakarta (2015), and Bangkok (2016). The next SEACOMP is planned to be held at Ilo-Ilo, Philippines on 1-3 December 2017.

Furthermore, the ASEAN College of Medical Physics (ACOMP) has been launched on 24 October 2014 at the 14th SEACOMP in Ho Chi Minh City, Vietnam [7]. The vision of ACOMP is to make it the premier education and training centre for medical physics in ASEAN region and beyond. The first activity of ACOMP was held in Malaysia on 11-14 November 2015 in conjuction with the AAPM/ISEP workshop on Medical Imaging. The second activity was held at Kuala Lumpur, Malaysia on 5-6 August 2016 with focous on Safety, Optimization, Dosimetry and Quality Control in Interventional Radiology. The third activity was held in conjuction with the 13th SEACOMP on 10 December 2015 at Yogyakarta, Indonesia. Recently, the forth activity was held in conjunction with the International Conference on Medical Physics (ICMP) at Bangkok, Thailand on 11 December 2016. The next upcoming ACOMP event will be the "School on Monte Carlo" from 10 - 14 July 2017, which is organized by the Institut Teknologi Bandung, Indonesia in collaboration with Indonesian Association of Physicists in Medicine. Beside the congresses and ACOMP activities, the medical physics capacity building in the region has been initiated to enhance the academic environment, such as external examiner exchange for master thesis and the students exchange.

In order to establish the scientific achivement in the region, the committees have also initiated joint research or

publication for two or more institutions to produce the scientific papers and publish in high impact journals. For example, the collaboration activity has been initiated between Universitas Indonesia with University of Malaya and Katholieke Universiteit Leuven. In addition, Institut Teknologi Bandung has also intiated collaborations between California State University and University of Kyushu to work together on joint research and publication.

To enhance the achievements of medical physics development in the region, the committee planned to establish an exchange program for external assesors of clinical residency program; sharing clinical supervisors among SEAFOMP residents; enhancing ACOMP activity as continuing professional development; and establishing travel grant schemes for young medical physicists to attend the regional medical physics activities.

III. CONCLUSIONS

The recognition of medical physics profession in SEAFOMP countries varies according to the respective governments. Although such recognition is still less than 60% (out of nine countries), the number and scale of activities for medical physicists, nationally or regionally, has been increasing and proven to be a channel to accelerate the recognition in all SEAFOMP countries. SEAFOMP is now paying special attention to advance the development of medical physics profession in the region, especially for Vietnam, Cambodia, Myanmar and Brunei Darussalam.

IV. REFERENCES

1. Official Website for Association South East Asian Nations. Available at www.Asean.org. Retrieved on 27 February 2017
2. Official website for South East Asian Federation of Organizations for Medical Physics (SEAFOMP). Available at www.seafomp.org. Retrieved on 27 February 2017
3. S. Eav, S. Schraub, P. Dufour, D. Taisant, C. Ra, P. Bunda. Oncology 2012;82:269–274
4. Tomas Kron, H. A. Azhari, E. O. Voon, et al. Medical physics aspects of cancer care in the Asia Pacific region: 2014 survey results. Australas Phys Eng Sci Med (2015) 38:493–501
5. K Ng, R Pirabul, A Peralta, D Soejoko. Medical physics is alive and well and growing in South East Asia. Australas Phys Eng Sci Med. 1997;20(1):27-32.
6. KH Ng, JHD Wong. The South East Asian Federation of Organizations for Medical Physics (SEAFOMP) - Its History and Role in the ASEAN Countries. Biomed Imaging Interv J 2008; 4(2):e21
7. The ASEAN College of Medical Physics (ACOMP) – The first two years (to be published in the same issue of MPI)

Contacts of the corresponding author:

Author: Supriyanto Ardjo Pawiro
Institute: Department of Physics, FMIPA Universitas Indonesia
Street: Kampus UI
City: Depok
Country: Indonesia
Email: supriyanto.p@sci.ui.ac.id

ANNEX

The list of postgraduate program in Medical Physics at SEAFOMP countries

Country	University Name	Person in Charge	Website and contact
Indonesia	Universitas Indonesia	Dr. Supriyanto Ardjo Pawiro	http://magister.fisika.ui.ac.id Email: supriyanto.p@sci.ui.ac.id
	Diponegoro University	Dr. Wahyu Setia Budi	http://www.mif.undip.ac.id/ Email: wahyu.sb@fisika.undip.ac.id
	Bandung Institute of Technology	Dr. Freddy Haryanto	http://www.fi.itb.ac.id Email: freddy@fi.ui.ac.id
	Brawijaya University	Dr. Johan Noor	http://fisika.ub.ac.id Email: jnoor@ub.ac.id
Philippines	University of Santo Tomas	Agnette Peralta, MSc	http://graduateschool.ust.edu.ph/wp-content/uploads/2014/10/medphysics_2015.pdf Email : apperalta2004@yahoo.com
Malaysia	University of Malaya	Dr. Jeannie Hsiu Ding Wong	https://www.um.edu.my/academics/master/medicine/master-of-medical-physics Email : jeannie.wong@ummc.edu.my
	Universiti Sains Malaysia	Dr. Norlaili Ahmad Kabir	http://www.ips.usm.my/index.php/article-coursework/190-master-of-science-medical-physics Email: norlailikabir@usm.my
Thailand	Chulalongkorn University	Dr. Anchali Krisanachinda	http://w.md.chula.ac.th/radiology/program/program.php Email: kanchali@chula.ac.th
	Mahidol University	Dr. Puangpen Tangboonduangji	www.grad.mahidol.ac.th Email: raptb@mahidol.ac.th
	Chiang Mai University	Dr.Narongchai Asavapromporn	http://www.med.cmu.ac.th/dept/radiology/Rad/learn.htm Email: nncnchawapu@mail.med.cmu.ac.th

THE ASEAN COLLEGE OF MEDICAL PHYSICS (ACOMP) –
THE FIRST TWO YEARS

K. H. Ng[1], A.P. Peralta[2], A. Krisananchinda[3], S. Suriyapee[3], D.S. Soejoko[4], J.C.L. Lee[5], N. T. Tran[6],
N.T. Chau[7], F. Haryanto[8], S.A.Pawiro[4], C.H. Yeong[1], N. Jamal[9], M.R.Z. Tecson[10], S. Chhom[11]

[1] Department of Biomedical Imaging, University of Malaya, Kuala Lumpur, Malaysia
[2] Office for Health Regulation, Department of Health, Manila, Philippines
[3] Department of Radiology, Chulalongkorn University, Bangkok, Thailand
[4] Physics Department, University of Indonesia, Jakarta, Indonesia
[5] Division of Radiation Oncology, National Cancer Centre, Singapore
[6] Department of International Cooperation, VINATOM, Hanoi, Vietnam
[7] Unit of PET-CT & Cyclotron, Cho Ray Hospital, Ho Chi Minh City, Vietnam
[8] Physics Department, Bandung Institute of Technology, Bandung, Indonesia
[9] Planning and International Relation Division, Malaysia Nuclear Agency, Bangi, Malaysia
[10] Medical Physics and Health Physics Services, Inc, Manila, Philippines
[11] National Cancer Centre, Calmette Hospital, Phnom Penh, Cambodia

Abstract— **The Association of Southeast Asian Nations (ASEAN) formed on August 8, 1967, is a geo-political and economic organization of 10 countries: Brunei, Cambodia, Indonesia, Laos, Malaysia, Myanmar, Philippines, Singapore, Thailand and Vietnam. The idea of forming the South East Asian Federation of Organizations for Medical Physics (SEAFOMP) was first conceived in 1996 and she was officially accepted as a regional chapter of the International Organization of Medical Physics (IOMP) during the Chicago World Congress in 2000. Another regional organization, the ASEAN College of Medical Physics (ACOMP), was born in October 2014 at the 12th Southeast Asian Congress of Medical Physics held in Ho Chi Minh City, Vietnam. The founding chairman of the College is Professor Kwan Hoong Ng. The secretariat is located in Jakarta, Indonesia. The vision is to make the ACOMP the premier education and training centre for medical physics in ASEAN and beyond. To achieve this vision, members will galvanise their talents to develop sustainable activities. For the first two years, four activities have been successfully organized including topics such as imaging physics, digital radiography, and interventional radiology. Some future activities planned include schools on Monte Carlo simulation, advanced radiation dosimetry, radiation emergency and disaster management, non-ionizing radiation protection, and a project on radiation dosimetric inter-comparison.**

Keywords— **Education and training, medical physics organization, professional development**

I. INTRODUCTION

Medical physics is rapidly advancing in the world and the situation is the same in South East Asia. Medical physicists have played a pivotal role in the development of new technologies that have revolutionized the way medicine is practiced today. They have been transforming scientific advances in the research laboratories to improving the quality of life for patients [1-2].

II. ABOUT ASEAN

The Association of Southeast Asian Nations commonly known as ASEAN is a geo-political and economic organization of 10 countries located in Southeast Asia, which was formed on August 8, 1967. The member countries are Brunei, Cambodia, Indonesia, Laos, Malaysia, Myanmar, Philippines, Singapore, Thailand and Vietnam. The motto of ASEAN is "One Vision, One Identity, One Community". Its aims include the acceleration of economic growth, social progress, cultural development among its members, and the promotion of regional peace [3].

Figure 1: Map of South East Asia.

It is interesting to compare some aspects of ASEAN and European Union (EU) [4,5] The total land area of ASEAN is 4,479,210 km^2 while that of EU is 4,381,376 km^2. The estimated population of ASEAN is 608 million (2012) while that of EU is 507 million (2014). However, EU has 24 'official and working' languages while ASEAN has adopted one 'official' language, namely English.

The SEA-EU-NET has been formed to foster cooperation in science, technology and innovation (STI) between Europe and Southeast Asia. Strategic opportunities for S&T cooperation have been identified, and there is opportunity to participate in the European Union's Horizon 2020 Framework Programme for Research and Innovation. [6]

III. SOUTH EAST ASIAN FEDERATION OF ORGANIZATIONS FOR MEDICAL PHYSICS (SEAFOMP)

The idea of setting up an organization for Southeast Asian medical physics societies was first conceived in 1996. During the International Organization of Medical Physics (IOMP) World Congress in Nice, the formation of S the South East Asian Federation of Organizations for Medical Physics (SEAFOMP) was endorsed by member countries and it was officially accepted as a regional chapter of the IOMP at the Chicago World Congress in 2000 [7]. SEAFOMP congresses have been held regularly since its inception and these congresses have stimulated much growth and progress in medical physics in the region. The history of SEAFOMP and her role in ASEAN has been well documented [8,9]. SEAFOMP members have been actively collaborating with international organizations such as the American Association of Physicists in Medicine (AAPM), Australasian College of Physical Scientists and Engineers in Medicine (ACPSEM), Institute of Physics and Engineering in Medicine (IPEM), Asia Oceania Federation of Organizations for Medical Physics (AFOMP), IOMP, International Atomic Energy Agency (IAEA), World Health Organization (WHO), International Commission on Non-Ionizing Radiation Protection (ICNIRP), and Abdus Salam International Centre for Theoretical Physics (ICTP) in hosting and organising conferences, workshops and courses.

IV. BIRTH OF THE ASEAN COLLEGE OF MEDICAL PHYSICS (ACOMP)

After a long gestation period, another regional organization, the ASEAN College of Medical Physics (ACOMP) was born on October 23th- 25th, 2014 at the 12th Southeast Asian Congress of Medical Physics in conjunction with the 14th Asia-Oceania Congress of Medical Physics held in Ho Chi Minh City, Vietnam. SEAFOMP EXCOM unanimously elected Professor Kwan Hoong Ng, president-emeritus of the SEAFOMP as the founding chairman of the College.

Figure 2. Some of the authors who were present during the SEAFOMP council meeting held in HCM City, Vietnam on Oct 25, 2014.

The secretariat is located in Jakarta, Indonesia. We hope to emulate the successful models of the AAPM and EFOMP summer schools.

The vision is to make the ACOMP the premier education and training centre for medical physics in the ASEAN region and beyond. Both physical and virtual campuses are being established. Emphasis will be placed on supporting the lesser developed countries.

The objectives of the ACOMP are to:

• enhance the standard and quality of education and training of medical physicists,

• provide continuing professional development (CPD) programmes, and

• promote the continuing competence of practitioners of medical physics.

V. THE FIRST TWO YEARS

First workshop organized by ACOMP - "AAPM/IOMP/ISEP Imaging Physics Workshop", 11-14 Nov 2015 at Kuala Lumpur, Malaysia

A four-day international imaging physics workshop entitled "AAPM/IOMP/ISEP Imaging Physics Workshop 2015" was held at the Armada Hotel, Petaling Jaya, Malaysia, from 11 - 14 November 2015. The workshop was jointly organized by the Medical Physics Subgroup of Institute of Physics, Malaysia and University of Malaya, Kuala Lumpur, in collaboration with International Scientific Exchange Program (ISEP) of the American Association of Physicists in Medicine (AAPM). The workshop was endorsed by the International Organization of Medical Physics (IOMP) and supported by multiple local and international professional bodies, including Southeast Asian Federation of Organizations for Medical Physics (SEAFOMP), ASEAN College of Medical Physics (ACOMP), Malaysian Association of Medical Physics (MAMP), Malaysian College of Radiology (MCOR), Malaysian Oncological Society (MOS) and Malaysian Society of Radiographers (MSR).

For the first time being held in Malaysia, the workshop hosted six world-leading medical physicists from the AAPM including Professor Cheng B Saw (the Chair of ISEP), Professor John M Boone (President of the AAPM), Professor Geoffrey D Clarke (UT Health Sciences Centre, Texas, USA), Professor Michael O'Connor (Mayo Clinic, Minnesota, USA), Associate Professor Dr. Jihong Wang (MD Anderson Cancer Centre, Texas, USA) and Associate Professor Dr. Aaron Kyle Jones (MD Anderson Cancer Centre, Texas, USA). The members of the faculty also include three distinguished speakers from the Ministry of Health, Malaysia. They are Mr. Zunaide B. Kayun @Farni (Deputy Director, Radiation Health and Safety Section), Mr. Nik Mohamed Hazmi Bin Hj Nik Hussain (Deputy Director, Allied Health Science Division) and Mr. Ahmad Shariff Bin Hambali (Deputy Director, Medical Device Authority).

Figure 3. A group photo taken during the opening ceremony of the AAPM/IOMP/ISEP Imaging Physics Workshop at the Armada Hotel, Petaling Jaya, Malaysia on 11-14 Nov 2015.

The workshop was accredited for Continuing Medical Education (CME, approved by the Ministry of Health, Malaysia), Continuing Professional Development (CPD Category A3: 15 credits), Medical Dosimetrist Certification Board (MDCB: 23 credits) and Commission on Accreditation of Medical Physics Education Programs (CAMPEP: 24.5 credits).

The focus of this workshop is towards the needs of the medical imaging professionals, including radiologists, oncologists, medical physicists, medical dosimetrists, radiographers, technologists as well as researchers who are involved in the practice of diagnostic, nuclear and oncologic imaging. A comprehensive program which covered most of the recent medical imaging modalities such as digital radiography, mammography, computed tomography, magnetic resonance imaging (MRI), functional MRI, hybrid nuclear imaging and image-based radiotherapy and treatment planning was conducted. The theme of the workshop was "*Building Foundations for Sound Clinical Practice*". It was hoped that through an enhanced understanding of the fundamental physics in this rapidly growing specialty, the level of expertise in medical imaging can be elevated to improve the healthcare and wellness of the people in our region, said the organizers.

Officiated the opening ceremony was Professor Dr. Awang Bulgiba Awang Mahmud, Deputy Vice Chancellor (Academic & International), University of Malaya. A total of 214 local and international participants attended this workshop, of which, 202 participants were from Malaysia and 12 were from other countries including Australia, Brunei, Indonesia, Philippines, Qatar and Singapore. Among the 214 participants, 32% were medical physicists, 27% radiographers, 20% students, 5% researchers, and 16% of other specialties.

The workshop was also an event to celebrate the 3rd International Day of Medical Physics, which falls on 7th November annually, to commemorate the birthday of Madam Marie Curie, the pioneer in radioactivity discovery.**econd workshop organized by ACOMP - "Workshop on Digital Radiography", 10 Dec 2015 during 13th SEACOMP, Yogyakarta, Indonesia**

The second workshop organized by ACOMP was held during the 13th SEACOMP at Yogyakarta, Indonesia on 10 Dec 2015. The theme of the workshop was on digital radiography. The workshop aimed to review the basic principles, image quality and artifacts, as well as some routine quality control (QC) tests in digital radiography. The speakers included Prof Dr Kwan Hoong Ng (Director of ACOMP), Dr. Napapong Pongnapang (University of Mahidol, Thailand) and Dr. Chai Hong Yeong (University of Malaya, Malaysia). Approximately 40 – 50 participants have attended the workshop.

Figure 4. The first ACOMP Workshop on Digital Radiography, Yogyakarta, Indonesia, 10 Dec 2015.

Third workshop organized by ACOMP - "Interventional Radiology Workshop", 5-6 Aug 2016 at Kuala Lumpur, Malaysia

The two-day workshop on Interventional Radiology: Safety, Optimization, Dosimetry and Quality Control" was held on 5th and 6th August 2016 in Kuala Lumpur. The workshop was jointly organized by the Medical Physics Subgroup of Malaysian Institute of Physics and University of Malaya (UM) in collaboration with ACOMP.

The workshop was endorsed by the Malaysian Ministry of Health (MOH), Malaysian Society of Interventional Radiology (MYSIR) and Malaysian Society of

Radiographers (MSR). Several local organizations, including Malaysian Nuclear Agency (MNA), Continuing Biomedical Imaging Education (CBIE) of University of Malaya, Medical Physics Unit of University of Malaya Medical Centre and University of Malaya Research Imaging Centre (UMRIC) supported the organization of the workshop.

This ACOMP Workshop featured several speakers including Professor Dr. Kwan Hoong Ng (ACOMP Director), Professor Dr. Basri Johan Jeet Abdullah (Consultant Interventional Radiologist, UMMC), Associate Professor Dr. Khairul Azmi Abdul Kadir (Head of the Department of Biomedical Imaging, UM), Assistant Professor Dr. Napapong Pongnapang (Mahidol University), Dr. Jeyaledchumy Mahadevan (President of MYSIR), Dr. Noriah Jamal (Director, Planning and International Relations, MNA), Mr. Zunaide B. Kayun (Deputy Director, Radiation Health and Safety Section, MOH), Dr. Jeannie Hsiu-Ding Wong (UM) and Dr. Chai-Hong Yeong (UM). The members of the faculty also include two speakers from UMMC, Mr. Mohammad Mudzakir Zainal Alam (Senior radiographer) and Ms. Noorhaniza Abu Hassan (Staff nurse).

A total of 64 local and international participants from six countries (Malaysia, Brunei, Indonesia, Qatar, Philippines and Australia) attended this workshop.

This workshop aimed to provide the latest updates on radiological safety, optimization, dosimetry and quality assurance related aspects in the field of interventional radiology. The program was designed such that the first day of the workshop was focusing on the physical principles and theory of multiple aspects in interventional radiology. Various expertises included interventional radiologists, radiographers, nurses, medical physicists and regulators have been invited to share their perspectives. The second day of the workshop was dedicated to practical / hands-on sessions, which was held at the Department of Biomedical Imaging, UMMC. Three modalities including two C-arm angiography systems (one biplane, one single plane) and a radiography/fluoroscopy system were used for the practical sessions. The topics for hands-on sessions included (1) patient dosimetry and measurement, (2) occupational dose assessment and radiation protection, and (3) quality control tests of the fluoroscopy systems.

Forth workshop organized by ACOMP - "Workshop on Digital Radiography", 11 Dec 2016 during ICMP2016, Bangkok, Thailand

The forth ACOMP workshop was held during the International Conference of Medical Physics (ICMP) at Bangkok, Thailand on 11 Dec 2016. The theme of the workshop focuses on the physical principles, image quality and quality control (QC) tests in digital radiography (DR).

Figure 5. Local organizing committee members and invited speakers.

Figure 6. Some of the workshop invited speakers, facilitators and participants in a relaxing moment.

Figure 7. Hands-on sessions on interventional radiology quality control and radiation safety.

DR is rapidly been developed in the last decade and has been gradually replacing computer radiography (CR) in many countries. It offers the potential for improved image quality and provides opportunities for advances in medical image management, computer-aided detection and teleradiology. This workshop aimed to provide comprehensive information on the physical principles and

instrumentation of DR. The main optimization techniques such as the use of automatic exposure control (AEC) and exposure index (EI) were discussed. The workshop also emphasized the physical QC tests in DR where image quality and artifacts were highlighted.

The workshop has attracted some 20 participants from ASEAN and other countries. The members of faculty included Prof. Dr. Kwan-Hoong Ng (Director of ACOMP) and Dr. Chai-Hong Yeong (University of Malaya, Malaysia).

Figure 8. ACOMP Workshop on Digital Radiography, held during the International Conference of Medical Physics at Bangkok, Thailand, 11 Dec 2016.

VI. THE FUTURE

ACOMP has planned several future activities:
• School on Monte Carlo simulation
• School on advanced radiation dosimetry
 • School on radiation emergency and disaster management
• School on non-ionizing radiation protection
• Regional inter-comparison in radiation dosimetry

To achieve this vision, members will need to galvanise their talents to develop sustainable activities, and will take advantage of information and communications technologies to achieve our goals. .

 ACOMP has been complementing the role of SEAFOMP by giving it an added impetus. We are witnessing rapid growth of medical physics in Southeast Asia [10]. In order to utilize diagnostic, interventional and therapeutic modalities optimally and safely we need to keep abreast and be well-educated and be innovative.

REFERENCES

1. Ng, K.H., *Medical physics in 2020: will we still be relevant?* Australas Phys Eng Sci Med, 2008. **31**(2): p. 85-9.
2. Ng, K.H., *Medical Physics in Asia — Where are we going?* Australas Phys Eng Sci Med, 2008. **31**(4): p. xi-xii.
3. Official website for Association of Southeast Asian Nations (ASEAN). Available at www.asean.org. Retrived on 31 Jan 2017.
4. Official website for European Union. Available at www.europa.eu. Retrieved on 31 Jan 2015.
5. Eurostat. Available at ec.europa.eu/eurostat. Retrieved on 31 Jan 2017.
6. http://www.sea-eu.net. Retrieved on 31 Jan 2017.
7. Official website for South East Asian Federation of Organizations for Medical Physics (SEAFOMP). Available at www.seafomp.org. Retrieved on 31 Jan 2017
8. K Ng, R Pirabul, A Peralta, D Soejoko. Medical physics is alive and well and growing in South East Asia. Australas Phys Eng Sci Med. 1997;20(1):27-32.
9. . KH Ng, JHD Wong. The South East Asian Federation of Organizations for Medical Physics (SEAFOMP) - Its History and Role in the ASEAN Countries. Biomed Imaging Interv J 2008; 4(2):e21
10. Kron T, Azhari HA, Voon EO, et. al. Medical physics aspects of cancer care in the Asia Pacific region: 2011 survey results. Biomed Imaging Interv J 2012, 2: e10

Corresponding author:

Author   : K.H.Ng
Institute : Department of Biomedical Imaging , Faculty of Medicine
Street   : University of Malaya, 50603
City   : Kuala Lumpur
Country : Malaysia
Email   : ngkh@ummc.edu.my

MEDICAL PHYSICS EDUCATION AND TRAINING IN BRAZIL: CURRENT SITUATION AND FUTURE DEVELOPMENT

Camila S. Melo[1], Larissa C.G. Oliveira[2] and Paulo R. Costa[1]

[1]Instituto de Física da Universidade de São Paulo, Grupo de Dosimetria das Radiações e Física Médica, São Paulo, Brazil
[2]Instituto de Radioproteção e Dosimetria (IRD/CNEN), Rio de Janeiro, Brazil

Abstract — The evolution of technologic applications in Medicine has been guided by concepts and methods of Physics and Engineering in the last century. The constant interaction among Physics professionals has been reinforced in activities related to health sciences, that is a characteristic of the Medical Physicist. The Medical Physics area in Brazil has been experiencing a period of growth and development, due to the increasing access to medical technology and its importance to diagnostic and treatment procedures. The Brazilian Health Authorities at the National Cancer Institute (INCA) estimate that approximately 600,000 new cancer cases will be diagnosed in 2016 – 2017 in Brazil. Therefore, the growing importance of early diagnostic and treatment of diseases such as cancer raises the need for qualified Medical Physicists. These professionals assist to ensure the quality of the facilities, equipment and treatment plans used in the health systems. In recent years, Brazil had the initiative to expand Medical Physics graduate and undergraduate programs and clinical training. Moreover, the government is investing in new equipment and creating regulatory standards for minimum quality maintenance of health services in the country. In the present work, an analysis of the Medical Physics status in Brazil was performed. It included the education, the Diagnostic Imaging equipment, training programs, the current mandatory national standards and perspectives for the development of the Medical Physics profession in Brazil.

Keywords — **Medical Physics, Education, Training, Professional qualification.**

Figure 1: The five regions and 26 states and one Federal District of Brazil[6].

I. INTRODUCTION

The Brazilian territory is geographically divided in five regions (North, Northeast, Midwest, Southeast and South) with 26 States and one Federal District where the capital is situated, Brasília (Figure 1)[1]. The country has an area of 8.515.767.049 km², a population of 24.66 people per square kilometer (62 per square mile)[1,2] and present a 1.774.72 billion of Gross Domestic Product (GDP)[3].

The National Cancer Institute (INCA) estimates approximately 600,000 new cancer cases will be diagnosed in 2016-2017 in Brazil[4]. Therefore, it is evident the importance of early diagnoses and treatment, which consequently, raises the need for qualified Medical Physicists to assist on the quality improvement of the diagnostic facilities and treatment centers[5].

An important step in this direction was the approval of Brazilian 11.129/2005 bill and the 1077/2009 regulation, which created the multidisciplinary residences in the professional field of health. As a consequence, new sites for training in different Medical Physics areas have been opened. In addition, the Ministry of Health recently announced the acquisition of 80 linear accelerators that would be distributed to attend the population of 63 cities around the country[7].

Hence, the need for qualified Medical Physicists has been growing in some areas in recent years. Consequently, the Brazilian education system has expanded as well as the Medical Physics career opportunities.

The aim of this study was to analyze the status of the education and training programs in Medical Physics in Brazil. In addition, the current mandatory national standards, the approximate number of Diagnostic Imaging equipment and perspectives for the development of the Medical Physics profession in Brazil are presented.

II. EDUCATION AND TRAINING PROGRAMS

Costa P.R[8] previously published a data survey regarding undergraduate, graduate, and clinical training levels in Medical Physics up to 2012. The present work will show a summary of these results and some updated information.

Undergraduate courses

The first undergraduate Medical Physics course established in Brazil started its activities in 1990. Eleven undergraduate programs were found in operation in the country up to 2012 and an estimated offer of 400 enrollment admissions per year[8].

The formal average duration of these undergraduation programs is 4.5 ± 0.5 years and the compulsory internship (practical/clinical training activities) differ between 0 to 720h[8]. This data is still representative, since the total number of undergraduate programs in Brazil remained eleven, as shown in Table 1, and no major changes have been identified in their curriculum grid.

Table 1: Universities with Medical Physics undergraduate courses in Brazil

Universities with Medical Physics undergraduate courses	Region	Initial Year
Pontifícia Universidade Católica do Rio Grande do Sul (PUCRS)	South	1990
Faculdade de Filosofia, Ciências e Letras de Ribeirão Preto (USPRP)	South east	2000
Centro Universitário Franciscano (UNIFRA)	South	2000
Universidade Federal de Sergipe (UFS)	North east	2001
Universidade Federal do Rio de Janeiro (UFRJ)	South east	2002
Universidade Estadual de Campinas (UNICAMP)	South east	2003
Universidade Estadual Paulista "Júlio de Mesquita Filho" - Campus de Botucatu (UNESP)	South east	2003
Centro Universitário da Fundação Educacional de Barretos (UNIFEB)	South east	2008
Universidade Federal de Uberlândia (UFU)	South east	2010
Universidade Federal de Goiás (UFG)	Midw est	2013
Universidade Federal de Ciências da Saúde de Porto Alegre (UFCSPA)	South	2014

Graduate courses

Thirteen Institutions with graduate programs in Physics with areas of concentration in Medical Physics or related fields were found in the previously published work corresponding to 140 opportunities for MSc, 93 to PhD and 23 direct-PhD[8]. The data on postgraduate studies remains uncertain nowadays, due to the lack of programs dedicated to Medical Physics, researches go into correlated areas such as Nuclear or Solid State Physics, even in other areas such as engineering and applied science to obtain their MSc and PhD titles.

The only significant novelty in this category of professional qualification since 2012 was the creation of the first Medical Physics professional master's degree at State University of Rio de Janeiro (UERJ). This program aims at training physicists in the Radiotherapy area[9].

Clinical Training programs

In Brazil, these programs are named "Residency Programs" and it has a minimum of 1152 hours of in classroom didactical instruction and at least 4608 hours of practical training determined by law. Nowadays, these programs offered 23 positions per year in the Radiotherapy area (RT), 2 positions in Nuclear Medicine (NM) and 9 positions in Diagnostic Radiology (RD), with 65% concentrated in the southeast region of the country.

There are other similar programs named "Professional Development Programs" with less hours of didactical instruction (~522 hours[8]) and practical training (~3396 hours[8]). These programs provided 3 positions in the Radiotherapy area and 1 in Nuclear Medicine, each position located in three different regions of the country (Northeast, southeast and Midwest).

III. CERTIFICATION IN MEDICAL PHYSICS AREA AND PROFESSIONAL CAREER

There are currently two categories of certifications for Medical Physicists in Brazil: (1) **Radiation Protection Supervisor - RPS** provided by the National Commission of Nuclear Energy (CNEN) and (2) **Specialist Certificate** provide by the Brazilian Association of Medical Physics (ABFM).

The recommendations for obtaining the Radiation Protection Supervisor certificate follow the regulation established in CNEN NN 7.01[10]. In order to be able to apply for the examination to become a SPR, the candidate must demonstrate at least 350 hours of experience in Radiotherapy and 200 hours in the area of Nuclear Medicine[10]. There is a total of 739 certified RPSs (295 in Nuclear Medicine and 444 in Radiotherapy) currently in Brazil, as shown in Figures 2 and 3[11]. It was possible to observe that the southeast region is the region with the highest number of supervisors (273 for RT and 165 for NM).

Figure 2: Regional distribution of Radiotherapy RPS [11].

Figure 3: Regional distribution of Nuclear Medicine RPS [11].

Nowadays, it is necessary a minimum experience of 3800 hours in the chosen area (initiated after the undergraduate program be concluded) in order to comply to the ABFM specialist certificate[12]. Currently, according to ABFM[12], there are 306 specialists in RT, 82 in RD and 42 in NM, distributed over the geographical regions of the country (Figure 4). It can be highlighted the predominance of certified physicists in the southeast region.

The Brazilian Association of Medical Physics (ABFM) was founded in 1969 by approximately 9 physicists and since then the number of members has increased considerably. The emergence of other undergraduate courses in medical physics, national congresses and specialist certification, the average membership increased from 8 per year until 1990 to 30 (up to 2001) and 54 (up to 2016). Currently, ABFM officially has 1345 active members. The temporal growth of ABFM members is shown in Figure 5.

Figure 4: Regional distribution of ABFM Certified Medical Physicists[12].

Figure 5: Temporal growth of ABFM members between 1969 to 2017.

Completing undergraduate, residency/training programs and certifications, the professional career can initiate in hospitals, clinics, and companies. Except for Radiotherapy, the recruitment of medical physicists as hospital staff is not a common practice, but over the past few years some vacancies have been opened in public hospitals for certified physicists, It is a common practice Medical Physicists create their own company and provide services to hospitals and clinics in the RT, RD and MN area. Otherwise, there are also vacancies in multinational companies for Medical Physicist positions that can diversify a lot, such as in software development, clinical applications support, product sales, product manager and others. Students of Medical Physics and/or Physics who continued their studies in postgraduate courses normally pursuit an opportunity in academic career.

IV.EQUIPMENTS IN BRAZIL

The technological base in Brazil has approximately 175000 Diagnostic Imaging equipment (data from private and public hospitals), being 89% in activity and 11% still without operational requirements (Annex A)[13]. Among the active equipment, 71% are in the private sector reflecting the greater investment of the private sector over the years. The percentage of no operational equipment in the public sector is approximately 5% and may be due to the installation cost of new equipment purchased or donated and maintenance of the broken devices.

The Southeast region concentrate 45% of the total equipment in use. This data highlights the great

technological base of the southeast region and justifies the high concentration of Medical Physics specialists in this area.

In addition to the officially registered equipment data, shown in Table 2, there are no official numbers available of treatment equipment in 236 radiotherapy facilities and 432 nuclear medicine facilities authorized by CNEN across the country[14].

It is important to emphasize that most of metropolitan areas it is possible to find updated technologies for diagnostic and treatment (DR, tomosynthesis, dual energy CT, IGRT, IMRT, radiosurgery, SPECT, PET-CT and PET-RM). Investigative technology, such as non-invasive biopsies with a 7T magnetic resonance imaging and a micro-PET imaging for the non-invasive, quantitative and repetitive imaging of biological function in living animals have also been used[15].

V. NATIONAL STANDARDS

The quality of installations and equipment in Brazilian health system and the safety of patient and workers are assured by the compliance of mandatory national standards. These standards were published by the National Commission of Atomic Energy (CNEN), the Ministry of Health (MS), the Department of Health Surveillance (SVS), the Ministry of Labour (ML), and the National Health Surveillance Agency (ANVISA).

The CNEN is responsible for establishing standards and regulations in radioprotection and regulating, licensing and supervising the production and use of nuclear energy in Brazil. The current regulations in the country cover the topic about Radiation Protection, Licensing of Radiating Facilities, Transport of Radioactive Materials, Requirements for Registration of Individuals for the Preparation, Use and Handling of Radioactive Sources and Management of Radioactive Rejection[16].

The MS/ANVISA created a National Guidelines for Radiation Protection in Medical and Dental Diagnostic Radiology (453/1998 regulation)[17] and a National Quality Program in Mammography (PNQM)[18].

The ML has a standard covering Safety and Health at work in health services. Ensuring those who work with Ionizing Radiation must have the proper training and monitoring.

In spite of several published national standards, there is a lack of more complete guides for quality control tests and respective reference levels. Therefore, it is a common practice Brazilian Medical Physicists base their quantitative evaluation of quality and dosimetric data on consult IAEA, ICRP, NCRP and AAPM publications.

VI. PERSPECTIVES OF THE DEVELOPMENT OF THE MEDICAL PHYSICIST PROFESSION AND NEEDS FOR THE NEXT 20 YEARS

The authors invited experienced Medical Physicists, all ABFM ex-presidents, to manifest their opinions regarding their point-of view regarding the perspectives of the development of the Medical Physics profession and the need in this field for the next 20 years. Ten professionals have replied to this request. The next paragraphs reflect a summary of these important opinions.

The recent classification of Medical Physics as a health profession by the MS was highlighted as a milestone according to the contributors. This classification allowed introduction of new residences programs in Medical Physics around the country. Many of these programs are nowadays supported and recognized by the Ministry of Health and Ministry of Education. Consequently, education and training has been improved and the number of certified medical physicists increased.

The Medical Physicists certification conducted by CNEN and ABFM are well-established processes, and they represent a fundamental stage for the professional development in Medical Physics. Additionally, the compulsory incorporation of certified radiotherapy and nuclear medicine professionals also reinforce the radiation protection culture. Although, ABFM certification be not mandatory, it have demonstrated be a differential qualification in the professional careers.

The contributors also highlighted that the country has an important technological base. It ensure the access to state-of-art technologies available in the major health facilities in the world. Therefore, the country is a reference in Latin America, in special in radiotherapy. In addition, recent investments in new linear accelerators equipment represents a positive perspective to the consolidation of Medical Physics profession. IAEA cooperative projects and training programs offered by manufacturers on new technologies also encourage the fortification of the profession.

The introduction of undergraduate and graduate Medical Physics courses and the consolidation of the residence programs allowed a satisfactory number of professionals in different working areas. Some of the contributors understand that the number of trained professionals currently meets the market requirement, and the number of new jobs may be lower than the number of the graduated/certified professionals in the next few years. It is difficult to consider all economical, educational and strategic aspects in order to balance adequately these numbers.

VI.CONCLUSIONS

The educational programs and equipment are concentrated in the Southeast region of the country, leading to a greater concentration certified Medical Physicists in this region. This demonstrates a need for investment in educational structure and health systems in order to decentralize these programs in the future, providing better access to medical physics education and professional distribution across the country.

The need of trained and experienced professional led to the consolidation of Residence Programs, as a consequence of the incorporation of the medical Physics as a health profession. Additionally, the certification processes annually offered by recognized institutions reinforces the need of highly qualified personal.

Dedicated Medical Physics graduate programs are not usual in the country few, which hinders entry and discourages students from initiating specific research in this area. This may be slowing major national developments in Medical Physics due to the lack of staff and laboratories dedicated to medical physics research.

The technology base of the country is diverse and contains state-of-art technologies. However, it also has a high concentration in the Southeast region. Quality control and preventive maintenance are deficit in some regions, especially out of the metropolitan centers. The causes widely vary, but the lack of qualified professionals, public policies and investments in these areas aggravate this scenario.

REFERENCES

1. Brazilian Institute of Geography and Statistics: IBGE Census: Brazil [internet]. Rio de Janeiro: Department of Population and Social Indicators. Available from: http://www.ibge.gov.br/home/default.php
2. OECD Environmental Performance Review: Brazil 2015. OECD Publishing, Paris. Available from: http://dx.doi.org/10.1787/9789264240094-en
3. Trading Economics: tradingeconomics.com [internet]. Available from: http://www.tradingeconomics.com/brazil/gdp
4. National Cancer Institute: Estimate 2016 – Cancer Incidence in Brazil. Rio de Janeiro: INCA, 2015. ISBN 978-85-7318-283-5.
5. S. Kodlulovich, L. Vasconcellos de Sá. *Medical Physics Education and Training in Latin America: Current Status and Challenges*. Medical Physics International Journal. 2013; 1(1):29-33.
6. Tourist Attractions in Brazil [internet / Modified]. Available from: http://www.brazilmycountry.com/tourist-attractions-in-brazil/
7. National Cancer Institute: Ministry of Health announced the acquisition of 80 linear accelerators. Available from: http://www2.inca.gov.br/wps/wcm/connect/agencian oticias/site/home/noticias/2013/saude_conclui_encomend a_de_oitenta_aceleradores_lineares
8. P.R. Costa. *Overview of medical physics teaching in Brazil*. Res. Biomed. Eng. 2015;31(3):249-256.
9. State University of Rio de Janeiro (UERJ)/ Education Foundation of Cancer [internet]. Available from: http://cancer.org.br/radioterapia/cursos/mestrado-profissional/
10. National Commission of Atomic Energy CNEN-NE-7-01. Certification of the qualification of radiation protection supervisors (Resolução CNEN 194/16). Available from: http://www.cnen.gov.br/certificacao-de-supervisores or http://appasp.cnen.gov.br/seguranca/normas/pdf/Nrm701.pdf
11. National Commission of Atomic Energy (CNEN) [internet]. Available from: http://www.cnen.gov.br/profissionais-credenciados.
12. Brazilian Association of Medical Physics (ABFM) [internet] Available from:http://www.abfm.org.br/index.php?site=prova_titulos_processo.php&m=5&ano_certificado=2017.
13. National Registry of Health Establishments (CNES) [interne]-Department of Informatics – DATASUS [internet]. Available from: http://cnes2.datasus.gov.br/Mod_Ind_Equipamento.asp
14. National Commission of Atomic Energy (CNEN) [internet]. Available from: http://www.cnen.gov.br/instalacoes-autorizadas
15. Folha de São Paulo News [internet]. Available from: http://www1.folha.uol.com.br/equilibrioesaude/2015/03/1 602162-ressonancia-superpotente-da-usp-permitira-autopsia-sem-abrir-cadaver.shtml
16. National Commission of Atomic Energy (CNEN) [internet]. Available from: http://www.cnen.gov.br/
17. Ministry of Health National: Guidelines for Radiation Protection in Medical and Dental Diagnostic Radiology (Ordinance 453/1998). Available from: http://saude.es.gov.br/Media/sesa/NEVS/Servi%C3%A7os%20de%20sa%C3%BAde%20e%20de%20interesse/portaria453.pdf
18. Ministry of Health: National Quality Program in Mammography (PNQM). Available from: http://bvsms.saude.gov.br/bvs/saudelegis/gm/2013/prt2898_28_11_2013.html

Contacts of the corresponding author:

Author: Camila Souza Melo
Institute: Grupo de Dosimetria das Radiações e Física Médica - IFUSP
Street: R. do Matão 1371 St., Butantã
City: São Paulo
Country: Brazil
Email: cmelo@if.usp.br

ANNEX A
Technology Park of Brazil in the area of Imaging Diagnostic

Equipment	North				Northeast				Midwest				South				Southeast			
	Private		SUS		Private		SUS		Private		SUS		Private		SUS		Private		SUS	
	Total	In Use	Total	In Use	Total	In Use	Total	In Use	Total	In Use	Total	In Use	Total	In Use	Total	In Use	Total	In Use	Total	In Use
Computed Mammography	50	49	35	34	175	172	140	138	81	81	42	42	105	103	74	72	269	266	138	136
Mammography (Stereotaxia)	50	46	28	24	205	197	97	91	85	81	25	24	146	143	71	70	391	368	150	138
Mammography	181	164	102	90	858	816	497	468	316	308	131	127	603	586	338	328	1955	1882	782	749
Film Processor	139	134	114	109	681	668	551	541	192	189	159	156	445	442	393	390	1049	1021	821	800
Computed Tomography	220	206	105	99	755	723	438	416	413	399	170	163	742	719	438	424	2000	1953	830	808
Hemodynamic	42	39	23	20	146	138	87	80	77	76	31	30	154	148	85	82	436	428	201	195
Bone Densitometry scanner	82	80	34	33	406	393	192	185	182	174	51	49	344	340	139	136	1050	1036	297	296
Fluoroscopy	42	38	26	23	180	171	114	108	95	84	54	44	293	283	202	195	998	852	467	439
Dental X-Rays	1860	1765	529	486	7720	7380	1985	1842	3472	3318	616	564	10764	8485	1215	1136	25740	24682	4156	3823
X-Rays	1244	1165	811	747	4547	4332	3057	2894	2120	2007	1286	1209	3578	3443	2308	2229	11713	5710	6057	5724
Ultrasound scanner	1253	1196	699	668	5340	5146	3131	3020	1799	1731	843	807	3647	3504	1872	1792	9453	4487	3735	3534
Color Doppler Ultrasound	626	602	246	236	2638	2575	1044	1005	1197	1165	365	352	2309	2237	909	867	6895	6640	2123	2065
Magnetic Resonance Imaging	107	99	57	52	340	328	191	182	178	170	57	54	400	391	222	214	1086	1066	373	366
Gamma camera scanner	53	50	28	27	163	161	93	91	99	96	38	35	150	146	81	79	468	448	210	204
PET/CT	0	0	0	0	7	7	6	6	3	2	2	1	12	12	11	11	20	20	13	13
TOTAL	5949	5633	2837	2648	24161	23207	11623	11067	10309	9881	3870	3657	23692	20982	8358	8025	63523	50859	20353	19290

Region of Brasil

EDUCATION AND CLINICAL TRAINING OF MEDICAL PHYSICS IN THAILAND

A. Krisanachinda[1], S.Suriyapee[1], K. Khamwan[1], T. Sanghangthum[1]

[1] Department of Radiology, Faculty of Medicine, Chulalongkorn University, Bangkok, Thailand

Abstract— **Medical Physics started in Thailand in 1959 at Siriraj Hospital. The education and training was established in 1971. Currently there are 5 programs, one offers the program for international students and Ph.D. in Medical Physics. As IAEA developed the Advanced Medical Physics in e-Learning and Enhancement (AMPLE) using MOODLE platform, Thailand piloted with Thai, Myanmar, Vietnamese and Nepalese residents and Thai Supervisors in diagnostic radiology, radiation oncology and nuclear medicine under the cooperation of Thai Medical Physicist Society (TMPS). Tutorials class and progress in training are set monthly for each program. The completion of competency training will be in 2018.**

Keywords— **education and training, medical physics, e-learning, assessment, assignment.**

I. INTRODUCTION

Medical physics is a profession classified by the International Labor Organization in 2011 [1]. The role and responsibility of the medical physicist refer to medical exposure, patient protection and safety. Specialized education, clinical training and competencies are required for the clinically qualified medical physicist [2]. The recognition of medical physicists remains a challenge [3].

II. EDUCATION AND CLINICAL TRAINING

The academic education program in medical physics provides the student the basic knowledge on a career in the regulatory, metrology, research and development. Further post graduate studies would be necessary to pursue for academic career in medical physics. In Thailand, the education program runs by 5 university hospitals capable of awarding M.Sc. and one for Ph.D. post graduate degree to remain sustainable by offering academic career development pathways. It is ensure the proper access to equipment for clinical practice and research in medical physics. Those university hospitals are listed in table 1.

Table 1 Five university hospitals offered education program

University Name	Hospital	Year	Program
Mahidol	Ramathibodi	1972	M.Sc.(Medical Physics)
Mahidol	Siriraj	1991	M.Sc.(Radiol.Science)
Chiang Mai	Chiang Mai	2001	M.Sc.(Medical Physics)
Chulalongkorn	KCMH	2002 / 2016	M,Sc.(Medical Imaging) / Ph.D.(Medical Physics
Naresuan	Chulabhorn	2015	M.Sc.(Medical Physics)

The need for medical physicists is according to the growth in technology and health care. Number of cancer centers, university hospitals and private hospitals with advanced radiology are increasing with standard facilities as detail in table 2.

Table 2 Facilities of radiotherapy and nuclear medicine in Thailand

Center	Bangkok	Suburb	Equipment			
			MP	Co-60	Linac	Brachy
Radiotherapy	17	19	98	14	66	28

Center	Bangkok	Suburb	Equipment				
			MP	PET	SPECT	DC	TU
Nuclear Medicine	14	8	20	10	50	50	25

MP – Medical Physicists, DC- Dose Calibrator, TU – Thyroid uptake

The facilities in diagnostic radiology are very large but the number of medical physics in diagnostic radiology is limited only in university hospitals and private hospitals of about 30 all over Thailand.

III. THAI MEDICAL PHYSICIST SOCIETY, TMPS

In 1979 Medical Physics Club of Thailand was set up from the alumni of medical physics program. The number of members was 30 and increasing every year. Thai Medical Physicist Society, TMPS, was established on June 12, 2001. The first annual meeting was co-hosted by Lopburi Cancer Center, Lopburi Province in February 2007. The Society becomes member of SEAFOMP, AFOMP and IOMP. TMPS hosted the first Asia- Oceania Congress of Medical Physics successfully in 2001 in Bangkok. Further from the annual meeting, TMPS hosted SEACOMP in 2004, AOCMP in 2009 and 2012 and ICMP in 2016. Currently, the number of active members is 150.

IV. CLINICAL TRAINING OF MEDICAL PHYSICIST

International Atomic Energy Agency (IAEA) Technical Cooperation (TC) had planned for the education and clinical training of medical physicist since 1991. Training materials for clinical training was prepared by Australian medical physicists. The regional project in Asia and Pacific RAS 6038 title 'Strengthening of Medical Physics through Education and Clinical Training' was approved. The first meeting on 'Regional Meeting for National Trainers to Initiate Trialing the Programme for Radiotherapy Specialty was hosted by TMPS and Chulalongkorn University in June 26-27, 2007 in Bangkok. Follow by the national workshop

on Radiation Oncology Medical Physics [4] (ROMP) clinical training on 28-29 June, 2007 for 5 training centers in Thailand as in Table 3. The 8 modules were arranged in clinical training guide. Minimum competency levels were agreeable among clinical supervisors. The 3 assignments were set for the month of 8, 16 and 24.

Table 3 ROMP Clinical Training in 2007

Hospital	Resident	Supervisor
King Chulalongkorn Memorial Hospital	3	2
Siriraj Hospital	2	2
Ramathibodi Hospital	3	2
Rajavithi Hospital	2	-
Chiang Mai University Hospital	2	1

The clinical training was supported by IAEA for mid-term and final assessments. Ten from twelve residents were successfully passed the assessment. The certification was organized at the 9th Asia Oceania Congress of Medical Physics held in Chiang Mai, Thailand (Fig. 1)

Fig. 1 ROMP Certification at the 9th AOCMP, Chiang Mai, Thailand. Prof. Rethy Chhem, Director of NAHU offered the Chairman at this event,

Diagnostic Radiology Medical Physics (DRMP) clinical training [5] was started in June 2010 with 6 residents from 3 centers as shown in Table 4. The 10 Modules and 45 Sub-modules with competency level on core knowledge and practical skill were agreeable among supervisors and residents. The training was completed in 2012 and the certification was arranged at the 12th AOCMP Chiang Mai Thailand.

Nuclear Medicine Medical Physics (NMMP) clinical training[6] started in June 2011 with 10 residents 5 clinical supervisors. (Fig. 2)

Table 4 DRMP Clinical Training in 2010

Hospital	Resident	Supervisor
King Chulalongkorn Memorial Hospital	4	1
Bumrungrad International Hospital	1	1
Phya Thai Hospital	1	-

Fig. 2 Orientation of 10 residents, 5 supervisors and 2 IAEA Experts on NMMP Clinical Training at Faculty of Medicine Chulalongkorn University in June 2011 (Table 5).

Table 5 NMMP Clinical Training in 2011

Hospital	Resident	Supervisor
King Chulalongkorn Memorial Hospital	3	1
Siriraj Hospital	2	2
Ramathibodi Hospital	1	-
Rajavithi Hospital	1	-
Chiang Mai University Hospital	1	1
Bumrungrad Hospital	1	-
Bangkok General Hospital	1	-
Chulabhorn Hospital	1	-

The NMMP Clinical Guide arranged 11 Modules and 57 Sub-modules. The final assessment supported by IAEA Expert and certification to 8 residents were arranged at the annual meeting of TMPS in 2014.

In February 24-26, 2016, IAEA National Workshop on 'Piloting e-learning in clinical training of medical physicists in diagnostic radiology, radiation oncology and nuclear medicine' was held to train AMPLE Moodle Platform. (Fig. 3)

28

Fig. 3   IAEA orientation on e-Learning in clinical training of ROMP, DRMP and NMMP at Chulalongkorn University Bangkok, Thailand

The 30 residents from 16 hospitals and 15 Clinical Supervisors from 8 hospitals applied for clinical training as shown in Table 6. There are 2 residents from Myanmar, 1 ROMP and 1 NMMP, 1 ROMP from Vietnam and 1 NMMP from Nepal participate in this training. The on line meetings were arranged for ROMP and DRMP in February and March 2017 to clarify the training methodology.

Table 6 ROMP Clinical Training in 2016

Clinical Training	Resident	Supervisor
Radiation Oncology	19	10
Diagnostic Radiology	7	2
Nuclear Medicine	4	3

CONCLUSIONS

In Thailand, the education and clinical training had been developed since 1972 until now for the 2 year graduated program, M.Sc. in medical physics and related fields. The clinical training in medical physics for sub specialty in radiation oncology, diagnostic radiology and nuclear medicine was started one by one in 2007 and completed in 2014. E-Learning in clinical training of medical physics started in Feb 2016 for ROMP, DRMP and NMMP simultaneously. The program is progressing as planned at the orientation. Residents are competence in several topics they had no experienced earlier. At the end of clinical training, the successful residents will work as clinically qualified medical physicists independently. They can train other young medical physicists and be able to strengthen medical physics in Thailand.

REFERENCES

1. Smith PHS, Nusslin F: Benefits to medical physics from the recent inclusion of medical physicists in the international classification of standard occupations. (ISCO-08), Med.Phys.Int 2013, 10-14.
2. International Atomic Energy Agency: Role and responsibility and education and training requirement for clinically qualified medical physicists, Human Health Series No.25, 2013, IAEA Vienna.
3. Meghzifene A: Call for recognition of medical physics profession, The Lancet 377, 1-2, 2011
4. International Atomic Energy Agency: Clinical training of medical physicists specializing in radiation oncology, Training Course Series No.37, 2009,IAEA Vienna
5. International Atomic Energy Agency: Clinical training of medical physicists specializing in diagnostic radiology, Training Course Series No.47, 2010, IAEA Vienna
6. International Atomic Energy Agency: Clinical training of medical physicists specializing in nuclear medicine, Training Course Series No.50. 2011, IAEA Vienna

Contacts of the corresponding author:

Author: Anchali Krisanachinda
Institute: Chulalongkorn University
Street: Rama IV Road
City: Bangkok 10330
Country: Thailand
Email: anchali.kris@gmail.com

EDUCATIONAL TOPICS

OPTIMIZING CLINICAL IMAGE QUALITY: AN EXPANDING ROLE FOR MEDICAL PHYSICISTS

Perry Sprawls

Sprawls Educational Foundation, www.sprawls.org

Abstract— **All modern medical imaging methods produce images in a digital format. This divides the patient body into small samples, or voxels, with corresponding pixels in the image. The size of the samples (voxels and pixels) has a major effect on image quality. The challenge is that the size generally has opposing effects on two image quality characteristics, detail and noise, and potential effects on radiation exposure to patients. For many methods the size can be adjusted with a combination of procedure protocol factors. An optimized procedure with an appropriate balance among the image quality characteristics and radiation exposure to patients requires a significant knowledge of physics. Medical physicists now have the opportunity to make additional contributions to image quality and radiation risk management through clinical consultations and educational programs including the topic of procedure optimization.**

Keywords— **Image Quality, Optimization, Radiation Exposure, Medical Physicists.**

I. INTRODUCTION

Medical physicists are the professionals who provide the knowledge and experience to insure adequate image quality for diagnostic imaging procedures and contribute to risk management relating to ionizing radiation. The quality of an image for a specific examination is determined by a combination of factors as illustrated in Figure 1.
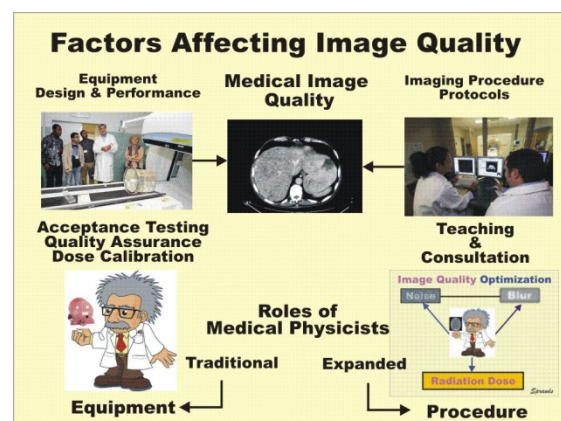

Fig. 1 Roles of Medical Physicists Related to Medical Image Quality

A starting point for image quality is the physical characteristics and design of the technology. This is unique to each imaging modality and the status of innovations and development. This generally determines both the overall capability and limits for producing images with specific quality characteristics. With respect to this, medical physicists can participate in the acquisition and installation process by reviewing specifications, consulting in the selection, and conducting acceptance testing to ensure the equipment can function as expected. The second issue is the continuing performance and maintenance of equipment that physicists verify through quality control and assurance testing and evaluations. These activities generally focus on the *equipment* and the *individual image quality characteristics*: contrast, detail/resolution, noise, and artifacts, along with radiation dose and risks issues.

II. OPTIMIZED IMAGE QUALITY: THE DIGITAL DILEMMA

Another major factor, and the one that has the greatest effect on image quality, especially for advanced modalities including CT, MRI, and digital radiography, is how the equipment is operated. Image quality for each clinical procedure is determined by a complex combination of adjustable technical parameters that collectively form the procedure protocol.

Virtually all imaging methods now produce images in a digital format. There are many advantages and values of digital images as illustrated in Figure 2.
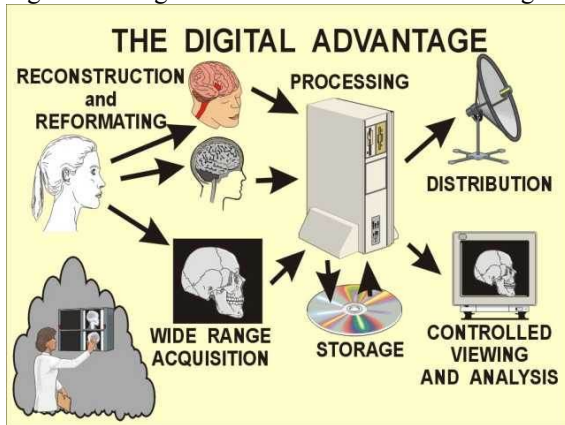

Fig. 2 An overview of the major advantages of digital medical images.

Digital imaging and technology is the foundation of our modern imaging methods and the ability to distribute and process images to improve healthcare around the world.

However, there is a characteristic of the digitizing process that has a major effect on image quality that must be taken into consideration. The digitizing process is a sampling process in which the human body is divided into discrete samples (voxels and corresponding image pixels) as illustrated in Figure 3
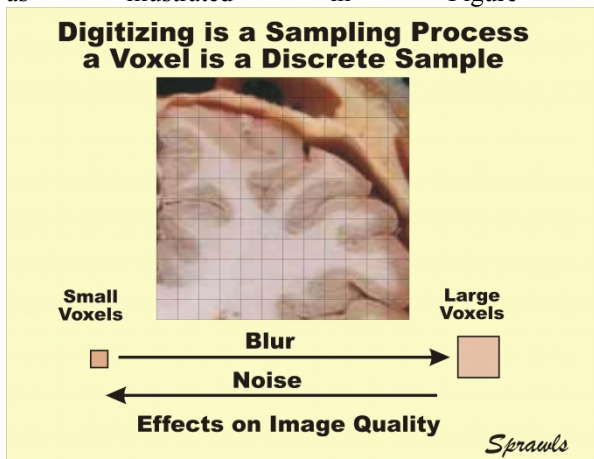

Fig. 3 The formation of digital images divides the human body into discrete samples, voxels, and corresponding pixels in the image.

The size of the sample (voxel/pixel) is usually adjustable when setting up an imaging procedure and also has a major and complex effect on image quality. And here is the dilemma: what is the best, or optimum, sample size for a specific imaging procedure? Digitizing is a blurring process. The challenge in selecting an appropriate size is that it affects two image quality characteristics, detail/resolution which is limited by blurring and noise, but in conflicting or opposing directions. It also is a determining factor in radiation

exposure to the patient for x-ray, including CT, procedures and acquisition time for MRI and some nuclear imaging methods.

The sample, typically the voxel, size is adjustable through the three protocol factors shown in Figure 4, using computed tomography as an example.
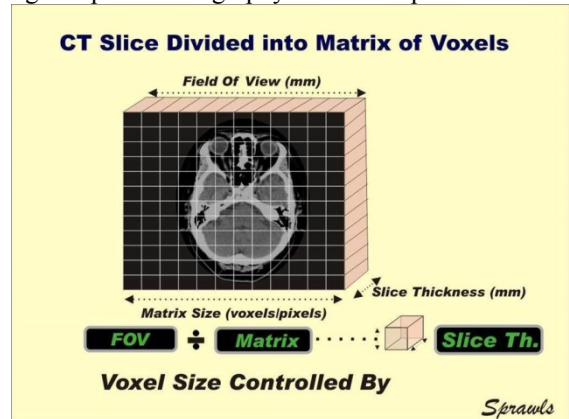

Fig. 4 The imaging protocol factors used to adjust voxel size.

For radiography and other non-tomographic imaging methods it is the image pixel that represents the sample and the size is the ratio of the field of view (FOV) to the dimension of the image matrix in pixels.

III. IMAGE BLURRING AND VISIBILITY OF ANATOMICAL DETAIL

The formation or conversion of an image in a digital format, for any modality, is a *blurring process*. Each voxel and corresponding pixel is actually a blur that adds to all of the other sources of blur in the imaging chain as illustrated in Figure 5.
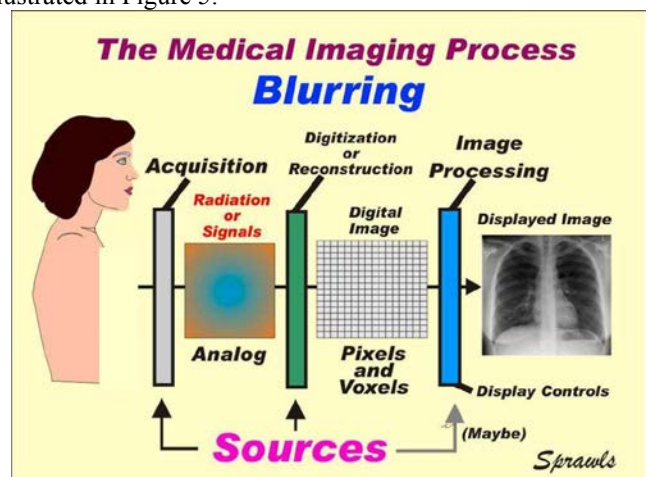
Fig. 5 The general sources of blurring for all imaging modalities.

Since voxel/pixel size and the blurring it produces is usually adjustable, a first thought might be to adjust it to the smallest possible value for each imaging procedure. That is not the appropriate action for three different reasons! The voxel/pixel size should be selected taking these factors into consideration.

Composite Blur: The blurring from digitizing an image adds to the blur from other sources within the system resulting in the total or composite blur in the image. For

radiography, including mammography, these sources are illustrated in Figure 6.

Fig. 6 Pixel size is one of the several sources of blurring in digital radiography. The sources combine to form the total or composite blur that will appear in the image.

A conventional model for determining the value or size of the composite blur is illustrated in Figure 7.
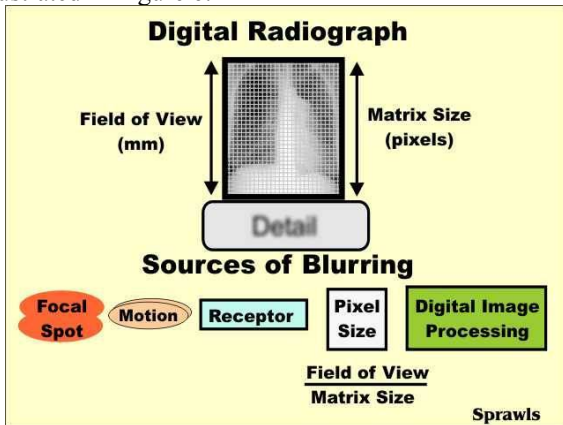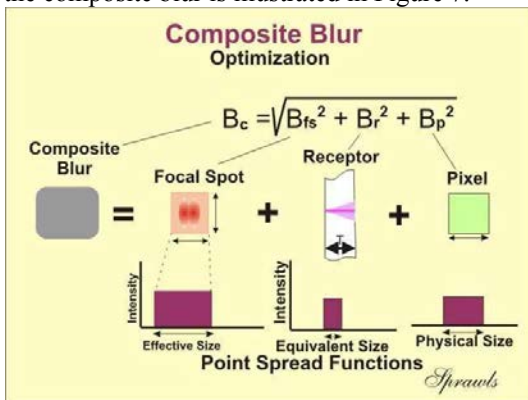

Fig. 7 A general relationship for determining the composite blur value in digital radiography.

The illustration here is for digital radiography, including mammography, but the mathematical relationship applies to all modalities. What must be considered are the factors limiting how much other sources of blurring can be reduced.

The selection of focal spot size is a compromise between image detail and heat capacity within the x-ray tube that limits the exposure, especially within a short time to minimize motion blurring, to form an image. The blurring produced within the receptor is generally a design characteristic relating to the thickness of the attenuation and conversion layer. If these sources of blur are already fixed for a specific radiography/mammography procedure the question then becomes, what is an appropriate pixel size? Should the pixel be made very small to reduce its blurring? There is actually a combination of two factors for not always using the smallest possible pixel size.

In general, adjusting the pixel blur size so that it is significantly smaller than the blur from other sources will have little effect on reducing the overall composite blur

and increasing visibility of detail. The other and generally most significant factor is that reducing pixel or voxel size *increases* image noise. This is for all imaging methods with the possible exception of ultrasound.

The Digital Dilemma: It is the conflicting effects of voxel/pixel size on image detail and image noise that is the "digital dilemma" and requires a comprehensive knowledge of physics and activities of experienced medical physicists to provide optimized imaging protocols that can provide adequate image quality for a specific clinical objective and with the lowest radiation exposure as appropriate.

We will now consider the specific effects of voxel/pixel size on image noise and then the overall process of image quality optimization and effects on radiation exposure.

IV. IMAGE NOISE AND VISIBILITY OF LOW CONTRAST OBJECTS

Noise is an undesirable image quality characteristic that specifically limits visibility of low contrast objects in the body. Many small objects, breast cancer calcifications for example, also have low contrast and their visibility is limited by noise in addition to blurring. In most imaging procedures the amount of noise in an image can be adjusted, either by equipment design or the adjustment of imaging protocol factors. That raises the question, if the noise can be adjusted and controlled why not set it to a very low level and have very high image quality? There are two reasons: changes in a procedure to reduce noise often result in increased blurring and loss of detail and also increased radiation exposure to the patient. Optimizing an imaging procedure is the process of using knowledge of physics to balance these opposing factors.

The sources of Image Noise: There is noise in images produced with all modalities. Even though the sources are different there are common characteristics, especially in relation to the digital structure of images. As illustrated in Figure 8 the digitizing process is not the source of the noise but it *controls* the amount of noise that appears in an image.
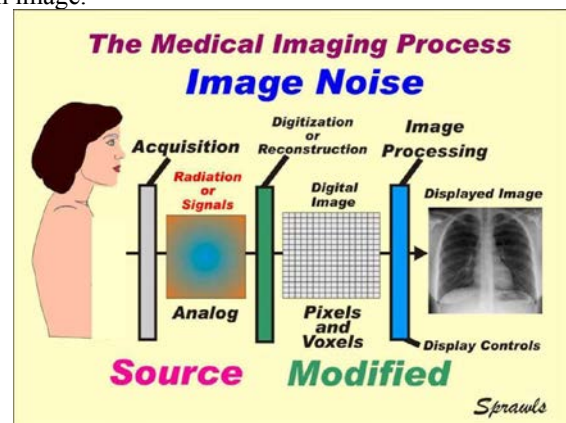

Fig. 8 The digital structure (voxel/pixel size) affects the value of the noise that comes from other sources and appears in an image.

For imaging methods using ionizing radiation--x-radiation and nuclear--the predominant source of noise is the statistical random nature of photons. This is especially true if the procedure is being conducted in the "quantum limited" mode to limit radiation exposure or acquisition time. With MRI the noise is from random RF emissions from within the body that are competing with the strength of the image RF signals that is controlled by voxel size. In all cases sample size is a controlling or modifying factor for the noise that appears in an image.

X-ray Image Noise: An important concept relating to x-ray image noise is illustrated in Figure 9.
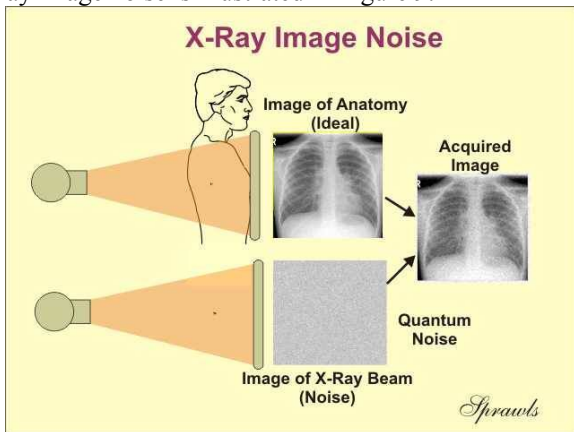

Fig. 9 The noise that appears in x-ray images is an image of the x-ray beam.

The noise is an image of the x-ray beam that is superimposed or added to the image of the anatomy. In the digitizing process of an x-ray image it is the number of photons in each sample (pixel) that determines the statistical variation which is the noise as illustrated in Figure 10.
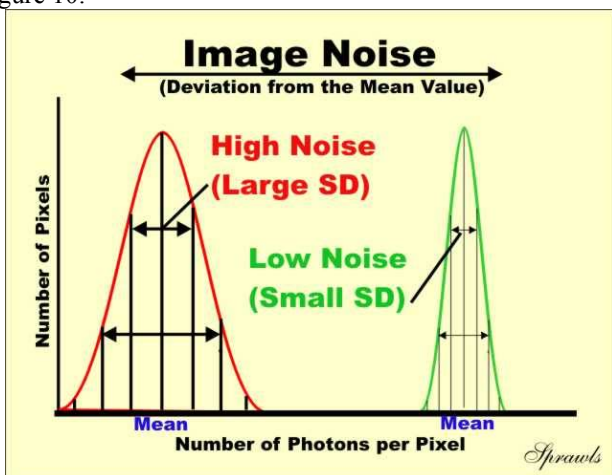

Fig. 10 The statistical distribution of photons among pixels and the relation to exposure.

There are two ways to increase the number of photons per pixel and reduce image noise. Both have adverse effects. One is to increase pixel size which increases blurring of the image. The other is to increase the exposure to the image receptor which also increases exposure to the patient.

Computed Tomography Image Noise: CT is an x-ray imaging method so the same principles regarding the source of noise apply as illustrated in Figure 11.
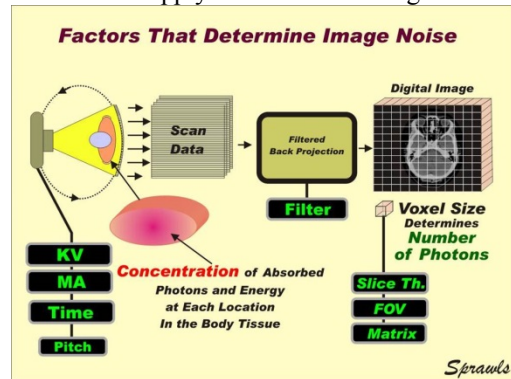
Fig. 11 The adjustable protocol factors that determine noise in CT images.

In addition to radiation dose and voxel size there is a third factor with a significant effect on CT image noise. It is the digital imaging processing algorithm or filter that is included in the "filtered" back projection image reconstruction process, sometimes referred to as the kernel. When setting up a protocol for a specific clinical procedure there is the opportunity to select from several different filters or kernels that affect image quality. The characteristics of these various filters vary among the different equipment manufacturers, who can provide information in their applications documents. However, there is a common issue that applies to all as illustrated in Figure 12.
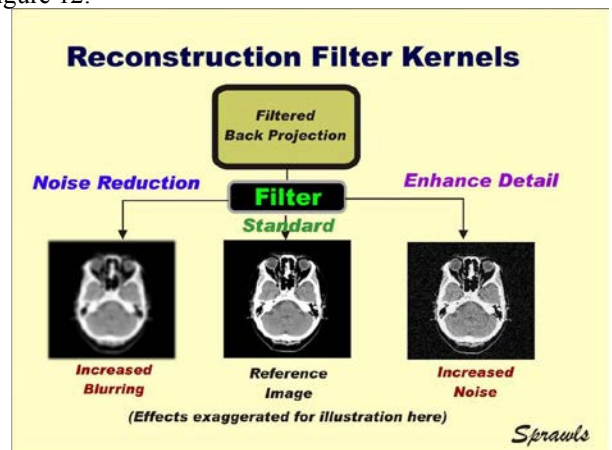
Fig. 12 Conflicting effects of CT reconstruction filters on image quality.

Digital processing an image to reduce noise is often done by mathematically blurring the image, such as by averaging adjacent pixels. Processing an image to enhance detail will typically increase the visibility of the noise. This is because noise is actually a high detail pixel-to-pixel variation in brightness. This is just another example of the opposing effects of image blurring and noise. Making changes in the imaging process to decrease one will increase the other.

V. RADIATION EXPOSURE TO PATIENTS AND IMAGE ACQUISITION TIME

In medical imaging there is always a cost, or "price to pay" for image quality. In the x-ray methods, including CT, it is the radiation exposure to the patient. In MRI it is the image acquisition time. In radionuclide or nuclear medicine procedures it can be a combination of radiation exposure and acquisition time. This is the third factor that enters into the optimization compromise or balance that needs to be achieved. Both radiation exposure and acquisition time (in MRI) are generally adjustable protocol factors that have direct effects on image quality.

As described above, the concentration of x-ray photons, or exposure, is the determining factor in image noise. As illustrated in Figure 10 noise is decreased by increasing the photons captured in each voxel or pixel.

The accepted approach in x-ray imaging is that the radiation exposure should be limited to a value that will produce the clinically necessary image quality. However, there is the realization that increasing exposure produces "better looking" images, even when the resulting quality is not required and might result in unnecessary exposure to patients.

With three competing factors, detail, noise, and radiation exposure, to be balanced, where do we start? An appropriate first step is to adjust the blurring to provide the clinically required visibility of detail. This involves selecting a voxel/pixel size that is generally equivalent to the other blur sources (focal spot, detectors. etc.) in the imaging system and is appropriate for the specific clinical procedure. This will range from approximately 0.2 mm for mammography to several mm in CT and MRI.

The selected voxel/pixel size becomes a factor for the noise. With the size now fixed because of image detail requirements it becomes necessary to increase radiation exposure or acquisition time to reduce the noise to an acceptable level.

One of the challenges in x-ray imaging, including CT, is determining what is an acceptable noise level for a specific clinical procedure which then establishes the lowest, but necessary, radiation exposure and dose. The judgment of the radiologist viewing the images is a key factor. Monitoring the radiation dose for the various procedures and comparing to reference values is the usual approach to optimizing the overall procedure. It is assumed that the reference values being used are related to image quality requirements and not more general regulatory limits.

V. THE ROLE OF THE MEDICAL PHYSICIST IN IMAGE QUALITY OPTIMIZATION

It is the conflicting effects of the three factors--image detail, image noise, and radiation exposure--that increase the complexity of modern imaging procedures and require knowledgeable medical physicists to achieve the appropriate image quality and radiation exposure for each clinical procedure as illustrated in Figure 13.
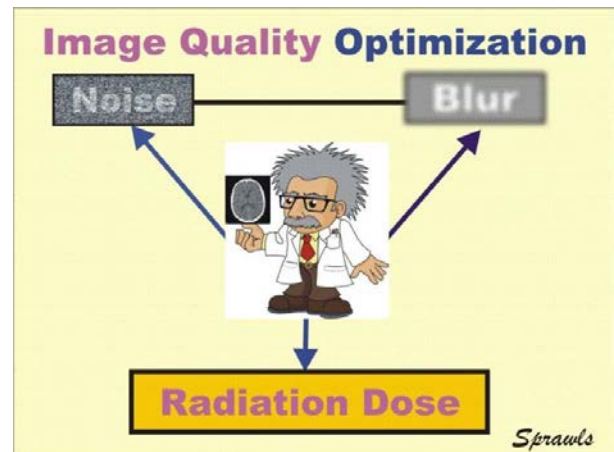

Fig. 13 Opposing factors that must be balanced to optimize an imaging procedure.

As medical physicists we are not usually capable in determining the image quality characteristics required for a specific clinical procedure, especially for the modalities of CT and MRI with the many variables, and we are not the ones who set up the protocols and actually control image quality. However, we are the professionals with knowledge of image quality characteristics, how they are related and controlled by protocol factors, and the overall issue of the process of optimization. The radiologists and imaging technologists are our connections to the actual imaging process and control of image quality.

A traditional role for medical physicists is monitoring and providing guidance on radiation exposure and dose to patients. This is a major contribution to the overall optimization process.

The very valuable role of medical physicists is that of educators and consultants. An effective educator and teacher require the combination of two things, personal experience and educational resources, especially visuals that can be used in classes, conferences, and other discussions.

Clinical Experience for Medical Physicists: For maximum effectiveness as educators, medical physicists need good knowledge of the imaging procedures as they are performed in the clinical environment. This can be achieved by observing clinical procedures giving attention to image characteristics and the selection of imaging protocol factors for a variety of examinations. The objective is not to know the details for every procedure but to have an understanding of the overall imaging process and how it is performed. This knowledge will enhance communications with radiologists and technologists both in class and conference discussions and in consultations within the clinic.

VI. EDUCATIONAL ACTIVITIES TO ENHANCE IMAGE QUALITY OPTIMIZATION

A major factor in obtaining optimum image quality with the various methods and procedures is a clinical

staff, radiologists and technologists, with knowledge of the physics principles relating to image quality, the control of image quality, and the concept of optimization as provided by the medical physicist. This requires both an expanded scope and content for traditional medical physics educational programs, especially for radiologists and residents, and an expanded role of medical physicists as educators/teachers.

A diagram, or mind map, for the image quality optimization program is shown in Figure 14.
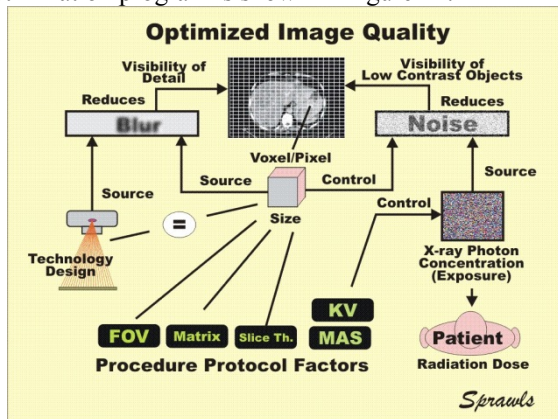

Fig. 14 A mind map giving an overview of the knowledge required to optimize image quality for digitized images.

The topic of image quality optimization can be an addition to an existing medical physics educational program or can be provided as a stand-alone course. An understanding of the concept and process of optimization requires foundation knowledge of image quality characteristics and the factors that affect and control those characteristics for each of the imaging modalities as illustrated in Figure 14. While the factors that determine image quality are specific for each modality the overall principle of optimization is the same as it relates to the digital structure and image characteristics.

A course to develop an understanding and capability for medical imaging procedure optimization for medical physicists, radiology residents, and other imaging professionals, will include these topics.

- Introduction and Overview of Medical Image Quality Characteristics
- Structure of Digital Images (pixels) and Imaged Body Segments (voxels)
- Image Contrast and Procedure Contrast Sensitivity
- Image Blurring, Visibility of Detail, and Effect of Digital Structure
- Spectral and Statistical Characteristics of X-radiation
- Image Noise, Effect on Visibility, Sources, Relation to Digital Structure
- Digital Radiography and Mammography, Factors That Affect Image Characteristics
- Computed Tomography, Factors That Affect Image Characteristics
- MRI, Factors That Affect Image Characteristics
- Radiation Quantities and Units, Emphasis on Dose to Patients
- Concept and Application of Medical Imaging Procedure Optimization

Resources to support these and related educational activities are available through the websites: www.sprawls.org/resources and www.sprawls.org/PhysicsWindows .

VII. CONCLUSION

The formation of medical images in a digital format is a sampling process in which the body is divided into voxels and the image into pixels. The size of the samples, voxels and pixels, has a conflicting effect on image quality and potential radiation exposure to patients. The voxel/pixel size is adjustable through a combination of imaging procedure protocol factors. A comprehensive knowledge of physics is required to optimize imaging procedures producing the necessary image quality and without unnecessary exposure to radiation or image acquisition times. The medical physicist is the imaging professional that provides this knowledge through consultations and educational activities.

AN e-LEARNING PACKAGE FOR PERSONAL DOSIMETRY TRAINING PURPOSES

M. Koutalonis[1], A.J. Porter[1], A.C. Moreton[1], E. Hogbin[1]

[1] Colchester Hospital University NHS Foundation Trust/Medical Physics Department, Colchester, UK

Abstract— **Personal dose monitoring is a legislative requirement under the Ionising Radiations Regulations 1999 (IRR99) in the UK. Regulation 18(3) says that "An employer who has designated an area as a controlled area shall not permit a person to enter or remain in such area in accordance with the written arrangements under paragraph 2(c), unless he can demonstrate, by personal dose monitoring or other suitable measurements, that the doses are restricted in accordance with that sub-paragraph". Members of staff who work in controlled areas with ionising radiation are therefore issued with personal dosimeters to monitor the doses they receive and satisfy the regulations. However, there is evidence that awareness of personal dosimetry among staff who work with ionising radiation is low. In particular, in our hospital it was noticed that, despite given relevant written instructions, some members of staff did not know how to distinguish among different types of dosimeters, which body position to wear each one at, what to do if they lose them, when to return them for replacement etc. As a result of this, an e-learning package was developed aiming to increase the awareness of matters relating to personal dosimetry among staff. The e-learning package consisted of training slides followed by a mandatory assessment. The training slides covered topics relevant to legislation on personal dosimetry, types of dosimeters and how to distinguish among each type, correct wearing of dosimeters, local investigation levels, when to return each dosimeter for replacement, what to do if it is lost etc. Awareness of our staff appears to have improved since the introduction of this e-learning package which is now mandatory for all new staff in order for them to be issued with a personal dosimeter.**

Keywords — **e-Learning, education, training, personal dosimetry.**

I. INTRODUCTION

Personal dose monitoring for members of staff working with ionising radiations is very important not only in order to comply with national and international regulations, but also to monitor the radiation doses that staff receive and to minimize the risk of any health effects. In the UK, the Ionising Radiation Regulations 1999 (IRR99) [1] have been implemented to comply with the European Council Directive 96/29 Euratom "Protection of health of workers and general public against the dangers arising from ionising radiation" [2]. Regulation 18(3) of IRR99 refers to personal dose monitoring of staff working in controlled areas.

Personal dose monitoring has been in use in hospitals for many years. Members of staff working with ionising radiations are issued with personal dosimeters that monitor the doses they receive over a period of time. Based on the type of work they perform, staff can be issued with various types of dosimeters: whole body dosimeters (most common), collar dosimeters, rings, wrist bands or eye dosimeters. Different types of dosimeters are used for different types of work, e.g. whole body dosimeters are used for most types of work (general radiography etc.); collar badges are mainly used in fluoroscopy; rings are used in Nuclear Medicine and Radiopharmacy and wrist bands can be used in interventional radiology and cardiology together with rings. Eye dosimeters are becoming more common following the latest recommendation for the reduction of the eye lens dose limit from the Basic Safety Standard of the European Union [3].

It is easily understood that members of staff, who perform complicated procedures and therefore who are issued with two or three different types of dosimeters, can get confused over various matters, such as which body part they should wear each one at, what is the correct orientation, when to return them for replacement etc. In our hospital, despite providing written instructions and information to our staff regarding their dosimeters, we have noticed in the past that their awareness is still low. In addition, several members of staff do not return their dosimeters for replacement at the specified times, something that has financial implications and also leads to inaccurate dose records.

Following these findings, it was decided to develop a mandatory e-learning package for all existing and new members of staff who work with ionising radiations in our hospital. E-Learning is becoming popular nowadays as it provides an easy and quick way of providing training to members of staff. Various e-learning packages are being published and one source of these in the UK for the health sector is the e-learning for Health website (e-LfH) [4]. The aim of this e-learning package was to increase the awareness of our members of staff on matters relating to personal dosimetry.

II. MATERIALS AND METHODS

The e-Learning package: The e-Learning package was developed using Microsoft Office PowerPoint2010®. It

consists of 21 slides (including a title slide and a final slide with instructions regarding the assessment). The main topics covered by the package are the following: legislation relevant to personal dosimetry; where can members of staff find information about personal monitoring; various types of dosimeters, what they are made of and which body part they should be worn at; when and where to return the personal dosimeters; consequences of late and non-returned dosimeters (financial, legislative enforcement and dose records); information on the storage of dosimeters; results from personal dosimetry; local investigation levels for staff doses; current dose limits and typical staff doses for various working environments. The slides include a combination of text as well as pictures showing for example the correct way of wearing the various types of dosimeters. Some example slides are presented in Figures 1, 2 and 3 that follow.
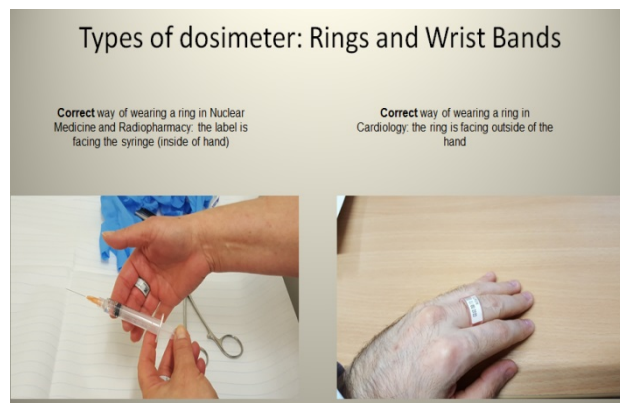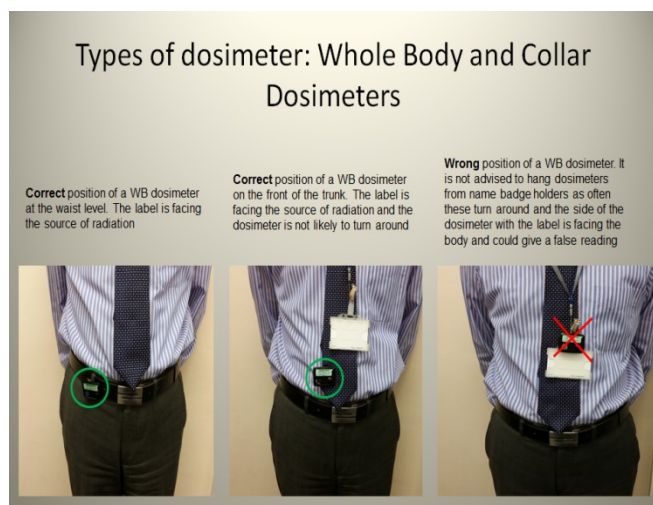

Fig. 1 Correct and wrong positioning of a whole body dosimeter
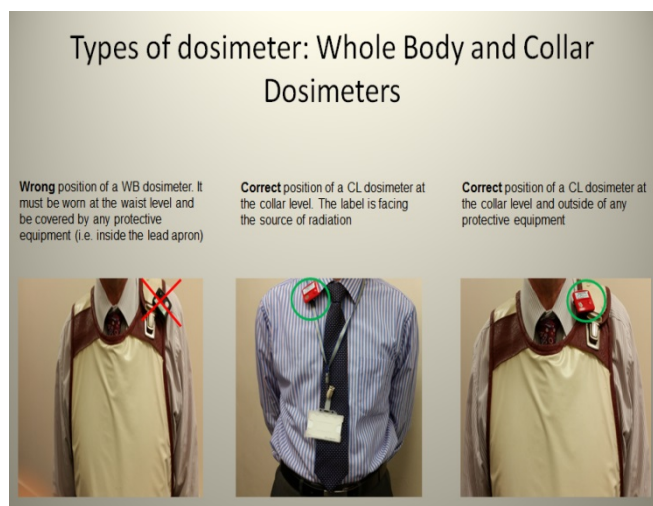
Fig. 2 Correct and wrong positioning of a whole body and collar dosimeter

Fig. 3 Correct way of wearing ring dosimeters in Nuclear Medicine, Radiopharmacy and Cardiology departments

The assessment: The training slides are followed by a mandatory assessment that consists of 10 multiple choice questions. Most of the questions have a choice of four possible answers while some others have two. Also, some questions have two correct answers that both need to be selected in order for the answer to be considered fully correct. Each question has a score of 10. The pass mark for the assessment was initially set to 80/100, although this is currently under review and likely to increase to 90/100. Upon successful completion of the training and the assessment, each member of staff is issued with a certificate which they submit to the Radiation Protection Section in order to be issued with their personal dosimeter(s). A copy of the assessment questions and answers is presented in the Appendix.

The e-learning package was submitted to the e-learning team of the Hospital and was entered on to the Hospital's e-learning system. This is now part of the mandatory training that all new members of staff requiring personal monitoring have to undergo before they can be issued with their personal dosimeter. Also, all existing members of staff that are monitored were asked to complete this training and provide Radiation Protection with their certificate. The training slides of the e-learning package are also available on our Department's website [5].

Statistical analysis of the results: Six months after the introduction of this e-learning package, the results were collected and analysed in order to evaluate the effectiveness of the package and review its content. Various statistical parameters were calculated to this end. These are summarized below:

Facility Index F: this is the mean score of all staff on each question and it is a measure of how easy or difficult a question is. It is calculated as $FI=X_{average}/X_{max}$, where $X_{average}$ is the mean credit obtained by all staff attempting the question and X_{max} is the maximum credit achievable for that question. In our case where most of the answers can be distributed dichotomically into correct/wrong categories, this index coincides with the percentage of staff that answered each question correctly. Table 1

shows a range of values for the facility index FI and their interpretation.

Standard Deviation (SD): this is a measure of the spread of scores around the mean score and therefore the extent to which the question can discriminate. If the FI index is very high or very low it is impossible for the spread to be large. However, a good SD does not automatically ensure good discrimination. A value of SD of less than about a third of the question maximum (i.e. 33%) in the table is considered not satisfactory in general.

Table 1 Facility Index (FI) and interpretation

FI range	Interpretation
5 or less	Extremely difficult or something wrong with the question
6-10	Very difficult
11-20	Difficult
21-34	Moderately difficult
35-64	About right for the average staff
65-80	Fairly easy
81-89	Easy
90-94	Very easy
95-100	Extremely easy

Random Guess Score (RGS): this the mean score that the members of staff would be expected to get for a random guess at each question. RGS is only available for questions that use a form of multiple choice, as in the case of this package's assessment. All random guess scores are for deferred feedback only and assume the simplest situation, e.g. for multiple response questions staff are told how many answers are correct. Values above 40% are unsatisfactory in general and show that True/False questions must be used sparsely in summative tests.

Intended and Effective weights: The intended weight is the question weight expressed as the overall test score while the effective weight is an estimate of the weight the question actually has in contributing to the overall spread of the scores. The effective weights should add to 100%.

The intended and effective weights are intended to be compared. If the effective weight is greater than the intended, it shows that the question has a greater share in the spread of scores than may have been intended. If it is less than the intended weight, it shows that it is not having as much effect in spreading out the scores as was intended.

The calculation of the effective weight relies on taking the square root of the covariance of the question scores with the overall performance. If a question's scores vary in the opposite way to the overall score, this would indicate that this is a very odd question which is testing something different from the rest. The effective weight of such questions cannot be calculated.

Discrimination Index: this is the correlation between the weighted scores on the question and those on the rest of the assessment. It indicates how effective the question is at sorting out able members of staff from those who are less able. The results of this index can be interpreted as shown in Table 2.

Table 2 Discrimination Index and interpretation

Index	Interpretation
51 and above	Very good discrimination
30-50	Adequate discrimination
20-29	Weak discrimination
0-19	Very weak discrimination
negative	Question probably invalid

Discrimination efficiency: this statistic attempts to estimate how good the discrimination index is relative to the difficulty of each question. A question which is very easy or very difficult cannot discriminate between members of staff of different ability because most of them get the same score on that question. Maximum discrimination requires a facility index in the range 30%-70% (although such a value is no guarantee of a high discrimination index). The discrimination efficiency will very rarely approach 100% but values in excess of 50% should be achievable. Lower values indicate that the question is not as effective at discriminating between staff of different ability as it might be and therefore is not a particularly good question.

III. RESULTS

At the time this study was performed, there were a total of 367 attempts to read the training slides and pass the assessment. These 367 attempts include several repeats from members of staff who either failed on their first attempt or they passed but wished to improve their pass mark (although the pass mark did not matter). The total number of first attempts (no repeats) was 272. This corresponds to the total number of staff that did the training. Of these 272, 25.7% (70 members of staff) failed while 74.3% (202 members of staff) passed (first attempts only).

An interesting fact is the time taken by each member of staff to complete the training slides and the assessment and its correlation with the pass/fail results. It is assumed that an average member of staff (regardless of experience) would need a minimum of 20 seconds in order to read each of the 20 slides and a minimum of 30 seconds to answer each of the 10 multiple choice questions of the assessment. This corresponds to a minimum time of approximately 12 minutes. Table 3 that follows shows the

distribution of times taken by staff to complete the training and the assessment, and their correlation to pass/fail rates.

Table 3 Time spent for the training slides and assessment

Time range (min)	No of attempts (1st only)	No of fails	% of total fails
< 7	215	64	91.4%
7 – 11	21	0	0.0%
> 11	36	6	8.6%

It is easily noticed from Table 3 that the majority of the staff (79% or 215 staff) completed the training faster than expected, taking less than 7 minutes. As a result of this, 64 of them (91.4% of the total number of fails on the first attempt) failed the assessment and had to repeat it. The majority of these however spent over 11 minutes in total, including the time they took to repeat the assessment (and perhaps read through the slides again).

The members of staff from the Radiology Department (radiographers and radiologists) form the largest group of staff that had to complete this training (75 staff – first attempts only). Of those, 22 (29%) initially failed the assessment and had to repeat it. Interestingly, out of these 22 staff that failed the assessment, 19 completed the training in less than 7 minutes and 15 in less than 4 minutes. The radiology department staff were also divided into more experienced (more than 10 years) and less experienced (less than 10 years) staff in order to investigate whether there is any correlation between experience and pass/fail rate. It was noticed that the time taken to complete the training was the dominant affecting factor for the pass/fail rate rather than the experience of each member of staff, as 33% of the more experienced staff and 37% of the less experienced staff failed the assessment.

The highest fail rate (25.9%) was noticed for Question 1, asking which regulations are related to the personal dosimetry. This was followed by a 25.2% fail rate for Question 4, which was asking the staff to select two correct answers out of four possible. The question was asking for how long the members of staff are expected to wear their whole body and collar dosimeters. 24.5% of our staff answered incorrectly Question 8, asking where the local investigation levels for staff doses can be found. Finally, 20.6% of the staff answered incorrectly Question 9, related to the correct orientation in which whole body and collar dosimeters, rings and wrist bands should be worn. This question was also asking for two correct answers out of four possible. The fail rates for the remaining six questions of the assessment were less than 10%. The lowest fail rate was noticed for Question 5 asking what the members of staff should do if their dosimeter is lost.

Table 4 that follows shows the Facility Index (FI), Standard Deviation (SD) and Random Guess Score (RGS) for each of the assessment questions. All questions had 367 attempts in total.

Table 4 Facility Index (FI), Standard Deviation (SD) and Random Guess Score (RGS) for each of the assessment questions

Q	FI	SD	RGS
1	74.1%	43.9%	25.0%
2	92.9%	25.7%	25.0%
3	94.6%	22.7%	50.0%
4	74.8%	40.0%	---
5	99.7%	5.2%	25.0%
6	90.5%	29.4%	25.0%
7	91.0%	28.7%	50.0%
8	75.5%	43.1%	25.0%
9	79.4%	38.7%	---
10	98.4%	12.7%	50.0%

Looking at the FI values from Table 3 and their interpretation from Table 1, it can be seen that most questions can be characterized as being fairly easy to extremely easy. This was the initial aim of the e-learning package assessment, to be simple and consist of questions that would test basic knowledge, rather than including difficult questions.

Questions 5 and 10 which are classified as extremely easy have led to a very low fail rate (very high FI) and also a very low SD (spread of scores around the mean). These questions may need to be modified or replaced when the e-learning package is next reviewed. The remaining 8 questions have an average SD value of about 34%.

Table 5 Intended Weight (IW), Effective Weight (EW), Discrimination Index (DI) and Discriminative Efficiency (DE) for each of the assessment questions

Q	IW	EW	DI	DE
1	10.0%	14.6%	28.2%	33.6%
2	10.0%	9.2%	20.7%	31.4%
3	10.0%	8.0%	16.5%	27.0%
4	10.0%	13.2%	23.3%	27.2%
5	10.0%	1.5%	0.8%	3.7%
6	10.0%	11.3%	31.1%	45.6%
7	10.0%	10.4%	23.9%	35.7%
8	10.0%	13.4%	18.4%	22.6%
9	10.0%	13.6%	30.9%	37.7%
10	10.0%	4.9%	12.7%	31.0%

Questions 4 and 9 were asking for two correct answers out of four possible and therefore do not have a calculated RGS value. The majority of the questions have a satisfactory RGS value of 25% as they provided four

possible answers. Questions 3, 7 and 10 have an RGS value of 50% because they provided two possible answers. These questions may be replaced in future versions of the e-learning package.

Table 5 above presents the Intended and Effective Weight (IW), (EW) for each assessment question, as well as their Discrimination Index (DI) and Discriminative Efficiency (DE). All questions had 367 attempts.

The Intended Weight for each question was the same and equal to 10%. As mentioned in the materials and methods section, the intended and effective weight scores should be compared. Ideally, they should be the same or as close as possible. Looking at Table 5, one can see that most questions have an EW of around 10% with the exception of Questions 5 and 10 where the EW is much lower than the IW. This means that these questions are not having as much effect in spreading out the scores as was intended. Questions 5 and 10 have already been identified as being extremely easy from the facility index analysis above.

Finally, the discrimination index and the discriminative efficiency were also calculated in Table 5. Looking at the DI results and their interpretation from Table 2, one can see that the majority of the questions fall into the categories of very weak discrimination, weak discrimination or adequate discrimination. Question 5 again, is considered probably invalid based on its DI value and Question 10 is just above the "question probably invalid" category. Similarly, most of the questions have a discriminative efficiency value of about 30% (with the exception of Question 5) which indicates that the questions are probably easier than expected and as a result they are not very effective at discriminating between staff of different ability. This result was also noticed above when analysing the Radiology Department results.

IV. DISCUSSION AND CONCLUSIONS

This e-learning package was developed aiming to increase the awareness of our staff working with ionising radiations on matters related to personal dosimetry. It was made mandatory to ensure that all staff will complete it. An assessment, consisting of questions testing basic knowledge rather than more difficult questions, was included in the package.

The analysis of the results showed that approximately one out of four members of staff failed the assessment on their first attempt. The majority of those who failed seem to have rushed while reading the e-learning package slides either due to limited time (e-learning can only be completed while at work) or because they felt confident with the content. This is an issue that needs to be looked at in the future. Also, it should be noted that the majority of the staff that attempted the training so far are already

being monitored and therefore have some experience with personal monitoring.

In addition, the analysis has showed that some of the questions of the assessment are probably too easy as they cannot discriminate between more and less experienced members of staff. These questions will be reviewed and modified in future versions of the package. The pass mark of 80% is also likely to increase to 90%, in accordance with most mandatory e-learning training packages in our hospital.

The process of unannounced audits on personal dosimetry is being introduced currently in various departments where members of staff work with ionising radiations. The audits look at topics covered by the e-learning package and aim to assess its efficiency in improving the awareness of our staff. Initial findings have showed that most staff wore the correct dosimeters and these were worn correctly (correct body part and orientation). Also, our staff seemed to have a better understanding of when the dosimeters need to be returned and what is the process for this. Some staff were also asked if they know/have seen their doses recently and most of them knew what doses they receive on average.

The developed e-learning package seems to be achieving its purpose to increase the awareness of our staff on matters related to personal dosimetry. Further assessment is necessary in the future as well as a review of the package to improve the training slides as well as the assessment questions.

REFERENCES

1. The Ionising Radiations Regulations 1999 at www.legislation.gov.uk/uksi/1999/3232/contents/made
2. Directive 96/29/Euratom – ionising radiation at www.osha.europa.eu/en/legislation/directives/73
3. Directive 2013/59/Euratom – protection against ionising radiation at www.osha.europa.eu/en/legislation/directives/directive-2013-59-euratom-protection-against-ionising-radiation
4. e-Learning for Health (e-LfH) at http://www.e-lfh.org.uk/home/
5. e-Learning package for personal dosimetry at "http://www.colchesterhospital.nhs.uk/medical_physics.shtml under Radiation Protection tab – Training Material" or at "http://www.colchesterhospital.nhs.uk/Personal%20Dosimetry%20Training.pdf"

Contacts of the corresponding author:

Author: Manthos Koutalonis
Institute: Colchester Hospital University NHS Foundation Trust
Street: Turner Road
City: Colchester
Country: UK
Email: Manthos.Koutalonis@nhs.net

APPENDIX

The e-learning package assessment (correct answers underlined)

Please note some questions refer to local practice only.

Question 1
Personal dosimeters are issued to members of staff who enter controlled areas to satisfy:
a) The Ionising Radiations (Medical Exposures) Regulations 2000
b) The Medical and Dental Guidance Notes
c) The Ionising Radiations Regulations 1999
d) The Environmental Permitting Regulations 2000

Question 2
What color is a whole body dosimeter and where should you wear it?
a) It is red and you should wear it at the waist level
b) It is black and you should wear it at the waist level
c) It is blue and you should wear it anywhere on your body
d) It is red and you should wear it on your collar/sleeve

Question 3
Which of the following statements is correct?
a) "A collar dosimeter should be worn on your collar or sleeve nearest to the source of radiation and outside any protective clothing"
b) "A whole body dosimeter should be worn on your collar or sleeve nearest to the source of radiation and outside any protective clothing"

Question 4
Which two of the following are correct?
a) WB and CL dosimeters are worn for three months
b) Rings and wrist bands are worn for three months
c) WB and CL dosimeters are worn for one month
d) Rings and wrist bands are worn for one month

Question 5
What should you do if your dosimeter is lost?
a) Inform the Trust's Chief Executive in writing
b) Inform your Radiation Protection Supervisor or Radiation Protection Section so that a replacement can be issued to you
c) Ring 999 and report it

d) None of the above. Wait until you receive another one at the end of the wear period

Question 6
How much is Radiation Protection Section charged for each non-returned whole body or collar dosimeter?
a) £5
b) £9
c) £14
d) £21

Question 7
Which of the following statements is correct?
a) "Personal dosimeters using LiF material to record the dose are sensitive to heat and direct sunlight"
b) "Personal dosimeters using LiF material to record the dose are not affected by heat and direct sunlight"

Question 8
Where can you find the current investigation levels for staff doses?
a) On the Hospital's Intranet, where all policies are stored
b) In the Head of Department's office
c) In the Local Rules for each controlled area
d) They are written at the back of each dosimeter

Question 9
Which two of the following statements are correct?
a) The Whole Body and Collar dosimeters must be worn with the label facing your body
b) The Whole Body and Collar dosimeters must be worn with the label facing away from your body
c) Rings and wrist bands must be worn with the label visible on the outside of the hand /wrist by all members of staff regardless of their type of work
d) Rings and wrist bands must be worn so that the chip is always exposed to the maximum amount of radiation

Question 10
Are you entitled to see your dose record?
a) Yes, my RPS/nominated person receives the results and I can ask Radiation Protection to show me my record by giving them notice
b) No due to data protection reasons

THE SOCIAL WEB: THE FUTURE IS NOW

G. Sánchez Merino[1,2]

[1] Department of Medical Physics and Radiation Protection, Araba Integrated Health Care Organization, Vitoria-Gasteiz, Spain
[2] Chair of EFOMP (European Federation Of Organizations For Medical Physics) Communications and Publications Committee, EFOMP, York YO24 1ES,UK

Abstract— **This paper presents a review of the Social Web and its tools in the context of professional and scientific activity. The utility of these tools is discussed and some success examples are presented.**

Keywords— **Internet, Communication, Social Networks, Social Media, Blog, Twitter, Facebook, LinkedIn.**

I. INTRODUCTION

In his 1945 article "As We May Think", Vannevar Bush described *the memex*, a device in which individuals would compress and store all of their books, records, and communications. The concept of the memex influenced the development of early hypertext systems, eventually leading to the creation of the World Wide Web, by Tim Berners-Lee 45 years later. Being an extraordinary concept, the memex has been largely surpassed by the current communication tools based on the World Wide Web.

If we concentrate on the scientific activity, we may ask ourselves: Can we really measure the impact of these new tools in this context? Have their use proved of any benefit for the scientific community and its activity? In August last year, The Guardian published two articles dealing with the subject of the utility of social media in research. The first was titled: "I'm serious academic, not a professional Instagrammer" and presented a strong critic about the use of social media in research. In a few days, an ironic response came up: "I'm a non-serious academic. I make no apologies for this", dealing, point per point, with the issues pointed out by the first article. At least, what is clear is that Social Media tools are controversial and a continuum debate is taking place around them in the scientific community.

My aim here is to present some Social Media tools, and to show how they can be used to be useful in the context of research activity. In particular, how they can be used in the communication of the science research and the spread of its culture.

II. ANATOMY OF SOCIAL MEDIA

Let's begin by answering to this question: What is Social Media? Social Media is a group of internet-based applications that build on the ideological and technological foundations of Web 2.0, and that allow the creation and exchange of User Content [2]. Web 2.0 is a term that was first used in 2004 to describe a new way in which software developers and end-users started to utilize the World Wide Web. Content and applications were no longer created and published by individuals, but instead were continuously modified by all users in a participatory and collaborative fashion. Web 2.0 can be understood as the platform for the evolution of Social Media. User Generated Content can be seen as the sum of all ways in which people make use of Social Media, and describes the various forms of media content that are publicly available and created by end-users.

There are two important concepts that are useful to understand the potential scope and impact of Social Media. The first one is the concept of *social presence*, developed by John Short, Ederyn Williams and Bruce Christie in 1976. According with social presence theory, media differ in the degree of social presence they allow to emerge between two communication partners. Degree of social presence is equated to the degree of awareness of the other person in a communication interaction, and it is influenced by the intimacy and immediacy of the medium. The face-to-face medium is considered to have the most social presence, and written, text-based communication the least. In text-based communication, an e-mail has a lower degree of social presence than, say, a WhatsApp communication. The higher the social presence, the larger the social influence that the communication partners have on each other's behavior.

Closely related is the idea of *media richness*, introduced by Richard L. Daft and Robert H. Lengel in 1986 as an extension of information processing theory. It is based on the assumption that the goal of any communication is the resolution of ambiguity and the reduction of uncertainty, and is used to rank and evaluate the ability to reproduce the information sent over a certain communication media. The degree of richness of any media is related with the amount of information they allow to be transmitted in a given time. In this sense, some media are more effective than others in resolving ambiguity and uncertainty due to the possibility to allow conversations between communication partners.

III. TOOLS FOR COMMUNICATION

There are currently several applications for Social Media, differing in their degree of richness and social presence. It is important to note that these are dynamic properties that depend on several factors that continuously evolve in time, as, for example, the popularity of the application. The three main categories of Social Media applications are presented below.

A. Bolgs

Blogs represent the earliest form of Social Media. A blog is a discussion or informational website consisting of discrete, often informal text entries ("posts"). Posts are typically displayed in reverse chronological order, so that the most recent post appears first, at the top of the web page. Blogs could be the work of a single individual, or of a small group, and often covered a single subject or topic. Generally, although not always, blogs offer the possibility to comment post engaging the end-user in the construction of the content.

A lot of things have changed since the first blog, Links.net, was created by Justin Hall in 1994. The current, more mainstream, platforms like Blogger or World Press allow end-users to add comments to the post, thus increasing the social presence of the media. Besides, with the help of content hosting platforms (see the ones discussed in Content Communities section), blogs are not limited to text content, but can include video or other media, and that increases their richness.

B. Content Communities

Content communities are web 2.0 applications oriented to sharing media content between users. They exist for a wide range of different media types like photos (Flickr), videos (YouTube and Vimeo) or presentations (Slideshare).

Usually, content communities allow the creation of personal or brand profiles and the sharing of content in a social network-like fashion. Another popular use is as a hosting platform for content to be shared in blogs or social media.

C. Social Networking Applications

A social networking service is an online platform that enables users to build social networks or social relations with people who share similar personal or career interests, activities, backgrounds or real-life connections. They are based on the creation of personal, institutional or brand information profiles, and on the interconnection of these profiles through the exchange of instant messages.

The most popular application for Social Networking is Facebook, created by Mark Zuckerberg along with his fellow Harvard College students and roommates in 2004. Facebook has around 1.7 billion monthly active users (December 31, 2016) which makes its potential for interaction and influence huge. Twitter was created in March 2006 by Jack Dorsey, Noah Glass, Biz Stone, and Evan Williams, and is another very popular tool. Users post and interact with messages restricted to 140 characters ("tweets").

Being two very popular tools, Twitter and Facebook have different levels of acceptance in the scientific community. According to a recent survey published in Nature [7], among a subset of researchers active in social networks, very different patterns of use were found. While the majority declares the utility of Twitter to comment, actively discuss and share research and contact peers, very few researchers declare this use of Facebook, and that the majority, in fact, declare not using Facebook professionally.

Social networks are a noisy communication channel, but with a high social presence due to the high degree of interaction they allow.

IV. TWITTER SUCCESSFUL USES CASES

In the last years several articles and reports had been published dealing with the use of social networks for the transmission of scientific information to society.

Li et.al. in their article "Tweeting disaster: an analysis of online discourse about nuclear power in the wake of the Fukushima Daiichi nuclear accident" studied how people used online tools like Twitter to communicate about global and local environment and health risk related to nuclear power. They stress the utility of this kind of tools inasmuch as "reflecting spontaneous and trending opinions, Twitter, along with many other social media tools, allows policymakers and crisis managers to understand the concerns of a group of informed citizens who are well engaged in a given issue".

Vinay Prabhu and Andrew B. Rosenkrantz arrive to similar conclusions in their article "Imbalance of Opinions Expressed on Twitter Relating to CT Radiation Risk: An Opportunity for Increased Radiologist Representation". In their study, they try to asses perspectives and information relating to CT and radiation risk on Twitter. What they found was that the large majority of content shared was either unfavorable or concerned regarding CT radiation risk. Besides, most shared articles were not peer-reviewed, and were posted by non-professionals without any relation with medical imaging. They advocate that "more active engagement on Twitter by radiologist and physicist and increased dissemination of peer-reviewed articles may

achieve a more balanced representation and alleviate concerns regarding CT radiation risk on social networks".

An interesting action in relation to the use of social networks in the communication of medical information is the Social Oncology Project. The initiative, which has been in operation for four years, has sought to take the view of cancer in society. In their last report a shift has taken to capture a more detailed snapshot on how the members of communities (an ecosystem that includes doctors, patients, media and advocates) communicate and relate. What they found is that Twitter can be a very powerful tool when professionals participate in the conversation with patients: "There was a clear interest in education—no cat videos or Reddit memes—but the sources each group shared varied and demonstrated the different veins of information each group tapped. Doctors were far more likely to share peer-reviewed publications, patients and advocates preferred well-established consumer information sources and video content, media often referenced news stories. These patterns were not absolute, however: everyone in the community consumed information from a wide range of places, and the only consistent similarity was the high quality of the content." [9]

V. DISCUSSION

It goes without saying that the use of social media is a personal choice. And it is not an easy one, as it implies a high level of exposure with which not everyone feels comfortable. But it has proved to be a powerful tool for professionals to engage with peers and society.

For institutions, it is almost an obligation if they want to communicate in an effective way with the public. As current Chair of Communications and Publications of the EFOMP, my greatest efforts are focused on strengthening the presence in social networks, an activity that we inaugurated last year with Twitter and LinkedIn accounts.

And for the worried with the excess of self-promotion using social media, a last advice: use the Kardashian index to keep the ego at bay ;-)

REFERENCES

1. "Memex." Wikipedia: The Free Encyclopedia. Wikimedia Foundation, Inc. Retrieved March 15, 2017, <https://en.wikipedia.org/wiki/Memex>
2. Andreas M. Kaplan, Michael Haenlein, Users of the world unite! The challenges and opportunities of Social Media, Business Horizons (2010), 53, 59-68
3. Imbalance of Opinions Expressed on Twitter Relating to CT Radiation Risk: An Opportunity for Increased Radiologist Representation
4. "Social Presence Theory." Wikipedia: The Free Encyclopedia. Wikimedia Foundation, Inc. Retrieved March 15, 2017, <https://en.wikipedia.org/wiki/Social_presence_theory>
5. "Media Richness." Wikipedia: The Free Encyclopedia. Wikimedia Foundation, Inc. Retrieved March 15, 2017, <https://en.wikipedia.org/wiki/Media_richness_theory>
6. Nan Li et.al. Tweeting disaster: an analysis of online discourse about nuclear power in the wake of the Fukushima Daiichi nuclear accident, Journal of Science Communication, 15(2) 201
7. Prabhu, V. and Rosenkrantz, A. B. Imbalance of Opinions Expressed on Twitter Relating to CT Radiation Risk: An Opportunity for Increased Radiologist Representation, Amrican Journal of Radiology, 2015
8. Richard Von Noorden Scientist and the Social Network, Nature, Vol 512, 2014
9. Social Oncology Project Report, 2016
10. "Kardashian Index." Wikipedia: The Free Encyclopedia. Wikimedia Foundation, Inc. Retrieved March 15, 2017, <https://en.wikipedia.org/wiki/Kardashian_Index>

Contacts of the corresponding author:

Author: Gaspar Sánchez Merino
Institute: Araba Integrated Health Care Organization
Street: Jose Atxotegi, s/n
City: Vitoria-Gasteiz
Country: Spain
Email: gaspar.m@gmal.com

TWITTER: @GSPRSM

INVITED PAPERS

The Appearance and Origin of Common Magnetic Resonance Imaging Artifacts, and Solutions for Alleviating Their Effects

Puneet S. Sharma, PhD[1] and John N. Oshinski, PhD [1,2].

[1] Department of Radiology and Imaging Sciences, Emory University School of Medicine, 1364 Clifton Road, Atlanta GA 30322
[2] Department of Biomedical Engineering, Emory University School of Medicine, 1364 Clifton Road, Atlanta GA 30322

Abstract – The appearance of image artifacts in magnetic resonance imaging (MRI) continues to be an area of confusion for many medical physicists. Much of the complexity in the appearance of artifacts comes from the fact that image data is acquired in frequency-phase space (k-space) and the artifacts' appearance is related to how the signal is transformed into image space. Here we give a brief non-mathematical explanation of the elements of image quality and image acquisition, and present many of the most common image artifacts in the context of this explanation. Solutions for eliminating or mitigating the effects of these artifacts are offered.

Keywords – MRI, Magnetic Resonance Imaging, Artifacts, Physics

1. INTRODUCTION

One of the pervasive truths about Magnetic Resonance Imaging (MRI) is that all acquisitions possess some degree of image artifacts. An image artifact is any feature that is present in an image that is not present in the original object. Sometimes artifacts are severe enough to obscure diagnostic interpretation or cause a mis-diagnosis, while others are insignificant or imperceptible to the radiologist. The medical physicist must be able to recognize artifacts and understand why they occur. Furthermore, it is important to outline possible remedies for more deleterious artifacts, and what personnel are most equipped to solve them (technologist, physicist, or vendor service engineer). MRI artifacts are generally classified into three broad groups: 1) Physiological-related, 2) System- or parameter-related, 3) Reconstruction-related.

Physiological artifacts evolve from the interaction between the subject and the MR system during acquisition. Specifically, it is important to understand how the MR pulse sequence is affected by the anatomy and physiology of interest. System-related artifacts stem from degradation or transient effects in the MR system and/or acquisition components. Establishing a local quality assurance (QA) program and periodic vendor-led preventative maintenance (PM) help recognize and ameliorate these issues. Reconstruction artifacts result from non-optimal implementation or failure of the reconstruction algorithm, such as artifacts arising from parallel imaging reconstruction.

In this article, we will outline the most common MR artifacts, including details about their mechanism, and we provide suggestions for possible solutions. We will pay special attention to pulse sequences and system configurations most usually affected by these artifacts. In addition, we will discuss aspects of a quality assurance program, especially the role of the MR Physicist in clinical practice. It is important to begin the discussion of artifacts by first considering the elements that constitute high quality MRI, followed by a brief review of k-space signal acquisition principles, then presentation and characterization of the artifacts.

1.2 ELEMENTS OF OPTIMAL MR IMAGE QUALITY

At its core, the goal of any modality and image acquisition strategy is to produce diagnostic information with consistently high image quality. Though this concept is abstract, high image quality can be defined empirically as possessing high signal- and contrast-to-noise, high resolution, and minimal artifacts, while achieving scan times as low as possible. This pursuit, however, is tempered by a variety of tradeoffs. In MRI, fast-imaging generally comes at the expense of each of these image characteristics, but primarily image resolution and signal-to-noise. Consider the basic equation for MR scan time (for 3D imaging) (1) :

$$Scan\ time = TR \times N_y \times N_z \times NSA \qquad [1]$$

Where TR is the sequence repetition time, N_y and N_z are the number of y- and z-phase encode steps, respectively, and NSA is the number of signal averages. It can be seen immediately that scan time is proportional to phase resolution (N_y and N_z) and signal strength (NSA), with repetition time largely dictated by the desired contrast of the image acquisition. There are more detailed parameters in an MRI acquisition that affect Equation 1, such as image matrix, slice thickness, slices, and bandwidth. These other parameters are typically defined by the requisite anatomical coverage, contrast sensitivity, and image resolution criteria set forth by radiologists and physicians based on specific needs for disease characterization. Though disease contrast resolution is of utmost importance in diagnostic MRI, the basic relationship that ultimately governs image quality is signal-to-noise ratio (SNR). MRI signal is proportional to the amount (and strength) of the magnetization in a voxel, and signal averaging. Measured noise, however, is proportional primarily to the acquisition readout bandwidth (BW_{read}), assuming other thermal and resistive components are relatively invariable. Hence the SNR per voxel (for 3D imaging) is:

$$SNR \propto K \cdot (\Delta x \cdot \Delta y \cdot \Delta z) \cdot \left(\sqrt{\frac{NSA \cdot N_x \cdot N_y \cdot N_z}{BW_{read}}} \right)$$

Where K represents all other imaging factors (coil, field strength, relaxation, tissue parameters, etc). The form of Equation 2 can be rewritten to describe relationships with other parameters, such as field-of-view (FOV), by substituting known equivalencies (i.e. $\Delta x = FOV/N_x$). This is beneficial when considering the consequences of fixed variables (such as Δx) on SNR (1).

The overlap between Equation 1 and 2 is clear, and one begins to understand the tradeoff among resolution, SNR, and scan time, especially the cost of high resolution imaging. For instance, if resolution N_y is doubled, SNR reduces by $1/\sqrt{2}$, while scan time is doubled. It is important to consider these costs quantitatively, but only in light of baseline SNR and scan time values. One may also choose to normalize SNR against scan time for better describing scan efficiency.

The complete picture of high MR image quality must also integrate equipment variables, contrast mechanisms, and imaging artifacts. While the former two elements can be gauged as part of preventative maintenance and disease-driven protocol criteria, respectively, and absorbed by the "K" term of Equation 2, image artifacts are primarily monitored and assessed qualitatively. In the sections to follow, we will investigate where and when artifacts present themselves, while later presenting methods to help track and resolve artifacts programmatically.

1.2. K-SPACE PRINCIPLES

The three broad MR artifact categories outlined earlier (System, Reconstruction, and Physiologic) have effects on

MR image acquisition that cause it deviate from the ideal scenario. MRI uses rapidly switching linear magnetic field gradients to specifically encode the origin of measured signal repeatedly over the duration of an acquisition. These gradients cause the image data to be acquired in frequency-phase space (or k-space), and therefore a significant emphasis is placed on the integrity of the raw (or k-space) data. As unwanted intrinsic and extrinsic factors alter the specific encoding and signal acquisition process, the measurement of MR data becomes discordant with expected phase- and frequency-encoded values. Whether raw data is collected all-together in one-TR, or periodically over multiple TRs, the relationship between the multiple encoded signals in k-space, and when they were temporally acquired, play an important role in predicting the prevalence of MR artifacts. For this reason, it is important to briefly discuss the key principles of 2D Fourier imaging and k-space.

In order to generate a grey-value for every voxel in the image, a method must be applied to spatially localize the spin density. The most widely used method is 2D Fourier imaging whereby applying a linear magnetic field gradient in one direction (e.g. x-direction) causes the Larmor frequency of the excited spin density to vary predictably across the field-of-view. The resultant (echo) signal (produced by either gradient or spin echo) is therefore regarded to be a combination of defined spatial-frequencies. The notion that a linear gradient provides a spatial- and time-dependent change in the precession frequency (and phase) of the spin density allows convenient interpretation using well-studied Fourier analysis. For the second dimension (i.e. y-direction), further frequency-encoding cannot be applied since unique assignment of spatial-frequency will not be possible for all unknown voxels. To overcome this, a brief linear gradient "pulse" is applied in the y-direction prior to frequency encoding. The consequence of a finite gradient is to impart a specific phase-shift along the second-dimension. To provide enough unique data to satisfy Fourier analysis and recover the original spin density, the process of phase-encoding is repeated every TR (or echo-signal), with the gradient amplitude incremented (ΔG_y) each time and followed by frequency encoding during data collection.

Since the individual ΔG_y step size and duration (τ_y) is known, the frequency-encoded echo signal can be measured and recorded into a particular "address" in k-space. The raw data points in k-space are discrete due to signal digitization, and therefore assigned k_y and k_x indices related by the equations:

$$k_x = \gamma G_x \Delta t$$
$$k_y = \gamma \Delta G_y \tau_y$$

In essence, each point in k-space (k_x, k_y) represents a spatial frequency, or oscillation "pattern". The intensity of the point signifies the weighted contribution of the frequency pattern to the original image features. The center of k-space represents low frequency patterns and, thus, the

majority of overall signal strength of the image. The periphery of k-space represents high frequency components, which more define the sharp signal changes in the image, such as near tissue interfaces and edges. Since the discrete Fourier transform connects the raw k-space data to image space, reconstruction is subject to transform properties, and artifacts in the acquired raw frequency-phase data transformed into the image data (1).

2.0. REVIEW OF MRI ARTIFACTS

The concepts of k-space acquisition and Fourier transform properties provide the medical physicist the background to understand the role of the MR acquisition process in the generation and appearance of image artifacts. However, the diagnosis of MR artifacts begins at the image level by recognizing distinct abnormalities in the image. It is important to distinguish image artifacts from poor signal-to-noise ratio or poor contrast-resolution, which are generally overcome through protocol optimization (although some poor SNR may be system- or electronics-related). In the sections to follow, we will describe the appearance and origin of commonly encountered artifacts, highlighting their sensitivity to system and reconstruction imperfections, patient physiology, and suggest solutions for mitigating or alleviating artifacts.

2.1. PHYSIOLOGIC ARTIFACTS: MOTION AND PHASE ENCODING EFFECTS

Appearance: Physiologic motion causes image artifacts, the most prevalent being image ghosting, *figure 1*. The "ghost" terminology originates from the observation of faint replicated copies of the imaged structures along the phase encode direction. Image ghosts may also be very distinct, especially if the moving object is high signal, such as fat or fluid. The occurrence of this artifact is a result of k-space sampling during the motion of an imaged object. In clinical practice, this is mostly caused by patient movement, breathing, blood flow, or cardiac motion. Even subtle motion, such as eye movement and swallowing, can cause motion-related ghosting.

Origins/Causes: The propagation of ghosts along the phase encode direction distinguishes them from other similar artifacts, such as truncation (or Gibbs "ringing") artifacts, which occur in all directions, and will be discussed later. The sensitivity to the phase encode direction evolves from the relatively slow sampling rate of phase encode steps relative to the motion of a moving object. The effective sampling rate in the phase encode direction is on the order of 1 to 100Hz (1/TR, for single-echo imaging), compared to kHz ($1/\Delta t = BW_{read}$) in the frequency encode direction. Therefore, during periodic motion, such as breathing in abdominal imaging, each phase step may encode information from a different diaphragm position over the course of an MR acquisition. This measurement inconsistency among the phase encode steps has two main consequences: 1) the absolute signal strength (due to inflow, tissue spin density, etc.) may vary between steps and 2) an additional phase shift is accrued due to tissue positional changes. Since MRI acquisitions assume the signal changes exclusively from k-space localization, this inconsistency causes k-space variability in the phase encode direction. This phase and signal variability is dependent on the sampling rate and the periodicity (and intensity) of the object motion.

Location: The properties of Fourier transform, which result from phase shifts in k-space due to *periodic* motion, cause a corresponding position shift of the object in the reconstructed image, resulting in ghosts. The degree of spatial shift is proportional to the displacement of the motion, so small motion results in ghosts with small displacements from the object. For *non-periodic* motion, the presentation of motion ghosts in images may appear somewhat random, especially if motion contains several harmonics, such as irregular breathing, eye-blinking, or gross head movements. In these cases, distinct ghosts are often not visualized, but rather blurring in the phase encoding direction predominates. If motion is fast enough, ghosts or blurring may also occur in the frequency encode direction. However, ghosting predominantly occurs due to motion is typically in the phase encoding direction.

Strategies for Alleviating Artifacts: Several methods are available to compensate for motion artifacts. A simple method is to swap the phase- and frequency-encode direction. Though not eliminated, this tactic can redirect motion ghosts into other directions, thereby revealing relevant anatomy. This performs best for small-dimensioned ghosts, such as those from vessels, eye-movement, swallowing, and peristalsis.

Since the variability of additional phase shifts in k-space dictate the occurrence of ghosts in the final image, synchronizing phase encode steps with motion eliminates inconsistencies. In the common case of respiration, this is accomplished through respiratory or navigator gating, in which a breathing belt or additional 1-D MR data across the diaphragm enables real-time tracking of abdominal and diaphragm movement. This system is configured to accept or discard raw data based on respiratory position, such as end-expiration. Though effective, respiratory gating has noteworthy shortcomings: 1) accepting only consistent data may result in lengthy scan times; and 2) an often integrated "data acceptance window" (+/- 2mm) may re-introduce some minor phase shifts, causing some subtle ghosts in the final image. When possible, routine abdominal imaging relies on breath hold imaging. However, its effectiveness clearly depends on patient cooperation, and fast imaging techniques optimized for quality and scan time. Modern MR systems are increasingly capable of high resolution breath hold imaging through advanced acceleration techniques, such as parallel imaging (2,3) and compressed sensing (2).

Data averaging is another method to reduce motion-induced ghosts. This is achieved by increasing the number

of signal averages (NSA), which also invariably increases scan time. MR signal averaging re-acquires each phase encode step, which is then combined to previous data prior to reconstruction. Essentially, data averaging reduces the degree of k-space variability by making phase transitions more gradual. While distinct phase ghosts can be eliminated, the result is more image blurring. The degree of effectiveness of this solution depends on the clinical application. Diffusion-weighted imaging (DWI) of the abdomen benefits from signal averaging since the subtle edge-blurring of large coherent tissue motion does not affect the small incoherent diffusion motion encoding imposed by the large diffusion-sensitizing gradients (4). Moreover, DWI is often acquired using a "single-shot" echo-planar (EPI) technique, which collects all phase-encode steps sequentially in less than 300ms. This pulse sequence strategy is itself motion-insensitive, since the k_y sampling frequency is significantly increased, effectively "freezing" bulk tissue motion. Single-shot MRI has also become routine for T2-weighted abdominal imaging. Some drawbacks persist, such as edge blurring, due to signal decay over the echo-train, and slice mis-registration for multi-slice acquisitions.

Another method to compensate for motion artifacts is to acquire k-space data with a radial trajectory. A radial trajectory through k-space is achieved by performing gradient frequency encoding in both the k_x and k_y directions, simultaneously. Similar to "single-shot" approaches, this allows the k-space sampling rate in each direction to be on the same order (kHz) during one TR. In addition to sampling k-space at a fast rate compared to object motion, the trajectory also passes though the center of k-space every TR period. This has a similar effect as signal averaging, since similar central k-space samples are acquired repeatedly, albeit at a higher rate. The amount of low k-space oversampling density is directly proportional to motion artifact reduction. However, a disadvantage is that high k-space data has subsequently lower sampling density, which introduces new artifacts, such as streaking. To achieve high motion-insensitive quality with radial k-space, lengthy scan times are often needed to provide sufficient sampling density.

3.0. SYSTEM-RELATED ARTIFACTS

3.1. NYQUIST GHOSTING

Appearance: Similar to motion, Nyquist ghosting are artifacts appear as distinct copies of the imaged object, propagated across the FOV in the phase encode direction, *figure 2*. The Nyquist ghost is often referred to as "N/2" ghosts, since the object is shifted half (N/2) the FOV in the phase encode direction. However, the object shift could be less (e.g N/8, etc) if the data acquisition is divided into more segments (e.g 4 segments). The effect is mainly seen with echo-planar imaging (EPI) or partial Fourier imaging, which requires rapid gradient switching to capture complete k-space data within a short duration (~100-

300ms). The Nyquist ghosts can be distinguished from motion induced ghosting described above by the periodic shift of ghosts across the field of view. In addition, the Nyquist ghosts have the same intensity for each ghost, which is not normally true in motion-induced ghosts.

Origins/Causes: The method of k-space sampling in fast imaging techniques such as EPI where all signal echoes are acquired in one segment, or "shot", uses a very high bandwidth, enabling accelerated data collection. Once each line of k-space is acquired, frequency-encode gradients are quickly (and equally) reversed. This rapid gradient switching is coupled with a defined increment in the phase encode gradient, resulting in a "zig-zag" trajectory through k-space, with every other echo signal measured with a reversed gradient polarity. The general assumption is that each echo is perfectly phase-centered for each gradient-reversal step. However, gradients cannot achieve instantaneous gradient reversal, even with maximum slew rates, but, rather, finite time is required for gradient ramp up/down. These slight timing delays explain the notion of the so-called "zig-zag" k-space trajectory, and may cause an additional phase in the measured signal. The high demands placed on balanced timing delays and consistent gradient reversals make EPI susceptible to phase offsets propagated throughout k-space. When there is a fixed phase offset between each adjacent echo measurement, the Fourier transform of raw data into image space results in an object displacement of half the FOV. This displacement is akin to those discussed with respiratory artifacts: if each phase-encode step acquired data alternatively between inspiration and expiration, ghost artifacts would resemble those associated with Nyquist EPI ghosts.

Most systems are well-calibrated and do not experience any inherent gradient timing delays (even though ramp-up, ramp-down times always exist). But the unique k-sampling of EPI methods make it susceptible to other factors that may introduce unpredictable signal phase shifts. Essentially, any B_0 inhomogeneity will have an influence on consistent spatial localization. However, the most common cause is eddy currents in the gradient coils. These additional currents are induced in response to the rapidly switching gradients during EPI acquisitions. In effect, eddy currents produce an additional local gradient magnetic field, which is then superimposed onto the prescribed acquisition gradients.

Strategies for Alleviating Artifacts: As an initial step, Nyquist ghosts can be mitigated by addressing the factors impairing field homogeneity. It is important to use higher-order, advanced shim settings to reduce local inhomogenities. However, the likely culprits of Nyquist ghosts, in the absence of patient motion, are the consequences resulting from the high gradient demands of EPI, such as eddy currents and other unforeseen timing delays. While some system architecture exists for eddy current compensation, it benefits to identify this root cause. The isolation of gradient-related Nyquist ghosts can be

accomplished through re-calibration by a service engineer, or replicated through local phantom testing. With an MR phantom, field homogeneity and object motion can be controlled during EPI scanning. Moreover, other rapid sequences, such as signal-shot TSE, which also demand consistent, phase-centered echoes, can also be tested to reveal evidence of residual gradient mis-timing effects. It is possible to reduce the demands to the gradient system by lowering the gradient strength and switching speed. However, this may introduce other artifacts in place of Nyquists ghosts, such as distortion due to reduced phase-encode sampling rate. Ultimately, routine system service by an engineer may be needed to confirm findings and recalibrate gradients.

Another factor that lessens the likelihood for Nyquist ghosts are mechanisms that reduce the sequence echo train length (ETL). As alluded earlier in this section, increasing the number of k-space "segments" reduces the propagation of phase errors over the complete data set. Though ghosts may persist if evident system timing imperfections are present, the N/2-appearance may not obscure image quality as significantly. Other methods to reduce ETL include reducing the phase resolution (less N_y points) or utilizing parallel imaging.

3.2. CHEMICAL SHIFT ARTIFACTS

Appearance: Two variations of the chemical shift artifact manifest in MRI. A type 1 chemical shift artifact typically occurs in the frequency encode (k_x) direction, and is the product of spatial misregistration between fat and water protons. The appearance is dark etching along boundaries between fat and other tissues. This artifact is sometime referred to as the 'india-ink' artifact, as tissues appear to be outlined in dark ink, *figure 3*. In echo-planar imaging (EPI), such fat misregistration typically occurs in the phase-encode direction, and is commonly visualized when fat suppression is not used or is inhomogeneous. A type 2 chemical shift artifact occurs in all directions and within tissue itself. It presents as complete signal loss at as tissue signal loss dependent on the proportion of fat/water voxel composition, *figure 4*. Type 2 chemical shift artifact is commonly associated with gradient echo techniques, and is often viewed as beneficial for assessing diffuse fatty tissues, such as liver, or identifying fat containing lesions.

Origins/Causes: The basis of chemical shift artifacts is the difference in precession frequency between fat and water protons (3.5ppm). At 1.5T, this difference (Δf) translates to an offset of 220Hz, while at 3T, the difference is 440 Hz. This distinction allows the precise estimation of the fat/water mis-registration in the image: given field-of-view (FOV), bandwidth (BW_{read}), and matrix size (N_x), one can calculate the spatial water-fat shift (WFS):

$$WFS = \frac{FOV \cdot \Delta f}{N_x \cdot BW_{read}}$$

If the WFS is greater than the spatial resolution in the frequency encode direction, some fat components will superimpose onto neighboring pixels, revealing dark boundary effects. This is the typical feature of type 1 chemical shift artifact. The misregistration is exacerbated at high field strength given equivalent parameters, due to increased Δf. It is also evident when matrix and/or bandwidth are low, or FOV is large. The prevalence of type 1 artifact to the frequency encode direction (for non-EPI sequences) is due to the relatively low readout BW of these sequences, as well as the fact that transverse magnetization is either refocused or spoiled for each echo measurement. This effectively negates the accumulation of precession-related offsets in the phase-encode direction.

Precession differences are also the source of type 2 artifact, which is mainly associated with gradient echo imaging. If fat and water protons coexist in one voxel, they will become progressively out-of-phase relative to each other following RF excitation (3). If the pulse sequence is precisely timed, there will be a particular time in which fat and water protons are 180 degrees out-of-phase, resulting in signal cancellation. At 1.5T, this time occurs approximately every 4.4ms, beginning with 2.2ms. At 3T it occurs every 2.2ms, beginning with 1.1ms. Some gradient-echo sequences are timed such that the echo time (TE) occurs when fat and water are opposed-phase, so that important information about fat containing lesions and tissues can be observed. Typical applications also include an "in-phase" acquisition, in which a second echo is measured when fat and water are coherent. It is important to note that signal loss due to opposed-phase effects is proportional to the fractional content of fat in the voxel, with 50% resulting is complete signal loss. However, if the fractional content is greater than 50%, signal amplitude will increase, with fat protons predominating voxel concentration. It is also important to note that type 2 chemical shift signal loss does not naturally occur in spin echo imaging. This is due to 180 degree RF refocusing, with TE selected to coincide with complete re-phasing of transverse magnetization.

Strategies for Alleviating Artifacts: From the equation above, type 1 chemical shift artifact can be corrected by selecting imaging parameters appropriately. Since FOV and matrix are often fixed due to application criteria, increasing bandwidth often remedies the artifact. This tactic also has less SNR penalty than increases in image resolution. Alternatively, frequency and phase directions can be swapped, in lieu of any parameter adjustment, as long as other artifacts, such as aliasing and motion, are not adversely affected. One must also be wary of chemical shift at high field strengths, since one-to-one transfer of imaging parameters will not be optimal; a proportional increase in BW is necessary to achieve the same WFS as lower field strength. Another solution to eliminate the appearance of fat shifts is to employ fat saturation. Though effective, this clearly alters the imaging

application, and may not be warranted in clinical application.

As mentioned above, type 2 chemical shift artifact is often desired in many clinical applications. However, it is usually common to acquire a corresponding in-phase image concurrently. Since other factors, such as iron deposition or susceptibility, may also contribute to signal loss on gradient echo images, it is recommended to acquire opposed-phase images using the first out-of-phase TE (1.5T: 2.2ms; 3T: 1.1ms). In other applications that do not call for interrogating fat composition, elimination of the type 2 artifact is achieved simply by acquiring data using in-phase TEs (1.5T: 4.4ms; 3T: 2.2ms), or using fat suppression. Note that incomplete fat suppression may still result in type 2-related signal loss, if TE is chosen near the opposed-phase TE.

3.3. SUSCEPTIBILITY-RELATED SIGNAL LOSS

Appearance: Areas of local signal loss, signal pile up (non-anatomical bright and dark areas near each other), and warping of geometry.

Origin/Causes: When external magnetic fields are applied to tissues, the tissues alter the applied magnetic field based on their physical and chemical composition. Magnetic susceptibility is a property that indicates how magnetization is effected in a tissue in response to applied magnetic field. Tissues that strengthen the applied magnetic field, are called *paramagnetic* and substances weaken the applied magnetic field are *diamagnetic*. When adjacent tissues have large differences in magnetic susceptibilities, they produce changes in the magnetic field, so the *local* magnetic field is then altered from its expected value. This can cause complete signal loss at the interface if the frequency change causes the signal to become far off from the resonance frequency. It also causes changes in the frequency distribution during frequency encoding, leading to mis-mapping of signal position in the images. The mis-mapping can cause signal 'pile-up' where signal from different locations are assigned to the same position due to incorrect frequency position, *figure 5*. The local alterations in the field induces a gradient in the field which increases signal dephasing. This accelerates the T2-decay of the signal and is often called T2* to differentiate it from conventional T2 effects.

The size of the susceptibility artifact is proportional to:

$$Degree\ of\ suscept\ artifact \propto \frac{(\Delta\chi) \cdot TE \cdot B_0}{BW_{read}}$$

Where $\Delta\chi$ is the susceptibility, TE is the echo time, B_0 is the magnetic field strength and BW_{read} is the readouts (frequency) bandwidth (4, 5).

Location: Susceptibility artifacts are present in areas where there is a large natural susceptibility ($\Delta\chi$) difference between two adjacent tissues. The most common location for these artifacts to occur is at tissue-air interfaces, including near the lung, in the nasal sinuses, or at the body surface. Areas in the brain or liver that may have a large iron buildup due to a pathologic state may also show susceptibility effects. Another other common location for susceptibility-induced artifacts is near any metal implants in or on the body. The metal is highly paramagnetic or even ferromagnetic, inducing large local changes in the magnetic field.

Susceptibility artifacts are most often present in gradient echo sequences, especially in gradient echo EPI sequences due to the large and rapidly changing magnetic field gradient applied in this sequences. Note that the use of the susceptibility effects to enhance tissue characterization has recently become an active area of research. S*usceptibility-weight imaging (SWI)* uses the effect of susceptibility to characterize tissue properties, and is especially useful for looking at iron content in the brain (5).

Strategies for Alleviating Artifacts: Susceptibility artifacts are ultimately due to dephasing of spins due to the presence of local magnetic field gradients. Ways to mitigate this dephasing include using a spin echo sequence instead of a gradient echo sequence. By examining the susceptibility equation, we can see that reducing the echo time or using an ultrashort TE sequence can reduce susceptibility artifacts. Increasing receiver bandwidth also reduces artifacts. Reducing pixel size can also reduce susceptibility by reducing the bandwidth per pixel in the image, but this comes at a signal-to-noise penalty. New MRI sequences which incorporate several of these susceptibility-reducing attributes have recently been developed by several MRI scanner manufacturers, especially for imaging in the present of metal implants for orthopedic applications (6). Finally, susceptibility induced artifacts are also proportional to the magnetic field strength, so they will be more pronounced at higher fields, such as 3.0 Tesla scanners (6) (7).

3.4. ALIASING/WRAPAROUND/FOLDOVER

Appearance: Objects from beyond the prescribed FOV are superimposed on the opposite side of the image in the phase-encoding direction.

Origins/Causes: The tissue that is outside the prescribed field of view (FOV) is still excited by the RF pulse and is subject to the applied magnetic field gradients. The phase encoding gradient imparts phase shifts of +/- 180° over this FOV in the phase encoding direction. Tissue that is outside the FOV will have a phase shift that is either >180° or < -180°. A phase shift of a signal is that is, for example, 181° is equivalent to a phase shift of -179° because of the cyclic nature of the MRI signal. Therefore signal outside of the FOV will be 'wrapped' to the other side of the image, *figure 6*. The frequency encoding direction is not affected by aliasing, as the frequencies above of beyond the receiver bandwidth are ignored.

Location: When the prescribed FOV is smaller than the object in PE direction, and coils are present that can detect signal from outside of the FOV, aliasing can occur.

Sometimes a small amount of aliasing in the image is tolerable if it can be easily identified, it does not interfere with the part of the image that is of concern clinically, and the region that is contains aliasing artifact can be seen in another imaging sequence.

Strategies for Alleviating Artifacts: The easiest way to remove the aliasing artifact is to increase the FOV. Of course increasing the FOV without increasing the number of phase encoding lines will reduce the image resolution, and increasing the number of phase encoding lines will increase the scan time. Saturation slabs can be placed over the area outside the chosen FOV to remove signal from the area that would normally wrap into the image. Additionally, the phase encoding direction can be aligned along the shortest dimension in the image to reduce the change of phase wrapping. Finally over-sampling in the phase encoding direction can be done. This is essentially acquiring (but not displaying) data in the phase encoding direction. Aliasing artifacts affect all types of MR sequences using Cartesian (line by line) acquisition of k-space. Aliasing in radial sequences is seen as noise and blurring.

3.5. RF NOISE/INTERFERENCE

Appearance: Zipper lines, checkerboards, or herringbone structures appearing in the image.

Origins/Causes: The receiver coils are designed to pick up signals from the tissue in the body. This signal is quite small and therefore antennas need to be quite sensitive at detecting small amounts of RF. If there equipment that is putting off signal frequencies near the receiver coils, they will be picked up. This can be electronic equipment in the MRI room, or a leak in the copper Faraday cage that surrounds and shields the MRI scanner room. These spurious signals will be placed in k-space and transformed through the Fourier transform into image artifacts. The zipper pattern sometime seen along one direction in the image is related to noise arising at a specific frequency. The herring-bone patterns are usually related to a noise spike in k-space and may be related to poor coil connections or poorly performing coils, *figure 7*.

Strategies for Alleviating Artifacts: Ensure that there is no electronic equipment that is operating the MRI scanner room that is not specifically designed for operation in an MRI environment. Ensure that there are no new penetrations in the shielding surrounding the MRI scanner room. Analyze the door to MRI suite for leaks in the seal, and ensure the door is closed during scanning. Check coil connections and integrity of pins on the coils.

3.6. DIELECTRIC EFFECT

Appearance: Shading or focusing across the image, usually with the brightest or darkest area of the image near the center.

Origins/Causes: Resonant frequency is proportional to the strength of the main magnetic field. The wavelength of the transmitted RF pulse is inversely proportional to the resonant frequency so it decreases with increasing main magnetic field. At higher the magnetic fields (3.0 Telsa and above), the wavelength of the transmitted RF pulse in on the order of the dimension of the objects being imaged, causing the strength of RF field to vary with spatial position. The effect has been referred to as "field-focusing", because flip angles are increased or "focused" near the center of the field of view (8). However, the effects can be quite variable and are not easily predicted. These effects can generally be ignored at 1.5T, but must be considered at 3.0T and above.

Strategies for Alleviating Artifacts: The easiest way to remove the dielectric effect is to scan at a lower magnetic field strength (1.5 Tesla of below). A method to reduce variations in signal intensity at 3.0 Tesla is to use dielectric pads made with a high dielectric constant that reduces RF pulse inhomogeneity. Finally, use of specialized 'tailored' RF pulses can reduce the variation of the flip angle across the FOV (9).

3.7. TRUNCATION ARTIFACT/GIBBS RINGING

Appearance: The truncation artifact is also known as *Gibbs ringing*. As the name implies, the artifact manifests as faint lines propagating from tissues edges, especially sharp edges between high contrast tissues, *figure 8*. Additionally, truncation artifact tends to fade away rapidly. This latter appearance distinguishes it from motion-related artifact, which present as distinct replicas of the object. Moreover, even subtle motion artifacts, which present small ghosts or blurred edges, can be differentiated from truncation artifact, since they often affect all tissue objects diffusely. Truncation artifact is specific to sharp transition edges, and may not affect all tissues in the FOV. Finally, truncation artifact appears mostly with lower resolution images, which may be an element of fast imaging techniques.

Origin/Causes: "Truncation" refers to the idea that k-space data is not continuous, but discretely sampled. This places a limit on the maximum encoded spatial frequency. From Fourier analysis, a sharp ("box-shaped") interface can only be approximated with an infinite number of frequency components. Since it is not possible in MR to sample an infinite number of spatial frequencies, finite frequency sampling limits the frequency components that can effectively describe the sharp edge. This translates to an overshoot and undershoot of sinusoidal signals in the vicinity of the interface, which gradually fade away. Moreover, if too few frequency components are used to approximate an interface, a false widening of that edge is presented. In terms of acquisition parameters, the maximum spatial frequency component (k_{max}) in both directions is defined by the product of the number of points (N_x and N_y), the gradient strength (G_x and G_y), and

sampling rate (dt). Therefore, for given bandwidth and gradient settings, the matrix in both the phase and frequency direction dictates the prevalence of truncation artifact. Since the phase resolution is typically lower, truncation artifact predominates in the phase encode direction.

Strategies for Alleviating Artifacts: The most commonly used solution for truncation artifacts are smoothing filters applied to k-space data prior to image reconstruction. An important tradeoff is image blurring, which may not be desirable in certain applications. If SNR is sufficient, resolution should be increased in the direction of ringing. This also includes the slice direction in 3D imaging, which is a commonly under-sampled for speed and improved SNR. Interpolation with zero-filling is often used to improve apparent resolution, but it does not concomitantly reduce truncation artifact, since it does not introduce new high spatial frequency data.

3.8. IMPROPER FAT SUPPRESSION

Appearance: Areas of high and low signal in regions of fat within the body when fat suppression is employed. One key advantage of a resonant frequency difference between water and fat protons is the ability to selectively *saturate* the magnetization of fat in MR images. Fat suppression has many applications, including eliminating confounding high signal from post-contrast T1 weighted imaging, and making edema and inflammation more conspicuous on T2-weighted imaging. A variety of methods exist for fat suppression, but the primary procedure is application of a chemical-shift sensitive RF excitation, centered on the resonant frequency of fat. In actuality, fat has up to six different resonant frequencies, with the most significant occurring at 1.3ppm, 2.1ppm, and 0.9ppm. For this reason, spectrally-selective RF pulses must also have a prescribed bandwidth, but must be limited to prevent intruding water resonance at 4.7ppm.

Ideal fat suppression should ensure uniform low signal intensity across the entire field-of-view, and among all slices, making the appearance of poor fat saturation clearly evident in most MR images. Poor fat suppression presents as regional elevation of fat signal intensity. It primarily occurs along the periphery of large field-of-view images, and in areas of complex or abnormal tissue geometry, such as the abdomen, neck, or breast, *figure 9*. Fat suppression is also rendered ineffective around metal implants, or significant gas/air interfaces. Moreover, large axial slice coverage, as in abdominal imaging, may suffer from non-uniform fat suppression on more superior and inferior slices.

Origins/Causes: The common theme among the locations of poor fat suppression is local field inhomogenity. In the majority of MR acquisitions, the frequency offset for fat suppression RF pulses are tuned based on global shimming procedures established before scanning begins. It does not subsequently adjust for field

inhomogeneities caused by local susceptibility changes. If certain voxels exist in regions of high susceptibility, such as adjacent to metal, the local resonant offset of fat will be more pronounced than predicted 1.3ppm, which is targeted by pre-tuned RF pulses. Sharp geometric transitions also cause voxels in this vicinity to possess resonant frequencies far different that default values. Additionally, local inhomogeneity may increase line broadening for fat resonances, which also may extend beyond the finite saturation bandwidth. All these instances cause the incomplete excitation of fat protons.

Separate from local susceptibility changes, large FOV imaging also causes regions of poor fat suppression, primarily along the periphery of the FOV. Fat –containing voxels located along the periphery are significantly far from isocenter, where field inhomogeneity also predominates. This also pertains to multi-slice axial imaging; poor fat suppression is often seen on first and last slices of axial data sets with large number of slices.

Another source of poor fat suppression is inefficient spectrally-selective RF pulses. Two important factors affect these RF pulses. First, even though a finite excitation bandwidth is tuned to 1.3ppm, sharp frequency cutoffs are difficult to achieve, especially over a small spectral range. Consequently, the bell-shaped profile may cause some varying excitation of resonances inside and outside the frequency bounds. The second factor is the B1 field, which defines excitation efficiency of the fat saturation pulses. Similar to B0 inhomogeneity, perturbations in B1 field causes the RF excitation flip angle to be spatially variant. Hence, certain fat voxels may experience different saturation flip angles than other, which results non-uniform suppression. Typically, diaelectric effects, such as those experienced at high field strengths, significantly alter B1 field uniformity.

Strategies for Alleviating Artifacts: An immediate solution to poor fat suppression is improving the fat suppression pulses themselves. Using longer pulse durations with selective phase dispersion, or adiabatic RF excitation help improve the spectrum of targeted fat protons. Alternatively, spectral excitation can be performed on water protons only, whose spectral amplitude and line width are usually more well-defined than fat.

Since fat suppression methods are generally spectrally-selective RF pulses, converting to *short-tau inversion recovery (STIR)* techniques offers increased suppression uniformity over broad FOVs and field inhomogeneity. STIR utilizes a non-selective 180 degree inversion (IR) pre-pulse timed to null the longitudinal magnetization of fat protons prior to image acquisition. The longitudinal T1 recovery of fat is approximately 250ms at 1.5T, and is adequately nulled using an inversion time (TI) of 150 to 160ms. Since the IR pre-pulse affects both fat and water proton resonant frequencies, all tissue will undergo longitudinal T1 recovery. Most tissues relax slower than fat, and will not be suppressed at the selected TI; however, they will incur reduced available magnetization, which

translates to reduced image SNR. There will be similar tissue T1 relaxation with STIR post-contrast administration, restricting its use as a surrogate for fat-suppressed contrast-enhanced T1 imaging.

Another strategy for improved fat suppression uniformity is to perform manual shimming of the main (B0) magnetic field. This can be accomplished with locally-assigned shim volumes, or manually shifting the spectral location of fat saturation pulses. Since the former routine optimizes field homogeneity over a selected region, other locations in the field of view may suffer greater variance in fat suppression uniformity. In any scenario, it is useful to observe the spectral peaks of fat and water following any shimming procedure when fat suppression uniformity is desired. Even though broad line widths may still persist, manual frequency adjustments help to resolve significant fat frequency shifts caused by off-resonance. This strategy can be further optimized by using smaller field-of-views, or fewer slices, thereby limiting the effective volume of shimming.

More systems are now equipped with sophisticated fat-water separation techniques. These methods evolved from the well-known 2-point Dixon method, which exploits the known fat/water resonant frequency difference to generate separate fat-only and water-only images based on two time-shifted echo acquisitions. Modern Dixon methods still incur a scan time penalty, but are very efficient for creating robust fat-suppressed (water-only) images. These techniques do not rely on field-sensitive spectrally-selective pulses, or non-selective IR pulses, which reduce SNR of all tissues. However, the overall efficacy of the reconstruction is highly dependent on producing a suitable B0 field map. Nonetheless, unfavorable fat/water swapping can persist in regions of significant B0 field inhomogeneity.

4.0. RECONSTRUCTION RELATED ARTIFACTS

Appearance: Foldover or Aliasing artifacts that appears in the center of the field of view, hotspots in the images, lower signal to noise in the image.

Origins/Causes: The availability of parallel imaging methods has tremendously improved the utility of MR in a variety of applications (10). Parallel imaging involves utilizing multi-array receive coils over the imaged region, and using their individually-specific coil sensitivity to reconstruct under-sampled k-space data. Scan times can be reduced by 2 or more time with parallel imaging, but the side effect is reduced SNR and some associated artifacts. Typically, the reduction in SNR is tolerated in many applications that warrant fast acquisitions, especially if inherent SNR is high, such as is present in balanced SSFP in cardiac imaging. Often significant amplification of noise is seen with parallel imaging, when reduction factors exceed 3. Furthermore, if mulit-array coils are not properly placed around the region of interest, more noise

amplification is seen. These relationships are captured in a general equation for SNR in parallel imaging:

$$SNR \sim \frac{1}{g \cdot \sqrt{R}}$$

Where g is the geometric factor, related to interdependence of coil elements and placement, and R is the parallel imaging reduction factor, which represents to degree of k-space under-sampling (11).

Other associated parallel imaging artifacts derive from the reconstruction method. One parallel imaging method reconstructs undersampled k-space data using multiple coil sensitivity images in image space (e.g SENSE). Artifacts with this method appear similar to image foldover, although the aliased regions typically appear in the center of the field of view, and are sometimes mistaken as signal "hotspots", *figure 10*. Another common parallel imaging technique estimates missing imaging information in k-space (e.g. GRAPPA). If missing k-space data is not effectively recovered, unwanted phase shifts may develop, resulting in ghost-like artifacts in the phase encode direction.

Origins/Causes: As shown in the equation above, unwanted amplification of noise is due to increased parallel imaging factors, as well as poor coil design of placement. When selected phase encode data is skipped to achieve scan acceleration, the resultant image is an aliased version of the original object. Image-based parallel imaging techniques, like SENSE, rely on a pre-calibration of coil element sensitivities for image reconstruction. The coil sensitivity profiles from each element serve to estimate true (un-aliased) voxel signal intensity. If pre-calibration of coil sensitivities performs perfectly, this data can be estimated mathematically with high accuracy. However, several scenarios cause imperfections, such as poor coil sensitivity maps (due to faulty elements), poor coil placement (resulting in poor object signal profiles), or poor matching of calibration maps with actual object position (due to patient movement), cause inaccurate true image data computation.

For k-space-based parallel reconstruction, such as GRAPPA, missing phase encode lines are estimated for each coil using fully sampled reference lines called autocalibration signals (ACS) (12). The missing data from one coil element is estimated from ACS data from all other coil elements, and from the behavior of neighboring data lines. In this way, full k-space data is estimated for each coil element, prior to reconstruction. A final image is produced by combining the individual coil images. This iterative estimation process in k-space is sensitive to motion, so subtle phase ghosts may be exacerbated in the image. Moreover, poor coil geometry or placement may cause incomplete estimation of individual coil images, resulting in exaggerated noise bands in areas of poor coil coverage.

Strategies for Alleviating Artifacts: One must first identify whether poor SNR, ghosts, or aliasing are a result of parallel imaging, or other physiological or technical factors. One may also exchange parallel imaging techniques to see if artifacts are resolved. Separate from removing parallel imaging altogether, some strategies are available to optimize the use of SENSE or GRAPPA methods. Proper coil placement is a significant cause of parallel imaging artifact, so care must be taken to first set up coil coverage that is favorable for parallel imaging. This means ensuring adequate multi-array coils in the phase encode direction, which is non-trivial when flexible multi-array coils are used for extremity imaging. Furthermore, spine imaging often only uses posterior multi-array coils. This configuration favors parallel imaging (i.e. phase encoding) only in the inferior-superior or left-right directions.

For image-based parallel imaging, an overly small FOV should not be used; some extended phase FOV will alleviate subtle unfolding reconstruction artifact. Furthermore, effort should be made to match the anatomic positioning between coil calibration scans and pulse sequences using parallel imaging. This may require calibration scans to be performed using similar breath hold instructions.

K-space-based parallel uses auto-calibration steps built into the acquisition, so parallel imaging ghosts are usually rare. However, the technique is more sensitive to patient motion, or inadequate reference coil sensitivities. Often, more auto-calibration reference lines are needed, which reduces the scan acceleration. Increased reference lines also alleviate central noise banding, which is common with parallel imaging.

Finally, users must be wary of malfunctioning elements on multi-array coils. Clearly, this will affect overall image SNR, but even slightly underperforming coil sensitivity profiles will accentuate artifacts on sequences using parallel imaging. Routine system and coil maintenance is vital for optimal performance of sequences using parallel imaging.

5.0. MR PHYSICIST'S ROLE: QUALITY ASSURANCE AND CLINICAL SERVICE

As discussed in the preceding sections, MR artifacts regularly degrade routine clinical imaging in a variety of ways. It is also evident that many image abnormalities can be readily identified and corrected. Even though general guidelines to avoid artifacts should be communicated to MR technologists, it is not often possible to address all artifacts as they happen, especially system-related artifacts across multiple MR systems. Therefore, strategies and programs must be developed by MRI physicists to periodically monitor and analyze system performance prospectively. Through proactive system assessment, an MR physicist can be best prepared for addressing issues before they occur, and discussing the outstanding needs to achieve a high quality diagnostic practice.

Though each MR system should have an established agreement with a vendor (or third-party) service engineer for preventative maintenance, overall system performance must be carefully evaluated and documented by an MR physicist. This begins with assessing the imaging capability of the MR system itself, which includes its basic system specifications (field and gradient strength, slew rate, effective field-of-view, etc.), as well as its array of imaging software applications (pulse sequence licenses, coil inventory, reconstruction options, etc.). From this survey, the physicist will have a better understanding of the limits of the system, thereby preventing subpar image quality, undesirable artifacts, or even unsatisfactory diagnostic results. This knowledge must be shared and discussed with all invested personnel, such as radiologists, technologists, and administration, but also used as ongoing insight into optimization strategies. This forms the primary goal of MR system hardware and software assessment: *to devise and implement optimized MR imaging protocols for clinical practice, with ongoing oversight and education of image quality and system performance.*

It is clear that the MR physicist's role is a balance between ensuring stable system performance and overseeing the varied aspects clinical MR operations. The specific division of these two roles may vary depending on the needs of the institution or involvement of other personnel in these areas. As mentioned, however, the essential duty is proactive system performance assessment. Beyond tabulating reports generated by service engineers and performing trend analyses, a comprehensive annual system performance evaluation should be performed to document baseline values for a variety of imaging metrics, such as geometric accuracy, contrast resolution, field and signal uniformity, slice thickness accuracy, and soft copy displays. Moreover, each system RF coil should be evaluated for signal-to-noise and signal uniformity, with deficiencies documented and relayed to appropriate service engineers. Importantly, this annual assessment will act as certification for local commission requirements for hospitals. There are ample resources available to assist in formulating and conducting an annual performance review, with the American College of Radiology (ACR) being the primary entity governing quality and accreditation in the United States. The ACR also provides guidelines and a multi-faceted MRI phantom, which facilitates performance testing. Recent changes to the ACR guidelines also call for a comprehensive assessment of the institution's MRI safety program, which should be conducted with delegated technologists, radiologists, and administrative leaders.

An MR physicist should also establish a weekly quality control program in partnership with MRI supervisors. Several guidelines exist regarding this effort, but essential tasks entail basic inventory and system visual checks by MRI staff, and limited phantom scanning to assess key performance metrics, such as geometric accuracy and low

contrast detectability. The MR physicist should oversee these weekly duties, monitor trends, and create action limits for deficiencies. The MR physicist should be also active in clinical MR operations. An important aspect of a proactive quality assurance in clinical MRI is the development and disseminating of MR educational materials for MRI staff. This involves establishing best practice MR protocols that limit the occurrence of MR artifacts with minimal technologist intervention. Examples of this effort include pre-programming appropriate FOVs, slice coverage, image contrast, image resolution, bandwidth, coil shimming, and motion compensation strategies into every protocol and sequence. In addition, the MR physicist should communicate these best practice imaging guidelines to MR staff to ensure compliance with protocols, while acting as an expert resource for feedback. This step is vital for revisiting protocols that are suboptimal. Similarly, an MR physicist should work in tandem with radiologists to translate clinical needs into MRI protocols, while suggesting appropriate imaging options based on the capabilities of the MR system. These important relationships with both MRI staff and radiologists are mutual feedback loops, with the overriding goal to efficiently achieve optimal diagnostic image quality on a routine basis.

The knowledge of an MR system's hardware and software capabilities plays an important role in an MR physicist's relationship with administrative leaders. Growth, innovation, and new imaging services in a department depend largely on updating or procuring new MR systems. It is important for MR physicists to engage themselves with administration and serve as expert advisors throughout the process of system purchase or modifications, including site planning, safety assessment, and system technical configurations.

REFERENCES

1. Brown R, Cheng, Y., Haacke, E., Thompson, M., & Venkatesan, R. Magnetic Resonance Imaging Physical Properties and Sequence Design (2nd ed.) ed. Hoboken: Wiley; 2014.

2. Feng L, Benkert T, Block KT, Sodickson DK, Otazo R, Chandarana H. Compressed sensing for body MRI. J Magn Reson Imaging. 2017;45(4):966-87. doi: 10.1002/jmri.25547. PubMed PMID: 27981664; PMCID: PMC5352490.

3. Dixon WT. Simple proton spectroscopic imaging. Radiology. 1984;153(1):189-94. doi: 10.1148/radiology.153.1.6089263. PubMed PMID: 6089263.

4. Schenck JF. The role of magnetic susceptibility in magnetic resonance imaging: MRI magnetic compatibility of the first and second kinds. Med Phys. 1996;23(6):815-50. doi: 10.1118/1.597854. PubMed PMID: 8798169.

5. Qiu D, Chan GC, Chu J, Chan Q, Ha SY, Moseley ME, Khong PL. MR quantitative susceptibility imaging for the evaluation of iron loading in the brains of patients with beta-thalassemia major. AJNR Am J Neuroradiol. 2014;35(6):1085-90. doi: 10.3174/ajnr.A3849. PubMed PMID: 24578278.

6. Hargreaves BA, Worters PW, Pauly KB, Pauly JM, Koch KM, Gold GE. Metal-induced artifacts in MRI. AJR American journal of roentgenology. 2011;197(3):547-55. doi: 10.2214/AJR.11.7364. PubMed PMID:21862795.

7. Oshinski JN, Delfino JG, Sharma P, Gharib AM, Pettigrew RI. Cardiovascular magnetic resonance at 3.0 T: current state of the art. J Cardiovasc Magn Reson. 2010;12:55. doi: 10.1186/1532-429X-12-55. PubMed PMID: 20929538; PMCID: PMC2964699.

8. Hoult DI, Phil D. Sensitivity and power deposition in a high-field imaging experiment. J Magn Reson Imaging. 2000;12(1):46-67. PubMed PMID: 10931564.

9. Sung K, Nayak KS. Design and use of tailored hard-pulse trains for uniformed saturation of myocardium at 3 Tesla. Magnetic resonance in medicine : official journal of the Society of Magnetic Resonance in Medicine / Society of Magnetic Resonance in Medicine. 2008;60(4):997-1002. doi: 10.1002/mrm.21765. PubMed PMID: 18816833.

10. Blaimer M, Heim M, Neumann D, Jakob PM, Kannengiesser S, Breuer FA. Comparison of phase-constrained parallel MRI approaches: Analogies and differences. Magnetic resonance in medicine : official journal of the Society of Magnetic Resonance in Medicine / Society of Magnetic Resonance in Medicine. 2016;75(3):1086-99. doi: 10.1002/mrm.25685. PubMed PMID: 25845973.

11. Pruessmann KP, Weiger M, Scheidegger MB, Boesiger P. SENSE: sensitivity encoding for fast MRI. Magnetic resonance in medicine : official journal of the Society of Magnetic Resonance in Medicine / Society of Magnetic Resonance in Medicine. 1999;42(5):952-62. PubMed PMID: 10542355.

12. Griswold MA, Jakob PM, Heidemann RM, Nittka M, Jellus V, Wang J, Kiefer B, Haase A. Generalized autocalibrating partially parallel acquisitions (GRAPPA). Magnetic resonance in medicine : official journal of the Society of Magnetic Resonance in Medicine / Society of Magnetic Resonance in Medicine. 2002;47(6):1202-10. doi: 10.1002/mrm.10171. PubMed PMID: 12111967.

Contact:
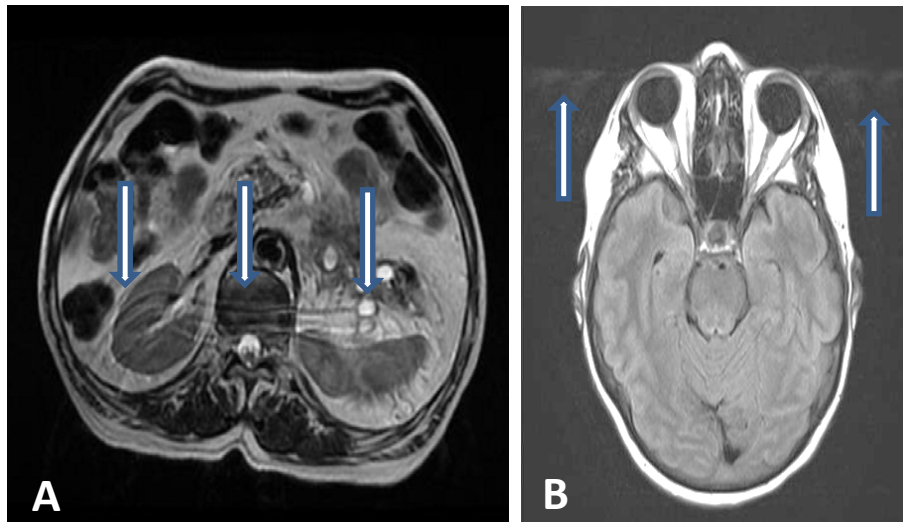Phone: 404-727-5894
Email: jnoshin@emory.edu

Figure 1. Motion and Phase Encoding Artifacts. Motion between phase encoding steps causes tissue to see different gradient strengths throughout the imaging process causing non-reproducible phase shifts between k-space lines. The results of this after the Fourier transform is misplacement of tissue related to the periodicity and extent of motion. This is most commonly seen as 'ghosting' of bright tissue such as vessels or fat in the phase encoding direction of the image. A) Respiratory ghosts on Axial T2 TSE; B) Non-periodic ghosts from eye movements on Axial T2 FLAIR.
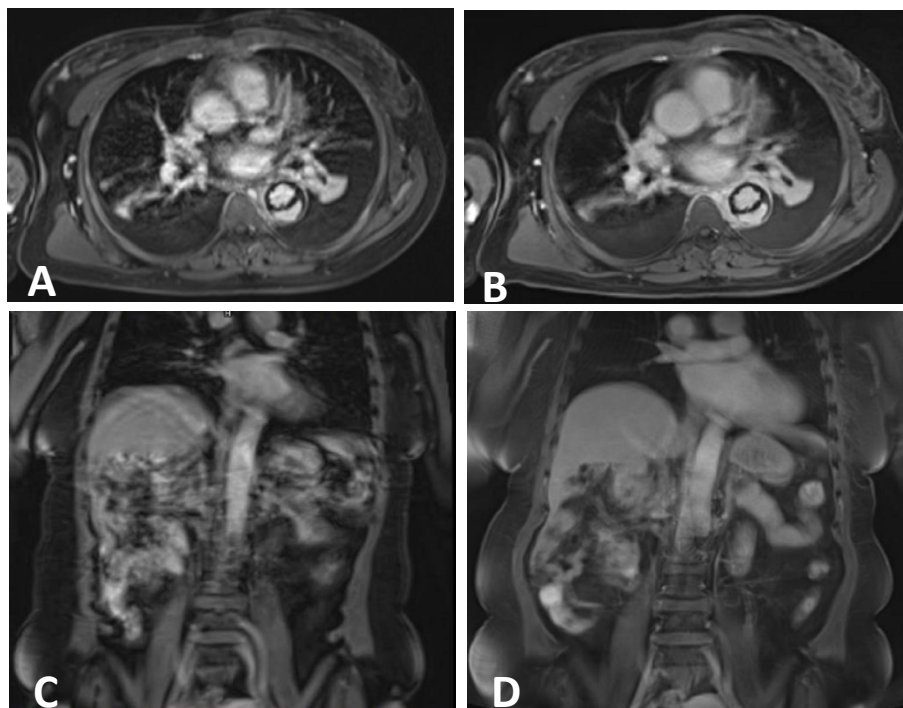
Figure 2. Motion and Respiratory Compensation. Poor breath holding may cause motion ghosts and/or blurring (A, C). Radial k-space sampling is an effective way to lessen the appearance of high signal ghost propagation by oversampling the center of k-space. Longer scan times are required to adequately sample the periphery of k-space to recapture image detail (B, D)
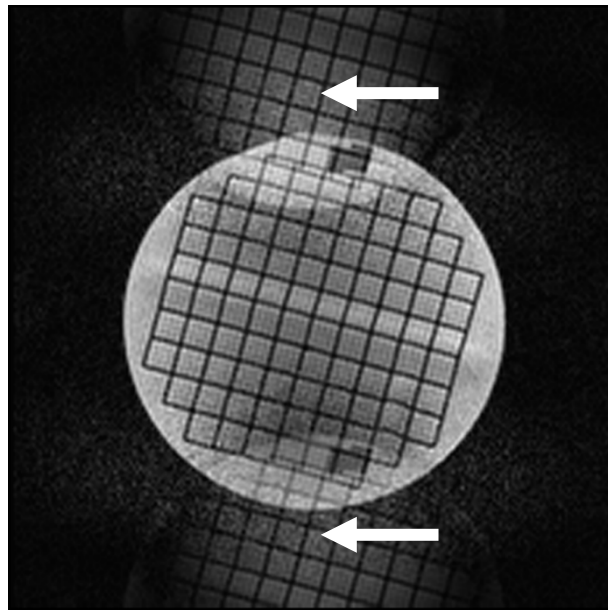
Figure 2. Nyquist Ghosting. Nyquist ghosting are artifacts appear as distinct copies of the imaged object, propagated across the FOV in the phase encode direction in EPI or other fast imaging techniques. They are related to a phase shift acquired during rapid gradient switching in accelerated imaging techniques. The White Arrow show the Nyquist ghosts.
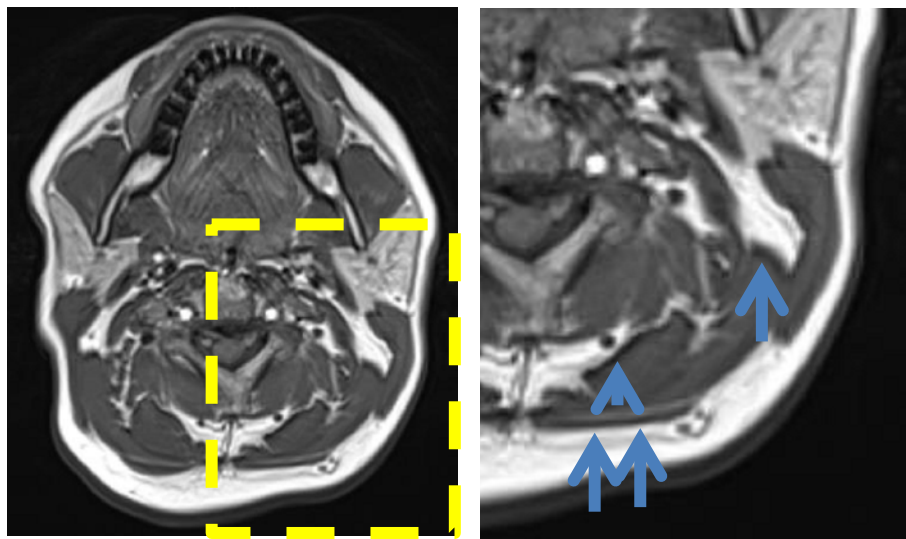
Figure 3. Chemical Shift Artifacts – Type 1. Chemical shift artifact of the first kind is caused by fat and water having slightly different procession frequencies. If the imaging bandwidth is too low, these differences in frequencies can cause a displacement in the location of fat relative to other tissues in the image space. The result is a black line (blue arrows) at the interface of fat and water where the displacement occurs. (see inset) For spin echo, chemical shift occurs in the frequency encode direction, while for echo-planar, it occurs in the phase encode direction
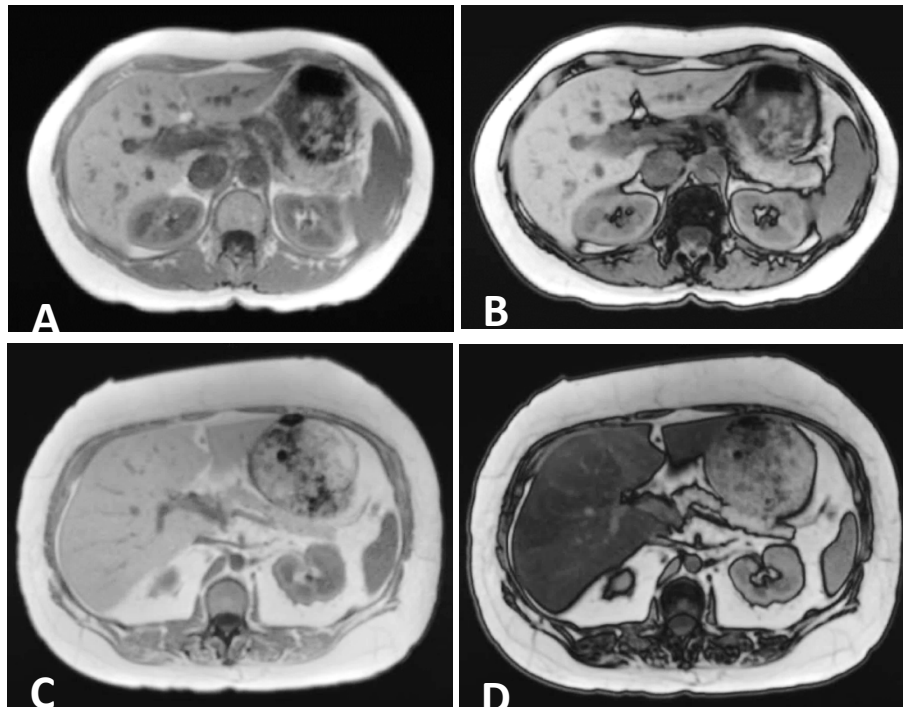
Figure 4. Chemical Shift Artifacts – Type 2. Chemical shift artifact of the second kind is also caused by fat and water having slightly different procession frequencies. At certain echo times the fat and water can be in-phase and other echo times they can be out of phase. When voxels contain both water and fat, in-phase images will add together to increase signal in a voxel (A, C). When fat and water are out of phase, fat and water will cancel each other and reduce signal along fat-water interfaces(B, D). When a subject has fatty liver disease., liver signal is reduced, proportional to the fat percentage (D).
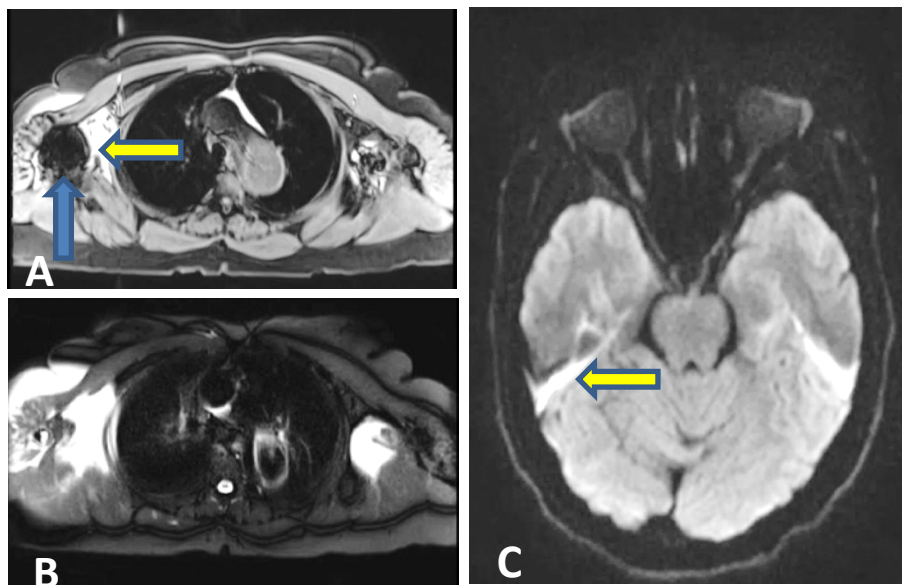
Figure 5. Susceptibility-Related Signal Loss and Signal Pile-up. When adjacent tissues have different magnetic properties or magnetic susceptibility, the *local* magnetic field is altered from its expected value, leading to signal mis-mapping in the images, or signal 'pile-up' (yellow arrow). It can also lead to local alterations in the field which change the signal from the resonant condition resulting in complete signal loss (blue arrow). A) This artifact was due to a metal implant, and is significant on gradient-echo imaging; B) Signal loss/distortion is reduced using TSE; however fat-sat is non-uniform around significant inhomogeneity. C) signal distortion pile-up on DWI due to air-tissue susceptibility interface
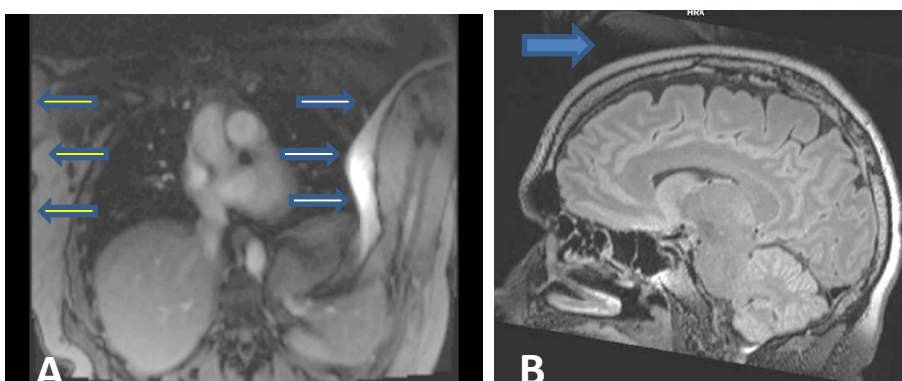
Figure 6. Aliasing / Wraparound / Foldover Artifact. The artifact occurs when tissue outside of the field of view receives the RF excitation pulse and generates a signal which is outside the readout bandwidth. The results is tissue 'wrapping around' to the other side of the image in the phase encoding direction. (A) The white arrows show the wrapped or aliased tissue and the yellow arrow show the edge of the prescribed FOV, which does not include the arm. Solution include increasing the FOV, using phase over-sampling, or pre-saturating tissue outside the FOV. B) On axial 3D imaging, aliasing may also occur in the slice direction, as seen on this sagittal reconstruction (blue arrow)
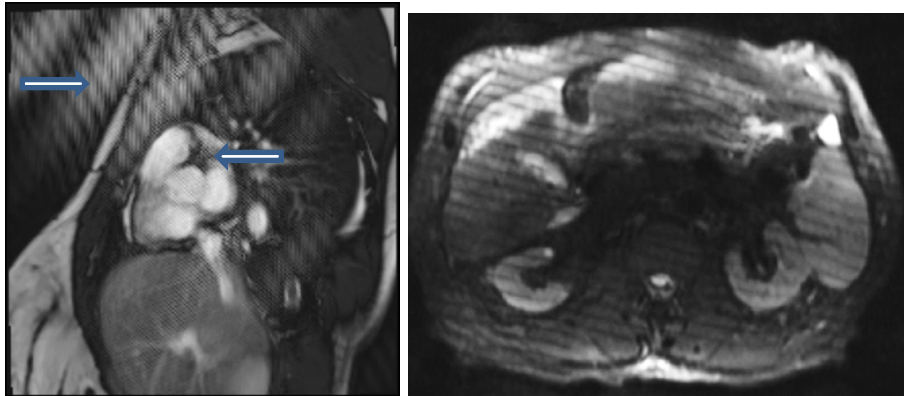
Figure 7. RF noise / Interference. If signals unrelated to the MR signal from tissue, but in the frequency range of the expected signal in the image, are present in the scanner room, they will be detected by the RF receiver coil. These noise signal will be put into k-space and transformed into the image. Because of the spatial frequency distribution of k-space, these signal will appears as 'zipper' or herringbone' artifacts.
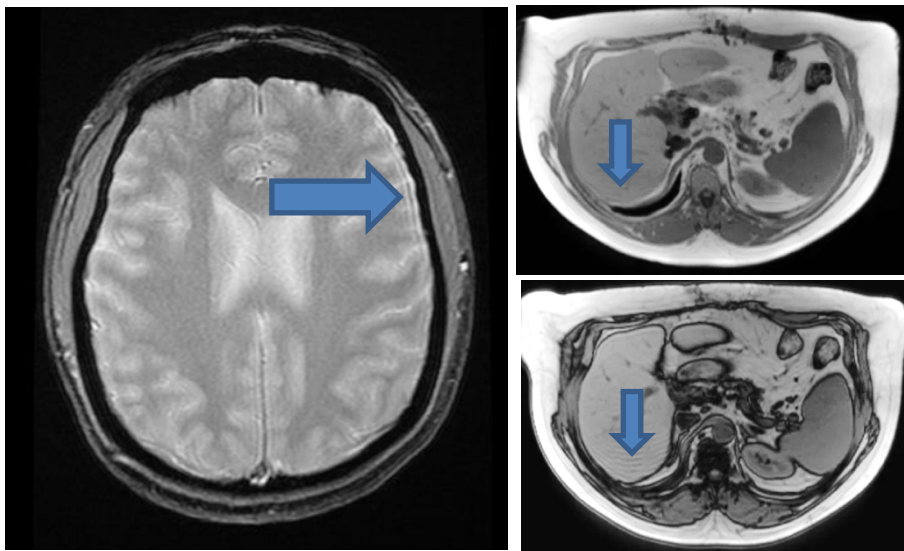

Figure 8. Truncation Artifact / Gibbs Ringing. Gibbs ringing is a result of truncating the acquisition of higher spatial frequencies in k-space. The lack of acquisition of high spatial frequencies causes edges in the image that have sharp boundaries in space and high signal intensity differences to appear to have a ringing effect. This is an artifact of the Fourier transforms being unable to represent a steep signal-step in image space. Ringing will evolve from high contrast edges if the resolution is low, which typically occurs in the phase encode direction, as in these examples (blue arrows).

Computed Tomography Dosimetry: From Basic to State-of-the-art Techniques

K. Matsubara[1]

[1]Department of Quantum Medical Technology, Faculty of Health Sciences, Kanazawa University, Kanazawa, Japan

Abstract— **In this review, the basic and state-of-the-art techniques for evaluating radiation dose in computed tomography (CT) are described. CT dose index (CTDI) and dose-length product are indicators for measuring, comparing, and communicating the radiation output of a CT system. Although volume CTDI ($CTDI_{vol}$) is not the absorbed dose of an actual patient, the American Association of Physicists in Medicine (AAPM) has proposed conversion factors to translate CTDIvol into patient dose estimates at the center of the scanned volume to obtain size-specific dose estimates. Recently, several disadvantages of CTDI have been noted, especially for wide-beam CT. To eliminate these disadvantages, the International Electrotechnical Commission has described a modified CTDI definition that covers wide-beam CT. The AAPM has proposed measuring the accumulated dose at the scanning range midpoint to estimate the equilibrium dose instead of measuring CTDI. This review also introduces methods of obtaining the average organ dose from point measurements and Monte Carlo calculation, which are generally used for estimating the patient dose in CT.**

Keywords— **computed tomography, dosimetry, computed tomography dose index, dose-length product**

I. INTRODUCTION

Since the computed tomography (CT) scanner was first introduced for clinical use, the medical information derived from CT scans has contributed to saving many lives not only in developed countries but also in developing countries worldwide. The evolution of CT scanners has greatly enhanced their value in medical diagnosis. However, radiation doses in CT examinations have become relatively higher than those in radiological examinations [1]. The dose to an individual from one CT examination does not cause radiation-induced biological effects, but it is crucial to manage radiation dose in CT examinations appropriately.

When considering radiation dose in CT examinations, it is important to understand that the absorbed dose distribution within each patient differs from that of other X-ray examinations (e.g., radiography and fluoroscopy). This is because the X-ray beam is narrowed by passing through the collimator, and the exposure is controlled by using an X-ray tube that is rotated around the patient. Hence, specific methods must be used for evaluation of radiation doses in CT scans.

II. COMPUTED TOMOGRAPHY DOSE INDEX

The CT dose index (CTDI) is a basic method for describing the doses delivered by CT scans [2]. CTDI is based on measuring the kinetic energy released per unit mass (kerma) of air in cylindrical polymethyl methacrylate phantoms 16 cm (for adult head and child) and 32 cm (for adult body) in diameter (Fig. 1). The index is measured from one axial CT scan and is calculated by dividing the air kerma by the product of slice thickness and the number of slices. The CTDI is defined by the following equation:

$$\text{CTDI} = \frac{1}{BW} \int_{-\infty}^{+\infty} D(z)\,dz \tag{1}$$

where BW is the nominal X-ray beam width along the z-axis, and $D(z)$ is the dose profile along the z-axis, which consists of primary and secondary (scattered) radiation, from a single acquisition. The unit of CTDI is mGy.
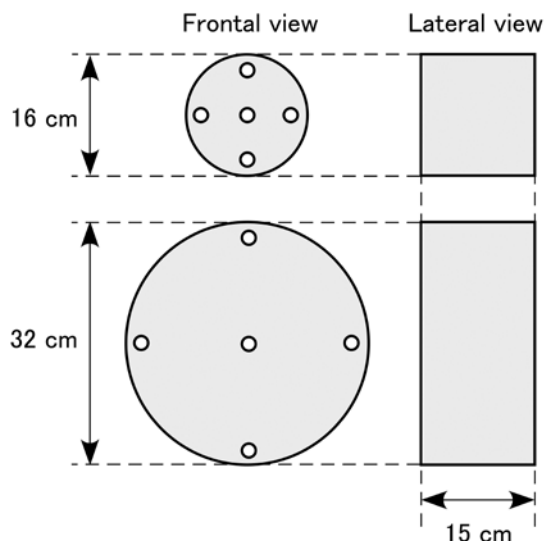

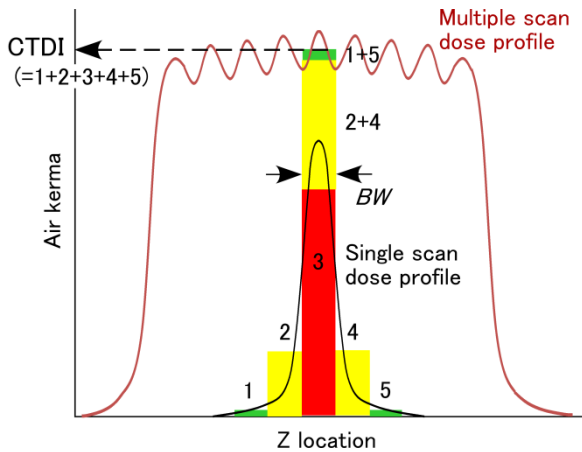Fig. 1 Schematic of the polymethyl methacrylate phantoms

Fig. 2 Meaning of CTDI. When the radiation dose from a single scan equals the sum of areas 1 to 5, CTDI represents the sum of areas 1 to 5 divided by *BW*.

The index is measured by using a single acquisition, but it can be used to estimate the average dose from multiple acquisitions when the table is incremented during acquisitions. If all of the scatter tails are measured and the table increment equals *BW*, the result represents the average value in the central portion, which has the length of *BW*, of the multiple scan dose profile (Fig. 2).

A pencil-type ionization chamber that has a 100-mm active length is inserted in the phantom's holes to measure the index. However, the chamber can only measure the primary dose and scatter tails within a 100-mm length along the z-axis [3]. The index, which is called $CTDI_{100}$, is defined by the following equation:

$$CTDI_{100} = \frac{1}{BW} \int_{-50mm}^{+50mm} D(z)dz \tag{2}$$

Air kerma between the central and peripheral regions of the phantom are different in CT scans. To take this difference into consideration, the weighted CTDI ($CTDI_w$) is defined by the following equation:

$$CTDI_w = \frac{1}{3} \cdot CTDI_{100,c} + \frac{2}{3} \cdot CTDI_{100,p} \tag{3}$$

where $CTDI_{100,c}$ is $CTDI_{100}$ at the center of the phantom and $CTDI_{100,p}$ is the average of the $CTDI_{100}$ at four points along the periphery of the phantom. In other words, $CTDI_w$ represents the average air kerma over the in-plane direction [4].

To represent the dose for a consecutive CT scan, it is essential to take pitch, gaps, or overlaps into consideration. $CTDI_{vol}$ is defined by the following equations.

1. In the case of sequential acquisitions:

$$CTDI_{vol} = \frac{BW}{I} \cdot CTDI_w \tag{4}$$

2. In the case of helical acquisitions:

$$CTDI_{vol} = \frac{1}{p} \cdot CTDI_w \tag{5}$$

where *I* is the table increment between each acquisition, and *p* is the pitch factor (= table feed per rotation/nominal X-ray beam width along z-axis). From these equations, the local air kerma for a specific CT protocol can be obtained. $CTDI_{vol}$ is the most familiar dose parameter because it is regulated to be displayed on the console of CT scanners [2].

As a dose descriptor in CT, the multiple scan average dose (MSAD) is also used. The air kerma for a certain part of the cylindrical polymethyl methacrylate phantom (Fig. 1) with multiple acquisitions is measured by using a small dosimeter, such as a thermoluminescent dosimeter (TLD) or radiophotoluminescent glass dosimeter (RPLD) [2]. Theoretically, the MSAD and CTDI are equivalent dose values because MSAD equals the dose value integrated over the dose profile for one rotation, which is equal to the CTDI. In the early days of CT, direct measurement of the MSAD was generally performed, but it required multiple scan acquisitions, which placed heavy loads on the X-ray tube [5].

One should know that the $CTDI_{vol}$ is not the absorbed dose of an actual patient, but CTDI is an indicator for measuring, comparing, and communicating the radiation output of a CT system [6]. For estimating patient doses from $CTDI_{vol}$, the American Association of Physicists in Medicine (AAPM) has released conversion factors to translate $CTDI_{vol}$ into patient dose estimates at the center of the scanned volume, which are described in section V [7].

Recently, some disadvantages of CTDI have been pointed out [8-12]. First, a 100-mm-long pencil ionization chamber used to collect the dose may not be sufficiently long to measure all of the tails of the scattered dose distribution. Second, the phantoms used for CTDI measurements are shorter than an adult torso and so do not produce as much scattered radiation as would occur in a typical adult. To address these limitations, the International Electrotechnical Commission (IEC) has described a modified CTDI definition in Amendment 1 of the third edition of report 60601-2-44. The definition of $CTDI_{100}$ [equation (2)] is retained for a nominal X-ray beam width along the z-axis of ≤40 mm; when the width is >40 mm, the $CTDI_{100}$ is defined as follows (Fig. 3):

$$CTDI_{100} = \frac{1}{BW_{Ref}} \int_{-50mm}^{+50mm} D(z)dz \cdot \frac{CTDI_{Air,BW}}{CTDI_{Air,Ref}} \tag{6}$$

where BW_{Ref} is the reference nominal X-ray beam width along the z-axis, which is at or near 20 mm, $CTDI_{Air,BW}$ and $CTDI_{Air,Ref}$ are the CTDI in air for the desired and reference nominal X-ray beam widths along the z-axis, respectively. CTDI in air is defined by the following equation:

$$\text{CTDI}_{\text{Air}} = \frac{1}{BW} \int_{-L/2}^{+L/2} D(z)dz$$

(7)

where L is the air kerma integration length, which is set to the desired nominal X-ray beam width along the z-axis plus 40 mm, with a minimum total length of 100 mm. When L is >100 mm, a pencil-type ionization chamber that has an appropriate active length is prepared, or a pencil-type ionization chamber that has a 100-mm active length is used by performing a two- or three-step measurement (Fig. 4). This methodology has been adopted by the International Atomic Energy Agency in its Human Health Report 5 [13].
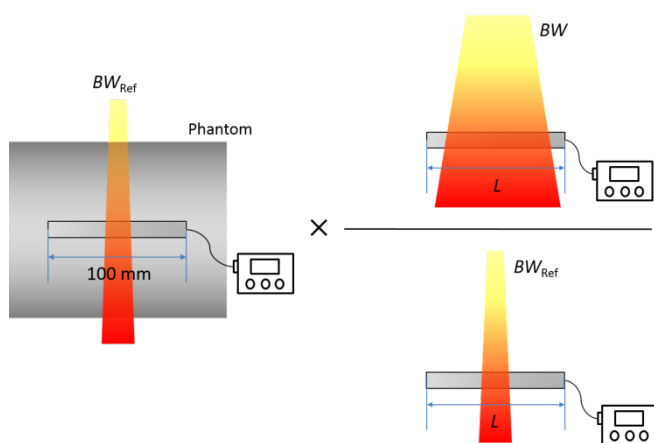
Fig. 3 Modified CTDI definition for an X-ray nominal beam width along the z-axis of >40 mm
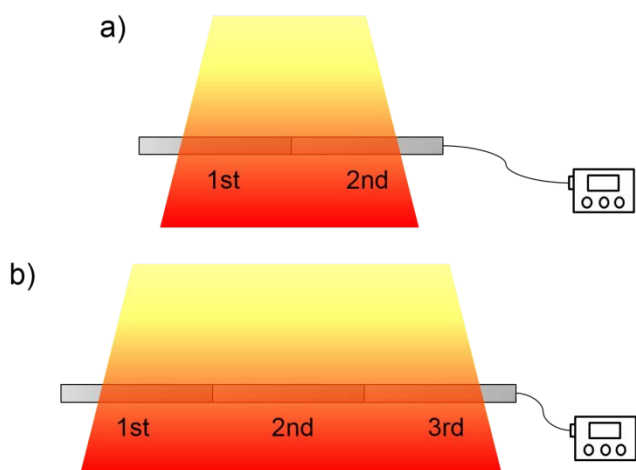
Fig. 4 Two- and three-step measurement process to measure CTDI by using the modified CTDI methodology

III. DOSE-LENGTH PRODUCT

The dose-length product (DLP) represents the total dose over a whole scan and is defined by the following equations.
1. In the case of sequential acquisitions:

$$\text{DLP} = \text{CTDI}_{\text{vol}} \cdot \Delta d \cdot N$$

(8)

2. In the case of helical acquisitions:

$$\text{DLP} = \text{CTDI}_{\text{vol}} \cdot L$$

(9)

3. In cases in which the table is not incremented during acquisitions:

$$\text{DLP} = \text{CTDI}_{\text{vol}} \cdot n \cdot L$$

(10)

where Δd is the table increment per rotation, N is the number of acquisitions, L is the scanning length, and n is the number of slices generated from one sequential acquisition. The unit of DLP is mGy·cm. DLP is also used as an indicator of radiation output of a CT system, but the patient effective dose can be estimated from DLP by using the following equation:

$$\text{E} = k_{\text{E}} \cdot \text{DLP}$$

(11)

where k_{E} is the conversion factor (mSv·mGy^{-1}·cm^{-1}) that depends on patient age and scanning regions [14].

The concept of effective dose was introduced by the International Commission on Radiological Protection in 1977 [15] and revised in 1991 and 2007 [16,17]. Tissue weighting factors, which are used for calculating the effective dose, have also been revised according to the latest findings with regard to the radiation effect for each organ or tissue.

IV. EQUILIBRIUM DOSE METHOD

A previous study showed that the dose at the center of the scan range may increase with longer phantoms and scan lengths, and asymptotically approaches the equilibrium dose for large scan lengths [8,18,19]. The relationship between equilibrium dose and CTDI is shown by the following equation:

$$D_{\text{eq}} = \frac{CTDI}{p}$$

(12)

where D_{eq} represents the equilibrium dose for a large scanning length.

The AAPM has released report 111, "Comprehensive Methodology for the Evaluation of Radiation Dose in X-Ray Computed Tomography" [18]. In this report, the AAPM has proposed measuring the accumulated dose at the midpoint of the scanning range, which is defined in the equation below, to estimate the equilibrium dose instead of measuring the CTDI.

$$D_L(0) = \frac{1}{a} \int_{-L/2}^{L/2} f(z)dz$$

(13)

where $D_L(0)$ is the accumulated dose at the midpoint of the scanning range, a is the scan interval, and $f(z)$ is the full dose profile.

For estimating the equilibrium dose from the accumulated dose, the equilibrium function $H(L)$,

$$H(L) = \frac{D_L(0)}{D_{eq}} \tag{14}$$

is required theoretically. The report stated that the equilibrium dose method needs phantoms that are sufficiently long. For example, a water-filled, 30-cm diameter, and 50-cm long phantom is designed to be transported empty, and once placed on the table, it can be filled with water. The AAPM-International Commission on Radiation Units and Measurements CT phantom comprises high-density polyethylene and is 30-cm in diameter and 60-cm long. The phantom is designed to be modular with three different sections. The cylindrical polymethyl methacrylate (PMMA) phantoms, which are used for measuring CTDI, can also be used to be assembled contiguously for requisite lengths. A previous paper has showed that the phantom length that is required for the radiation dose profile measurement should be at least 75 cm (five PMMA phantoms) with the maximum beam width of 160 mm [20].

For measuring $D_L(0)$, a thimble ionization chamber with an active length of 20–35 mm for charge collection and a nominal collection volume of at least 0.6 cm^3 should be used (Fig. 5a). A small solid-state detector can also be used for this purpose [20,21] (Fig. 5b).
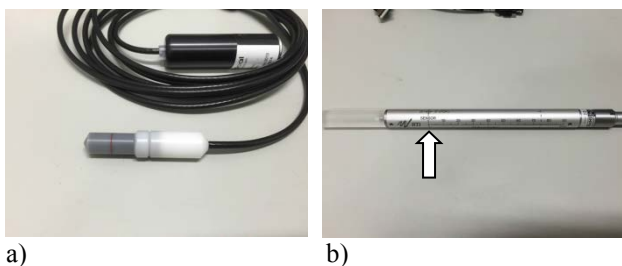

a)   b)

Fig. 5 Examples of small dosimeters for measuring accumulated dose at the midpoint of the scanning range: a) a Farmer-type 0.6-cm^3 ionization chamber (10X6-0.6CT; Radcal, Monrovia, CA, USA), b) a small solid-state detector (placed 3 cm from the end of the probe [white arrow]. CT Dose Profiler; RTI Group AB, Mölndal, Sweden)

V. SIZE-SPECIFIC DOSE ESTIMATES

Although CTDI$_{vol}$ is not the absorbed dose of an actual patient, the AAPM released report 204, "Size-Specific Dose Estimates in Pediatric and Adult Body CT Examinations" [22], which provided conversion factors as a function of geometric patient size to translate CTDI$_{vol}$ to patient dose estimates at the center of the scanned volume, which was named size-specific dose estimates (SSDE).

In this report, four different measurements of torso thickness are used to represent patient size: the anteroposterior dimension (AP), the lateral dimension (LAT), the sum of the dimensions (AP + LAT), and the effective diameter (square root of the product of AP and LAT). For example, Mueller et al. [23] showed that SSDE estimates the rectal absorbed dose reasonably during CT colonography.

However, X-ray attenuation is the fundamental physical parameter that affects absorption of X-rays and thus, is more relevant than geometric patient size. Hence, the AAPM released report 220, "Use of water equivalent diameter for calculating patient size and SSDE in CT" [24], which provided conversion factors as a function of X-ray attenuation to calculate SSDE for all patients, with little or no user intervention.

Previous work has proposed the concepts of a water-equivalent area and diameter [25-29]. The water-equivalent area can be represented in terms of CT numbers, as shown in the following equation:

$$A_w = \sum \frac{\mu(x,y)}{\mu_{water}} \cdot A_{pixel} = \sum \left(\frac{CT(x,y)}{1000} + 1 \right) \cdot A_{pixel} \tag{15}$$

where A_w is the water-equivalent area, A_{pixel} is the area of a pixel in the CT image, μ is the linear attenuation coefficient, and $CT(x,y)$ is the CT number of a voxel. The water-equivalent diameter is shown by the following equation:

$$D_w = 2\sqrt{A_w / \pi} \tag{16}$$

where D_w is the water-equivalent diameter. A previous study showed that using the water equivalent diameter from one image in the center of the scan range and the mean CTDI$_{vol}$ from the entire scan provided a sufficiently accurate method for calculating the mean SSDE for CT examinations of the torso in adults [30].

Estimating the water-equivalent diameter can only be performed by using reconstructed CT images. Although two studies have shown that patient attenuation can be estimated by using CT localizer radiography [26,27], the CT localizer radiograph-based method for estimating the water-equivalent diameter is not recommended because it requires calibration of the CT localizer radiograph pixel values in terms of water attenuation.

VI. PHYSICAL MEASUREMENTS

Obtaining the organ dose from point measurements is another effective method in CT dosimetry. Sectioned and drilled phantoms, such as the Alderson RANDO phantom [31-33] and ATOM phantom [34-37], are used (Fig. 6). These phantoms accept small dosimeters, such as TLD [31,33], RPLD [32], metal-oxide-semiconductor field-effect transistor dosimeters [35,36,38], semiconductor detectors

[21,37], photo diode dosimeters [39,40], and optically stimulated luminescence (OSL) dosimeters [41].

The energy dependency of these small dosimeters within the energy range generally used in CT is relatively high; hence, they must be calibrated with the effective energy used. One of the methods for calibration is to compare dose values with those of an ionizing chamber by using a diagnostic X-ray system. The chamber and small dosimeters are placed adjacent to each other at the same distance from the X-ray focus in an irradiated field. Radiographic or radiochromic film may also be used instead of small dosimeters. The film is placed between any two contiguous sections, which are then sealed with black tape to prevent any exposure of the film to light.

Fig. 6 An example of an anthropomorphic phantom (ATOM model 702; CIRS, Norfolk, VA, USA); it has holes for inserting small dosimeters

When TLD, RPLD, or OSL are used as small dosimeters, they should be initialized beforehand by heating (TLD and RPLD) or irradiating visible light (OSL). After initializing, the initial dose values should be read. Then, they are placed at the drilled holes that are located corresponding to targeted tissues and organs. Thereafter, the phantom is placed on the CT table and scanned. If possible, the scan should be performed multiple times by using separate sets of small dosimeters to reduce uncertainty and random error.

After scanning, the small dosimeters are removed from the phantom, and the dose values are read after adequate time has passed (for TLD) or preheating has been performed (for RPLD) to stabilize the obtained values. Examples of adequate times are 1 h for BeO and from 12 to 24 h for $CaSO_4$.

As shown in the following equation, the absorbed dose for each organ is obtained by multiplying the averaged value of the organ or tissue, the calibration factor of the small dosimeters, and the ratio of mass energy-absorption coefficients for each organ or tissue to air:

$$D_T = (M_T - M_I) \cdot k_C \cdot \frac{(\mu_{en} / \rho)_T}{(\mu_{en} / \rho)_A} \qquad (17)$$

where M_T is the averaged dose value from the small dosimeters placed at locations corresponding to each organ or tissue, M_I is the averaged initial dose value, k_C is the calibration factor of the small dosimeter, $(\mu_{en}/\rho)_T$ is the mass energy-absorption coefficient for each organ or tissue, and $(\mu_{en}/\rho)_A$ is the mass energy-absorption coefficient for air.

VII. SIMULATION METHOD

Without using anthropomorphic phantoms and small dosimeters, the absorbed dose for each organ or tissue for typical clinical CT scanner models and scan protocols can be calculated on the basis of Monte Carlo (MC) simulation software. One example is the ImPACT CT Patient Dosimetry Calculator software (St. George's Hospital, London, UK) (Fig. 7) [42]. This software uses the National Radiological Protection Board MC dose data sets produced in report SR250 [43] and provides normalized organ dose data for irradiation of a mathematical (Medical Internal Radiation Dose [MIRD]) phantom.
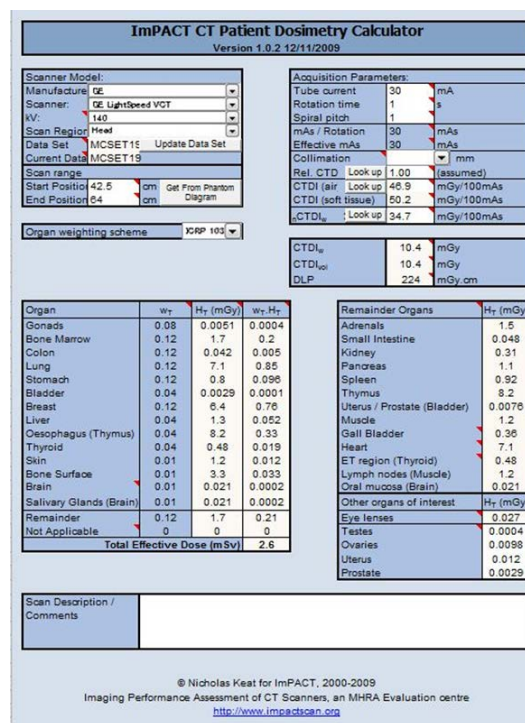

Fig. 7 ImPACT CT Patient Dosimetry Calculator [42]

There are other MC simulation programs, such as CT-Expo [44], ImPACTDose [45], and WAZA-ARIv2 [46]. CT-Expo offers dose calculation for adults, children, and infants, and takes into account overbeaming, overranging, and dose modulation (longitudinal and three-dimensional) effects. ImPACTDose offers anthropomorphic phantoms represented by 12 phantoms of both sexed and different ages (newborn, 1, 5, 10, 15 years old and adult) as well as

two voxelized human phantoms. The WAZA-ARIv2 is a web-based CT dose calculator, that can calculate organ doses of 18 body types of patients, including adults and children. The Particle and Heavy Ion Transport Code System (PHITS) [47] has been used for developing this web-based software.

In addition, there are several types of MC packages that are used for CT dosimetry, such as Monte Carlo N-Particle eXtended (MCNPX) [48-53] and Electron Gamma Shower (EGS) [54,55]. When the MC packages are used, source models of the CT scanner and human models need to be set manually for calculating absorbed doses in CT.

VIII. CONCLUSIONS

In this review, the basic and state-of-the-art techniques for evaluating radiation dose in CT are described. Understanding these techniques is necessary not only for measuring, comparing, and communicating the radiation output of a CT system but also for estimating patient dose in CT. Medical physicists should understand these techniques clearly before performing quality control in CT and optimizing patient dose and scanning protocols.

ACKNOWLEDGMENT

REFERENCES

1. United Nations Scientific Committee on the Effects of Atomic Radiation (2010) Sources and effects of ionizing radiation, UNSCEAR 2008 Report to the General Assembly with Scientific Annexes, Volume I. United Nations, New York, NY, USA
2. Shope TB, Gagne RM, Johnson GC (1981) A method for describing the doses delivered by transmission x-ray computed tomography. Med. Phys. 8:488–495
3. International Electrotechnical Commission (2009) Particular requirements for the basic safety and essential performance of X-ray equipment for computed tomography. Medical electrical equipment – Part 2-44, International Electrotechnical Commission, Geneva, Switzerland
4. Leitz W, Axelsson, B, Szendrö G (1995) Computed tomography dose assessment: a practical approach. Radiat. Prot. Dosimetry 57:377–380
5. McCollough CH, Lenq S, Yu L, et al. (2011) CT dose index and patient dose: they are not the same thing. Radiology 259:311–316
6. American Association of Physicists in Medicine (2008) The measurement, reporting and management of radiation dose in CT, AAPM Report 96. American Association of Physicists in Medicine, College Park, MD, USA.
7. American Association of Physicists in Medicine (2011) Size-specific dose estimates (SSDE) in pediatric and adult body CT examinations. American Association of Physicists in Medicine, College Park, MD, USA
8. Dixon RL (2003) A new look at CT dose measurement: beyond CTDI. Med. Phys. 30:1272–1280
9. Mori S, Endo M, Nishizawa K, et al. (2005) Enlarged longitudinal dose profiles in cone-beam CT and the need for modified dosimetry. Med. Phys. 32:1061–1069
10. McCollough CH (2006) It is time to retire the computed tomography dose index (CTDI) for CT quality assurance and dose optimization: against and proposition. Med. Phys. 33:1190–1191
11. Dixon RL (2006) Restructuring CT dosimetry: a realistic strategy for the future–requiem for the pencil chamber. Med. Phys. 33:3973–3976
12. Boone JM (2007) The trouble with CTDI100. Med. Phys. 34:1364–1371
13. International Atomic Energy Agency (2011) Status of computed tomography dosimetry for wide cone beam scanners, IAEA Human Health Report 5. International Atomic Energy Agency, Vienna, Austria
14. Valentine J (2007) Managing patient dose in multi-detector computed tomography (MDCT), ICRP Publication 102. Ann. ICRP 37:1–79
15. International Commission on Radiological Protection (1977) Recommendation of the International Commission on Radiological Protection, ICRP Publication 26. Ann. ICRP 1
16. International Commission on Radiological Protection (1991) 1990 recommendation of the International Commission on Radiological Protection, ICRP Publication 60. Ann. ICRP 21
17. Valentine J (2007) The 2007 recommendation of the International Commission on Radiological Protection, ICRP Publication 103. Ann. ICRP 37:1–332
18. American Association of Physicists in Medicine (2010) Comprehensive methodology for the evaluation of radiation dose in X-ray computed tomography, AAPM Report 111. American Association of Physicists in Medicine, College Park, MD, USA
19. Li X, Zhang D, Liu B (2013) Monte Carlo assessment of CT dose equilibration in PMMA and water cylinders with diameters from 6 to 55 cm. Med. Phys. 40:031903
20. Lin PP, Herrnsdorf L (2010) Pseudohelical scan for the dose profile measurements of 160-mm-wide cone-beam MDCT. Am. J. Roentgenol. 194:897–902
21. Herrnsdorf L, Björk M, Cederquist B, et al. (2009) Point dose profile measurements using solid state detectors in characterization of computed tomography systems. Nucl. Instrum. Methods Phys. Res. Sect. A. 607:223–225
22. American Association of Physicists in Medicine (2011) Size-specific dose estimates (SSDE) in pediatric and adult body CT examinations, AAPM Report 204. American Association of Physicists in Medicine, College Park, MD, USA
23. Mueller JW, Vining DJ, Jones AK, et al. (2014) In vivo CT dosimetry during CT colonography. AJR. Am. J. Roentgenol. 202:703–710
24. American Association of Physicists in Medicine (2014) Use of water equivalent diameter for calculating patient size and size-specific dose estimates (SSDE) in CT, AAPM Report 220. American Association of Physicists in Medicine, College Park, MD, USA
25. Huda W, Scalzetti EM, Roskopf M (2000) Effective doses to patients undergoing thoracic computed tomography examinations. Med. Phys. 27:838–844
26. Menke J (2005) Comparison of different body size parameters for individual dose adaption in body CT of adults. Radiology 236:565–571
27. Toth T, Ge Z, Daly MP (2007) The influence of patient centering on CT dose and image noise. Med. Phys. 34:3093–3101
28. Wang J, Christner JA, Duan X, et al. (2012) Attenuation-based estimation of patient size for the purpose of size specific dose estimation in CT. Part I. Development and validation of methods using the CT image. Med. Phys. 39:6772–6778
29. Wang J, Duan X, Christner JA, et al. (2012) Attenuation-based estimation of patient size for the purpose of size specific dose estimation in CT. Part I. Development and valudation of methods using the CT image. Med. Phys. 39:6764–6771
30. Leng S, Shlung M, Duan X, et al. (2015) Size-specific dose estimates for chest, abdominal, and pelvic CT: effect of intrapatient variability in water-equivalent diameter. Radiology 276:184–308
31. Groves AM, Owen KE, Courtney HM, et al. (2004) 16-detector multislice CT: dosimetry estimation by TLD measurement compared with Monte Carlo simulation. Br. J. Radiol. 77:662–665

32. Matsubara K, Koshida K, Suzuki M, et al. (2009) Effective dose evaluation of multidetector CT examinations: influence of the ICRP recommendation in 2007. Eur. Radiol., 19:2855–2861

33. Lechel U, Becker C, Langenfeld-Jäger G, et al. (2009) Dose reduction by automatic exposure control in multidetector computed tomography: comparison between measurement and calculation. Eur. Radiol. 19:1027–1034

34. Cody DD, Moxley DM, Krugh KT, et al. (2004) Strategies for formulating appropriate MDCT techniques when imaging the chest, abdomen, and pelvis in pediatric patients. AJR. Am. J. Roentgenol. 182:849–859

35. Litmanovich D, Tack D, Lin PP, et al. (2012) Female breast, lung, and pelvic organ radiation from dose-reduced 64-MDCT thoracic examination protocols: a phantom study. AJR. Am. J. Roentgenol. 197:929–934

36. Lungren MP, Yoshizumi TT, Brady SM, et al. (2012) Radiation dose estimations to the thorax using oragan-based dose modulation. AJR. Am. J. Roentgenol. 199:W65–W73

37. Matsubara K, Lin PJ, Fukuda A, et al. (2014) Differences in behavior of tube current modulation techniques for thoracic CT examinations between male and female anthropomorphic phantoms. Radiol. Phys. Technol. 7:316–328

38. Ramani R, Russell S, O'Brien P (1997) Clinical dosimetry using MOSFETS. Int. J. Radiation Oncology Biol. Phys. 37:959–964

39. Fujii K, Aoyama T, Yamauchi-Kawaura C, et al. (2009) Radiation dose evaluation in 64-slice CT examinations with adult and paediatric anthropomorphic phantoms. Br. J. Radiol. 82:1010–1018

40. Yamauchi-Kawaura C, Fujii K, Aoyama T, et al. (2010) Radiation dose evaluation in head and neck MDCT examinations with a 6-year-old child anthropomorphic phantom. Pediatr. Radiol. 40:1206–1214

41. Zhang D, Li X, Gao Y, et al. (2013) A method to acquire CT organ dose map using OSL dosimeters and ATOM anthropomorphic phantoms. Med. Phys, 40:081918

42. ImPACT CT scanner evaluation group at http://www.impactscan.org/

43. The National Archives at http://webarchive.nationalarchives.gov.uk/

44. Science & Technology for Radiology at http://www.sascrad.com/

45. ImpactDose at http://ct-imaging.de/en/ct-software-e/impactdose-e.html

46. WAZA-ARIv2 at http://waza-ari.nirs.qst.go.jp/

47. Sato T, Niita K, Matsuda N, et al. (2013) Particle and Heavy Ion Transport Code System PHITS, Version 2.52. J. Nucl. Sci. Technol. 50:913–923

48. Zhang D, Cagnon CH, Villablanca JP (2012) Peak skin and eye lens radiation dose from brain perfusion CT based on Monte Carlo simulation. AJR. Am. J. Roentgenol. 198:412–417

49. Lee C, Kim KP, Long DJ (2012) Organ doses for reference pediatric and adolescent patients undergoing computed tomography estimated by Monte Carlo simulation. Med. Phys. 39:2129–2146

50. Gu J, Xu XG, Caracappa PF, et al. (2013) Fetal doses to pregnant patients from CT with tube current modulation calculated using Monte Carlo simulations and realistic phantoms. Radiat. Prot. Dosimetry 155:64–72

51. Figueira C, Becker F, Blunck C, et al. (2013) Medical staff extremity dosimetry in CT fluoroscopy: an anthropomorphic head voxel phantom study. Phys. Med. Biol. 58:5433–5448

52. Zhang D, Cagnon Ch, Villablanca JP, et al. (2013) Estimating peak skin and eye lens dose from neuroperfusion examinations: use of Monte Carlo based simulations and comparisons to CTDIvol, AAPM Report No. 111, and ImPACT dosimetry tool values. Med. Phys. 40:091901

53. Khatonabadi M, Zhang D, Mathieu K, et al (2012) A comparison of methods to estimate organ doses in CT when utilizing approximations to the tube current modulation function. Med. Phys. 39:5212–5228

54. Caon M (2013) The ratio of ICRP 103 to ICRP60 calculated effective doses from CT: Monte Carlo calculations with the ADELAIDE voxel paediatric model and comparisons with published values. Australas. Phys. Eng. Sci. Med. 36:355–362

55. Haba T, Koyama S, Ida Y (2014) Influence of difference in cross-sectional dose profile in a CTDI phantom on X-ray CT dose estimation: a Monte Carlo study. Radiol. Phys. Technol. 7:133–140

Contacts of the corresponding author:

Author: Kosuke Matsubara, Ph.D.
Institute: Kanazawa University
Street: 5-11-80 Kodatsuno
City: Kanazawa
Country: Japan
Email: matsuk@mhs.mp.kanazawa-u.ac.jp

HISTORY

HISTORY OF MEDICAL PHYSICS – A BRIEF PROJECT DESCRIPTION

Tabakov, S.[1,2],

[1] EMITEL Project Coordinator, King's College London, UK,   [2] President IOMP (International Organization of Medical Physics)

I. INTRODUCTION

Medical Physics is a relatively young profession and medical physicists began to be employed in hospitals around the time of the introduction of X-ray equipment in medicine. At the same time the profession is very dynamic and new methods/equipment are constantly developed, introduced and replaced. This creates a need for a reference source showing the development of the profession and the progression of ideas. Such source is naturally a project describing the history of the profession. The projects aim will be to show the creation and the evolution of different equipment and methods, as well as their clinical application; the overall development of the profession and the main contributors in the various topics in medical physics.

The project results will be a very useful source of information for future new developments and will provide a canvas for future updates. Very importantly, the project results will be a written proof of the significant role played by medical physicists in contemporary medicine.

The idea about this project came at one of the EMITEL Encyclopedia project meetings (Lund, 2007) when its Consortium was discussing to include in the Encyclopedia of Medical Physics names of prominent medical physicists. It was decided that due to time restrictions of the EMITEL EU-funded project this is not viable at the moment. Soon after this I came up with the idea that the Encyclopedia experience might be used for the preparation of a concise project/book, dedicated to the development of our profession. The project was revived late in 2015 and discussed in the IOMP Publication Committee and IOMP Executive Committee. As a result it was decided the project to be developed as an international, IOMP-led activity.

Elements of medical physics history already exist in various Overviews/Reviews related to specific methods or equipment. Their authors will be contacted for collaboration on the project, as well as any colleagues willing to help with this important initiative.

The project results will be a Compendium of various independent Volumes, as per the different branches of the profession. The results will be used not only by medical physicists, but also by medical doctors and other related professionals. The Compendium will be useful to researchers dealing with the stages of development/evolution of specific methods/equipment. The Compendium will be very useful to a broad audience and will create an excellent visibility for our profession.

The project will start with the time around the discovery of X-rays. The years before this period are very well described in Francis Duck's book "Physicists and Physicians", published by IPEM in 2013.

II. INITIAL STRUCTURE OF THE COMPENDIUM

The Compendium will have independent Volumes/Parts, which will reflect the main areas of development of medical physics, including:
1. Diagnostic Radiology (X-ray) Imaging
2. Computed Tomography
3. Radiotherapy (External beam)
4. Radiotherapy (Brachytherapy)
5. Nuclear Medicine Imaging
6. Ultrasound Imaging
7. Magnetic Resonance Imaging
8. Optical Systems and NIR in Medicine
9. Medical Informatics
10. Radiation Measurement and Protection in Medicine
11. Medical Physics – Professional Development
12. Medical Physics – Education&Training Development

Additional Volumes might be included to this initial spine (e.g. current methods as nanotechnology use, etc).

III. IDEA FOR THE SYSTEM OF PROJECT WORK

Each Volume of the Compendium will be relatively independent and will have its own Leads/Editors, who will prepare the internal structure of the Volume (its Chapters/Sub-chapters) and will invite colleagues to write these Chapters. This way the team for each Volume could span to more than 20 Contributors (especially when large Chapters have to be written). All these Contributors will write in parallel their Chapters and Sub-chapters, but will regularly send information about their progress to the Editors.

Each Chapter/Sub-chapter inside a Volume will refer to specific types of equipment and/or methods. The evolution of these will be described in a chronological manner – e.g.: what medical need existed, how the equipment/method idea has emerged; how it has developed; how it has been introduced into practice; how it has evolved; how it has been replaced by others OR has phased out OR has provided the background of something else, etc. These will be supported by a Reference list of the main publications (one system of citation to be used in all Volumes). It will be important the chronological order of development to be also applied for the Content of the Volume (when possible).

All Chapters and all Volumes of the Compendium will be developed in independent time periods. These will start and be completed at different times (some earlier, others later) depending on the teams and topics. When the content of one Volume is written, it will go through a Refereeing process (by another team of Colleagues). Their work will also be in independent periods of time. The Referees will also be listed as Contributors to the Volume. The development of the Compendium will pass through several "iterations". The methodology of the projects will roughly follow the methodology of development of the Encyclopedia of Medical Physics project (www.emitel2.eu). This methodology was consulted at the time with historians.

The project will aim to present a comprehensive view of our professional history, this way its expected each volume to be at least around several hundred pages (depending on the topic). This will produce a significant overall size, whose development will take several years. The References to the respective Chapters and Sub-chapters will have to be kept relatively brief (the essential publications). The number of pages used for References (in each Volume) will be additional to the overall Volume size. The workload, distributed to many colleagues, will present a project, which will not be too difficult to develop (judging again by the experience with the Encyclopedia of Medical Physics).

Initially the project will start with several Volumes as a trial and later will expand to the development of other Volumes. When one Volumes are ready, it will be printed as an Annex to the respective issue of the free online Journal of IOMP Medical Physics International (MPI). These Volumes will gradually form the Compendium *History of Medical Physics*.

The Editors and Contributors will have to have a broad view on the Volume topic and detailed knowledge about some of its parts. Care should be taken to have strong emphasis on the evolution of ideas over time (not so much on the current research). Early pioneers of some equipment/methods can be specially invited to contribute to the Volume. Many of the equipment and methods have been invented by members of AAPM and IPEM and this should be taken into consideration when selecting Editors/ Contributors.

IV. AUTHORING AND COPYRIGHT

Each Contributor will be asked to prepare his/her Chapter/Co-Chapter free of charge. In case the Contributor uses students for Literature search, the names of these will be included as Contributors.

All Contributors, Editors and Referees form the overall team of Contributors to the respective Volume. Their names will be written next to the Respective Chapter/Sub-chapters in the Content of the book. All these names will continue to stay in the future updates (i.e. names cannot be excluded).

All Contributors should agree that the overall copyright will be with IOMP. In case of future paper print of the Compendium (or its Volumes), the income will be used solely for supporting the global development of the medical physics profession.

In case a Publisher wants to publish on paper the Compendium or some of its Volumes (in their existing form), the Publisher could have a License to Publish, but not the copyright (IOMP will hold the copyright of the electronic publication). This would allow future updates by the future IOMP teams, independently from the Publisher. This would further allow the electronic form of the Compendium (a sequel of e-books) to be updated at any time by the future teams of colleagues. This way the *History of Medical Physics* will form a life record of the development of our profession.

Corresponding Author: Slavik Tabakov, President IOMP, e-mail: slavik.tabakov@emerald2.co.uk

INTERVIEW WITH PROFESSOR JOHN MALLARD

I. INTRODUCTION

During 2016 the International Organization for Medical Physics (IOMP) approved a new International Award in Medical Physics named after Professor John Mallard, OBE, FRSE, FIPEM.

The name of Professor John Mallard was selected for this award, as he played a crucial role in the development of two of the world's most important medical technologies – Magnetic Resonance Imaging and Positron Emission Tomography. He is also one of the Founders of IOMP; was the first IOMP Secretary General, later IOMP President and also Founding President of IUPESM.

The IOMP John Mallard Award will honour a medical physicist who has developed an innovation of high scientific quality and who has successfully applied this innovation in clinical practice (e.g. equipment, software, methodology), or who has led a team developing this innovation. This Award will be given triennially at the IOMP International Conference on Medical Physics (ICMP).

The winner of the first John Mallard Award was Professor Paul Marsden, Director of PET Medical Physics at King's College London and Guy's and St Thomas' PET Centre. He was selected to receive the IOMP John Mallard Award for his contribution to the development and clinical application of hybrid imaging using simultaneously PET and MRI. The inaugural John Mallard Award was presented at the 22nd ICMP, December 9 – 12, 2016 in Bangkok, Thailand.

Several months before the award presentation the IOMP Past Secretary General Prof. Peter Smith and the current IOMP President Prof. Slavik Tabakov visited Prof. John Mallard at his home in Aberdeen, where S Tabakov took an interview with him.

II. INTERVIEW

Slavik Tabakov: Dear colleagues, we are here with Professor John Mallard, the first Secretary General of the International Organisation of Medical Physics. In fact, the founder of the organisation together with other distinguished colleagues from the UK, Sweden, Canada and the United States. We are here on the occasion of the International Award in Medical Physics named after Professor John Mallard. It is a privilege to be here with him and his wife Fiöna, to hear some of his advice to all of us and also to share some of his memories. Professor Mallard, could you please tell us how did you decide to begin your career in medical physics?

John Mallard: Well, I had been at what was then University College Nottingham, which was a College of the University of London. My Professor was Professor L.F. Bates who was a magnetism man. He had developed, during WWII, a method to protect iron ships from magnetic mines. Immediately after the war the Atomic Energy Research Establishment at Harwell wanted to know the magnetic properties of Uranium which of course they were using for the first nuclear pile, atomic pile and so on. I had the task of measuring those magnetic properties. Iron was always an impurity. We obtained many samples with different levels of iron in, so that we could measure the magnetic susceptibility and project back to the magnetic susceptibility of the pure Uranium. That was my PhD work. I was appointed as a demonstrator in the Physics Department at University College Nottingham then. But it was clear that I had to move on as the Department was fully staffed. I saw an advertisement in the paper for a job in a hospital in Liverpool which was at the Liverpool Radium Institute. This institute had been given a gram of Radium – I think there were five of them in the country – to use for radiotherapy purposes. I applied for this job and much to my surprise I got it. I must confess that one of the major attractions was that it was a much better salary than any of the other jobs that were being advertised at the time!

So I moved to Liverpool and I was fortunate to work with a Dr T Chalmers (known for the Szilard-Chalmers nuclear reaction). He and his colleagues, particularly Mr Herbert, introduced me to the use of radioactive I-131 for measuring thyroid function. I did a lot of that, measuring thyroid function in patients. Then we started learning how to image the thyroid by moving what, at that time, was a collimated Geiger counter, and eventually became a collimated scintillation counter, over the neck to build an image of the shape and size of the thyroid in the neck. You could find

tumours in the thyroid and abnormalities of function, cysts and so on. I worked with many patients at that time. And then a job came up at Hammersmith Hospital in London which is now part of Imperial College. I managed to get that job and I built the first scanner, which started off being used for just the thyroid gland. It was based on a floating-top couch. You put the patient on the floating-top couch and moved it in centimetre steps. You measured the activity at each step so that you could build up an image of the distribution of I-131.

There was also a cyclotron at Hammersmith. The very first medical cyclotron in the world. Dr Constance Wood's Medical Research Council Radiotherapeutic Research Unit had this cyclotron and they were able to make other isotopes which led us to I-132, with a much shorter half life. We could carry out studies on children which you couldn't do with I-131 because the radiation dose would have been too high. I was able to have other isotopes, particularly an isotope of arsenic which localised in brain tumours, because the brain tumour breaks down the myelin sheath on the outside of the nervous fibres. The arsenic is able to penetrate, so that where there is a brain tumour you get an increased concentration of the arsenic. With our scanner we were able to image that and we set up a brain tumour scanning service which I think was the first one in the world. All the patients were sent to us from a neurosurgeon at Atkinson Morley's hospital in South London. They were sent over with a nurse and I was told: "you do your thing and tell me what you think". So I sent the nurse back with a report that said there was a tumour in a certain position in the brain, it was so big and so on. And after about eighteen months he came on the phone and said: "you know, you're doing remarkably well, I'm able to operate on most of your patients and I find the tumour is where you say it is and it helps me a lot". So that was how the first brain tumour scanning series went. I'm running out of steam now, where do we go?

ST: You were also involved in the pioneering of a whole body magnetic resonance scanner and a PET scanner, how did this equipment develop? How did the ideas come through and how were they implemented in practice?

JM: Well, the idea of the Positron Emission Tomography Imager is that you have a pair of scintillation counters on either side of the head or the body. The radioactive arsenic is localised by the two counters being activated at the same time by the positron disintegration, which is within a fraction of a millimetre from the actual radioactive decay. It gave a much more accurate localisation of the tumour than you could get from normal gamma ray imaging. That was the beginning of PET, Positron Emission Tomography. It was more complicated than before of course, you had to have two counters and digital processing, but it was a big improvement.

MRI came much later. I think sub-consciously I had always been looking for a use of magnetism in medicine. Never found one, but then we started getting this idea of possibly being able to localise things with magnetic resonance. I built up a team of physicists led by the brilliant Dr Jim Hutchinson. And the first image we took was of a mouse, which had been killed immediately before it was put into a small MR imager. We killed it by breaking its neck and the first image showed very clearly, exactly where the neck had been broken. So from then on it became a fight to get this technique from looking at a mouse, to looking at a whole human being. And that took 23 years. But once that was achieved, we scanned our first patient on April the 26th 1980. It was a man from Fraserburgh, Scotland, who had a very large malignant growth in his liver which was known about, but what they didn't know was that there was also a secondary deposit in one of his spinal discs. That was picked up on the whole body MRI. So for our very first patient, the MRI showed information that they didn't have before.

ST: It is so important that your innovations were immediately implemented into clinical practice. That is why we decided to award the John Mallard Award to a scientist who not only discovered something, but also actively implemented it into medicine, because this is what we do. We are at the interface between science and medicine.

JM: Yes, well it is not a bit of good doing it in the lab is it? You have got to go out and use it on patients and get some practical results. I am very pleased that it has gone as well as it has. I have got a leaflet somewhere about the latest magnet from Siemens, I think it's 7 Tesla. Good heavens! Our first one was 0.04 of a Tesla, Mark I. Mark II was 0.08 Tesla and now it is 7 Tesla, which gives superb visual resolution compared to our Mark I and Mark II. But at the time that was the highest field strength we could achieve with sufficient uniformity over the body.

ST: Yes, but the important things are the ideas and the methods which are working now and improving constantly. One other thing that you have done amongst the many contributions to medical physics is your work to help other countries to develop their own medical physics programmes. As President of the IOMP, I really want to thank you on behalf of many colleagues around the world, now 84 countries, for the establishment of the International Organisation for Medical Physics. You were there from the very beginning and you were the first Secretary General. What are your memories of this time, back in 1963?

JM: Well, Sweden was always very much to the fore and I remember Dr Sven Benner of Uppsala, who was always very interested in developing Medical Physics. The other interesting thing is that Hungary was always to the fore. I wrote a lot of letters to people in Hungary. At that time they were firmly behind the Iron Curtain, so how they managed to correspond with me, very much in the West, I really don't

know, but they did. We were all keen to develop medical physics. Another country that always surprised me was Japan, Japan corresponded a lot. I am not quite sure how many countries I was corresponding with - it was either 34 or 43. I suppose it was 34. If there was more than one centre in the country I tried hard to encourage them to set up a national committee so that they could affiliate that country to the beginning of IOMP.

ST: Yes, and now we have 84 countries with about 24 000 members around the world. This is something that you started. You were also President of the IOMP at the beginning of the 1980's alongside your work with magnetic resonance. What would be your advice to colleagues around the world, young colleagues, for their work in the field of medical physics?

JM: Try hard to improve it, try hard to do something new. Try hard to think of something a bit different and develop that: push it as much as you can. Don't just sit there and accept what is the accepted version because there is always something beyond that if you can think of it or find it.

ST: I have to say that a lot of us have worked in this field, we are here with Prof. Peter Smith who was also Secretary General of the IOMP and he was very much involved in the establishment of Medical Physics as a separate profession. This was an achievement of IUPESM and you were the first president of IUPESM. How do you see the future of this field?

JM: Well, I worry sometimes: has it reached its zenith, will it fade away a bit, with less new things coming along? There is a tendency throughout the world isn't there, for the biologists to take over. And I have always been told, for donkey's years, oh well the biochemists are going to solve everything. And all I can say is that they haven't solved everything yet have they? So I am sure Medical Physics will still have a part to play.

ST: There is a future and we always have to believe that there is more to be discovered. We haven't even scratched the surface of nature, and I think that in the future medicine and medical physics will continue to have a strong link, especially when many countries work together.

JM: I think that probably the next most important development will be nanotechnology. Trying to develop that so that we can direct treatment in whatever form it might be, exactly to the right place. Probably that is the next step. But I am afraid that is a bit beyond me.

ST: There will be others now to go along the road which you have paved. Thank you very much indeed on behalf of

all of my colleagues from the International Organisation of Medical Physics, from the UK IPEM, and all of us.

JM: Thank you very much indeed, thank you.

Special gratitude is to be extended to Prof. Peter Smith, Past Secretary General of IOMP, and Past Treasurer of IUPESM, who initiated the renewed link of IOMP with Prof. John Mallard and facilitated the meeting with him and his wife Mrs Fiöna Mallard at their home in Aberdeen.

With Prof. Mallard during the interview (August 2016) – left to right: John Mallard, Slavik Tabakov, Peter Smith

III. Video address from Professor John Mallard to the ICMP2016 delegates

I am in my ninetieth year, so these are really the ramblings of a very old man. I know that you're all medical physicists and I think that you are all very fortunate because you are able to use your science to help people. Both your routine work and your research work helps to treat them, and helps to diagnose their illnesses. With research, I think it is very important to persevere and keep going. All advances take a lot of time. MRI was twenty three years from the idea to making it work on the whole body. IOMP is the wonderful organisation which ensures that every advance is made known worldwide, and I am both proud and humbled by the award which IOMP has set up in my name. I'm very grateful. And I hope that it spurs people on to contribute significantly to our very wonderful field of science. Enjoy it and learn as much as you can from your Congress in Bangkok. How I wish I could be with you. Thank you very much for listening. .

MEDICAL PHYSICS PROFESSIONAL BODIES IN THE UNITED KINGDOM: A BRIEF HISTORY

Keevil, S [1,2]

[1]Department of Medical Physics, Guy's and St Thomas' NHS Foundation Trust, London, UK
[2]Department of Biomedical Engineering, King's College London, London, UK

Abstract –**The Institute of Physics and Engineering in Medicine (IPEM) is the UK-based professional body and learned society for medical physics and engineering. Its members include clinical scientists and technologists working in healthcare, as well as colleagues in academia and industry. The Institute has a strong reputation internationally for its scientific and professional work. IPEM was established in its current form in 1997, but it continues the legacy of several earlier organisations, including the world's first professional organisation for medical physics, the Hospital Physicists' Association (HPA), which played a significant role in the establishment of the International Organisation for Medical Physics (IOMP). This article gives a brief account of the history and heritage of IPEM, focusing particularly on its medical physics legacy.**

Keywords – **IPEM, medical physics, history**

I. INTRODUCTION

On 24th September 1943, a group of around 30 men and women gathered at the offices of the British Institute of Radiology (BIR) in London and decided to establish '…a body… to interest itself in and discuss matters arising out of the natural interests of those engaged in hospital physics' [1]. The following day a name was chosen for this new 'body': the Hospital Physicists' Association (HPA). And so, over the course of two days, the first organisation in the world dedicated to medical physics was both born and christened, dedicating itself to the application of physical science to the relief of human suffering even while the Second World War was still raging.

The relationship between physics and medicine of course has a much longer history than this mid-twentieth-century date would suggest. Some of the greatest scientists in history, including Leonardo da Vinci (1452-1519) and Ibn al-Haytham (965-c1039), sought to use physical principles to understand the functioning of the body, and indeed much of what we now think of as physiology is really applied physics. By the nineteenth century, physics-based technology was pervasive in medical practice and research. There are several published accounts of the fruitful relationship that developed over the centuries between the two fields of endeavour [2, 3]. As in many other walks of life, the role of physics and physicists applying their expertise to medicine was mainly to provide explanations and tools for use by others: physicists themselves were not yet involved directly in clinical practice. But the growing dependence of medicine on physical science led to a requirement for physics teaching in medical schools, which therefore established academic physics departments that in due course were to provide a springboard for something more [2].

The closing years of the nineteenth century were *anni mirabiles* for physics. Within the space of four years, Wilhelm Röntgen (1845-1923) discovered x-rays, Henri Becquerel (1852-1908) discovered radioactivity, and Pierre and Marie Curie (1859-1906 and 1867-1934, respectively) discovered radium and isolated radioactive isotopes. These discoveries were to revolutionise not only our understanding of fundamental physics, but also medical practice. Astonishingly, X-rays were in clinical use for imaging within three months of their discovery. By the summer of 1896 radiation was being used to treat cancer too, and at around the same time the harmful effects of radiation became apparent. It soon became clear that safe and effective clinical use of radiation required input from physicists; physicists who would not simply invent tools for others to use, as had been the case before, but who would be directly involved clinically.

In some UK teaching hospitals, this emerging need was conveniently met by drawing on the expertise of local academic physicists. So, for example, Professor Gilbert Stead (1888-1979) was appointed as Honorary Consultant Physicist to Guy's Hospital, in addition to his academic duties at Guy's Hospital Medical School. Elsewhere, hospitals employed their own physicists directly, with the first in the UK being Sidney Russ (1879-1963), appointed by the Middlesex Hospital in 1913. Russ was later the inaugural holder of the oldest chair in medical physics in the world, the Joel Professorship of Physics Applied to Medicine

By 1932 there were 10-12 hospital-based medical physicists in the UK, and by the beginning of the Second World War there were 35-40. The time was right for a dedicated organisation to support this new but rapidly growing profession.

II. THE HOSPITAL PHYSICISTS' ASSOCIATION (HPA)

Sidney Russ was unanimously elected as the first Chairman of the HPA at the inaugural meeting in 1943, and work began in earnest. The fortieth anniversary of the

Association was marked by publication of a detailed history [1], which has formed the basis of much of this section of the present paper.

Reading the early history of the HPA, it is clear that the pattern of learned society activities was established early on: scientific meetings, publications, and of course social events (see Figure 1)! These early years also witnessed the forging of strong, mutually beneficial relationships with allied organisations such as the BIR, Faculty (later Royal College) of Radiologists, and Society of Radiographers. Whilst initially work focused purely on clinical applications of ionising radiation, the activities and structure of the Association rapidly adapted to encompass a broader range of medical physics topics. Later strong links were established with government departments, giving the Association and subsequently the Institute an influential voice in policy development, the implementation of legislation and the development of professional guidelines.
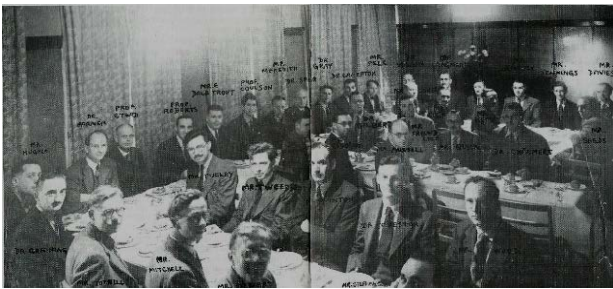
Figure1. HPA annual dinner 1949. At the centre of the top table is Charles Coulson, at the time Professor of Theoretical Physics at King's College London. At least seven medical physicists with links to King's and its associated hospitals are also in the picture.

A key early initiative was the 'Diagrams and Data Scheme'. This facilitated sharing of scientific data and good practice between members for mutual benefit, a concept still at the core of IPEM's activities today. In 1956 the HPA was instrumental in the establishment of *Physics in Medicine and Biology*, now published by IPEM in association with IoP Publishing, and one of the leading international journals in the field. Publication of specialist reports, often containing advice that is regarded as authoritative internationally, is a further activity strongly associated with IPEM which also began early on in the life of the Association.

Another concern for the Association from its earliest years was the pay and conditions of employment of hospital physicists. This became particularly important following the establishment of the UK National Health Service (NHS) in 1948, at which point such matters became the subject of national negotiation rather than local agreement at individual hospitals, and in 1977 the HPA registered as a trade union in order to strengthen its position in these discussions.

Membership of the HPA grew from 53 in 1943 to 627 in 1965 and nearly 1500 by the early 1980s. The Association was open to medical physicists, but not to technicians working in the field. In 1952, a meeting was held at Guy's Hospital, chaired by Gilbert Stead who was then President of the HPA, to establish the separate Hospital Physics Technicians' Association (HPTA), later renamed the Association of Medical Technologists (AMT) [4].

Education and training were key concerns of the HPA from its early days, and formal discussions about the establishment of a training programme for medical physicists date back to 1963. After lengthy consideration, a graduate training scheme was established in 1981, involving staff rotating through different specialisms to broaden their knowledge.

As the first organisation of its kind in the world, the HPA naturally took a leading role in the development of the medical physics profession globally. The Association was instrumental in discussions leading to establishment of the International Organisation for Medical Physics (IOMP) in 1963 and hosted the inaugural International Conference on Medical Physics (ICMP) in Harrogate in 1965. The HPA was also heavily involved in establishment of the European Federation of Organisations for Medical Physics (EFOMP) in 1980. Over the years there were many bilateral initiatives with colleagues in the developing world, and this continues to feature in IPEM's international strategy.

III. THE INSTITUTE OF PHYSICAL SCIENCES IN MEDICINE (IPSM)

By the early 1980s, it was felt that it would be best to distinguish the scientific and professional work of the HPA more clearly from its trade union role. To this end, the Institute of Physical Sciences in Medicine (IPSM) was established in 1982, and registered as a charity in 1984. The HPA continued solely as a trade union, with its other activities transferred to IPSM. Initially, although the HPA and IPSM were legally separate organisations, it was not possible to join one without also joining the other, the Council of the Institute and Board of the Association had identical memberships, and a single individual was president of both. But the two bodies gradually became more distinct, and in 1993 the HPA merged with the Manufacturing, Science and Finance Union (MSF) and separated completely from IPSM [5]. As a result of subsequent mergers between trade unions, the HPA became a national branch of Unite the Union in 2007.

The new membership structure of IPSM included categories of corporate membership, for the first time conferring the right to postnominal letters for those qualified in medical physics specifically. Membership of the Institute (MIPSM) initially required six years of responsible experience, shorter for those who completed the IPSM Training Scheme. Fellowship (FIPSM) was established as a distinction level of membership, requiring demonstration of

a high standard of scientific achievement and professional responsibility.

Until the early 1990s, it was the exception rather than the rule for new entrants to the profession to undertake the IPSM Training Scheme. Most new staff trained 'on the job' in a specific role, often with little opportunity for exposure to other medical physics specialisms. In 1990 a new career structure for NHS scientists was introduced by the government, which for the first time recognised the need for structured initial training and established a training grade (known as 'Grade A') for this purpose. Supernumerary posts funded by Regional Health Authorities, not individual hospitals, were in place throughout the country by 1994 [5]. Thus the IPSM Training Scheme became the standard route for training of medical physicists in the NHS, a situation which was to continue until the 2010s.

IV. THE INSTITUTE OF PHYSICS AND ENGINEERING IN MEDICINE (IPEM)

The Biological Engineering Society (BES) was founded in 1960 to provide a 'home' for the growing number of engineers working in biomedicine, as well as medical practitioners and biologists with an interest in engineering [6]. It has always been difficult to draw a clear dividing line between medical physics and biomedical engineering, and there were a number of joint initiatives with the HPA and IPSM in areas such as training. A Memorandum of Understanding signed by the presidents of both organisations in 1992 envisaged ever closer cooperation, and in 1995 members of IPSM and BES voted by a clear majority (90% and 95%, respectively) for full merger [7]. After lengthy consideration, senior officers of the new organisation decided on the name 'Institution of Physics and Engineering in Medicine and Biology' (IPEMB). However, this name proved unpopular with the membership, and in 1997 was changed to 'Institute of Physics and Engineering in Medicine' (IPEM), although many regretted the implied loss of the link with biology.

The BES had a much more diverse membership base than IPSM, and several additional categories of IPEM membership were needed to accommodate, for example, medically qualified individuals and technologists. Opening up of membership to technologists was a particularly significant development, and led to discussions with the AMT that resulted in a further merger in 1997. This completed the process of mergers and name changes that led to the establishment of IPEM in essentially the form that is has today (see Figure 2). IPEM now has a membership of over 4000, including individuals working (or simply interested) in all aspects of medical physics and engineering.
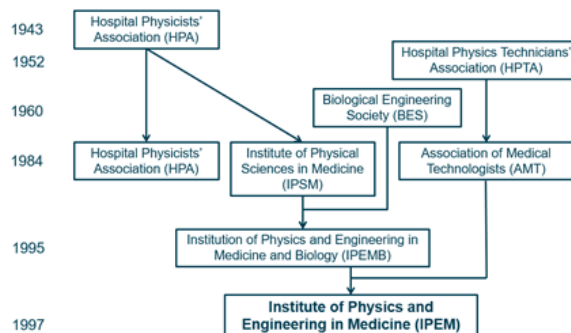
Figure 2. The evolution of UK professional bodies in medical physics and engineering.

Since its formation, IPEM has built on the legacy and reputation of its predecessor organisations and become 'one of the most effective professional bodies in the field of healthcare' [8]. One of IPEM's key strengths is that it brings together both physical sciences and engineering applied to medicine, something that is surprisingly rare internationally. The Institute is licensed by both the Engineering Council and the Science Council in the UK and can award professional registration in both disciplines (CSci, CEng, RSci, IEng, EngTech and RSciTech) to suitably qualified members. Internationally, it is a member of both IOMP and the International Federation for Medical and Biological Engineering (IFMBE).

State registration for scientists working in healthcare, as a means of ensuring professional competence and so protecting the public, was first proposed in the 1980s, and in 1994 a joint 'indicative register' was established by IPSM and other professional bodies in the sector. In 2000 state registration became a legal requirement, and 'clinical scientist' (encompassing medical physicists and other groups of scientists in healthcare) became a legally protected title. This was clear and important recognition of the role that medical physicist play in patient care. In 2000, IPEM also established the Register of Clinical Technologists (RCT), with strong links to the Institute's Technologists Training Scheme. The RCT was accredited by the Professional Standards Authority (PSA) in 2015. As a result of changes in government policy, this is currently the closest available equivalent to state registration for clinical technologists.

The IPEM Training Scheme provided the main route to clinical scientist registration for medical physicists and clinical engineers until 2011. In that year, radical changes to scientist training were introduced by the government, and a National School of Healthcare Science was established to deliver these new training programmes in England. Although IPEM no longer runs the training scheme, it was able to influence the structure of training significantly, so that the programme now followed by all trainee clinical scientists bears more than a passing resemblance to the former IPEM scheme. IPEM is also heavily represented in

the structures overseeing and supporting the new training arrangements.

As noted earlier in this article, many early medical physicists came from an academic background. Over the years there has been a steady and healthy flow of scientists moving between academic and clinical work. State registration has made this more difficult in recent years, and IPEM's close involvement with NHS training and workforce issues has led the Institute to have a strong focus on that sector. With responsibility for NHS training removed, IPEM is now reinforcing its position in the academic sector. In 2015 it was agreed that the scientific work of the Bioengineering Society, an informal grouping of academic biomedical engineers, would be transferred to IPEM.

The first joint conference will be held in September 2017 (see https://www.ipem.ac.uk/ConferencesEvents/MPECME Ibioeng2017.aspx). Further changes to membership structures have loosened links to NHS training and employment and so made membership more attractive to academic and industrial colleagues. In this way the Institute is building on its strong legacy and consolidating its position as the leading professional body in medical physics and engineering, bringing together clinical and academic activity under a single umbrella to the benefit of both and ultimately of the public that, as a charity, IPEM exists to serve.

REFERENCES

1. Haggith J.W. (Ed.) (1983). History of the Hospital Physicists' Association. (Newcastle upon Tyne: Hospital Physicists' Association).
2. Keevil S.F. (2012) Physics and medicine: a historical perspective. Lancet 379 1517-24.
3. Duck F.A. (2013) Physicists and Physicians. A History of Medical Physics from the Renaissance to Röntgen. (York: Institute of Physics and Engineering in Medicine).
4. Arkley W. (2006) The Association of Medical Technologists 1952-2001. Scope 15 Heritage Supplement 33-38.
5. Dendy P. (2006) The Institute of Physical Sciences in Medicine (IPSM) 1983-95. Scope 15 Heritage Supplement 18-26.
6. Meldrum S. (2006) The Biological Engineering Society 1960-95. Scope 15 Heritage Supplement 12-17.
7. Wells P. (2006) The Birth of the IPEM 1995-97. Scope 15 Heritage Supplement 27-32.
8. Griffiths P. (2006) The First Decade of the IPEM 1995-2005: the Development of the IPEM into a Professional Body. Scope 15 Heritage Supplement 39-45.

Contacts of the corresponding author:

Author: Stephen Keevil
Institute: Department of Medical Physics, Guy's and St Thomas' NHS Foundation Trust
Street: St Thomas' Hospital, Westminster Bridge Road
City: London, SE1 7EH
Country: United Kingdom
Email: stephen.keevil@kcl.ac.uk

BOOK REVIEWS AND COLLABORATING TOPICS

COLLABORATING TOPICS AND BOOK REVIEWS

Moyed Miften [1]

[1] Professor and Chief Physicist, Department of Radiation Oncology, University of Colorado School of Medicine, USA

Hendee's Radiation Therapy Physics, Fourth Edition by Todd Pawlicki, Daniel J. Scanderbeg, George Starkschall. 327 pp. WILEY Blackwell, Hoboken, New Jersey, 2016. Price $149.95 (Hard Cover). ISBN: 978-1-4398-2582-2.
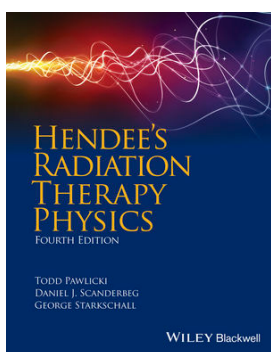
V. DESCRIPTION

Hendee's Radiation Therapy Physics, Fourth Edition, is an up-to-date edition of the well-known text book *Radiation Therapy Physics.* The book presents an overview of the physics involved in radiation therapy, ranging from theoretical principles to current treatment planning and delivery techniques. Specifically, the book presents theory, discusses relevant clinical treatment techniques, and covers the technology used in the fields of external beam therapy, brachytherapy, and stereotactic radiosurgery, as well as quality assurance (QA) and patient safety for these fields.

VI. PURPOSE

The field of radiation therapy has seen tremendous advancements over the past 10 years; therefore, a new edition of *Radiation Therapy Physics* is needed. The book meets the objectives of updating the third edition, which include i) removing outdated materials such as the use of film and conventional simulators, ii) expanding the chapters on digital imaging and Computed Tomography, and iii) adding new chapters on image-guided radiation therapy (IGRT) and adaptive radiation therapy (ART), proton radiation therapy, radiation therapy informatics, and QA, quality improvements and safety in radiation therapy. In doing so, the authors focuses on building upon the 3rd edition's strong foundation in which a wide-array of topics that span all areas of radiation therapy including advanced fields are covered, thereby making the book relevant to the educational needs in radiation therapy.

VII. AUDIENCE

The book is directed at radiation oncology residents as stated by the authors. However, I found the book useful for medical physics students, medical dosimetrists or physicists starting a career in medicine, and clinical physicists who want to use the book as a quick reference guide.

VIII. CONTENTS/FEATURES

The book has 20 chapters that cover the following major sections: basic nuclear physics and radiation interactions with matter; measurements, calibrations, and dosimetry; imaging and treatment planning; computer systems and informatics; brachytherapy; and radiation protection and quality assurance. Furthermore, the book discusses new advancements for various treatment modalities and describes new treatment techniques and technologies, including IMRT, protons, IGRT and ART, and patient safety and quality improvements. The book is concise but comprehensive in scope. Information and data are presented in a balanced way and in an easy-to-read format. Each chapter includes up-to-date references for each subject and

includes problem and answers sets for self-testing, a desirable feature for students. All chapters have numerous illustrations and practical examples.

IX. ASSESSMENT/COMPARISON

With the rapid development and implementation of advanced planning, imaging, and delivery technologies, the book provides a platform to disseminate knowledge on these new areas in addition to conventional radiation therapy. The field of radiation therapy is continuously evolving in new directions. Our field is seeing additional integration of imaging modalities with radiation therapy, such as Ultrasound, PET and MRI, additional imaging and delivery techniques that track tumors in real time, and a greater interest in Carbon particle therapy. While the book does not cover all these areas, it provides a substantial overview of current treatment techniques and technologies in radiation therapy. *Hendee's Radiation Therapy Physics,* fourth edition, is a valuable educational resource worthy of being added to our radiation therapy text book library.

REPORT OF AN UPDATE TO THE PERSIAN TRANSLATION OF MEDICAL PHYSICS TERMS: EMITEL INTERNATIONAL DICTIONARY

Behrouz Rasuli[1], Ali Mahmoud-Pashazadeh[2], Azam Niroomand-Rad[3], E. Ishmael Parsai[4]

[1] Department of Radiology Technology, Behbahan Faculty of Medical Sciences, Behbahan, Iran. [2] Persian Gulf Nuclear Medicine Research Center, Bushehr University of Medical Sciences, Bushehr, Iran. [3] Department of Radiation Medicine, Georgetown University Medical Center, Washington DC, USA. [4] Department of Radiation Oncology, University of Toledo Medical Center, Toledo, Ohio, USA.

Abstract— **The aim of this paper is to introduce first update to the original online Persian translation of medical physics terms in the Multilingual Dictionary of Medical Physics Terms, available also at EMITEL (European Medical Imaging Technology e-Encyclopedia for Lifelong Learning), that is both accurate and common. Consistent with EMITEL objectives, periodic review of EMITEL terms is imperative to ensure the quality in the Persian language. This first update of Persian translation section of EMITEL, that provides significant improvements to the original one, is outcome of many hours of volunteering efforts by numerous contributors. In this report, we present a sample of revised words as searched in EMITEL based on the key words entered in its search engine, and present explanation of definition of the acronyms in English section of EMITEL. Attempts are made to review and revise all (4921) entries of EMITEL terms, whether a single word or combination of words, that are precise and frequently used by medical physicists in Iran. Revision of some sample words such as *Dose*, *Radiation*, *Image*, *Imaging*, *Radiotherapy*, *Ultrasound*, *Protection*, *MRI*, *Radiobiology*, *CT Scan*, *PET*, *Film* and *Detector* are also presented in this report.**

I. INTRODUCTION

With widespread use of online educational resources, some features of distant learning and educational technique have changed greatly in the past few years (1, 2). Online educational resources provide an easy-to-access complementary learning tools to students, teachers and educational organizations (3). One of these online tools is EMERALD (European Medical Radiation Learning Development) e-Learning material involving UK, Sweden, and Italy that was developed in late 1990's. Later on, in early 2000s EMERALD project was expanded and led to development of EMIT Multilingual Dictionary of Medical Physics Terms (International Dictionary). The latter was further expanded into EMITEL (European Medical Imaging Technology e-Encyclopedia for Lifelong Learning), including the respective translations of the International Dictionary (4). The International Dictionary was established to address the needs of medical physics professionals. It was initially founded in association with the European Federation of Medical Physics (EFOMP), then the project was joined by the International Organization of Medical Physics (IOMP) during the International World Congress of Medical Physics in Seoul, South Korea, in 2006 (4).

The International Dictionary first started with 7 languages (English, Swedish, Italian, French, German, Portuguese, and Spanish), and later 22 languages, including Persian, were added, thus forming the existing list of 29 languages (4). By mid-2000's the International Dictionary provided a foundation for the development of EMITEL e-Encyclopedia of Medical Physics with c.3200 terms (4). The full International Dictionary is now accessible from www.emitdictionary.co.uk, while the terms included in the e-Encyclopedia of Medical Physics are accessible from www.emitel2.eu - both as terms translation in 29 languages and as encyclopedic entries in English for each term (5).

According to IOMP statistics, over 4600 users visited the emitdictionary.co.uk website of the EMITEL from April to January, 2013 and over 10174 users visited the emitel2.eu website (4). Over 200 translators, experts in medical physics and related fields including (but not limited to) radiation therapy, diagnostic radiology, nuclear medicine, ultrasound imaging, magnetic resonance imaging and radiation protection, were involved in this massive undertaking (4). In this current update of the Persian translation, the ultimate goal was to introduce accurate and proper substitutes for English terms that are meaningful, practical, and reflect and convey the equivalent in the Persian language. As this was the first complementary step to revise the Persian section of the International Dictionary, the authors of the current report, besides introducing this project to the Persian-speaking medical physics communities, present a brief overview of the effort which resulted in a revised and enriched Persian section of the Dictionary at both web sites.

II. METHOD AND MATERIALS

The first version of Persian section of the International Dictionary was implemented in mid 2000s. This first version was the results of many hours volunteering efforts by Prof. Alireza Binesh, [Persian Coordinator], from Payam Nour University, Fariman, Iran, Dr. Ali Asghar Mowlavi, from Sabzevar Tarbiat Moallem University, Sabzevar, Iran, and Prof. Azam Niroomand-Rad, IOMP Past President from Georgetown University Medical Center, Washington DC, USA (4).

In this first update of Persian translation that started in late 2014 efforts were made to substitute some words, either as a single word or in combination with other words, that are "accurate" and in "common" use by current medical physicists in Iran. A comprehensive review of all (4921) EMITEL words was performed. After thorough examination, authors of this manuscript found that some Persian translations were not consistent or practical for Persian-speaking medical physicists. In addition, in some cases few extra words had to be added to make the Persian translation more clear and concise. Moreover, in some cases corrections were made to eliminate misconceptions of the exact meaning of the words that were incorrect.

Lastly, with the objective of enriching Persian translation of the Dictionary, attempts were made to identify over 45 acronym of abbreviated words in the English section of the International Dictionary that were described accordingly.

III. RESULTS AND DISCUSSION

After careful examination of all (4921) entries of the Persian translation of terms, they were updated at the Dictionary web site: www.emitdictionary.co.uk. (8)

Those of the terms (c.3200), used also in the EMITEL Encyclopedia, were also updated. Like any other online websites with e-learning materials, EMITEL International Dictionary was also updated in several languages and that update of Persian translation was a timely task.

Our criterion for update of Persian section of EMITEL dictionary was to suggest those Persian equivalent words for English terms that are more practical and more commonly used by medical physicists in Iran (6). In some cases, however, some words had to be replaced completely since there were some errors either in spelling or in concept. To ensure correct and precise Persian translation, where it was necessary, comments of experts were also included to provide the best translation for the English terms.

Table 1 compares our proposed translation of a few Persian words for update of Persian section of the International Dictionary that we believe are "common and correct" translations as compared with the existing ones. As shown in Table 1, some of the words such as "Build up dose", "Dose tolerance", "Time dose fractionation" and "Radiation biology" were translated word by word rather than as a whole phrase, which did not convey the true concept of the phrase. In a few words such as "Functional MRI", "Radiation quality", "Film crystals" and "lead protection" some errors in translations were seen and were corrected. At the writing of this paper, we expect our proposed update is uploaded in both websites www.emitdictionary.co.uk; and EMITEL www.emitel2.eu and can easily be accessed by the readers.

Moreover, the Persian translation team of International Dictionary - both past and present contributors - have tried to find the most appropriate and commonly used Persian words that are equivalent to the English terms. However, there were some limitations for this task. The most obvious one was to translate the abbreviated English terms that are common in English language, but not in Persian language. Therefore, when these abbreviated terms were identified, their acronyms were spelled out with their corresponding Persian translation accordingly, such that they are meaningful to Persian speaking medical physicists in Iran and elsewhere.

Lastly, authors of this paper hope that with the combined efforts of our translation teams (past and present) we are able to provide comprehensive and precise translation of the Persian section of Multilingual International Dictionary and EMITEL that can enhance quality e-learning in Persian language and ultimately be useful for the education and training of medical physicists for all Persian speaking population of the world (7).

IV. REFERENCES

1. Wang Y, Sun C. Internet-based real time language education: Towards a fourth generation distance education. Calico Journal. 2013;18(3):539-61.

2. Zhao Y. Recent developments in technology and language learning: A literature review and metaanalysis. CALICO journal. 2013;21(1):7-27.

3. Rutten N, van Joolingen WR, van der Veen JT. The learning effects of computer simulations in science education. Computers & Education. 2012;58(1):136-53

4. S Tabakov VT, M Stoeva, A. Cvetkov , F Milano S-E Strand5, J-Y Giraud, C Lewis. Medical Physics Thesaurus and International Dictionary. Medical Physics International Journal. 2013;1(2):140-144.

5. EMITEL e-Encyclopedia of Medical Physics 2014 [Available from: http://www.emitel2.eu/.

6. Ishmael Parsai et al. PARSA Dictionary, The Oxford Translator. Tehran, Iran: Azad University; 2017.

7. Seyed Rabi Mahdavi, Behrouz Rasuli, Azam Niroomand-Rad. Education and training of medical physics in Iran: the past, the present and the future Physica Medica. 2017;(accepted manuscript).

8. EMIT Medical Physics e-Dictionary only, 2006, [Available from: http://www.emitdictionary.co.uk/.

Corresp. Author: Azam Niroomand-Rad, e-mail: azam@georgetown.edu

Table 1. Proposed "common and correct" translations for some of the medical physics terms in EMITEL that required revision

EMITEL Term	Translation in EMITEL	Common and correct translation
CT (Computed Tomography)	ترموگرافی محاسبه شده	برش نگاری رایانه ای
Functional MRI (fMRI)	MRI کارآمد	MRIفانکشنال / مبتنی بر عملکرد بافت / عملکردی
Interventional MRI	MRI وقفه ای	MRI مداخله ای
Build up dose	دز ترقی	دز (ناحیه) انباشت
Dose Area Product	سطح دز ایجاد شده	حاصل ضرب دوز در سطح میدان تابش
Dose calibrators	درجه بند سازهای دز	کالیبراتورهای دوز
Dose conversion factors	عامل های واگردانی دز	عامل های تبدیل دوز
Dose length product	طول دز تولیدی	حاصل ضرب دوز در طول اسکن
Dose monitoring	دیدبانی دز	پایش دز
Dose tolerance	رواداری دز	تحمل دز
Dose width product(DWP)	پهنای دز حاصله	حاصل ضرب دز در عرض(میدان)
Implant dose distribution	توزیع دز تزریقی	توزیع دز اطراف چشمه کاشت شده (در براکی تراپی)
Integral dose	دز کامل	دز تجمعی
Normal organ dose tolerance	تحمل دُز اندام بهنجار	دز نرمال تحمل بافت
Normal tissue dose	دُز بافت بهنجار	دز نرمال بافت
Normalized treatment dose	دز دومانی بهنجار شده	دز درمانی بهنجار / نرمال
Percentage depth dose	درصد دز ژرف	درصد دز عمقی
Time dose fractionation	جزء به جزء سازی دُز زمانی	تقطیع دز (تقسیم دز کل به دز در چند جلسه در پرتو درمانی)
Asymmetric film screen	پرده فیلم بی‌تقارن	فیلم اسکرین های نامتقارن
FFD (Focal film distance)	فاصله کانونی فیلم	فاصله فیلم تا نقطه کانونی تیوب
Film badge	نشان فیلم	فیلم بج/ بج فیلم
Film crystals	بلورهای لایه نازک	کریستال (دانه های بلور در امولسیون) فیلم
Acquisition modes for digital image	مدهای یابش برای تصویر رقمی	روش های داده گیری برای تصویر دیجیتال
Analogue image	تصویر مانسته	تصویر آنالوگ
Image artifact	دست ساخته تصویر	آرتیفکت تصویر
Image fusion	ذوب تصویر	ادغام تصویر، ترکیب تصویر
Image guided radiotherapy	تصویر راهنمای رادیوتراپی	پرتو درمانی با هدایت تصویر
Portal image	تصویر مدخل	تصویر پورتال
Lead protection	حفاظت از آثار سوء سرب	حفاظ سربی
Extra focal radiation	کانون اضافی تابش	تابش تولید شده در لامپ اشعه ایکس غیر از نقطه کانونی
Radiation biology	تابش زیستی	زیست شناسی پرتوی
Radiation exposure	نوردهی تابش	پرتوگیری / پرتودهی تابش
Radiation monitoring	تنظیم تابش	پایش پرتوی
Radiation quality	کمیت تابش	کیفیه تابش
Bolus- radiotherapy	رادیوتراپی قطعه ای	بلوس رادیو تراپی/ پرتو درمانی
Inverse radiotherapy planning	برنامه‌ریزی رادیوتراپی وارون	طراحی درمان معکوس

RAD-AID, AN ORGANIZATION BRINGING RADIOLOGY TO RESOURCE-LIMITED REGIONS OF THE WORLD

Nikita Consul [1], Melissa Culp [2], Elise Desperito [3], Miriam Mikhail [2,4]

[1] Columbia University, College of Physicians & Surgeons, New York, NY, USA
[2] RAD-AID International, Chevy Chase, MD, USA
[3] Department of Radiology, Columbia University Irving Medical Center, New York, NY, USA
[4] RAD-AID International, Consultant Diagnostic Radiologist based in Geneva, Switzerland

I. INTRODUCTION

Resource-limited regions around the world stand to benefit greatly from sustainable global health initiatives, inclusive of both ionizing and non-ionizing medical uses of radiation. Optimal infrastructure for medical imaging and radiotherapy is difficult to establish. The World Health Organization has estimated that radiology is inadequately available to more than half the world's population [1,2]. Ultrasound and low-cost radiography may be more widely accessible, but imaging such as CT, MRI, and nuclear modalities remain inaccessible in many world regions [3], though they represent crucial diagnostic and interventional tools in modern medicine [4]. Addressing burden of disease and striving towards the goal of universal healthcare - according to evidence-based guidelines, clinical knowledge benchmarks, and best practices - obligates both medical imaging and radiotherapy.

RAD-AID seeks to bring imaging modalities to resource-limited regions and to promote appropriate use of them, at a time when interest in global health radiology is increasing [2]. RAD-AID, in addition to sharing radiological tools and technologies, also supports teaching initiatives on a range of topics - for example, optimal image acquisition, radiation protection, PACS, DICOM, and image interpretation [5]. This supports team building of staff and trainees, alike, as they ally with RAD-AID to deliver radiology-related aid to regions in need [2], and has inspired the expansion of RAD-AID chapters across 53 ACGME-accredited academic medical centers - with on-site projects in over 20 countries [3,6]. Associated capacity building by the entire RAD-AID team (e.g. radiologists, medical physicists, radiologic technicians/radiographers, ultrasound technologists/sonographers, IT professionals, and/or more) as relevant to the particular project bolsters the building of sustainable practices which maximize the population's benefit from integration or improvement of radiology into the Member State's healthcare services [1,5].

RAD-AID was founded in 2008 by a few members of Johns Hopkins University, and has since burgeoned to over 6100 volunteers from around the world, including 53 university-based chapters and on-site projects in 21 countries [6].

Project Sites, 2017
Africa
    Cape Verde
    Ethiopia
    Ghana
    Kenya
    Liberia
    Malawi
    Nigeria
    South Africa
    Tanzania
    Uganda
Asia
    Bhutan
    China
    India
    Jordan
    Kazakhstan
    Laos
    Nepal
Latin America and the Caribbean
    Guatemala
    Guyana
    Haiti
    Nicaragua

II. GLOBAL HEALTH

RAD-AID applies a stepwise approach to project planning: (1) economic development, (2) technological innovation, (3) clinical model implementation, (4) educational approaches, and (5) public health policies [7]. Working with local stakeholders - to ensure sustainability after implementation - requires assessment of items (1), (3), and (5) [1]. Clinical applicability quantifies the program's direct benefit for the patient population, for which (2) and (3) are particularly useful. Moreover, transfer of skills in using the introduced technologies entails onsite assessments (4).

As part of the aforementioned multidisciplinary approach, RAD-AID developed and trademarked (2009) a

tool utilized before and during deployment of radiology improvement programs, the Radiology-Readiness Assessment (Figure 1) [6]. As part of the assessment, data are collected to evaluate pre-existing availability of community resources and to identify local and regional medical needs. Then, an optimally impactful, achievable plan is created, with measurable deliverables, to target radiology needs. Implementation often includes equipment installation and clinical workflow design. Training constitutes an essential step, considered an opportunity for reciprocal education, and is discussed further in the section entitled "Educational Support". Finally, the overall project and program results are analyzed in efforts towards further improvements and innovations [7].
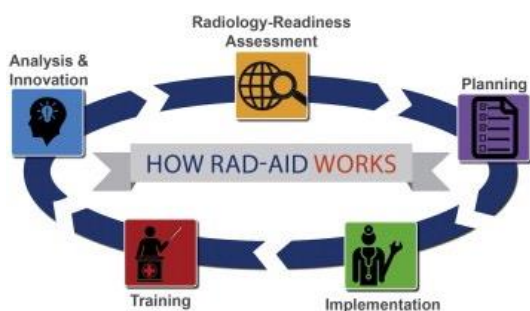
Figure 1. The steps of RAD-AID's Radiology-Readiness Assessment allow for data-driven design and implementation of a program based on the medical needs of a community that are solvable with radiology.

One such successful project, a direct result of the RAD-AID Radiology Readiness Assessment, is a mobile women's health care outreach program called Asha Jyoti ("Ray of Hope" in Hindi) in Chandigarh, India, which provides screening for breast cancer, cervical cancer, and osteoporosis in a decentralized, sustainable, and cost-effective manner[8]. This is a joint effort by RAD-AID, Philips Healthcare, and a local government medical center, the Post Graduate Institute of Medical Education and Research. Since the Asha Jyoti launch in 2012, more than 10,000 underserved women in northern India have been screened, thousands of whom live far from public hospitals and otherwise would receive no care [8]. Regular educational interventions on an annual or bi-annual basis by teams of residents and attending physicians through RAD-AID enable quality assurance of both image acquisition and interpretation.

III. EDUCATIONAL SUPPORT

RAD-AID's Chapters Network has implemented a common curriculum for radiology residents that provides global health training and allows chapter members to work in inter-

institutional chapter teams. Academic training programs have incorporated international elective rotations supported by RAD-AID grants, technology, PACS support, project guidance, and educational materials [3]. To assist residents and students in adopting roles that are both helpful and not beyond their scope of training during their exposure to and assistance in promoting optimal global health [5,9], RAD-AID has committed to providing clear objectives for projects and training for the settings and contexts within which projects are implemented [1].

Examples of resident international elective programs include RAD-AID chapters at Emory University and New York-Presbyterian Weill Cornell Medical Center, with projects located in Ethiopia. Other resident project initiatives include employing online learning management systems in Nicaragua and Haiti, implementing PACS platforms (Ethiopia, Ghana, Nepal, Haiti, Nicaragua), performing demonstrations of procedures (Nicaragua, Guyana, Ethiopia, Haiti, Malawi), or reporting back on implementation of image-based screening (Bhutan, India) [3].

As of this year, RAD-AID has extended its RAD-AID Certificate of Proficiency in Global Health Radiology to medical students, and has launched an elective course to be offered to medical students at the Columbia University College of Physicians & Surgeons beginning March 2017. The course is a four-week clerkship that incorporates didactic teaching from radiology faculty on global health, online modules pertaining to the Certificate of Proficiency, as well as a RAD-AID project overseas [3].

IV. MEDICAL PHYSICS AT RAD-AID INTERNATIONAL

RAD-AID uses a multidisciplinary approach to address areas of need in diagnostic imaging. Medical physicists are an important part of the organization. One such example is the Lao Friends Hospital for Children where RAD-AID has partnered since the hospital opening in 2015. RAD-AID supports the department of radiology via education for the local imaging personnel and human capacity building. Medical physicists consulted extensively on the radiography room design and radiation safety procedures to ensure best practice. For its work in Laos, RAD-AID received the 2017 Healing Asia Award from Friends without a Border.

Physicists are providing team support and on-site acceptance testing for the RAD-AID CT educational programs in Guyana and Haiti. Medical physicists are joining teams of radiologists, technologists, and other healthcare professionals to provide education about quality management testing, radiation protection, and protocol

design as relates to CT imaging. From the beginning, medical physicists have been an essential part of this program creation and will join teams on the ground as part of implementation in 2017.

RAD-AID supports the goals of radiotherapy and education of radiation oncology professionals. In 2010, RAD-AID began the Cancer Imaging and Treatment Initiative in western China, which has since expanded to include programs in Kenya and Tanzania. In these initiatives, physicists play a vital role in providing education and in promoting the importance of the physicist role in the multidisciplinary team of radiotherapy.

Additionally, some RAD-AID partner locations, such as Tanzania, show an emergence of functional imaging techniques so all scopes of medical physics are critical for success in outreach initiatives. In stepwise approach supporting in-country human capacity building, the participation of medical physicists in RAD-AID International contributes to the mission of sustainable impact in radiology—including medical imaging and radiotherapy.

V. Conclusions

RAD-AID International is a growing non-profit organization dedicated to expanding access to radiology, and in some cases radiotherapy as well, in resource-limited regions of the world. By using its Radiology-Readiness Assessment, RAD-AID continues to generate programs around the world in communities where radiology can improve health. With an increasing level of interest from allied professionals, RAD-AID seeks to continue to foster relationships with the team of professionals required for medical imaging infrastructure, ministries of health, relevant facilities, and/or academic medical institutions in its partner nations and to provide education in global health to healthcare professionals. Like IOMP, RAD-AID

International is a non-state actor officially affiliated with the WHO, and RAD-AID both welcomes and needs input from the medical physics community as part of a team, multidisciplinary effort. The Radiology Readiness Assessment and subsequent planning of programs feature aspects for which medical physicists serve a vital role, including but not limited to radiation protection.

To learn more and get involved, please visit https://www.rad-aid.org

References

1. Mollura DJ, Lungren MP. *Radiology in global health : strategies, implementation, and applications.* New York: Springer; 2014.
2. Tahvildari AM, Atnafu A, Cosco D, Acosta A, Gupta D, Hudgins PA. Global health and radiology: a new paradigm for US radiology resident training. *J Am Coll Radiol.* 2012;9(7):516-519.
3. Kesselman A, Soroosh G, Mollura DJ, Group R-ACW. 2015 RAD-AID Conference on International Radiology for Developing Countries: The Evolving Global Radiology Landscape. *J Am Coll Radiol.* 2016;13(9):1139-1144.
4. Diagnostic Imaging: What is it? When and how to use it where resources are limited? World Health Organization; 2001.
5. Ostensen H, Volodin V. Diagnostic imaging in developing countries: considerations for improvement. *Eur Radiol.* 2000;10 Suppl 3:S397-398.
6. RAD-AID. Introduction and Brief History. 2017; https://www.rad-aid.org/about-us/.
7. Culp M, Mollura DJ, Mazal J, Group R-ACW. 2014 RAD-AID Conference on International Radiology for Developing Countries: The Road Ahead for Global Health Radiology. *J Am Coll Radiol.* 2015;12(5):475-480.
8. Mango VL, Ha R, Nguyen B, et al. RAD-AID Asha Jyoti Mammogram Quality Assessment in India: Optimizing Mobile Radiology. *J Am Coll Radiol.* 2016;13(7):831-834.
9. Shah S, Wu T. The medical student global health experience: professionalism and ethical implications. *J Med Ethics.* 2008;34(5):375-378.

International Day of Medical Physics
2017 IDMP Award

The IOMP is pleased to announce the IDMP Award. This award recognises excellence in Medical Physics with a particular view of promoting medical physics to a larger audience and highlighting the contributions medical physicists make for patient care. The IDMP Award is linked to the International Day of Medical Physics (IDMP) from which it takes its name. This year we celebrate the 150th anniversary of Madame Marie Sklodowska-Curie's birth. The 2017 IDMP theme is *"Medical Physics: Providing a Holistic Approach to Women Patients and Women Staff Safety in Radiation Medicine"*.

The 2017 IDMP Award will be given on the occasion of the celebration of the International Day of Medical Physics (IDMP) and will be announced on November 5, 2017.

The IDMP Award consists of an IOMP certificate, and additionally a short biography of the awardee will be published in the IOMP Newsletter *Medical Physics World*.

Criteria for selection:

- The recipient of the award shouldbe a professional medical physicist holding a master's or higher degree or equivalent, who is an active member of the relevant Medical Physics society.
- The recipient should have taken active part in promoting medical physics, nationally or internationally.
- The recipient should have performed original and/or applied work of high scientific quality, or made a significant professional contribution to Medical Physics in the past three years.

Nominating Procedure

- The award will be widely advertised on the IOMP mailing list and website.
- The President of each IOMP Regional Organisation is kindly requested to nominate **three medical physicists** from her/his respective region. The Presidents of AAPM and COMP are kindly requested to nominate jointly three medical physicists from the North American region. Nominees should be full members of an IOMP National Member Organization (NMO).
- Self-nomination will only be considered in exceptional circumstances.
- Nominations are to be made to the chair of the IOMP Awards and Honours Committee (AHC)
- The nomination should include the following:

1. A letter of not more than 1,000 words evaluating the nominee's achievements and identifying the specific work to be recognized.
2. A Curriculum Vita including all publications and professional contributions to Medical Physics organizations.

Nominations should be sent to Dr. Simone K. Renha, Chair of the IOMP Awards and Honours Committee (AHC) at **simone@cnen.gov.br** by **September 8, 2017**. Submissions should be in the form of: MS Word or PDF document. Nominations will be acknowledged by e-mail. If you do not receive an acknowledgement within 72 hours please contact Dr. Simone or the Secretary General of the IOMP at**sg.iomp@gmail.com**.
One medical physicist from the three nominations per region will be selected by the AHC to receive the award.
The winners will be announced on **November 5, 2017**.

WELCOME TO PINK CITY JAIPUR

17th Asia-Oceania Congress of Medical Physics "AOCMP - 2017"
In conjunction with
38th Annual Conference of Association of Medical Physicists of India "AMPICON - 2017"

4th - 7th November 2017
Jaipur, India

Organized by
Department of Radiological Physics, SMS Medical College, Jaipur ,India
Under the auspices of
Asia Oceania Federation of Organizations for Medical Physics (AFOMP) &
Association of Medical Physicist of India (AMPI)

Visit us at:
Www.aocmp-ampicon2017.org

"Advances in Medical Physics: Shaping the Future of Modern Healthcare"

AOCMP - 2017

AMPICON - 2017

Organized by:

Co-sponsored by:

Endorsed by:

AFOMP   AMPI   OMP   AAPM   MEFOMP

Prof. Arun Chougule,Org.Chairman

II/38,Gandhi Nagar , Jaipur (Rajasthan) India Mobile+919928140113,
Mail to us at - arunchougule11@gmail.com, aocmp2017@gmail.com,visit us at - http://www.aocmp-ampicon2017.org

Jaipur **"*Pink city of India*"** is most celebrated city of legendary Rajputana, the land of Rajput valour, still retains its beauty and charm despite the process of modernization. It was founded in 1727 AD and still retains its splendid valour. The **17th Asia Oceania Congress of Medical Physics (AOCMP 2017)** and **38th Annual Conference of Association of Medical Physicist of India (AMPICON 2017)** being organised at SMS Medical College and Hospital, Jaipur "Pink City" during 4th to 7th November 2017.

Jaipur is well connected by road/rail/air with rest of the country. November-December is peak tourist season, so please plan your travel in advance. We suggest you to keep at least 2 days free after the conference dates for sightseeing while planning your travel plan The weather in Jaipur and Rajasthan is generally very pleasing in November and hope delegates will enjoy their stay at Jaipur. Kindly keep visiting conference website "**www.aocmp-ampicon2017.org**" for regular updates.

Registration Details & Deadlines

Category	Early Bird Till 31st August 2017	Upto 30th September 2017	After 30th September 2017
Foreign Delegates			
AFOMP & MEFOMP Member	US$ 250	US$ 350	US$ 450
NON Member	US$ 300	US$ 400	US$ 500
Associate Delegate	US$ 150	US$ 250	US$ 300
Student Delegate	US$ 150	US$ 250	US$ 300
Trade Delegate	US$ 1000	US$ 1500	US$ 2000
Indian & SAARC Delegates			
AMPI Member	Rs. 3000	Rs. 4000	Rs. 5000
NON Member	Rs. 4000	Rs. 5000	Rs. 6000
Associate Delegate	Rs. 1500	Rs. 1800	Rs. 2500
Student Delegate	Rs. 1500	Rs. 1800	Rs. 2500
Trade Delegate	Rs. 5000	Rs. 6000	Rs. 8000

Event	Date
Registration Open	On 01.07.2016 (1st July 2016)
Early Bird Registration	Up to 31.08.2017 (31st August 2017)
Regular Registration	Up to 30.09.2017 (30th September 2017)
Late Registration	After 30.09.2017 (30th September 2017)
Opening Of Abstract Submission	From 01.01.2017 (1st January 2017)
Closing Of Abstract Submission	On 30.06.2017 (30th June 2017)
Opening Of Trade Participation	From 01.01.2017 (1st January 2017)
Closing Of Trade Participation	On 30.09.2017 (30th September 2017)

The Payment can be made by sending **Demand Draft** in the favor of **AOCMP & AMPICON 2017** payable at Jaipur, Rajasthan (India) or by online transfer to conference account by NEFT/link provided on website. Don't forget to retain transaction reference number in case of online transfer , The account details for online transfer is:-

Name of bank: IDBI BANK LTD, VAISHALI NAGAR BRANCH, JAIPUR
ACCOUNT NAME: AOCMP & AMPICON 2017
BRANCH CODE: 273
IFSC CODE: IBKL0000273
BRANCH ADDRESS: F-28, GAUTAM MARG,OPP RELIANCE FRESH, NEAR AMRAPALI CIRCLE, VAISHALI NAGAR JAIPUR PIN: 302021
Account no. : 0273104000189071
Swift code: IBKLINBB013

Prof. Arun Chougule, Org.Chairman

II/38,Gandhi Nagar , Jaipur (Rajasthan) India Mobile+919928140113,
Mail to us at - arunchougule11@gmail.com, aocmp2017@gmail.com,visit us at - http://www.aocmp-ampicon2017.org
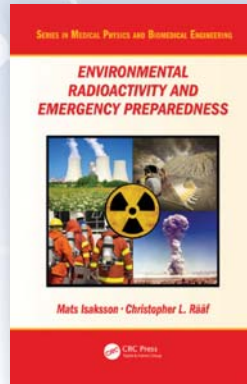
EXCLUSIVE DISCOUNTS FOR MEMBERS OF THE IOMP
on new books in the *Series in Medical Physics and Biomedical Engineering*, the official book series of the IOMP
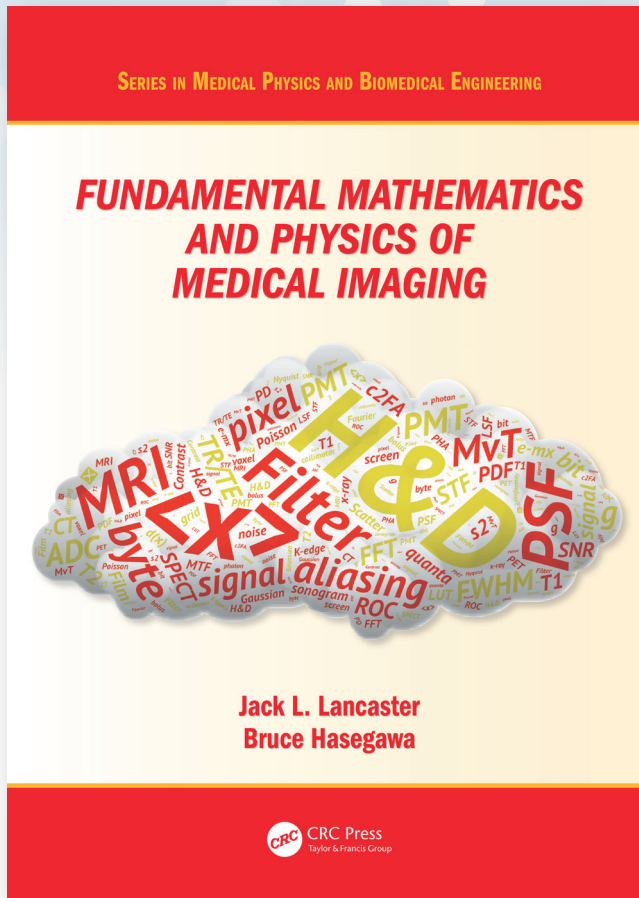
Fundamental Mathematics and Physics of Medical Imaging

Jack Lancaster, Research Imaging Institute, University of Texas Health Science Center at San Antonio, Texas, USA & Bruce Hasegawa

Authored by a leading educator, this book teaches the fundamental mathematics and physics concepts associated with medical imaging systems. Going beyond mere description of imaging modalities, this book delves into the mechanisms of image formation and image quality common to all imaging systems: contrast mechanisms, noise, and spatial and temporal resolution, making it an important reference for medical physicists and biomedical engineering students. This is an extensively revised new edition of *The Physics of Medical X-Ray Imaging* by Bruce Hasegawa (Medical Physics Publishing, 1991), and includes a wide range of modalities such as X-ray CT, MRI and SPECT.

Key Features:

- Covers underlying physics and mathematics at a level appropriate for all medical imaging modalities
- Extensive homework problems within each chapter, with answers in a solutions manual.
- The solutions manual also includes optional homework problems that can be used periodically in lieu of those in the textbook.
- Extensive figures and equations throughout the book.
- Several chapters include example questions and answers.
- Many of the homework problems can be solved using Mango, a freely distributed image processing software found on the author's website at: http://ric.uthscsa.edu/mango/

Table of Contents:

Basic Concepts. Overview. Medical Imaging Technology & Terminology. Digital Imaging in Diagnostic Radiology. **Intermediate Concepts.** Physical Determinants of Contrast. Mathematics for Linear Systems. Spatial Resolution. Random Processes. Noise and Detective Quantum Efficiency. **Advanced Concepts.** Noise-Resolution Models. The Rose Model. Receiver Operating Characteristics (ROC) Analysis. **Dynamic Imaging.** Digital Subtraction Angiography (DSA). Temporal Filtering. **Tomographic Imaging.** X-Ray Computed Tomography (CT). Single Photon Emission Computed Tomography (SPECT). Magnetic Resonance Imaging (MRI).

September 2016 • 978-1-4987-5161-2

To view our full range of books and order online visit: **www.crcpress.com**
email: orders@crcpress.com • 1-800-634-7064 • 1-859-727-5000 • +44 (0)1235 400524

CRC Press
Taylor & Francis Group

Master of Advanced Studies in Medical Physics

January 2018 – December 2019

A two-year training program by ICTP and Trieste University under the patronage of the Trieste University Hospital

Applications are now being accepted for the 2018-2019 Master of Advanced Studies in Medical Physics. The program provides young, promising MSc graduates in physics or equivalent (mainly from low- and medium-income countries that are members of the UN, UNESCO or IAEA) with the skills to be recognized as clinical medical physicists in their home countries.

The first year of the program is dedicated to theoretical training, while the second year places in one of the program's network hospitals for clinical training. The language of instruction is English.

Topics include:

· Anatomy and physiology
· Radiobiology
· Radiation physics
· Radiation dosimetry
· Medical physics imaging
· Physics of diagnostic imaging
· Physics of nuclear medicine
· Physics of radiation oncology
· Radiation protection
· Statistics for medicine

Directors and Council Board:

R. LONGO, Trieste University, Italy (Director)
R. PADOVANI, ICTP, Italy (ICTP Coordinator)
L. BERTOCCHI, ICTP, Italy
M. DE DENARO, University Hospital, Trieste, Italy
E. MILOTTI, Trieste University, Italy
L. RIGON, Trieste University, Italy

Further information:

http://www.ictp.it/programmes/mmp.aspx

mmp@ictp.it

How to apply:

Online application:
http://www.ictp.it/programmes/mmp.aspx

Female scientists are encouraged to apply.

Grants:

A limited number of full or partial scholarships will be awarded to successful candidates from developing countries, thanks to the support of the IAEA and ICTP.

Deadline:

15 April 2017

The programme is accredited by the IOMP

IAEA International Atomic Energy Agency *Atoms for Peace*

INFORMATION FOR AUTHORS

PUBLICATION OF DOCTORAL THESIS AND DISSERTATION ABSTRACTS

A special feature of Medical Physics International (on line at www.mpijournal.org) is the publication of thesis and dissertation abstracts for recent graduates, specifically those receiving doctoral degrees in medical physics or closely related fields in 2010 or later. This is an opportunity for recent graduates to inform the global medical physics community about their research and special interests.

Abstracts should be submitted by the author along with a letter/message requesting and giving permission for publication, stating the field of study, the degree that was received, and the date of graduation. The abstracts must be in English and no longer than 2 pages (using the MPI manuscript template) and can include color images and illustrations. The abstract document should contain the thesis title, author's name, and the institution granting the degree.

Complete information on manuscript preparation is available in the INSTRUCTIONS FOR AUTHORS section of the online journal: www.mpijournal.org.

For publication in the next edition abstracts must be submitted not later than /august 1, 2014.

INSTRUCTIONS FOR AUTHORS

The goal of the new IOMP Journal Medical Physics International (http://mpijournal.org) is to publish manuscripts that will enhance medical physics education and professional development on a global basis. There is a special emphasis on general review articles, reports on specific educational methods, programs, and resources. In general, this will be limited to resources that are available at no cost to medical physicists and related professionals in all countries of the world. Information on commercial educational products and services can be published as paid advertisements. Research reports are not published unless the subject is educational methodology or activities relating to professional development. High-quality review articles that are comprehensive and describe significant developments in medical physics and related technology are encouraged. These will become part of a series providing a record of the history and heritage of the medical physics profession.

A special feature of the IOMP MPI Journal will be the publication of thesis and dissertation abstracts for will be the publication of thesis and dissertation abstracts for recent doctoral graduates, specifically those receiving their doctoral degrees in medical physics (or closely related fields) in 2010 or later.

MANUSCRIPT STYLE

Manuscripts shall be in English and submitted in WORD. Either American or British spelling can be used but it must be the same throughout the manuscript. Authors for whom English is not their first language are encouraged to have their manuscripts edited and checked for appropriate grammar and spelling. Manuscripts can be up to 10 journal pages (approximately 8000 words reduced by the space occupied by tables and illustrations) and should include an unstructured abstract of no more than 100 words.

The style should follow the template that can be downloaded from the website at:

http://mpijournal.org/authors_submitapaper.aspx

ILLUSTRATIONS SPECIAL REQUIREMENTS

Illustrations can be inserted into the manuscript for the review process but must be submitted as individual files when a manuscript is accepted for publication.

The use of high-quality color visuals is encouraged. Any published visuals will be available to readers to use in their educational activities without additional approvals.

REFERENCE WEBSITES

Websites that relate to the manuscript topic and are sources for additional supporting information should be included and linked from within the article or as references.

EDITORIAL POLICIES, PERMISSIONS AND APPROVALS

AUTHORSHIP

Only persons who have made substantial contributions to the manuscript or the work described in the manuscript shall be listed as authors. All persons who have contributed to the preparation of the manuscript or the work through technical assistance, writing assistance, financial support shall be listed in an acknowledgements section.

CONFLICT OF INTEREST

When they submit a manuscript, whether an article or a letter, authors are responsible for recognizing and disclosing financial and other conflicts of interest that might bias their work. They should acknowledge in the manuscript all financial support for the work and other financial or personal connections to the work.

All submitted manuscripts must be supported by a document (form provided by MPI) that:

• Is signed by all co-authors verifying that they have participated in the project and approve the manuscript as submitted.

• Stating where the manuscript, or a substantially similar manuscript has been presented, published, or is being submitted for publication. Note: presentation of a paper at a conference or meeting does not prevent it from being published in MPI and where it was presented can be indicated in the published manuscript.

• Permission to publish any copyrighted material, or material created by other than the co-authors, has been obtained.

SUBMISSION OF MANUSCRIPTS

Manuscripts to be considered for publication should be submitted as a WORD document to: Slavik Tabakov, Co-editor: slavik.tabakov@emerald2.co.uk

MANUSCRIPT PROPOSALS

Authors considering the development of a manuscript for a Review Article can first submit a brief proposal to the editors. This should include the title, list of authors, an abstract, and other supporting information that is appropriate. After review of the proposal the editors will consider issuing an invitation for a manuscript. When the manuscript is received it will go through the usual peer-review process.

Fig. 1 Medical Physics International Journal

ANNEX

IMPLEMENTING STEREOTACTIC RAPIDARC TREATMENTS INTO CLINICAL ROUTINE: FROM ALGORITHM CONFIGURATION TO TREATMENT VALIDATION

A. Van Esch [1,2,3], F. Sergent [2,3], K. Basta [3], P. Bertrand[4], C. Corbice[4], E. Fontaine[4], L. Hambach[2], A. Blavier[2], C. Clermont[2], D.P. Huyskens[1,2,3]

[1] 7Sigma, QA-team in radiotherapy physics, Kasteeldreef 2, 3150 Tildonk, Belgium

[2] Université catholique de Louvain, CHU-UCL Namur, Service de radiothérapie, Place L Godin 15, 5000 Namur, Belgium

[3] Centre Hospitalier de Mouscron, Avenue de Fécamp 49, 7700 Mouscron, Belgium

[4] CHU de la Réunion, Site GHSR, Av. Francois Mitterand BP305, 97448 Saint-Pierre, Réunion

Abstract: **Purpose: This work aims to aid the medical physicist with the safe implementation of RapidArc (RA) (Varian Medical Systems, Palo Alto, CA) stereotactic radiotherapy treatments (SRS/SBRT) into clinical routine, from treatment planning system (TPS) configuration to patient plan verification. Implementation procedures are applicable to different Varian linear accelerators, either equipped with a standard Millennium 120MLC or a high-definition HDMLC, but always with on-board imaging.**

Methods: A systematic approach was used to assure proper control of the different aspects of the implementation. First, an extensive series of detectors (all from PTW, Freiburg, Germany) – from numerous single detectors to the 1000SRS/Octavius4D 3D dose measurement system - were carefully benchmarked to assess their dosimetric characteristics, their precision and their practical usefulness. This benchmarking was performed independently of the TPS. Second, the necessary measurements were performed to include small field data in the Analytical Anisotropic Algorithm (AAA) and Acuros (AXB) algorithm configuration. Third, validation of the Eclipse small field dose calculation was performed for both algorithms, starting off with static gantry (small) MLC fields and ending with RA SRS/SBRT test plans. Finally, pre-treatment QA procedures were implemented, executed and analyzed on all patient treatments.

Results: While one can do a substantial part of the basic validation with a single, high resolution, directionally independent detector, a water phantom and a small solid water phantom to hold this detector, a single measurement is insufficient to assess the geometric precision of the dose-fall off during arc delivery. Given the safety requirements for stereotactic treatments, it is therefore highly recommended to invest in a detector system that can provide 2D and 3D dose information as well. The 1000SRS was found to provide very reliable planar dose measurements and, in combination with the Octavius4D system, measurement-based 3D dose reconstructions. It is also the most efficient method, especially when multiple lesions are concerned. From the battery of validation measurements, it was found that, although the algorithm configuration as well as the MLC modeling within the Eclipse TPS could benefit from further improvements, the currently obtained results are within clinical acceptance for the specific requirements of stereotactic treatment plans.

Conclusions: Target localization remains the key aspect of successful stereotactic radiotherapy and should be carefully addressed according to the treatment site. However, from a dosimetric point of view, when the appropriate measurement equipment is available, safe implementation of stereotactic RA treatments should be within reach of all radiotherapy departments outfitted with an up to date Clinac (or TrueBeam) and state-of-the-art on-board imaging.

Keywords: **Stereotactic RapidArc, clinical implementation**

I. INTRODUCTION

Intracranial brain lesions have long been treated with stereotactic radiosurgery (SRS) on equipment specifically dedicated to this high dose, high precision technique. Gradually, the extremely hypofractionated treatment technique has expanded to include small lesions outside of the brain and spine, introducing stereotactic body radiotherapy (SBRT) in e.g. liver and lung. Delivering such high doses per fraction requires high conformity and steep dose fall-off to avoid irradiating organs at risk. It necessitates appropriate patient immobilisation and image-guidance for patient set-up. Technology has evolved significantly since the onset of SRS/SBRT. Current day linear accelerators have gained in geometric and dosimetric precision, allow more advanced treatment optimisation and delivery techniques such as IMRT and VMAT, and are often standard equipped with on-board kV imaging and CBCT. Because of the rising amount of literature reporting favourable therapeutic outcome of SRS/SBRT for a variety of clinical indications [1-12], it is no wonder that there is a growing interest to implement SRS/SBRT treatments on these widely available treatment units. Although requirements for immobilization, treatment planning and delivery can vary significantly with disease site, quality assurance and safety issues are similar: the delivery of high dose fractions implies that the margin of error is much smaller than for conventional radiotherapy. Even small inaccuracies in target localization can lead to serious under-treatment of the target or severe overdosage to the adjacent normal tissue. When adjacent normal tissue includes high-risk organs, fractionated stereotactic radiotherapy (FSRT)

can be used to provide additional normal tissue protection [13].

While the most essential aspect of all stereotactic treatments is undoubtedly the high precision treatment localization during all steps of the treatment process, implementing this treatment technique into clinical routine also presents challenges from a dosimetric point of view as small field dosimetry comes with its own specific problems [14]. Reports of past accidents are an unfortunate testimony of this [15-20]. Given the beneficial therapeutic possibilities when stereotactic treatments are made available, it is therefore the purpose of this work to provide practical guidelines on the safe implementation of stereotactic treatments on readily available radiotherapy equipment, more specifically, on Varian (Varian Medical Systems, Palo Alto, CA) linear accelerators in combination with the Varian Eclipse treatment planning system (TPS). As stereotactic treatments on the Novalis (Brainlab, Feldkirchen, Germany) linear accelerator in combination with the dedicated iPlan TPS (Brainlab) have been around for a while, this is a well-established solution and numerous publications on the subject already exist [21-25]. The iPlan stereotactic treatments are primarily non-coplanar, conformal arc treatments. The standard dose calculation algorithm in the iPlan software is the single pencil beam model. It is robust and works well for SRS. It is unfortunately less well adapted for SBRT, especially in highly heterogeneous media such as lung. With the availability of VMAT (RapidArc® (RA)) in combination with the more advanced dose calculation algorithms such as the Anisotropic Analytical Algorithm (AAA) and Acuros (AXB) in the Eclipse planning system, there is a growing desire to include stereotactic treatment planning into the Varian integrated environment. A number of publications exist on this subject already [26-41], presenting mostly planning studies but also reporting clinical treatments. On the topic of dose calculations in lung lesions, planning studies present a comparison between the AAA and AXB calculations or compare the respective dose calculations to measurements in heterogeneous phantoms. Conclusions are unanimous: AXB dose calculations are superior to AAA when it comes to heterogeneity corrections. While lung SBRT is very sensitive to the heterogeneity correction method, it is less dependent on small field dosimetry as the lung lesions generally require larger field sizes than cranial SRS. It is even so that for lung SBRT, the Eclipse dose calculation algorithms often do not even have to be specially configured below the standard minimum field size of 3x3cm^2. This does not hold for cranial SRS for which the small field data definitely need to be added to the algorithm configuration. Initial assessments of the AAA and AXB accuracy for small fields were reported and found to be promising [42]. Numerous and elaborate guidelines on TPS validation for stereotactic treatments exist, but these are all general guiding principles and not solution specific [14]. In addition, with the rising interest in stereotactic treatments, improved single detectors and user friendly 2D and 3D measurement devices have

become commercially available relatively recently, potentially liberating the medical physicist from the tedious and error prone film or gel dosimetry. Dosimetric characteristics of almost all of the available detectors have been reported in literature, but mostly on a fundamental basis and not in the framework of TPS-specific usefulness [43, 44-46]. Silicon diode detectors are commonly used but are not dosimetrically water equivalent, resulting in energy dependence and fluence perturbation for field sizes with a dimension below 1 cm. The relatively new synthetic microDiamond (PTW, Freiburg, Germany) detector provides superior water equivalence to diode detectors but has a slightly larger cross-section than diodes. It has become clear that, up to date, there is no real-time detector available that can accurately measure output factors down to field sizes of 5 mm without the use of correction factors. Numerous groups have worked to derive appropriate correction factors through comparison with Monte Carlo simulations, Gafchromic EBT2 film and plastic scintillators [47, 48, 49]. Unfortunately, beyond field dimensions of the order of 1 cm, the exact values of the tabulated correction factors differ between publications, sometimes by considerable amounts. The origin of the differences is difficult to trace, but they at offer another illustration of the delicacy of small field data acquisition. It is, however, not the goal of our work to elaborate on the small(est) field correction factors. On the contrary, while these factors may be applicable for stereotactic dose delivery through cones or other fixed field apertures, their practical use in modulated stereotactic treatment delivery is unfortunately very limited. Even for the simple output factor measurements, while correction factors exist for a 1x1 cm² field, rectangular fields up to 1x40 cm² need to be acquired for algorithm configuration and there are no published values for these narrow, elongated field dimensions. Moreover, in clinical practice, when validating patient treatments consisting of modulated fields with aperture openings that vary during delivery, applying such correction factors is simply not feasible from a practical point of view. In this study, we therefore study the different detectors without the use of any field size dependent correction factor. This more pragmatic approach allows us to assess which detectors qualify for use in clinical practice when varying beam apertures complicate the use of appropriate correction factors.

The extensive literature on different detectors can be overwhelming and does not necessarily facilitate the choice. It is, however, important to not blindly select a detector based on its fundamental properties but to also take into account the practical implications of the detector choice for the task at hand. As the latter are often hard to judge without actually purchasing the equipment, we have tried to present a practical overview specific to the needs of the Eclipse TPS and the RapidArc treatment modality.

The manuscript outlines a procedure for performing basic benchmarking of available QA equipment. Once the behaviour of the chosen detector(s) has been confirmed and/or quantified, one can proceed to the small-field specific

algorithm (AAA or AXB) configuration and subsequent validation. As a final step, possible patient QA procedures are addressed and compared. With the QA steps outlined from start to finish, we hope to aid the medical physicist with the safe implementation of stereotactic RA treatments into clinical routine.

As VMAT optimization offers new possibilities for optimizing the dose distribution to the target, the traditional non-uniform stereotactic target coverage can now be made more homogeneous through VMAT delivery. Whether or not the customary 70 to 100% dose gradient in the target needs to be maintained or whether it would be beneficial to strive towards a more uniform dose distribution, is a clinical debate and beyond the scope of this work. On a similar note, now that the treatment beam output within an arc can be better optimized, the need for elaborate couch rotations should be subjected to critical revision. Reducing the number of couch rotations in a plan facilitates accurate patient localization by means of the on-board imaging and therefore merits serious consideration. Although the actual RA optimization is again not the subject of this manuscript, the choice of treatment geometry does have an impact on the possible QA procedures. We therefore address all geometries, from drastically non-coplanar to entirely coplanar arc delivery.

For the medical physicist, dosimetric issues are similar between SRS, SBRT and FSRT as they are mostly related to the small field size rather than to the dose per fraction. For the purpose of this work, we will therefore reduce the amount of acronyms used and refer to all of the above as stereotactic radiotherapy (SRT).

II. METHODS AND MATERIALS

All data were acquired on either a Clinac iX (Varian) dual energy accelerator (6&18 MV (at CH Mouscron), 6&23 MV(at CHU Réunion)) equipped with a 120 Millennium MLC (120MLC) or on a NovalisTX (Brainlab) (at CHU Namur) linear accelerator (6MV, 6MV_SRS and 18MV) equipped with the high definition MLC (HDMLC). The focus being on stereotactic treatments, all presented data in this work concern the 6MV or 6MV_SRS treatment beams. The Clinac iX units have a Varian IGRT treatment couch while the NovalisTX treatment unit has a Brainlab Exact couch. Both can perform on-board imaging (kV, MV (aS1000) and CBCT) while the NovalisTX has an additional ExacTrac (Brainlab) positioning system. Stereotactic treatments in routine can either be planned as RapidArc treatments with the Eclipse treatment planning system (Varian), or as conformal arc treatments with either Eclipse or the iPlan software (Brainlab). While conformal arcs were used in the validation process, the final objective is to use RA delivery for SRT patient treatments. In Eclipse, dose distributions were calculated by means of the Analytical Anisotropic Algorithm (AAA v11.0.31) or the Acuros (AXB v11.0.31) algorithm.

Table 1: Overview of PTW detector characteristics relevant to stereotactic data acquisition. the electron diode dE (TW60012), the stereotactic diode dSRS (TW60018), the photon diode dP (TW60008), the microDiamond μD (TN60019), the 3D PinPoint Pp3D (TN31016) and the Semiflex3D Sf3D (TN31021). Although the Octavius1500 and 1000SRS (both PTW, Freiburg, Germany) are two-dimensional arrays rather than single detectors, their presence in table 1 serves to characterise the individual ion chambers of the 2D composition.

	d E	d SRS	d P	μ D	Pp3 D_{rad}	Pp $3D_{ax}$	Sf3 D	1000 SRS	Oct1 500
radius (cm) (vendor given)	0.06	0.06	0.06	0.11	0.145+	0.145	0.275++	~0.16+++	~0.28++++
sensitivity (nC/Gy) (measured)	169.8	169.4	130.0	1.1	0.4	0.4	2.0	/	/
Field size dependence (normalised to 5x5 cm² open field dose and relative to μD measurement)									
MLC in XxY (cm²)									
0.5x0.5 in 1x1	1.025	1.032	1.025	1.000	0.773	0.839	0.492	1.038	0.606
0.5x1 in 1x2	1.012	1.022	1.012	1.000	0.888	0.931	0.693	1.029	0.892
1x1 in 2x2	1.005	1.009	0.999	1.000	0.929	0.962	0.818	1.021	0.971
2x2 in 3x3	1.000	1.000	0.999	1.000	0.992	0.996	0.988	1.010	0.966
3x3 in 5x5	1.000	1.000	0.999	1.000	1.002	0.999	1.000	1.004	0.989
5x5 (no MLC)	1.000	1.000	1.000	1.000	1.000	1.000	1.000	1.000	1.000
Directional dependence (relative to axial measurement in Ruby)									
Gantry rotation (couch 90°)									
315	0.93	0.92	0.71	1.00	1.01	/	1.00	/	/
0	0.90	0.89	0.83	1.00	1.00	/	1.00	/	/
45	0.97	0.966	0.98	1.01	1.00	/	1.00	/	/
90	1.00	1.00	1.00	1.00	1.00	/	1.00	/	/

+ length = 2.9 mm, ++ length = 6.5 mm, +++ volume = 2.3x2.3x0.5 mm³, ++++ volume = 4.4x4.4x3 mm³

At the onset of the implementation of SRT treatments, it is most essential to first quantify the mechanical precision of the different components. By means of the Winston-Lutz test [53] (or an in-house developed equivalent setup) and the portal imager, we have quantified the mechanical precision of the isocentric rotation of the gantry, the collimator, the treatment couch and the on-board imaging. To obtain a precise jaw calibration, we also made use of the portal imager rather than trusting the light field or using a film measurement. The mechanical precision of the gantry and MLC in RA delivery mode are monitored by the Snooker Cue test [54].

II.1. Detector evaluation

As field dimensions approach detector dimensions, the impact of the detector choice on the measurement outcome becomes critical. Much literature has already been attributed to this subject, especially when it comes to single detectors [43,44-46], and it is not the purpose of our work to present another in-depth characterisation of the different detectors available. However, we do aim to present a practical overview of the detectors and measurement methods in view of their possible usefulness for dose calculation algorithm configuration and validation and for routine treatment QA. This benchmarking is performed entirely independent of the TPS.

0D: Point dose measurements

We have made use of the following PTW (Freiburg, Germany) detectors: the electron diode dE (TW60012), the stereotactic diode dSRS (TW60018), the photon diode dP (TW60008), the microDiamond μD (TN60019), the 3D PinPoint Pp3D (TN31016) and the Semiflex3D Sf3D (TN31021). An overview of the single detectors and some of their basic characteristics is given in the upper part of table 1, including their relevant dimensions and sensitivities. Although we refer to these measurements as '0D, point dose measurements', the 'point' inevitably encompasses the detector volume and therefore includes the dose-volume effect. Although the Octavius1500 and 1000SRS (both PTW, Freiburg, Germany) are two-dimensional arrays rather than single detectors, their presence in table 1 serves to characterise the individual ion chambers of the 2D composition. The Octavius1500 array consists of 1405 vented cubic ion chambers – of 0.44x0.44x0.3 cm³ each –

mounted below a 0.5 cm polystyrene build-up layer and arranged on a 27x27 cm^2 surface area in a checkerboard pattern [55]. The 1000SRS array consists of 977 liquid-filled ion chambers - 0.23x0.23x0.05 cm^3 – distributed over a 11x11 cm^2 surface area: 400 ion chambers provide complete coverage of the inner 5x5 cm^2 surface area whereas the remaining chambers are distributed in a 0.5 cm center-to-center grid over the rest of the surface. [55]

A practical overview of the field size dependence was obtained by performing a series of dose measurements on the beam axis for collimator settings going from 1x1 to 5x5 cm^2 in combination with MLC (HDMLC) fields of dimensions 0.5x0.5 cm^2 to 3x3 cm^2. All data were acquired with 200 Monitor Units (MU), at depth = 8.5 cm and source-phantom distance SPD = 91.5 cm. We made use of a set of customized PMMA blocks of 5x10 cm^2 surface area and different thicknesses. A suitable insert was made for every detector. All data were acquired axially, i.e. with the beam axis along the detector axis, except for the Pp3D$_{rad}$ for which the beam incidence was perpendicular to the detector axis. The field size dependence of the arrays was measured in the same conditions by means of solid water plates (PTW) placed on top of the arrays. The daily output variation of the treatment unit as well as any possible deviations due to non-water equivalence of the PMMA were corrected through a cross-calibration factor based on the 5x5 open field measurement and the theoretically expected dose in water for all detectors. From the above measurements, the sensitivity (nC/Gy) could also be deduced and compared to the vendor specifications.

As mentioned above, we do not wish to take field size dependent correction factors into account and aim to assess the practical usability of the different detectors when not doing so. In order to present the results in an orderly fashion, we have decided upon the microDiamond as the reference detector. Although contradictory results [47,48,50,51,52] have been published regarding this detector's field size dependence for the smallest field dimensions (0.5 to 1 cm), a recent publication of Francescon et al. [49], re-confirms the original findings by Morales et al [51] and Chalky and Heyes [52] that microDiamond correction factors are within 1% down to a 7.6 x 7.7 mm MLC field size, and even within 1.5 % for cone sizes down

to 5 mm. (suggesting that the overresponse due to the mass-density effect is well-balanced by the volume averaging effect). We have therefore taken the doses measured by the microDiamond detector (and cross-calibrated to the 5x5 cm^2 field) as the reference values and have normalised all other detector data to these values in table 1 for comparison (thereby accepting a possible ~1-1.5% imprecision in the small(est) field data).

To assess the directional dependence, we made use of
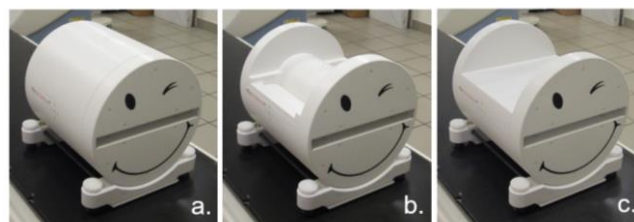
Figure 2: Modular Octavius4D measurement unit consisting of (a) the large diameter top (Oct4D_Maxi), (b) the SRS top (Oct4D_Mini) and (c) the flat top (Oct4D_Flat) which can all be used in combination with the 1000SRS 2D array.

Ruby, a geometric PMMA phantom developed for use in stereotactic treatment QA (figure 1a). All of Ruby's orthogonal cross-sections (transversal, coronal and sagittal) have an octagonal shape with sides of 6 cm, resulting in a total phantom thickness of 14.5 cm. Different detector inserts allow the use of all of the above single detectors. The directional dependence of the detectors can easily be assessed by irradiating Ruby with different combinations of gantry and couch rotations without the need for different MU calculations. All beam incidences orthogonal to the square 6x6 cm^2 surface areas have the same SPD: with the couch rotation set to 90 degrees, the gantry was positioned at 315, 0, 45 and 90 degrees (table 1 and figure 1b), respectively. All data were acquired with 128 MUs, delivering 1 Gy to the isocentre with a 3x3 cm^2 field size (which should be large enough to exclude an impact of the detector dimensions compared to the field size). The phantom and detector position were verified by means of the on-board imaging (orthogonal kV images or CBCT) prior to data acquisition and better than 0.5 mm in all directions. No directional dependence measurements were performed for the 2D arrays. The directional dependence of the Octavius1500 has been reported elsewhere and, like the 1000SRS, it should preferably be used only in a simple orthogonal setup or in the rotational Octavius4D unit [55].

1D & 2D: *water phantom scans and planar dose acquisition systems*

Depth dose measurements were performed in a MP3-M water phantom (PTW) for square fields of 1x1, 2x2, 3x3,4x4,10x10, 26x26 and 40x40 cm^2 at SPD = 95 cm with all of the above listed detectors. The detectors were positioned by means of the TrueFix (PTW Freiburg) system
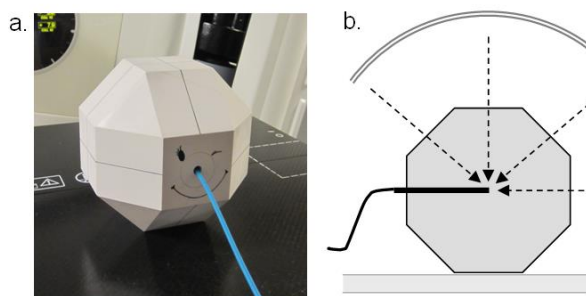

Figure 1: a. Ruby, the small solid water phantom used with various point dose detectors. All orthogonal cross-sections of the phantom have an octagonal shape with 6 cm sides. b. The angular incidences (dashed arrows) used to assess the detector's directional dependence with the couch (or phantom) rotated by 90 degrees. The double-lined arrow indicates the gantry rotation.

to take their effective point of measurement into account. Both the water phantom and the gantry were carefully verified with a spirit level to ensure that the detector remained at the centre of the field at all times during the scan. The central position of the detector was furthermore confirmed at shallow and large depth by means of two orthogonal profile scans acquired with small step size (1 mm) around the penumbra region. During the depth dose scans, the acquired signal was not divided by the signal of a reference chamber because the physical presence of the latter would risk having an impact on the measurement for the smallest field sizes. This approach is justified because of the stability of the linac's dose rate output during data acquisition. Furthermore, the measurement range was not adjusted in between scans with the same detector so the signal could be converted to the dose for a 200MU delivery through cross-calibration to the 10x10 cm^2 measurement.

To compare the dosimetric precision (absolute dose level and geometric resolution) with which the different point detectors can measure profiles, scans were acquired in the water phantom for a single static artificial MLC field (MLC120), containing 8 cm long open field strips of different widths (0.5, 1.0 and 1.5 cm wide, corresponding to 1, 2 and 3 adjacent open leaf pairs, respectively), alternating with 1 cm wide strips of 2 closed leaves. The field size defined by the jaws was 10x10 cm^2. Scans were performed perpendicular to the MLC leaves at SPD = 95 cm and depths 5, 10 and 15 cm. Similar to the depth dose data, scans were converted to the absolute dose for a 200 MU delivery through cross-calibration of the detector signal with an open 10x10 cm^2 field. The same MLC pattern was also measured with the 1000SRS 2D array in solid water (200 MU). At each depth, the 1000SRS array was cross-calibrated to the dose obtained for a 5x5 cm^2 open field in water (100 MU) at the maximum dose rate (600 MU/min for 6MV). As an additional planar measurement system, we included the MV portal imager (aS1000, Varian) and delivered the above static MLC field (200 MU) to the aS1000 MV imager using the integrated image acquisition mode. The imager panel was calibrated for this dosimetric acquisition mode using the profile correction files from the preconfigured package [57].

3D: volumetric dose reconstruction in the modular Octavius4D rotational unit

The modular Octavius4D (Oct4D) measurement system provides a 3D dose reconstruction that is entirely measurement-based and independent of the information contained in the TPS dicom dose (or dicom plan) file. The phantom consists of a rotational base in which a variety of 2D arrays can be inserted and upon which three different tops can be mounted, depending on the purpose of the measurement and the type of treatment (figure 2). For standard treatment localisations, the Octavius729 or Octavius1500 array would be used in combination with the standard top, creating a 32 cm diameter cylinder as shown in figure 2a (Oct4D_Maxi) [55]. For stereotactic treatments, the SRS top generates a 17 cm diameter cylinder (figure 2b),

to be used along with the 1000SRS (Oct4D_Mini). Although the 1000SRS array can also be used in the standard setup, the SRS top corresponds to a more realistic diameter for e.g. intracranial stereotactic treatments. The third, flat solid water top (figure 2c, Oct4D_Flat) is not designed to be used for 3D dosimetry but for treatment unit QA. It can, however, also be useful to measure the projection of the treatment delivery into a single plane during arc treatment, analogous to the portal image acquisition but in a 5cm deep water equivalent setup rather than in an amorphous silicon environment. The inclinometer mounted on the gantry ensures that the rotation unit always rotates along with the gantry, thus keeping the 2D array perpendicular to the beam axis at all times.

The measured dose as a function of gantry angle is stored in the measurement file every 200ms. Upon loading this file in the Verisoft software, the 3D dose in a homogeneous cylindrical phantom is reconstructed: for every stored gantry angle, the 2D measurement data are extrapolated to the rest of the cylinder by applying a percentage depth dose (PDD) curve through every measurement point. The total 3D dose is then reconstructed as the sum of these individual contributions and linearly interpolated to a user specified dose grid. For the stereotactic dose reconstruction, we have set the grid to 1 mm (instead of the default 2.5 mm). The software decides on the field size for which to select the PDD based on the effective surface of the array irradiated for every gantry angle. The set of PDD curves needed for this reconstruction should be acquired beforehand in a water phantom. As we have been routinely performing QA of RA treatments on the previous (non-modular) Octavius4D model (diameter 32 cm), such a set had long been measured in our department at SPD = 85 cm with an ionisation chamber (0.125 cm^3 Semiflex, PTW) for field sizes ranging from 27x27 to 3x3 cm^2 and subsequently extrapolated down to a virtual 0x0 cm^2 field size to cover all field sizes that could possibly be needed during the reconstruction process. This PDD set will be further referred to as PDD$_{85}$. With the possibility of using both the standard as well as the SRS top in the modular system, however, it needs to be verified whether the PDD$_{85}$ set can be used for both phantom compositions and whether the theoretical extrapolation below 3x3 cm^2 does not introduce deviations for stereotactic treatment fields. We have therefore acquired additional PDDs in the water phantom at SPD= 91.5 cm and SPD = 84 cm, i.e. at the exact SPDs of the Oct4D_Mini and the Oct4D_Maxi setup, respectively. We have measured the PDDs of simple open fields (27x27 down to 1x1 cm^2) and of the stereotactic MLC fields listed in table 1. The Sf3D was used for effective field openings above 5x5 cm^2 while all smaller dimensions where measured with the dSRS. The open field PDDs at SPD 91.5 cm were also used to generate alternative PDD sets for Verisoft (PDD$_{91.5}$). The small fields (X, Y or MLC ≤ 5 cm) were subsequently measured with the 1000SRS array in the Oct4D_Mini and Oct4D_Maxi. The 3D doses were reconstructed in Verisoft with the

relative electron density of the Oct4D material set to 1.00 and using both PDD sets (PDD_{85} and $PDD_{91.5}$) on all data. The PDD along the beam axis of the reconstructed doses was then exported from Verisoft and compared to the PDDs measured in the water phantom at the same SPD. As the Verisoft 3D dose reconstruction has no prior knowledge of the actual collimator or MLC position but selects the PDD solely based on the effectively measured field dimensions, these test fields allow an assessment of the validity of this approach by comparing the truly measured PDD with the Verisoft reconstructed PDD, for both open and MLC fields. (Although the water phantom PDDs were acquired with a flat water surface instead of the curved shape of the cylindrical phantom, the consequences of this geometric discrepancy are negligible when focussing on small field sizes, for which the curve of the cylindrical surface is too small to noticeably impact the shape of the depth dose on the beam axis.)

Finally, a number of simple rotational test deliveries were created around spherical target structures of 1.0, 1.5 and 3.0 cm in diameter. Conformal arc plans were generated by adjusting the MLC and jaws tightly around these targets, bearing in mind minimum jaw settings of 1x1 cm^2. In addition to the conformal arcs, RA plans were created on each of the three targets with a single arc per plan. To facilitate interpretation of the data, the collimator was kept at 0°. All of these arcs were measured with the 1000SRS array in both Oct_Mini and Oct_Maxi. The absolute dose reconstructed by Verisoft at isocentre was compared to the absolute dose measurement performed with the Pp3D and μD inserted into the rotational phantom by means of the dedicated solid water insert. Both the 1000SRS and the point detectors were cross-calibrated to the theoretical dose of a 5x5 cm^2 field at the center of a water equivalent cylinder of 32 cm or 17 cm diameter, respectively.

II.2. Dose calculation algorithm configuration and validation

II.2.1. Algorithm configuration

Upon configuring a dose calculation algorithm with beam data measured in a water phantom, it is not only important to know the characteristics of the detector used for these acquisitions, but also to understand which aspects of the data are of importance to the configuration of the calculation model and which are not. In short, it is often most beneficial to understand the process of the algorithm configuration before starting with the actual beam data acquisition.

The AAA and AXB dose calculation algorithms require the same basic beam data input for configuration: a series of open field PDDs, profiles of these open fields at five different depths, diagonal profiles of the largest field size at the same five different depths and output factor measurements (performed at a depth beyond d_{max}). Although a minimum amount of data needs to be provided, the choice

of field sizes is pretty much left up to the user, as long as the largest field is included. For standard algorithm configuration, users usually measure beam data for fields ranging between 3x3 cm^2 and 40x40 cm^2. The purpose of the configuration module is to characterize the phase space of the photon beam. Once the modelling of the parameters describing this phase space is complete, the measured PDDs and profiles will no longer be used during the actual dose calculations. Only the output factors are still involved in the monitor unit (MU) calculation.

In theory, if one wishes to calculate small field dosimetry with the AAA or AXB algorithm, one can simply do so by using the 'standard' algorithm configuration without including any additional small field data into the beam configuration data set: the algorithm will calculate depth doses and profiles according to the configured phase space and extrapolate MUs to smaller field sizes than the ones specified in the output factor table. As especially the latter is clearly not advisable, we present an overview of the (additional) measurements that were performed to include small field dosimetry in the AAA and AXB configuration in order to investigate their respective impact on the precision of the stereotactic dose calculation compared to the 'standard' configuration

Small field depth doses and profiles:

During beam configuration, Eclipse will ignore PDD measurements for field sizes below 2x2 cm^2 based on the assumption that PDDs for very small field sizes are easily subject to measurement imprecision and therefore more likely to deteriorate rather than improve the phase space modelling . It is therefore a waste of effort to try and carefully measure the 1x1 cm^2 PDD for beam configuration. A similar reasoning holds for the small field profiles. Although it would be tempting to measure the field profiles with a high resolution detector to accurately reproduce the penumbra at the field edge, this sharp penumbra gradient is not used in the phase space modelling, precisely because of its known detector dependency. It is more important to have a reliable dose measurement of the profile tails under the jaws than it is to have a sharp penumbra. For all of the above reasons, we made use of the Sf3D ion chamber for the complete basic beam data acquisition. As an ion chamber it produces a reliable dose measurement under the jaws and because it can measure PDDs down to 2x2 cm^2, all data can be acquired with a single detector. The only other detector that is equally versatile would be the μD, but as the latter has a lower sensitivity than the Sf3D, data acquisition will have to be slowed down or yield a smaller signal-to-noise ratio than the Sf3D.

Small field output factors:

In contrast to the small field depth dose and profile measurements, the output factors have a more visible impact on the configured data. They result in the calculation of additional collimator backscatter factors and directly impact the MU calculation for the small field dimensions. Before

the acquisition of the small field output factors (dimensions < 3 cm), the calibration of the jaws was carefully verified for all treatment units and adjusted where necessary to obtain the highest possible positional accuracy (< 0.5 mm) for each individual jaw. Output factors were measured in isocentric conditions at SPD = 95 cm and depth = 5 cm with the Sf3D for field dimensions down to 3 cm (X or Y). Additional data were acquired with the dE, dSRS and μD for field dimensions between 1 and 3 cm, with additional measurement points for the 4x4 and 5x5 cm^2 fields to confirm a seamless merge of both data sets. The overlapping measurements for the X = 3 cm or Y = 3 cm fields provide an additional check.

Both dose calculation algorithms (AAA and AXB) were configured with the above acquired input data, the only difference being the size of the point source set to 0 mm for AAA and 1 mm for AXB, according to Varian recommendations [42,58].

MLC parameterisation:
The MLC parameters were derived according to our standard method for IMRT or RA implementation, making use of the Octavius1500 2D array in solid water (SPD = 95 cm, depth = 5 cm), measuring four different fields: first a static open field with the same collimator settings as the subsequent MLC fields (12x24 cm^2 for the 120MLC, 12x20 cm^2 for the HDMLC), second a static field with closed MLC to derive the overall leaf transmission, third a dynamic sweeping gap field (with a gap of 5 mm) to derive the dosimetric leaf gap (DLG) parameter modelling the rounded leaf tips and fourth a dynamic delivery in the shape of a chair [59] to make sure we have a consistent set of MLC parameters and have not compensated possible errors in the transmission measurement by introducing a suboptimal value for the DLG. Although the tongue and groove effect of the MLC is taken into account in the calculation in a similar fashion as the DLG, albeit in the direction perpendicular to the MLC leaves, this is a parameter that can not currently be adjusted by the user and therefore requires no configuration measurements. Even so, an additional test series was performed to assess the dosimetric precision of its modelling in Eclipse v11. They are therefore described in the below paragraph concerning the algorithm validation rather than configuration.

II.2.2. Algorithm validation

Although the AAA and AXB algorithms need only few additional data in order to be configured for small field dosimetry calculations, careful validation is advisory as the small field dose calculation pushes the algorithm to the limits.

In order to validate both algorithms, we have reused the (MLC) fields (static and dynamic) for which data had already been acquired during the detector validation, adding more field sizes (with and without MLC) wherever

desirable. Whereas measurements for the detector characterisation could be performed on either the NovalisTX or the Clinacs, for the dose calculation validation, similar datasets were always acquired on all treatment units.

0D: point dose validation:
The measurements in the solid water blocks (SPD = 91.5 cm, depth = 8.5 cm) were calculated in Eclipse on an artificial water phantom with both AAA and AXB. The calculation resolution was set to 2.5 mm (AAA$_{res2.5}$ and AXB$_{res2.5}$) and to 1.0 mm (AAA$_{res1.0}$ and AXB$_{res1.0}$). Measurements were performed with the dE, dSRS and μD detector.

1D & 2D: dose profiles and planar dose validation:
The water phantom depth dose data acquired for the validation of the Oct4D dose reconstruction process were also used for the validation of AAA and AXB. Calculations were performed with 200 MU in the same conditions as the measurements, i.e. on a rectangular phantom at SPD = 91.5 and 84 cm. Similarly, dose profiles were calculated for the MLC field containing the narrow strips of opened and closed leaves (SPD = 95 cm, d = 5, 10, 15 cm, 200 MU) and compared to the measurements. In addition, to allow an indirect but easy evaluation of the changes in the photon fluence as a function of calculation resolution, portal dose images were predicted from the four calculated plans (AXB$_{res1.0}$, AAA$_{res1.0}$, AXB$_{res2.5}$ and AAA$_{res2.5}$), providing us with images based on photon fluences with resolutions 0.5, 1.0, 1.25 and 2.5 mm, respectively. (The portal dose prediction algorithm had been configured with the beam data from the preconfigured package.) These were compared to each other as well as to the portal image acquired with the aS1000 MV imager panel.

The 1000SRS and aS1000 2D detectors are also practical for the validation of the Eclipse MLC modelling. The MLC transmission and DLG parameter values were optimized during the configuration to achieve good agreement between dose calculation and measurement. The tongue and groove effect, however, is subjected to further investigation. Maximal tongue and groove effect was achieved by creating a dynamic treatment field consisting of two complementary static MLC segments. The first segment (100 MU) has all impair leaf pairs opened to form a 5 cm gap while all other leaf pairs remain closed under the jaws. In the second segment (100 MU), the impair leaves are closed while the pair leaves create the 5 cm openings. This dynamic MLC was used in combination with different jaw settings to investigate the tongue and groove for all leaf widths present in both MLC types. The portal imager was used to provide a high-resolution image of the tongue and groove pattern and compare it to the dosimetric image that was predicted based on the photon fluence calculated by Eclipse. For the portal imager, jaws were set sufficiently large to include all leaf widths within a single measurement. The predicted image was calculated from the AXB$_{res1.0}$ dose calculation,

corresponding to a 0.5 mm internal fluence resolution. Data were also acquired with the high resolution 1000SRS array in between solid water plates (SPD = 95 cm, depth = 5cm). To make full use of the high detector density in the central part of the array, a symmetric 5x5 jaw opening allows measurement of the tongue and groove pattern for the central leaves (2.5 mm (HDMLC) and 5 mm (120MLC), respectively). The array was then moved longitudinally to measure another 5x5 field, this time with highly asymmetric jaw settings to also include the outer leaves (5 mm (HDMLC) and 10 mm (120MLC), respectively). Measurements were compared to the corresponding calculations.

3D: volumetric dose validation:

As the 3D dose reconstructions obtained with the Oct4D_Mini and Oct4D_Maxi phantom were first independently validated by means of water phantom (for the static gantry) and point dose measurements (for the arc plans), these can now be used to verify the accuracy of the 3D dose calculation algorithms. Both the static gantry and the rotational plans were recalculated with $AAA_{res1.0}$ and $AXB_{res1.0}$ and dose distributions were exported for comparison in the Verisoft software.

II.3. Patient QA

Having benchmarked the precision with which different measurement methods can be relied upon and the dosimetric accuracy that can be expected from the TPS in simple plan deliveries, we can commence the validation of real stereotactic RA patient treatments.

The patient plans encompass a variety of treatment localisations. Single lesions were mostly treated with the isocentre placed within the lesion. RA optimizations were performed either with the commonly used non-coplanar arc setup (with multiple couch rotations) or, if possible, with coplanar or slightly non-coplanar arc delivery. Multiple lesions were either treated with multiple isocentres (in which case they can simply be regarded as multiple single lesion treatments when it comes to treatment QA) or with a single isocentre. In the latter case, if lesions are well separated, we treat both lesions with separate arcs, albeit all with the same isocentre. If they are closely spaced, we optimized on both volumes in the same arc, but add additional arcs to allow for more modulation. The plan quality that can be obtained with these different beam geometries depends on the size and location of the lesion(s) but as this is not the subject of this manuscript, it will not be elaborated on. However, as we do use all of the above setups in clinical routine, the QA protocol needs to be able to handle all of them. We have therefore first prepared two test patients on the Clinac iX, one with a single lesion (1Meta) (diameter ~ 1.5 cm) and one with two separate lesions (2Meta) of different sizes (diameters ~ 2 and 1 cm, respectively) but relatively closely spaced (center-to-center distance of ~ 3 cm). Both cases were planned with three different treatment approaches regarding couch movement: firstly, the more traditional, radically non-coplanar setup was used with multiple couch rotations, secondly a plan was optimized for a coplanar arc geometry and lastly, a nearly-coplanar setup (with couch rotations set at 10 and 350 degrees) was used to avoid concentrating the dose outside of the target into a single cross-section of the brain whilst still minimizing couch rotation. These six treatment plans were validated in-depth with the following measurement methods:

0D) µD and Pp3D in Ruby: for every lesion, the phantom position was optimized to have the detector at the centre of the lesion. To avoid mistakes and minimize inaccuracies during set-up, a CBCT was acquired (without couch rotation) for every localisation and the phantom position was adjusted accordingly. Subsequently, for every point dose measurement, the entire treatment plan was delivered preserving the original couch rotations. Once positioned, no more image-guided adjustments to the phantom were made for the different couch rotations. Dosimetric deviations due to a possible imprecision in the couch movement are therefore inherently included in the measurement.

3D) 1000SRS in Oct4D_Maxi and Oct4D_Mini: a verification plan is generated in Eclipse to calculate the expected dose in the Oct4D phantom ($AAA_{res1.0}$ and $AXB_{res1.0}$). For both the measurement and calculation, couch rotations are set to zero. 3D dose distributions are exported for the total dose as well as for the individual arcs.

In addition, all routine stereotactic patients treated on the NovalisTX were verified with the 1000SRS/Oct4D_Maxi until the modular Octavius became available and from then on verification has been carried out with the 1000SRS/Oct4D_Mini combination instead. As AXB is not yet available for routine purposes on the NovalisTX, all of these plan verifications were calculated with $AAA_{res1.0}$. Point dose measurements were carried out occasionally.

To analyze the 3D dose information, the standard gamma criteria accepting 3% dose differences (local (%L) or global (%G)) in combination with a 3 mm distance to agreement (DTA) are deemed inappropriate for stereotactic treatments. While we can be more tolerant on the absolute dose level in the high dose area, we aim to be more precise regarding the location of the dose peak. We have therefore performed all 3D gamma analysis (γ_{3D}) with a DTA of 1 mm while varying the local dose criterion. Volumetric gamma evaluation scores were obtained for different isodose levels by means of the volumetric gamma analysis tool in Verisoft, representing the percentage of points that pass the criteria within the volume delineated by the given isodose level. To allow focus on the high dose area, as levels of interest, we have opted for the 90%, 70% and 50% isodose volumes. The local dose criterion was varied between 3% and 5% to

investigate if – and at which tolerance level - near-perfect ($\geq$ 99%) pass rates (PR) could be achieved.

III. RESULTS

Firstly and importantly, after careful recalibration of the jaws, submillimeter precision was achieved for all mechanical components on all treatment units when evaluated in static mode. In RA treatment mode, the successful use of the Snooker Cue test assured a dynamic rotational precision within 1 degree, even under extreme acceleration and deceleration conditions. An appropriate procedure was implemented to ensure that these mechanical precisions are maintained over time.

III.1. Detector evaluation

0D: Point dose measurements

Table 1 provides an overview of the dosimetric characteristics for the different detectors relevant to stereotactic dose measurements. To assess the field size dependence, the data were first normalized to the 5x5 open field measurement for each detector. The microDiamond measurement was then chosen as the reference [49] and all measured output factors were divided by the one measured with the μD. The diodes have the smallest radii (0.06 cm)

and the highest sensitivity, making them all well suited for dose measurements down to dimensions of 1 cm in orthogonal measurement conditions. Even for smallest measured field dimension of 0.5x0.5 cm², deviations are only $\sim$ 3%. The single ion chambers can all be used with good accuracy down to 2x2 cm^2, but start to diverge by 4 to 50 % below. In spite of its dimensions similar to the Pp3D, the central chamber of the 1000SRS proves to be a good dose detector down to the smallest field size as well. The vented ion chambers of the Oct1500, however, cannot be relied upon for accurate dose measurements of field sizes below 3cm.

From table 1, it is furthermore apparent that apart from the Pp3D and Sf3D ion chambers, only the μD shows a directional independence. The diodes all measure a considerably lower signal when not irradiated axially.

Although the sensitivities widely differ between the different detectors, this did not really affect the outcome in table 1 as all data could simply be acquired with high enough dose to obtain a good signal to noise ratio.

1D & 2D: water phantom scans and planar dose acquisition systems

To compare the measured depth dose data between different detectors, figure 3 shows a plot of the relative difference between the different PDDs. All PDDs were first normalized to a depth of 5 cm and then divided by the supposed reference PDD. For the small field dimensions (< 3 cm), we opted for the dSRS as the baseline, whereas for
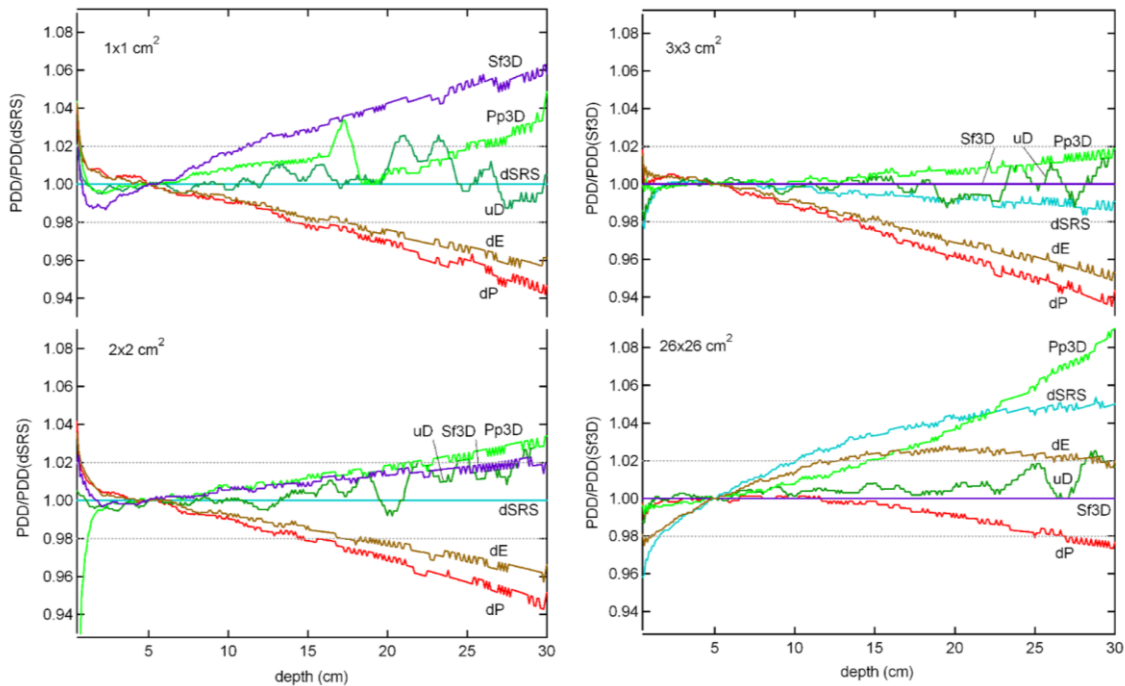

Figure 3: Comparison between depth dose curve measurements using the different detectors listed in table 1. For field sizes 1x1 and 2x2 cm²(graphs on the left side), the acquired PDDs are normalized to the dSRS PDD. For the larger field sizes (graphs on the right), data are normalized to the Sf3D measurement. The horizontal, dotted lines indicate the 2% interval around the reference PDD.
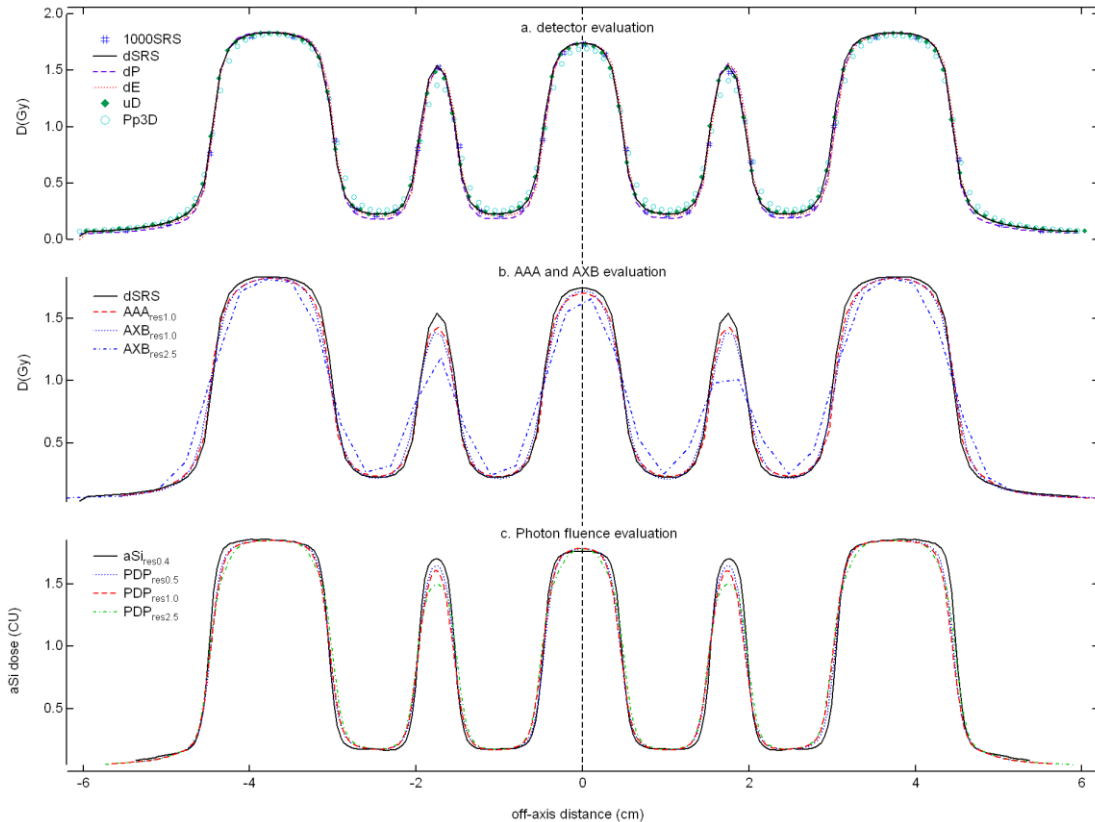
Figure 4: Profiles for the MLC striped field: (a) detector evaluation: profiles measured at SPD = 95, depth = 5cm with different high resolution point dose detectors: the lines correspond to the diode measurements (dSRS: solid black, dP: dashed mauve, dE:dotted red) the μD (solid green diamonds), the Pp3D (open cyan circles). A line profile was also extracted from the 1000SRS planar measurement (dark blue hashtags). (b) AAA and AXB evaluation: comparison between reference measurement (dSRS, black solid line) and different dose calculations: resulsts for $AAA_{res1.0}$ and $AXB_{res1.0}$ are similar, displaying a slightly too broad penumbra and too low dose in the narrow peaks. On the central axis, the $AAA_{res1.0}$ dose calculation is 1% lower than the corresponding AXB dose calculation. Dose calculations with 2.5 mm resolution ($AAA_{res2.5}$ not shown but similar to $AXB_{res2.5}$) are drastically too broad. (c) Photon fluence evaluation: profile comparison between portal dose images predicted with different fluence resolution showing the same gradual decline of the peak in the narrowest strips as well as the increased broadening of the penumbra. The measured dosimetric image is also displayed (solid black line) and shows sharper penumbra and higher peaks.

the larger dimensions ($\geq$ 3cm), all data are displayed relative to the Sf3D acquisition. The dotted horizontal lines indicate the 2% interval above and below these baseline PDDs. The dE and dP come out as the least suitable for overall small field PDD acquisition, deviating by more than 2% at larger depths (>15 cm). The μD appears to be the most versatile detector, agreeing with the baseline PDDs within 2% over the whole field size range. However, the numerous bumps and valleys are a reflection of the noisier aspect of the data acquired with this detector, in spite of the considerably longer acquisition times used. The ion chamber capable of accurately measuring small field PDDs down to 1x1 cm^2 is the Pp3D, but this detector is suboptimal for larger fields. The Sf3D demonstrate nearly equally versatile behaviour as the μD, but with better signal-to-noise ratio: this detector is suitable for all field sizes, with the exception of the smallest 1x1 cm^2 field.

The impact of the detector resolution can be observed in the profiles acquired for the MLC-striped field shown in figure 4a. All diodes and the μD have a sufficiently small resolution to accurately reproduce the dose peaks corresponding to the open MLC strips. The 0.145 cm diameter of the Pp3D has the expected broadening effect on the profiles that can mostly be observed from the decrease in the 0.5 cm and 1 cm wide dose peaks, accompanied by the increase of the low dose measured in between the peaks. In spite of its similar ion chamber dimensions, the 1000SRS, however, does not display this broadening effect and demonstrates behavior expected of a spatial resolution of the order of 1 mm rather than 2.4 mm. The dose maxima or the narrow peaks also agree very well with the ones observed with the diodes. In the valleys shielded by the MLC, dP consistently reports the lowest dose whereas the Pp3D overestimates the dose. The other detectors all show good agreement, with the μD and dSRS being ever so slightly higher than the dE and the 1000SRS.

The aSi acquired images cannot be compared to water phantom measurements as they do not provide dose to water and are therefore not added to figure 4a. Without an image prediction algorithm, they can basically only be used to verify the geometry of the field and MLC outline. They are therefore only presented in figure 4c and will be evaluated in more detail during the TPS validation.

3D: volumetric dose reconstruction in the modular Octavius4D rotational unit

Figure 5 displays a selection of small (MLC) field depth dose curves as measured in the water phantom and as extracted from the 3D dose reconstructed by the Verisoft software. The Oct4D data in the upper half of the graph are obtained from measurements in the Oct4D_Maxi setup, while the lower half corresponds to Oct4D_Mini. Both were reconstructed with the two PDD reference sets. Upon close inspection, we observe that the 3D dose reconstruction along the beam axis is most accurately reproduced when a PDD set is used that was acquired with a SPD similar to the phantom setup: the Oct4D_Maxi dose reconstruction has a near-perfect agreement with the water phantom data when the PDD_{85} is used while slight deviations in the slope of the depth dose are observed when applying the $PDD_{91.5}$

reference set. The inverse is true for Oct4D_Mini for which the $PDD_{91.5}$ reconstructed data are superior. However, it needs to be said that the observed deviations with the non-corresponding PDD sets are small and only visible for off-isocentre distances larger than 2.5 cm, i.e. outside of the 3D volume that will be reconstructed from the ion chamber data in the central part of the detector. Furthermore, the slightly different slope will be partially annihilated in the 3D reconstruction of rotational delivery. Also noteworthy: although the PDD_{85} reference data-set was created with extrapolated rather than measured PDDs below 3x3 cm^2, these extrapolated data seem to yield equally good small field dose reconstruction as the $PDD_{91.5}$ for which depth doses were actually measured down to 1x1 cm^2.

For the arc treatments measured with the 1000SRS no difference could be distinguished between the dose reconstructions with the different PDD sets. The reconstructions shown in figure 6 have been generated with PDD_{85}. As can be seen, all Oct4D_Maxi measurements report an isocentric dose that agrees within 1% with the µD measurement. The Pp3D measures an equally good agreement for the conformal arcs on the 1.5 cm (figure 6b) and 3.0 cm (not shown) target, but underestimates the dose
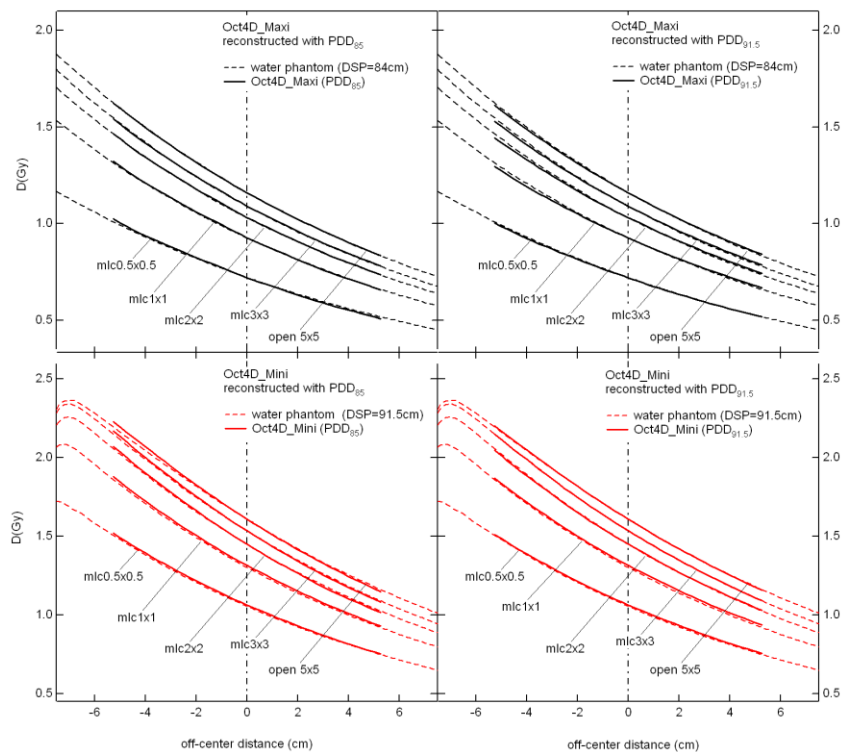
Figure 5: Comparison between water phantom measured PDDs and Oct4D reconstructed PDDs for Oct4D_Maxi and Oct4D_Mini. Small field (open and MLC) PDDS as measured in the water phantom are represented by the dashed lines at SPD = 84 cm (black, upper graphs) and SPD = 91.5 cm (red, lower graphs). The solid lines represent the PDDs extracted from the Oct4D_Maxi (upper graphs) and Oct4D_Mini (lower graphs) dose reconstruction using two different PDD reference sets. Graphs on the left were reconstructed with the PDD_{85}, graphs on the right were reconstructed based on the $PDD_{91.5}$. Comparison shows that best results are obtained when a PDD set adapted to the actual phantom SPD is used.
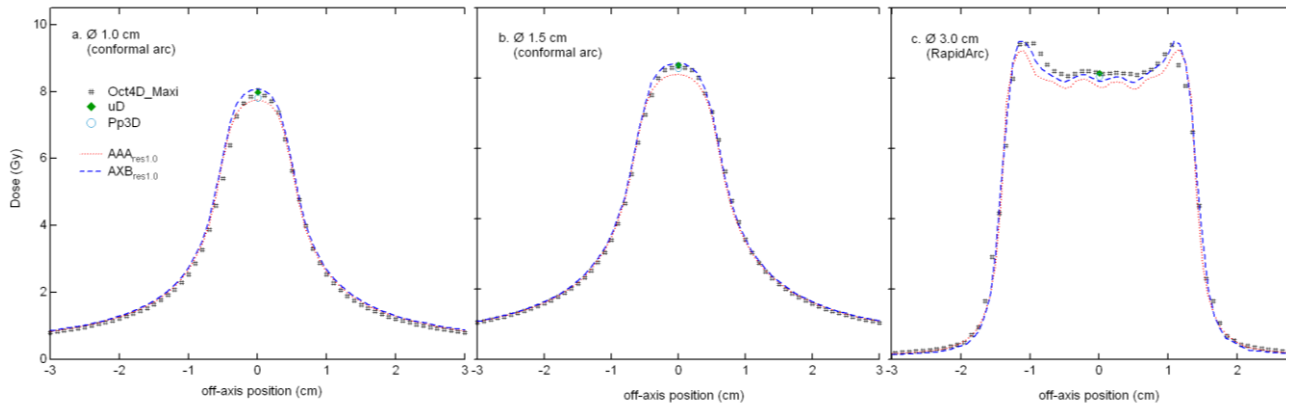
Figure 6: Results on the conformal and RA plans made on simple spherical targets of (a) 1.0 cm, (b) 1.5 cm and (c) 3.0 cm diameter. Symbols represent the different measurements: black hash tags are profiles extracted from the Oct4D_Maxi dose reconstruction. Coronal cross-sections indicating the position of the extracted profile are shown in the insets. Point dose measurements with the µD (green, solid diamonds) and Pp3D (light blue, open circles) at the isocentre are also displayed. Red dotted lines and dashed blue lines represent the AAA$_{res1.0}$ and AXB$_{res1.0}$ calculations, respectively.

of the smallest PTV by 3% (figure 6a). Similar results are obtained when comparing the RA measurement at isocentre between the µD,Pp3D and Oct4D_Maxi. The RA plan on the largest target is shown as an example in figure 6c.

III.2. Dose calculation algorithm configuration and validation

3.2.1. Algorithm configuration

Both dose calculation algorithms were successfully configured. Compared to the original, 'large field' algorithm configuration, no significant difference was observed in the calculated phase space parameters, apart from the fact that both the output factor table and the collimator backscatter factors now contain values down to a 1x1 cm^2 field size.

For the 120MLC, the leaf transmission was set to 1.5 %, providing an acceptable compromise of the overall transmission for both the 0.5 and 1.0 cm wide MLC leaves. The sweeping gap measurement provided a fairly flat total dose delivery and agreed well with TPS calculation for a DLG set to 0.14 cm. For the HDMLC, however, the overall leaf transmission is higher for the inner leaf area (1.25 %) than for the outer leaf area (1.1 %). As the inner leaves are predominantly used during (stereotactic) treatments, we have set the leaf transmission to 1.25 %. The DLG value was set to 0.09 cm to obtain good agreement between measured and calculated data for the central leaves. The results on the tongue and groove modeling are presented in figure 7. The portal images (upper graphs) indicate a promisingly good overall agreement between the measured and calculated photon fluence for both MLC types, as long as the calculation is performed with a sufficiently high resolution. This satisfactory agreement is also found in the comparison between the 1000SRS measurements and the dose calculations for the 120MLC, for the central (middle

graph of figure 7a) as well as for the outside leaves (bottom graph of figure 7a) as dose measurements and calculations intertwine. For the inner leaves of the HDMLC, however, the calculated dose level is systematically lower than the measurement (middle graph of figure 7b). Although the individual leaf positions could still be distinguished in the predicted portal dose image, this is no longer so for the in-phantom dose calculation. The Eclipse dose calculation grid not only smoothens out the tongue and groove effect, it also overestimates its impact on the dose reduction. The off-axis measurement on the HDMLC confirms the above findings (lower graph of figure 7b): while the overall dose level below the 2.5 mm leaves is ~ 7% too low, the 5 mm leaves are more adequately modeled as measurement and calculation overlap again.

3.2.2. Algorithm validation

0D: point dose validation:

Although many more jaw/MLC combinations were measured and calculated for the algorithm validation, table 2 shows a representative selection of the data as a function of field size, algorithm and calculation resolution. A lot can be learned from careful inspection of these simple datapoints. Firstly and most clearly, the absolute calculations for the small fields (≤ 2x2 cm^2) are unacceptable when calculated with a 2.5 mm calculation grid, regardless of the algorithm. Results for this calculation grid are only shown for the HDMLC, but were comparably poor for the 120MLC. For the 1 mm dose resolution, however, it can be observed that agreement between measurement and calculation is better for data obtained on the Clinac iX than on the NovalisTX: the field dimensions below 2x2 cm^2 show a ~ 2% larger deviation on the NovalisTX than on the Clinac iX. To investigate whether this should be attributed to a difference in the algorithm configuration or to the different MLC types, the datapoints for the HDMLC were recalculated with the
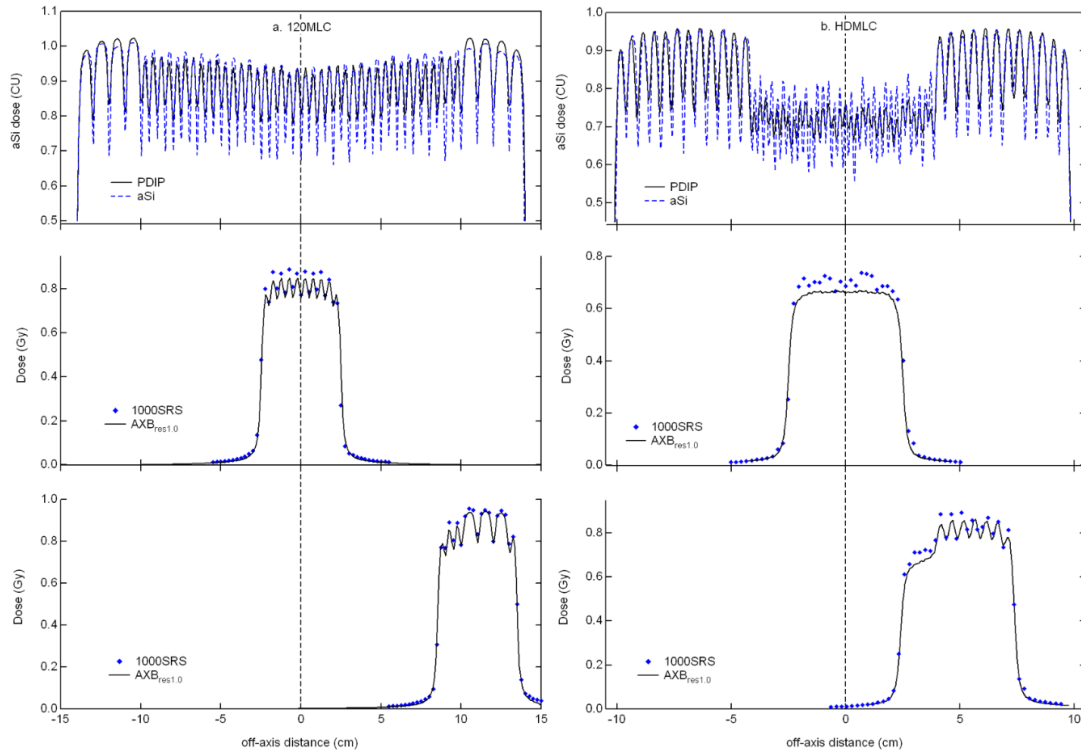
Figure 7: Evaluation of the tongue and groove model in Eclipse for the 120MLC (a. graphs on the left) and HDMLC (b. graphs on the right) by means of the step and shoot MLC plan with alternating leaf pair openings. Profiles perpendicular to the leaf movement are extracted from the planar measurements. The upper graphs display the high-resolution aS1000 (aSi) portal dose measurement (dashed blue line) and the portal dose predicted image (solid black line) based on the photon fluence as modeled by Eclipse during the $AXB_{res1.0}$ dose calculation. The middle graphs show the 1000SRS measurement (solid blue diamonds) for a central $5x5cm^2$ field opening - including only the central leaves into the results - while the lower graphs have a highly asymmetric 5x5 field-of-view to include both MLC widths for every MLC type. Dose calculations are shown for $AXB_{res1.0}$ (solid black lines).

Clinac iX algorithm configuration. (Although these treatment units do not officially have matched beam characteristics, when comparing their depth doses, profiles and output factor measurements in water, they appear near-identical, apart from a small (< 2%) difference in the field flatness, visible only in the profiles of the largest field sizes.) When recalculated with the Clinac iX beam data (not shown), agreement between measured and calculated dose is very similar for both MLC types, confirming that the inferior outcome on the NovalisTX in table 2 is beam data rather than MLC related. Best results were obtained with $AXB_{res1.0}$ on the Clinac iX: all point dose calculations

agreed within 2.5 % with the corresponding measurement. While results for $AXB_{res1.0}$ are slightly better than for $AAA_{res1.0}$ on the Clinac iX , the latter showing agreement within ~5 % for the smallest field sizes, this improvement is less systematic for the NovalisTX. Overall results on the NovalisTX are very good down to dimensions of 2 cm, below which deviations rise from ~ 5 % for the 1x1 cm^2 field to ~ 10% for the smallest 0.5x0.5 cm^2 field opening. To investigate whether the differences between AAA and AXB could be related to their respective differences in internal fluence resolution, an additional calculation was performed on the NovalisTX with AAA set to a resolution

Table 2: Point dose data measured with a μD for a selection of small field MLC/jaw combinations at SPD = 91.5, detph 8.5 cm (200 MU). The table lists the deviations observed for the Clinac iX and NovalisTX between measurement and calculation for different dose calculation conditions: values are shown for both algorithms at 1 mm dose calculation resolution (AAA$_{res1.0}$ and AXB$_{res1.0}$). For the Novalis, values are also listed for a 2.5 mm resolution (AAA$_{res2.5}$ and AXB$_{res2.5}$). The AAA$_{res1.25}$ calculation was added as it uses to the same internal fluence resolution as AXB$_{res2.5}$.

MLC in XxY (cm² in cm²)	Clinac iX, (120MLC)			NovalisTX (HDMLC)					
	μD (Gy)	AAA res1.0	ACUr es1.0	μD (Gy)	AAA res1.0	ACUr es1.0	AAA res2.5	ACUr es2.5	AAA res1.25
0.5x0.5 in 1x1	/	/	/	1.028	-7.56%	-10.74%	-32.74%	-69.97%	-10.74%
0.5x1 in 1x2	1.195	-2.37%	-0.58%	1.178	-5.35%	-4.57%	-12.54%	-15.98%	-7.06%
no MLC in 1x1	1.272	0.89%	0.89%	1.297	-0.20%	-0.92%	-1.95%	-3.33%	-0.71%
1x1 in 1x1	1.268	-0.61%	0.30%	1.285	-0.20%	-0.61%	-2.47%	-3.65%	-0.30%
1x1 in 2x2	1.308	-4.63%	-2.16%	1.296	-5.63%	-4.41%	-8.86%	-7.80%	-6.42%
2x2 in 3x3	1.444	0.40%	-0.10%	1.450	-2.04%	-2.88%	-3.20%	-2.77%	-0.91%
3x3 in 5x5	1.540	0.10%	-0.30%	1.535	0.89%	-0.30%	0.10%	-0.10%	0.20%
no MLC in 5x5	1.610	0.20%	0.10%	1.610	0.79%	-0.30%	0.20%	-0.3%	0.20%

of 1.25 mm, effectively obtaining the same internal fluence resolution as AXB$_{res2.5}$. As expected, results were slightly worse than for the AAA$_{res1.0}$ calculation, but still considerably better than the AXB$_{res2.5}$ results for field openings with dimensions smaller than 2cm, indicating that deviations can not be ascribed to the fluence resolution only.

The three different MLC/jaw combinations all resulting in a 1x1 cm² field opening (no MLC in a 1x1 cm² open field and 1x1 cm² MLC in 1x1 cm² and 2x2 cm² jaws) illustrate another tendency: for the smallest MLC openings, agreement between calculation and measurement improves as jaw positions approach the MLC outline. This is systematically observed for both treatment units. Although not shown in table 2, this tendency mostly manifests itself for jaw sizes smaller than 5x5 cm². For the 5x5 cm² jaw opening, all data for MLC apertures with dimensions of at least 1 cm, agree within 3% with the AAA$_{res1.0}$ and AXB$_{res1.0}$ calculation, in spite of the much larger jaw opening.

Additionally, it can be observed that the different MLC characteristics –especially the dosimetric leaf gap - between the HDMLC and the 120MLC have no noticeable impact on the absolute isocentric dose for beam aperture dimensions of 1 cm or more. Even for the 0.5x1 cm² measurements, the DLG can only be held accountable for a fraction of the 3% dose difference between measurements on the NovalisTX and on the Clinac iX as the open field output factor for the 1x2 cm² jaws already differs by 2% as well (not shown).

1D& 2D: water phantom scans and planar dose validation

In order to eliminate the absolute dose difference (MU calculation) from the depth dose evaluation, figure 8 displays the calculated depth doses for AAA$_{res1.0}$ and AXB$_{res1.0}$ at SPD 91.5 cm, normalized to the absolute dose measured in water by means of the above (table 2) established correction factor at a depth of 8.5 cm. The measured depth dose curves in figure 8 are the ones acquired with the dSRS.

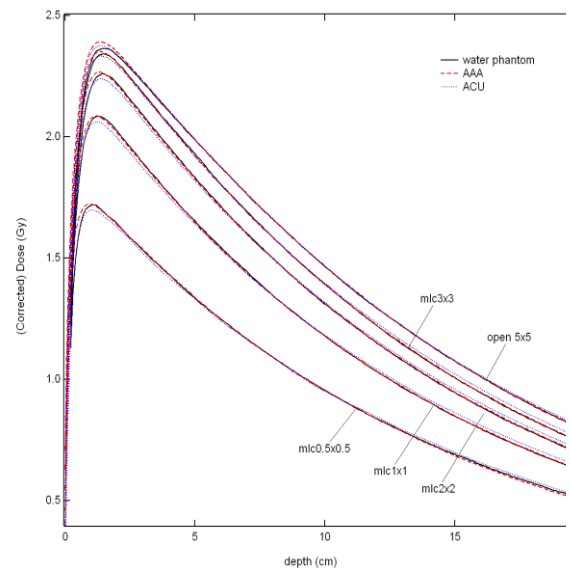*Figure 8: Comparison between measured and calculated depth dose curves for small (MLC) fields. Calculated PDDs were normalized to the measurement at 8.5 cm depth to correct for the absolute dose difference in the calculation. Except for the data in the build-up area, the relative shape of the PDD is perfectly reproduced for the AAA$_{res1.0}$ calculation while minor deviations are observed for the AXB$_{res1.0}$ data (<1%).*

When ignoring the absolute difference, $AAA_{res1.0}$ produces a visually perfect reproduction of the shape of the measured small field PDD, except in the build-up area. PDDs calculated for the MLC fields with $AXB_{res1.0}$ diverge slightly (up to ~ 1%) from the measured data as the distance from the normalization point (at 8.5 cm depth) increases. The 5x5 open field depth dose, however, matches the measured one. The $AXB_{res1.0}$ dose in the build-up area also differs more from the water phantom data than the $AAA_{res1.0}$ calculated dose. Depth doses calculated at the other SPDs were similarly rescaled to the water measurement at a fixed depth (not shown) and they all demonstrate results analogous to the ones in figure 8.

The transversal profile measured (dSRS) across the MLC striped pattern is compared to both calculation algorithms in figure 4b. Overall agreement is consistent with the deviations found in the absolute point dose comparisons as a function of MLC opening: for the 0.5 cm, 1 cm and 1.5 cm wide strips, $AAA_{res1.0}$ underestimates the peak dose by 8%, 2.5% and 0.7 %, respectively, while $AXB_{res1.0}$ reports 10%, 1.3% and 0.7% too little. From the profiles, however, it can also be observed that the summit of the 0.5 cm gap is only ~ 0.1 cm wide, making the absolute dose difference very dependent on the exact location of the dose calculation grid points. Although the detector diameter (0.12 cm) is somewhat larger than the calculation grid (1 mm), the calculated profiles are slightly more diffuse than the measured profile: apart from the dose underestimation at the center of the narrow peaks, both $AAA_{res1.0}$ and $AXB_{res1.0}$ display a small broadening of the penumbra. A dose calculation with the 2.5 mm grid is only displayed for AAA in order not to overload the graph, but the results for $AXB_{res2.5}$ look equally inadequate. Following the above established inferior results for the $AAA_{res2.5}$ and $AXB_{res2.5}$ calculations, these will henceforth be excluded from the presented data.

The ~0.4 mm resolution of the portal imager permits an up-close inspection of the photon fluence as measured by the aS1000. Although the Varian portal dose prediction algorithm was not yet validated for small field dosimetry, it does provide an indirect view on the actual photon fluence used during the Eclipse dose calculation (for both AAA and AXB) as it simply convolves this fluence with a single pencil beam (and rescales it with a number of correction factors to try and obtain the expected absolute dose level). Figure 4c displays the profiles extracted from the acquired dosimetric image along with the image predictions based on the $AXB_{res1.0}$ fluence (0.5 mm resolution) and the $AAA_{res1.0}$ and $AAA_{res2.5}$ fluences (1.0 and a 2.5 mm fluence resolution, respectively). As the resolution changes from 0.5 mm to 2.5 mm, the reduction in the fluence maximum of the narrowest strip is most apparent, along with the gradual broadening of the penumbra region. For the wider strips, the maximum of the peak is not considerably affected.

3D: volumetric dose validation

Analysis of the simple, conformal arcs show near-perfect agreement (<1%) for the $AXB_{res1.0}$ calculation and a 2 to 4 % too low dose for the $AAA_{res1.0}$ calculation on the 1.5 and 1.0 cm target, respectively (figure 6a and 6b). For the 3.0 cm target, $AAA_{res1.0}$ also matches the calculation within 1 % accuracy for the conformal arc plan (not shown). For the (simple) Rapidarc plans, however, the agreement between measured and calculated 3D dose is inferior to the near-perfect results obtained for the conformal arcs. The least favorable results are now obtained for the plan made on the largest target, shown in figure 6c. Although the shape of the dose distribution appears to be adequately reproduced, the overall dose is underestimated by ~ 4 % and ~ 2% for $AAA_{res1.0}$ and $AXB_{res1.0}$, respectively. The MLC movements of these RapidArc deliveries are more modulated than those of the conformal arcs, resulting in a smaller average MLC opening compared to the jaw settings. For the RapidArc delivery shown in figure 6c, an average MLC opening of ~ 2 cm^2 moves within the $3.0x2.8$ cm^2 collimator setting. The observed absolute discrepancy is therefore in accordance with what was found during the point dose validation of the different jaw/MLC combinations on the Clinac iX with the 120MLC.

3.3. Patient QA

An in-depth analysis was performed on the two test patients made for this purpose on the Clinac iX. Table 3a aims to summarize the obtained measurements compared to the dose calculations. In the left half of the table, the μD measurements in Ruby show good agreement with the dose calculations for almost all lesions. $AAA_{res1.0}$ reports a slightly lower maximum dose than $AXB_{res1.0}$, especially at the level of the smallest lesion of the '2Meta' patient. This lesion is the only one for which one of the μD measurements shows an underdosage of more than 3% for $AXB_{res1.0}$. The positive sign of the dose deviation for the Pp3D indicates that the detector's diameter is too large for this lesion. For the other lesions, however, Pp3D measurements are most satisfactory.

The right half of table 3a summarizes the evaluation by means of the 1000SRS/Oct4D systems. We judged the 3D gamma evaluation score for the 70 % isodose volume (γ_{3D} (iso70%)) to be the most representative statistical parameter for data interpretation. On Oct4D_Maxi, $AAA_{res1.0}$ calculations show inferior agreement to the measurement than $AXB_{res1.0}$ calculations. For nearly all plans, the dose tolerance needs to be relaxed to 5% to obtain a 99% PR, a condition that is already achieved for a 3% dose limit when using $AXB_{res1.0}$. This difference between AAA and AXB is only prominent in Oct4D_Maxi and not in Oct4D_Mini; illustrating that the tendency of AAA to underestimate the dose in narrow MLC openings becomes more pronounced with increasing depth. For AXB, no such depth dependence

could be deduced from the Oct4D data. Even so, nearly all plans do reach a 99% PR for the 5%L,1mm criteria. The only exception is the non-coplanar treatment of the double lesion, for which only the AXB calculation on Oct4D_Mini passed the 99% PR with a dose tolerance of at least 5%. This poor outcome is due to the inappropriate use of the total dose rather than the field-by-field evaluation. For the coplanar and nearly coplanar dose delivery, the Oct4D without couch rotation still results in a reasonable representation of the patient 3D dose distribution. For a single lesion located at isocentre, this method even holds for the radically non-coplanar arc setup ('1Meta_nonCP') as the high dose is delivered to isocentre regardless of the couch rotation. For the multiple lesions case, however, the high dose peaks are no longer situated at isocentre and the absence of the true couch rotation during QA makes the resulting 3D dose totally unrepresentative of the patient 3D dose: high dose areas in the non-rotated phantom do not necessarily correspond to high dose areas in the patient and vice versa. As the 70% isodose becomes a clinically irrelevant parameter in this summed dose matrix, the importance of the poor outcome of the γ_{3D} (iso70%) is equally hard to judge. The different arcs of this non-coplanar dose delivery were therefore evaluated on an individual basis and each of the arcs showed a PR of the same quality as the total plans for the coplanar and nearly coplanar cases, thereby confirming the adequate agreement between dose calculation and delivery for every arc individually.

*T*able 3: Overview of the QA results obtained on SRT treatment plans verified by means of point dose measurements in Ruby and by means of the 1000SRS/Oct4D system. Parallel validations with all methods on the Clinac iX are presented in part (a): single('1M') and multiple lesions('2M') were treated with non-coplanar ('_nonCP'), coplanar ('_CP') and nearly coplanar ('_nearCP') arc geometries. For the point dose measurements in Ruby, the percent deviations between the calculated and measured dose is given for every lesion. The '2M' plans therefore have two values per plan: the smallest deviation always corresponds to the largest lesion. The right half of part (a) lists the percentages of points that pass the γ_{3D} analysis within the 70% isodose volume. Local dose difference criteria were varied fro 3%L to 5%L, while the DTA was kept fixed at 1mm. The scores are given for Oct4D_Maxi as well as for Oct4D_Mini. Part (b) of the table only lists results for Oct4D_Mini measurements compared to $AAA_{res1.0}$ dose calculations as this is what is currently used in clinical routine on the NovalisTX. Scores are shown for a representative selection of 10 patients (P1-P10).

a. Clinac iX, 120MLC

	Ruby & μD		Ruby & Pp3D		Oct4D_Maxi γ_{3D} (iso70%), DTA = 1mm				Oct4D_Mini γ_{3D} (iso70%), DTA = 1mm			
					$AAA_{res1.0}$		$ACU_{res1.0}$		$AAA_{res1.0}$		$ACU_{res1.0}$	
	$\Delta AAA_{res1.0}$	$\Delta ACU_{res1.0}$	$\Delta AAA_{res1.0}$	$\Delta ACU_{res1.0}$	3 %L	5 %L	3 %L	5 %L	3 %L	5 %L	3 %L	5 %L
1M_NonCP	-1.3%	-0.5%	-0.7%	0.1%	96.7	100	100	100	99.6	100	99.7	100
1M_CP	-2.5%	-1.2%	-1.2%	0.3%	97.8	99.8	100	100	99.6	99.8	99.7	99.9
1M_nearCP	-2.4%	-1.1%	-1.6%	-0.3%	95.1	99.1	99.6	100	99.7	100	100	100
2M_nonCP	-0.7% -1.8%	0.1% 0.0%	-0.8% 4.0%	0.1% 5.9%	84.4	92.2	94.9	97.5	92	98	94.4	99.5
2M_CP	-1.6% -3.3%	0.0% 0.1%	-0.6% 5.8%	1.2% 7.1%	98.8	100	100	100	100	100	100	100
2M_nearCP	-1.7% -5.0%	0.1% -3.9%	-1.5% 6.7%	0.3% 8.0%	98.3	100	99.7	100	99.9	100	99.8	100

b. NovalisTX, HDMLC

	Oct4D_Mini γ_{3D} (iso70%), DTA = 1mm	
	$AAA_{res1.0}$	
	3%L	5%L
P1	83.4	95.3
P2	81.6	100
P3	67.1	90.9
P4	94.4	100
P5	74.9	91.1
P6	96.9	99.9
P7	88.2	97.8

The third part of table 3 lists a representative selection of stereotactic arc treatments on the NovalisTX for which pre-treatment QA was performed with Oct4D_Mini. Results are markedly inferior to those obtained on the Clinac iX: none of the plans come even close to achieving 99% PR for the 3%L,1mm criteria and even for the lenient 5%L,1mm settings, only 4 out of 10 plans pass. As most of these are single lesion cases, the deviations can not be attributed to the use of an inappropriately summed plan for non-coplanar delivery. On the contrary, for some cases individual arcs were compared to their corresponding calculation and similarly low-grade outcomes were observed. Dose calculations with $AXB_{res1.0}$ did not bring about a systematic improvement. Only two obvious differences exist between both treatment units: the algorithm configurations and the MLC type. As it was observed during algorithm validation that for the very small MLC fields results are better for the beam data configured on the Clinac iX than those on the NovalisTX, treatment plans on the NovalisTX were recalculated with the Clinac iX algorithm version and vice versa. Although these recalculations confirmed the slight improvement when using the Clinac iX algorithm configuration, they were insufficient to explain the marked inferiority of the results for patient QA on the NovalisTX. The additional problems are therefore suspected to be related to the HDMLC, in particular to the underestimation of the dose in areas of considerable asynchronous leaf movement, resulting in a pronounced tongue and groove effect. Although the exact impact of this effect is difficult to quantify, from the leaf movement one can judge whether a dose delivery will be subject to a lot of tongue and groove effect or not. The simple observation of the leaf movement for the different plans listed in table 3 supports the hypothesis that HDMLC VMAT arcs with more pronounced asynchronous leaf movement indeed have lower pass rates.

IV. DISCUSSION

Careful and systematic benchmarking of commercially available dosimetry equipment requires time and effort but

this investment is easily won back when the practical knowledge gained from it can be put to good use when choosing an appropriate detector for a specific task at hand, when interpreting measurement results (knowing their expected precision) or when troubleshooting. Without appropriate, TPS independent benchmarking, one cannot be certain if observed deviations are detector or TPS related, or both. This is especially true for stereotactic treatments where very small dimensions and high dose (rate) delivery are combined, pushing both the detector and the dose calculation to the limits of their capabilities.

Combining the step-by-step detector evaluation with background knowledge of the dose calculation algorithm configuration firstly helps with the detector choice for beam data acquisition. When upgrading an existing AAA or AXB configuration – typically already configured down to a 3x3 cm^2 field size – to include small field dose calculation, the only data that really need to be added are the small field output factors. As all diode detectors were found to be equally suitable for this, and as most radiotherapy departments have at least one of these available, no additional purchases need to be made for this part of the stereotactic treatment implementation. Note that, while the appropriate detector choice may be important, it is also essential to carefully verify (and possibly adjust) the jaw calibration before initiating the output factor measurements.

When basic beam data for AAA and/or AXB need to be acquired from scratch, however, our preferred detector for PDD and profile scans would be the Sf3D as this detector can comfortably be used for the whole field range (from 2x2 to 40x40 cm^2). Even though depth dose and profile data for the 2x2 cm^2 field size are not actually required and contribute very little –if anything- to the algorithm configuration, the 2x2 cm^2 PDD acquisition can be put to use for the algorithm validation. The Sf3D can also be used for output factor measurements down to 3x3 cm^2, below which one needs to switch to one of the diode detectors or to the μD. Although the μD is definitely the most versatile detector as it can go down to 1x1 cm^2 (for PDDs, profiles and output factors) because of its excellent spatial resolution, on the down side it has a low sensitivity and requires considerably longer sampling times to achieve good signal-to-noise ratio. This may not look like a big disadvantage on paper, but when acquiring beam data it does start to feel like one as the evening progresses. In addition, as the 1x1 cm^2 PDD and profile scans are in any case totally ignored during the configuration process, there is little benefit in using the μD for beam data acquisition. The inferior resolution of the Sf3D is not an issue for the Eclipse basic beam data acquisition as the penumbra region is also ignored during the configuration process. However, if high resolutions profiles or small field PDDs do need to be acquired in a water phantom for purposes other than the AAA or AXB configuration, our preference would go to the dSRS because of its high sensitivity and its good agreement

with the ion chamber in the low dose areas (below the MLC or below the jaws) at all depths.

While very little – if any – additional equipment needs to be foreseen for the algorithm configuration, validation can be extremely cumbersome without the appropriate tools. Past incidences in different radiotherapy centers as well as our own validation results clearly demonstrate that accurate absolute dose calculation in small fields is not a given.

A minimum requirement for validation and subsequent patient QA would be a high resolution single detector that shows good directional independence (such as the μD or Pp3D) and a small solid water phantom in which to fit the detector (such as an assortment of small solid water blocks of several thicknesses or a phantom like Ruby). The static MLC/jaw combinations provide a simple test and a good indication of the accuracy of the absolute dose calculation that can be expected for small MLC openings in different jaw sizes. We have observed that some algorithm configurations give better results than others but we have not been able to determine the underlying cause, making it all the more advisable to effectively perform such measurements. When carried out with a single detector in a water phantom, these test do take some time, but when solid water blocks or a phantom like Ruby are available, and the plans have been prepared in Eclipse beforehand, 15 minutes machine time suffice for the whole measurement sequence. For point dose validation of the conformal and RA arc treatments during the validation process, Ruby was most successful in combination with the μD, but the Pp3D can also be used as long as one is aware of its tendency to underestimate the actual dose as field dimensions become very small (≤ 1 cm). The Pp3D has the drawback of possibly reporting overly optimistic agreement for field sizes for which both the detector and the dose calculation underestimate the actual dose. Although spherical phantoms exist and have the distinct advantage of being directionally independent by design, we have a preference for geometric structures with flat surfaces as they are easy to place on the treatment couch (or couch extension), to align to the field crosshairs and lasers and they do not need any specific mounting accessory to prevent them from rolling. The geometric structure is also easily matched to its CBCT image, further facilitating accurate phantom setup. With a directionally independent detector inserted, this very simple phantom allows accurate point dose verification of the patient treatments in the exact same geometry as the actual treatment plan, including couch rotations. While the QA procedure is quite straightforward for single lesion treatments at isocentre, it becomes more cumbersome and error-prone for treatments with multiple lesions as a separate verification plan needs to be made per lesion and each time, the detector needs to be positioned at the center of the lesion rather than at isocentre. As we find that we treat more and more multiple lesions with a single isocentre, this is an important drawback. In addition, the single point dose measurement is just that: a single point dose. It does not

provide any information on the location or accuracy of the dose drop-off at the edge of the target, even though this is an important factor in stereotactic treatments. Nor can the single point measurement provide much assistance during trouble-shooting.

For a more in-depth validation, the most efficient and multipurpose validation tool by far is the 1000SRS. While high resolution profiles can indeed be acquired in a water phantom like we have done, the acquisition process is tedious and the analysis is cumbersome as it requires extensive manual data manipulation before an actual comparison with the TPS data can be performed in third party data analysis software. Great care needs to be taken when converting the measured profiles into absolute dose, but as the absolute dose level is one of the weak links in the dose calculation, this step is quite essential. As the profiles extracted from the orthogonally irradiated 1000SRS array compared so well to the water phantom profiles obtained with the μD or dSRS at all three depths (5, 10 and 15 cm), profile acquisitions in the water phantom were further abandoned and replaced by 2D planar dose measurements with the 1000SRS instead. In fact, both the small MLC output factor data (down to 0.5×0.5 cm^2) and the profile comparisons experimentally reflect a spatial resolution that would be of the order of ~1 mm instead of the 2.4 resolution defined by the actual chamber dimensions. The previously reported dose rate and field size dependences of the 1000SRS [56] were simply handled through an appropriate choice of cross-calibration conditions: we mostly used a 4x4 cm^2 or 5x5 cm^2 rather than a 10x10 cm^2 reference field and irradiated at maximum dose rate (600MU/min for 6MV, 1000MU/min for 6MV_SRS). The static validation fields were always delivered with this constant, maximum dose rate and the high dose levels of the real treatment plans cause the dose rate to always be at (or close to) its maximum level as well, even for RA treatments.

For validation of the stereotactic arc treatments, the 1000SRS needs to be combined with the Oct4D rotational phantom. Both the Oct4D_Maxi and Oct4D_Mini were validated independently of the TPS dose calculation and both were found to give equally reliable measurement based dose reconstructions. Although the 3D dose is slightly better reconstructed when phantom-specific PDD sets (PDD$_{85}$ and PDD$_{91.5}$, respectively) are used, the effect of this is only apparent in static acquisitions of single fields but hardly visible in dose reconstructions of rotational deliveries. As we now have both PDD sets available, we do alternate between them accordingly, but from a practical point of view, it can be safely assumed that a single PDD set suffices for patient QA. Although both phantom diameters produce correct dose reconstructions, there are a few practical disadvantages to the Oct4D_Maxi compared to Oct4D_Mini with respect to stereotactic plan QA. Firstly, the large diameter regularly invokes memory problems in the Eclipse TPS because of the 1 mm calculation grid (for both AAA and AXB), causing the dose calculation to fail. And even if the calculation in the full phantom is successful, the

calculation process takes a very long time and the exported dose file is so large that memory issues sometimes arise in the Verisoft software as well. It is therefore advisable to reduce the calculation volume but this needs to be done manually, hindering automated verification plan creation. In addition, our data have shown that AAA results are inferior in the large phantom. Although this is attributed to a genuine deviation in the dose calculation, it may be argued that 15 cm could be too large a depth to reflect clinical relevance, especially for intracranial stereotactic treatments. None of these issues are encountered with the Oct4D_Mini. The one drawback encountered with both Oct4D compositions, on the other hand, is the removal of planned couch rotations, in the phantom calculation as well as in the delivery. For single lesions or for multiple lesions with (nearly) coplanar treatment arcs, it is sufficient to compare the summed doses of the different arcs to the total calculated dose by means of the γ_{3D}(iso 70%) and visual assessment of the summed data. For multiple lesions treated with a single isocentre and a radically non-coplanar setup, this summed dose without couch rotation becomes totally distorted and impossible to interpret. For these cases, the results are preferably analyzed for each individual arc. Although this is more time-consuming on the analysis side, it does not add any machine time to the QA procedure and it is still much more efficient and less error-prone than the repetitive treatment delivery per lesion with Ruby.

From the algorithm validation performed on Clinac iXs and the NovalisTX, we can draw a number of general conclusions. Firstly, one conclusion holds for all dose calculations: if deviations are observed in the high dose area, they are always underestimates of the true dose. Secondly, a large error that can easily be made and subsequently overlooked is the accidental use of the 2.5 mm dose calculation grid. As the default calculation resolution is usually set to 2.5 mm for standard treatments, the planner needs to actively change this resolution when performing stereotactic treatment optimization. Fortunately, when a verification plan is created on a phantom, it uses the same calculation resolution as the plan of origin and the QA will detect the dose discrepancy. Third, near-identical looking basic beam data can result in beam configurations of different precision. This needs to be investigated further as it points towards instability in the algorithm configuration. Although it cannot be helped for now, it can at least be diagnosed, allowing the physicist to estimate beforehand how accurate the final dose calculation will be and to take this into account during plan evaluation. In our study, excellent results (<3%) were obtained on the Clinac iX units with AXB$_{res1.0}$. On the NovalisTX, this accuracy was only achieved for simple MLC field dimensions of at least 2 cm. Fourth, while the Eclipse modeling of the dynamic MLC appears satisfactory for the 120MLC, it is the cause of additional deviations for the HDMLC on the NovalisTX. The overall MLC transmission can only be modeled by a single parameter in Eclipse, regardless of the leaf width.

While a sensible average value for all leaves can be determined for the 120MLC, for the HDMLC the overall MLC transmission is noticeably higher for the high definition central leaves than for the outer leaves. Even more important than the transmission could be the tongue and groove model. The dose calculation is too low in areas irradiated through highly asynchronous leaf movement. This effect is moderate for the 120MLC but can go up to 8% for the HDMLC. As a result of the above, ironically, dosimetric results for the stereotactic treatments are better on the conventional Clinac iX units than on the NovalisTX.

Having benchmarked the QA equipment and the dose calculation precision, a decision needs to be made regarding the acceptance criteria to be used for patient QA. The traditional 3%G,3mm gamma evaluation (with a 95 % pass rate) is ill adapted to the clinical needs of stereotactic treatments on almost all aspects. Firstly, it would be unrealistic to state that a 3% accuracy in the high dose area is mandatory. Given the traditional dose prescription to the 50, 70 or 80% isodose level (depending on the delivery approach) around the target and the ensuing dose non-uniformity within the target, dose homogeneity in the target is not the goal in stereotactic treatment planning. The goal is to achieve the prescribed lower dose limit tightly shaped around the target. Within the target, the dose can go up to 100%, but there is no consensus on whether or not this is clinically necessary. Underestimating the true dose to the lesion by a few percent is therefore no cause for alarm. However, when deviations become larger than e.g. 5%, the clinician's opinion could be invoked to decide whether the measured overdosage at the level of the lesion is acceptable. Secondly, while we are willing to be considerably more lenient on the maximum dose at the level of the lesion, we do not wish to allow for a 3 mm imprecision on the penumbra. The spatial precision of the gradient fall-off is an important aspect of the treatment. The DTA is therefore set to 1 mm. Admittedly, this is very close to the positional precision that can be achieved with the 1000SRS/Oct4D phantom setup. It is therefore sometimes necessary to perform an alignment of the measured and calculated 3D dose matrices in the Verisoft software. From the validation of a cohort of real patient plans, we have found that a 5%L,1mm gamma analysis on the 70% isodose volume gives a score that is representative for the clinically relevant agreement between measurement and calculation. Even so, we use this gamma analysis only as a guideline rather than as a pass/fail filter. We find that for these small volumes, for now, visual inspection of the data in e.g. the three orthogonal planes provides the most relevant and efficient analysis.

V. CONCLUSION

A compact procedure for benchmarking the different detector systems (from point dose to 3D dose) eligible for SRT measurements provided a clear and practical overview regarding their expected accuracy and their possible applications:

Embedding small field dose calculations into an already existing AAA and AXB algorithm configuration merely requires the additional input of small field output factors (down to 1x1 cm^2). For this, all diodes and the μD were found to be suitable. As quality and safety guidelines on SRT stress the need for TPS validation as well as patient-specific treatment QA, it is advantageous to select multipurpose detector systems that can serve for both. A single detector that is directionally independent is mandatory to permit verification of the total dose delivered through non-coplanar arcs. The μD is most suitable for this, but the Pp3D can also be used. When inserted into a phantom such as Ruby, the single detector can be used for the most basic validation of the TPS as well as for the most complex RA dose verification. The point dose measurement provides a relevant verification of the dosimetric precision of the high dose level (in static or arc delivery), but does not provide any reassurance on the location of the dose fall-off. The latter can easily and reliably be verified with the 1000SRS/Oct4D combination. Whereas the Oct4D_Mini has some practical advantages over the Oct4D_Maxi, both systems were carefully validated and – when appropriately cross-calibrated - provide equally reliable measurement-based dose reconstructions.

Using the above selected detector systems, AAA and AXB validation on the Clinac iX (120MLC) and the NovalisTX (HDMLC) revealed differences in algorithm precision between different treatment units. As the origin of this difference remains unknown, it further emphasizes the need to validate individual algorithm configurations. It was also found that the Eclipse modeling of the HDMLC should be further improved, especially with respect to the tongue and groove effect. On the Clinac iX, the obtained results were excellent for AXB and AAA, undoubtedly within clinical acceptance. On the NovalisTX, results were inferior to the Clinac iX. Because of the above mentioned deviations, the calculated dose systematically underestimated the real dose by a few percent (2-7%, depending on the patient plan). But also for the NovalisTX, all results were judged to be within clinical acceptance for SRT treatments.

REFERENCES

[1] R. Timmerman, R. Paulus, J. Galvin, J. Michalski, W. Staube, J. Bradley, A. Fakiris, A. Bezjak, G. Videtic, D. Johnstone,J. Fowler,E. Gore, and H. Choy. "Stereotactic body radiation therapy for inoperable early stage lung cancer," JAMA 303, 1070-1076 (2010). doi: 10.1001/jama.2010.261

[2] D.E. Heron, R.L. Ferris, M. Karamouzis M, R.S. Andrade, E.L. Deeb, S. Burton, W.E. Gooding, B.F. Branstetter, J.M. Mountz, J.T. Johnson, A. Argiris, J.R. Grandis, and S.Y. Lai. "Stereotactic body radiotherapy for recurrent squamous cell carcinoma of the head and neck: results of a phase I dose-escalation trial," Int. J. Radiat. Oncol., Biol., Phys., 75(5), 1493-1500 (2009). doi: 10.1016/j.ijrobp.2008.12.075

[3] P. Baumann, J. Nyman, M. Hoyer, B. Wennberg, G. Gagliardi, I. Lax, N. Drugge, L. Ekberg, S. Friesland, K.A. Johansson, J.A. Lund, E. Morhed, K. Nilsson, N. Levin, M. Paludan, C. Sederholm, A. Traberg, L. Wittgren, and R. Lewensohn. "Outcome in a prospective phase II trial of medically inoperable stage I non-small-cell lung cancer patients treated with stereotactic body radiotherapy," J. Clin Oncol. 27, 3290-3296 (2009). doi: 10.1200/JCO.2008.21.5681

[4] K.E. Rusthoven, B.D. Kavanagh, H. Cardenes, V.W. Stieber, S.H. Burri, S.J. Feigenberg, M.A. Chidel, T.J. Pugh, W. Franklin, M. Kane, L.E. Gaspar, and T.E. Schefter. "Multi-institutional phase I/II trial of stereotactic body radiation therapy for liver metastases," J. Clin. Oncol. 27,1572-1578 (2009). doi: 10.1200/JCO.2008.19.6329

[5] K.E. Rusthoven KE, B.D. Kavanagh, S.H. Burri, C. Chen, H. Cardenes, M.A. Chidel, T.J. Pugh, M. Kane, L.E. Gaspar, and T.E. Schefter. "Multi-institutional phase I/II trial of stereotactic body radiation therapy for lung metastases," J Clin Oncol. 27, 1579-1584. (2009). doi: 10.1200/JCO.2008.19.6386

[6] M.T. Lee, J.J. Kim, R. Dinniwell, J. Brierley, G. Lockwood, R. Wong, B. Cummings, J. Ringash, R.V. Tse, J.J. Knox, and L.A. Dawson. "Phase I study of individualized stereotactic body radiotherapy of liver metastases," J. Clin Oncol. 27, 1585-1591 (2009). doi: 10.1200/JCO.2008.20.0600

[7] A.J. Fakiris, R.C. McGarry, C.T. Yiannoutsos, L. Papiez, M. Williams, M.A. Henderson, and R. Timmerman. "Stereotactic body radiation therapy for early-stage non-small-cell lung carcinoma: four-year results of a prospective phase II study," Int. J. Radiat. Oncol., Biol., Phys. 75, 677-682 (2009). doi: 10.1016/j.ijrobp.2008.11.042

[8] P. Baumann, J. Nyman, M. Hoyer, G. Gagliardi, I. Lax, B. Wennberg, N. Drugge, L. Ekberg, S. Friesland, K.A. Johansson, J.S. Lund, E. Morhed, K. Nilsson, N. Levin, M. Paludan, C. Sederholm, A. Traberg, L. Wittgren, and R. Lewensohn. "Stereotactic body radiotherapy for medically inoperable patients with stage I non-small cell lung cancer - a first report of toxicity related to COPD/CVD in a non-randomized prospective phase II study," Radiother. Oncol. 88, 359-367 (2008). doi: 10.1016/j.radonc.2008.07.019

[9] C.R. King, J.D. Brooks, H. Gill, T. Pawlicki, C. Cotrutz, and J.C. Presti "Stereotactic body radiotherapy for localized prostate cancer: interim results of a prospective phase II clinical trial," Int. J. Radiat. Oncol., Biol., Phys. 73,1043-1048 (2009). doi: 10.1016/j.ijrobp.2008.05.059

[10] R.V. Tse, M. Hawkins, G. Lockwood, J.J. Kim, B. Cummings, J. Knox, M. Sherman, and L.A. Dawson. "Phase I study of individualized stereotactic body radiotherapy for hepatocellular carcinoma and intrahepatic cholangiocarcinoma," J. Clin. Oncol. 26, 657-664 (2008). doi: 10.1200/JCO.2007.14.3529

[11] E.L. Chang, A.S. Shiu, E. Mendel, L.A. Mathews, A. Mahajan, P.K. Allen, J.S. Weinberg, B.W. Brown, X.S. Wang, S.Y. Woo, C. Cleeland, M.H. Maor, and L.D. Rhines. "Phase I/II study of stereotactic body radiotherapy for spinal metastasis and its pattern of failure," J. Neurosurg. Spine. 7,151-60 (2007). doi: 10.3171/SPI-07/08/151

[12] M.T. Milano, A.W. Katz, A.G. Muhs, A. Philip, D.J. Buchholz, M.C. Schell, and P. Okunieff. "A prospective pilot study of curative-intent stereotactic body radiation therapy in patients with 5 or fewer oligometastatic lesions," Cancer. 112, 650-658 (2008). doi: 10.1002/cncr.23209

[13] S.E. Combs, T. Welzel, D. Schulz-Ertner, P.E. Huber, and J. Debus. "Differences in clinical results after linac-based single-dose radiosurgery versus fractionated stereotactic radiotherapy for patients with vestibular schwannomas," Int. J. Radiat. Oncol., Biol., Phys. 76, 193-200 (2010). doi: 10.1016/j.ijrobp.2009.01.064

[14] T.D. Solberg, J.M. Balter, S.H. Benedict, B. A. Fraass, B. Kavanagh, C. Miyamoto, T. Pawlicki, L. Potters, and Y. Yamada, "Quality and Safety Considerations in Stereotactic Radiosurgery and Stereotactic Body Radiation Therapy," Practical Radiation Oncology, supplement material 2, 2-9 (2012) doi:10.1016/j.prro.2011.06.014

[15] P.Y. Borius, B. Debono, I. Latorzeff, J.A. Lotterie, J.Y. Plas, E. Cassol, P. Bousquet, F. Loubes, P. Duthil, A. Durand, F. Caire, A. Redon, I. Berry, J. Sabatier, and Y. Lazorthes. "Dosimetric stereotactic radiosurgical accident: Study of 33 patients treated for brain metastasis," Neurochirurgie. 56:368-373 (2010). doi: 10.1016/j.neuchi.2010.07.002

[16]. S. Derreumaux, C. Etard, C. Huet, F. Trompier, I. Clairand, J.F. Bottollier-Depois, B. Aubert, and P. Gourmelon. "Lessons from recent accidents in radiation therapy in France," Rad. Prot. Dosim. 131,130-135 (2010). doi: 10.1093/rpd/ncn235

[17] P. Gourmelon, E. Bey, T. De Revel, and J.J. Lataillade. "The French radiation accident experience: emerging concepts in radiation burn and ARS therapies and

in brain radiopathology," Radioprotection. 43(5), 23-26 (2008). doi: 10.1051/radiopro:2008761

[18] W. Bogdanich, K. Rebelo, "The Radiation Boom - A Pinpoint Beam Strays Invisibly, Harming Instead of Healing," The New York Times, New York, A1 (2010).

[19]. Elekta Bulletin 98-02-17, Leksell Gamma Knife, ''New 4-mm Helmet Output Factor,'' Feb. 17, (1998).

[20]. J.P. Gibbons, D. Mihailidis, C. Worthington, H. Alkhatib, R. Boulware, R. Clark, B. Dial, and W. Neglia. "The effect of the 4-mm-collimator output factor on gamma knife dose distributions," J. Appl. Clin. Med. Phys. 4,386-389 (2003). doi: 10.1120/1.1621375

[21] H. D. Kubo, C. T. Pappas, and R. B. Wilder, "A comparison of arc-based and static mini-multileaf collimator-based radiosurgery treatment plans," Radiother. Oncol. 45, 89-93 (1997).

[22] D. Leavitt, "Beam shaping for SRT/SRS," Med. Dosim. 23, 229-236 (1998).

[23] D. Solberg, K.L. Boedeker, R. Fogg, M.T. Selch, and A.A. DeSalles, "Dynamic arc radiosurgery field shaping: A comparison with static field conformal and noncoplanar circular arcs," Int. J. Radiat. Oncol., Biol., Phys. 49, 1481-1491 (2001).

[24] H. Benedict, F.J. Bova, B. Clark, S.J. Goetsch, W.H. Hinson, D.D. Leavitt, D.J. Schlesinger, and K.M. Yenice, "Anniversary Paper: The role of medical physicists in developing stereotactic radiosurgery," Med. Phys. 35, 4262-4277 (2008). doi: 10.1118/1.2969268

[25] J. Hazard, B. Wang, T.B. Skidmore, S.S. Chern, B.J. Salter, R.L. Jensen, and D.C. Shrieve, "Conformity of LINAC-based stereotactic radiosurgery using dynamic conformal arcs and micro-multileaf collimator," Int. J. Radiat. Oncol., Biol., Phys. 73, 562-570 (2009). doi: 10.1016/j.ijrobp.2008.04.026

[26] Y. Tsuruta, M.u Nakata, M. Nakamura, Y. Matsuo, K. Higashimura, H. Monzen, T. Mizowaki, and M. Hiraoka, "Dosimetric comparison of Acuros XB, AAA, and XVMC in stereotactic body radiotherapy for lung cancer," Med. Phys. 41(8) , 081715 (2014)
doi: 10.1118/1.4890592

[27] A. Fogliata, A. Clivio, G. Nicolini, E. Vanetti, and L. Cozzi, "Intensity modulation with photons for benign intracranial tumours: A planning comparison of volumetric single arc, helical arc and fixed gantry techniques," Radiother. Oncol. 89, 254–262 (2009). doi: 10.1016/j.radonc.2008.07.021

[28] F. Lagerwaard, O. Meijer, E. van der Hoorn, W. Verbakel, B. Slotman, and S. Senan, "Volumetric modulated arc radiotherapy for vestibular schwannomas," Int. J. Radiat. Oncol., Biol., Phys. 74, 610–615 (2009). doi: 10.1016/j.ijrobp.2008.12.076

[29] S. Subramanian, C. Srinivas, K. Ramalingam, M. Babaiah, S. T. Swamy, G. Arun, M. Kathirvel, S. Ashok, A. Clivio, A. Fogliata, G. Nicolini, K. S. Rao, T. P. Reddy, J. Amit, E. Vanetti, and L. Cozzi, "Volumetric Modulated Arc-based hypofractionated stereotactic radiotherapy for the treatment of selective intracranial arteriovenous

malformations: Dosimetric report and early clinical experience," Int. J. Radiat. Oncol., Biol. Phys. 82(3), 1278-1284 (2012). doi: 10.1016/j.ijrobp.2011.02.005

[30] W. Verbakel, S. Senan, J. Cuijpers, B. Slotman, and F. Lagerwaard, "Rapid delivery of stereotactic radiotherapy for peripheral lung tumors using volumetric intensity modulated arcs," Radiother. Oncol. 93, 122–124 (2009). doi: 10.1016/j.ijrobp.2009.03.029

[31] C. Ong, D. Palma, W. Verbakel, B. Slotman, and S. Senan, "Treatment of large stage I-II lung tumors using stereotactic body radiotherapy (SBRT): Planning considerations and early toxicity," Radiother. Oncol. 97, 431–436 (2010). doi: 10.1016/j.radonc.2010.10.003

[32] C. Ong, W. Verbakel, J. Cuijpers, B. Slotman, F. Lagerwaard, and S. Senan, "Stereotactic radiotherapy for peripheral lung tumors: A comparison of volumetric modulated arc therapy with 3 other delivery techniques," Radiother. Oncol. 97, 437–442 (2010). doi: 10.1016/j.radonc.2010.09.027

[33] C. Ong, W. Verbakel, J. Cuijpers, B. Slotman, and S. Senan, "Dosimetric impact of interplay effect on rapidarc lung stereotactic treatment delivery," Int. J. Radiat. Oncol., Biol., Phys. 79, 305–311 (2011). doi: 10.1016/j.ijrobp.2010.02.059

[34] D. Palma, J. van Sömsen de Koste, W. Verbakel, A. Vincent, and S. Senan, "Lung density changes after stereotactic radiotherapy: A quantitative analysis in 50 patients," Int. J. Radiat. Oncol., Biol., Phys. 81(4),974-978 (2011). doi: 10.1016/j.ijrobp.2010.07.025

[35] D. Palma, S. Senan, C. Haasbeek, W. Verbakel, A. Vincent, and F. Lagerwaard, "Radiological and clinical pneumonitis after stereotactic lung radiotherapy: A matched analysis of three dimensional conformal and volumetric modulated arc therapy techniques," Int. J. Radiat. Oncol., Biol.,Phys. 80, 506–513 (2011). doi: 10.1016/j.ijrobp.2010.02.032

[36] M. Bignardi, L. Cozzi, A. Fogliata, P. Lattuada, P. Mancosu, P. Navarria, G. Urso, S. Vigorito, and M. Scorsetti, "Critical appraisal of volumetric modulated arc therapy in stereotactic body radiation therapy for metastases to abdominal lymph nodes," Int. J. Radiat. Oncol., Biol., Phys. 75, 1570–1577 (2009). doi: 10.1016/j.ijrobp.2009.05.035

[37] M. Scorsetti, M. Bignardi, F. Alongi, A. Fogliata, P. Mancosu, P. Navarria, S. Castiglioni, S. Pentimalli, A. Tozzi, and L. Cozzi, "Stereotactic body radiation therapy for abdominal targets using volumetric intensity modulated arc therapy with RapidArc: feasibility and clinical preliminary results," Acta Oncol. 50, 528–538 (2011). doi: 10.3109/0284186X.2011.558522

[38] L. S. Fog, J. F. B. Rasmussen, M. Aznar, F. Kjær-Kristoffersen, I. R. Vogelius, S. A. Engelhom, and J. P. Bangsgaard, "A closer look at RapidArc radiosurgery plans using very small fields," Phys. Med. Biol. 56, 1853–1863 (2011). doi: 10.1088/0031-9155/56/6/020

[39] G. Clark, R. Popple, P.E. Young, and J. Fiveash, "Feasibility of single iso-centre volumetric modulated arc

radiosurgery for treatment of multiple brain metastases," Int.J.Radiat.Oncol.,Biol., Phys. 76, 296-302 (2010). doi: 10.1016/j.ijrobp.2009.05.029

[40] C. Mayo, L. Ding, A. Addesa, S. Kadish, T. Fitzgerald, and R. Moser, "Initial experience with volumetric IMRT (RapidArc) for intracranial stereotactic radiosurgery," Int. J. Radiat.Oncol.,Biol., Phys. 78, 1457-1466 (2010). doi: 10.1016/j.ijrobp.2009.10.005

[41] H. Wolff, D. Wagner, H. Christiansen, C. Hess, and H. Vorwerk, "Single fraction radiosurgery using RapidArc for treatment of intracranial targets," Radiat. Oncol. 5 (2010). doi: 10.1186/1748-717X-5-77

[42] A. Fogliata, G. Nicolini, A. Clivio, E. Vanetti, and L. Cozzi, "Accuracy of Acuros XB and AAA dose calculation for small fields with reference to RapidArc® stereotactic treatments," Med. Phys. 38, 6228-6237 (2011). doi: 10.1118/1.3654739

[43] R. Alfonso, P. Andreo, R. Capote, M. Saiful Huq, W. Kilby, P. Kjäll, T. R. Mackie, H. Palmans, K. Rosser, J. Seuntjens, W. Ullrich, S. Vatnitsky "A new formalism for reference dosimetry of small and non-standard fields," Med. Phys. 35, 5179–86 (2008) doi: 10.1118/1.3005481

[44] IPEM, Small Field MV Photon Dosimetry, IPEM Report No. 103 (Institute of Physics and Engineering in Medicine, New York, (2010).

[45] M. Schwedas, M. Scheithauer, T. Wiezorek, T.G. Wendt, "Radiophysical characteristics of different detectors for use in dosimetry." Z. Med. Phys. 17, 172-179 (2007).

[46] M. Bucciolini, F. B. Buonamici, S. Mazzocchi, C. De Angelis, S. Onori, and G. A. Cirrone, "Diamond detector versus silicon diode and ion chamber in photon beams of different energy and field size," Med. Phys. 30, 2149–2154 (2003). doi: 10.1118/1.1591431

[47] A. Ralston, M. Tyler,P. Liu,D. McKenzie and N. Suchowerska, " Over-response of synthetic microdiamond detectors in small radiation fields." Phys. Med. Biol. 59, 5873–81 (2014) doi: 10.1088/0031-9155/59/19/5873

[48] T. Underwood, B. Rowland, R. Ferrand and L. Vieillevigne, "Application of the Exradin W1 scintillator to determine Ediode 60017 and microdiamond 60019 correction factors for relative dosimetry within small MV and FFF fields." Phys. Med. Biol. 60, 6669–83 (2015) doi: 10.1088/0031-9155/60/17/6669

[49] P. Francescon, W. Kilby, J.M. Noll, L. Masi, N. Satariano and S. Russo, "Monte Carlo simulated corrections for beam commissioning measurements with circular and MLC shaped fields on the CyberKnife M6 System: a study including diode, microchamber, point scintillator, and synthetic microdiamond detectors." Phys. Med. Biol. 62, 1076–1095 (2017) doi: 10.1088/1361-6560/aa5610

[50] A. Ralston, P. Liu, K. Warrener, D. McKenzie and N. Suchowerska, "Small field diode correction factors derived using an air core fibre optic scintillation dosimeter and EBT2 film," Phys. Med. Biol. 57, 9 (2012) doi: 10.1088/0031-9155/57/9/2587

[51] J.E. Morales, S.B. Crowe, R. Hill, N. Freeman and J.V. Trapp, "Dosimetry of cone-defined stereotactic radiosurgery fields with a commercial synthetic diamond detector." Med. Phys. 41 111702 (2014) doi: 10.1118/1.4895827

[52] A. Chalkley and G. Heyes, "Evaluation of a synthetic single-crystal diamond detector for relative dosimetry measurements on a CyberKnife" Br. J. Radiol. 87 20130768 (2014) doi: 10.1259/bjr.20130768

[53] W. Lutz, K.R. Winston,and N. Maleki. "A system for stereotactic radiosurgery with a linear accelerator," Int J Radiat Oncol Biol Phys. 14(2), 373-381 (1998).

[54] A. Van Esch, D.P. Huyskens, C.F. Behrens, E. Samsoe, M. Sjolin, U. Bjelkengren, D. Sjostrom, C. Clermont, L. Hambach, and F. Sergent, "Implementing RapidArc into clinical routine: a comprehensive program from machine QA to TPS validation and patient QA," Med Phys. 38(9),5146-66 (2011). doi: 10.1118/1.3622672.

[55] A. Van Esch, K. Basta, M. Evrard, M. Ghislain, F. Sergent, and D. P. Huyskens, "The Octavius1500 2D ion chamber array and its associated phantoms: Dosimetric characterization of a new prototype" Med. Phys. 41, 091708 (2014) doi: 10.1118/1.4892178

[56] B. Poppe, T. S. Stelljes, H. K. Looe, N. Chofor, D. Harder and K. Willborn, "Performance parameters of a liquid filled ionization chamber array," Med. Phys.40, 082106 (2013). doi 10.1118/1.4816298

[57] A. Van Esch, D.P. Huyskens, L. Hirschi, C. Baltes, "Optimized Varian aSi portal dosimetry: development of datasets for collective use," J Appl Clin Med Phys. 14(6), 4286 (2013).doi: 10.1120/jacmp.v14i6.4286.

[58] E. Sham, J. Seuntjens, S. Devic, and E. B. Podgorsak, "Influence of focal spot on characteristics of very small diameter radiosurgical beams," Med. Phys. 35, 3317–3330 (2008). doi: 10.1118/1.2936335

[59] A. Van Esch, J. Bohsung, P. Sorvari, M. Tenhunen, M. Paiusco, M. Iori, P. Engström, H. Nyström, and D. P. Huyskens, "Acceptance tests and quality control_QC_ procedures for the clinical implementation of IMRT using inverse planning and the sliding window technique: experience from five radiotherapy departments," Radiother. Oncol. 65, 53-70 (2002)

author to whom correspondence should be addressed: ann.vanesch@7sigma.be